Mesh Refinement Strategies for the Adaptive Isogeometric Method

Dissertation

zur

Erlangung des Doktorgrades (Dr. rer. nat.)

der

Mathematisch-Naturwissenschaftlichen Fakultät

der

Rheinischen Friedrich-Wilhelms-Universität Bonn

vorgelegt von

Philipp Morgenstern

aus

Berlin

Bonn, 2017

Angefertigt mit Genehmigung der Mathematisch-Naturwissenschaftlichen Fakultät der Rheinischen Friedrich-Wilhelms-Universität Bonn

1. Gutachter: Prof. Dr. Daniel Peterseim

2. Gutachter: Prof. Dr. Carsten Burstedde

Tag der Promotion: 19.06.2017

Erscheinungsjahr: 2017

Acknowledgements

All parts of this thesis were written during my employment at the Institute for Numerical Simulation at the University of Bonn. Most of the time, I was funded by the German Research Foundation (DFG) in the Priority Program 1748 “Reliable simulation techniques in solid mechanics. Development of non-standard discretization methods, mechanical and mathematical analysis” under the project “Adaptive isogeometric modeling of propagating strong discontinuities in heterogeneous materials”.

Most of all I want to thank my advisor Prof. Dr. Daniel Peterseim for offering me this position in his workgroup, involving me into computational homogenization and sending me into Isogeometric Analysis, for the introduction to a widespread mathematical community, frequent encouragement, lenience and patience, and for the possibility to write this thesis. Also I am thankful to the other members of the committee, especially Prof. Dr. Carsten Burstedde who agreed to be the co-referee of this thesis. I want to thank all my co-authors for the extensive and fruitful joint work, and further special thanks go to Giancarlo Sangalli and Michael Scott for their interest and compliments that encouraged me to pursue my ideas on T-spline refinement, to Paul Hennig for the very rich and fruitful joint work and the permission to use his figures in this thesis, and to Markus Burkow for counterchecking the thesis.

Personal thanks go to all my family for their patience, for their encouragement and interest, for child-keeping and support in various ways, and to the instructors and participants of the choirmaster course that took place from 2013 to 2015 at the National Music Academy of Lower Saxony. Those weekends were invaluable for the whole period of my PhD studies.

Contents

1 Introduction

This thesis explains and discusses several mesh refinement strategies for the Adaptive Isogeometric Method. The Adaptive Isogeometric Method is a numerical method that combines concepts of Isogeometric Analysis, itself a hybrid research field bridging between Computer-Aided Design (CAD) and Finite Element Analysis, with local mesh refinement. In order to provide an overview to the reader, we briefly outline the histories of the involved research fields. We emphasize that each of the fields has a very rich history and the outlines below are far from being complete.

The Adaptive Finite Element Method The Finite Element Method (FEM) is a numerical method for the approximate solution of partial differential equations (PDEs), which was introduced in the field of aeronautic engineering during the 1950s [1], based on the method of weighted residuals that Boris Galerkin introduced in 1915 [2]. With the evolution of computer-aided engineering, the FEM caught widespread attention and is used until today throughout most branches of computational mechanics, such as aeronautics, biomechanics, automotive industries and many more. In the 1970s, this approach was combined with spatial adaptivity of the discretization, based on local estimates of the error between approximated and exact solution that could be computed having only the approximation, introduced by Ivo Babuška and Werner Rheinboldt in 1978 [3]. The FEM and its mesh-adaptive variant (AFEM) caught growing attention in the mathematical field of Numerical Analysis, and the proof of convergence of the Adaptive FEM in one dimension by Babuška and Vogelius [4] in 1984 was a first step to theoretically corroborate this new method. Beneath the following milestones were the introduction of a new marking strategy by Willy Dörfler [5] in 1996 (see Section 2.5), a proof of convergence of the AFEM in higher dimensions by Morin, Nochetto and Siebert [6] in 2002, and a first proof of optimal convergence rates for the AFEM with refinement and coarsening by Binev, Dahmen and DeVore [7] in 2004, but the algorithm proven to be rate-optimal was actually never implemented. Analogous results were proven without the need of a coarsening step in 2007 by Rob Stevenson [8] and 2008 by Kreuzer, Cascon, Nochetto and Siebert [9]. Diverse proofs of rate-optimality followed for different types of the FEM, and recently, rate-optimality has been proven in a general framework for a wide range of problems and discretizations by Carstensen, Feischl, Page and Praetorius [10].

Isogeometric Analysis In 2005, Hughes, Cottrell and Basilevs introduced the framework of Isogeometric Analysis (IGA) [11, 12] in order to revolutionize computer-aided manufacturing and design, which where facing growing difficulties in the transition process between design models and their assessment in engineering applications. As mentioned above, the (Adaptive) Finite Element Method is used, e.g., for the stress analysis in structural mechanics, and is therefore a very important and useful

tool for the evaluation and assessment of computer-aided structural designs. With the rapid evolution of computer capacities in the last decades, the complexities of designs have grown equally, and so did the capacities of engineering applications. However, the conversion between the data structures of design and engineering, in particular the re-meshing of the geometry, turned out to be of higher complexity and has recently become a bottleneck of the structural design process. In IGA, this conversion is avoided by using the shape functions and data structures from CAD as ansatz functions for a Galerkin Method. The advantage is obviously that this idea yields a workaround for an inevitably growing problem, but on the other hand, it threw back the theory of FEMs for at least two decades, since the approximation properties of a Galerkin scheme with shape functions from CAD applications were completely unknown. In the past ten years, the IGA community and the number of related research articles grew rapidly in both engineering and mathematics, and many fundamental mathematical results were achieved for this new kind of method, most of which can be found in the work of Beirão da Veiga, Buffa, Sangalli and Vàzquez [13].

Truncated Hierarchical B-splines Although data approximation with globally smooth piecewise polynomials has been investigated already throughout the 19th century, the history of Hierarchical B-splines is far more recent and is sketched here with the following few milestones. In 1988, in the context of computer graphics and modeling, Forsey and Bartels suggested overlaying B-splines of several hierarchical levels [14] in order to control small-scale features of a macroscopic geometry. Kraft's PhD thesis from 1998 [15, 16] introduced a mechanism for the selection of particular B-splines in order to form a basis, which was later applied in the IGA context [17, 18], and finally in 2012, Giannelli, Jüttler and Speleers proposed a truncation mechanism [19] that reduces the support of the Hierarchical B-splines and yields a partition of unity, also for the application in Isogeometric Analysis [20, 21].

T-splines In 2003, Sederberg, Zheng, Bakenov and Nasri introduced T-splines in the context of CAD as a new realization for B-splines on irregular meshes [22] that does not require the bookkeeping of a hierarchical basis, but nevertheless allows for local mesh refinement [23] in order to control small-scale geometry features. Shortly after, IGA was introduced, and T-splines were applied with promising results [24, 25], but were at the same time proven by Buffa, Cho and Sangalli to lack linear independence in certain cases [26], which actually excludes them from the application in a Galerkin method. Another algorithmic difficulty was revealed by Scott and Li in 2011 [27], who showed that the refinement suggested in [23] may not only yield linear dependencies between the shape functions, but also non-nested spline spaces, which compromises the theoretical approximation properties of the method as well as the preservation of exact geometry data during refinement. The issue on linear independence was solved by Li, Zheng, Sederberg, Hughes and Scott in 2012 [28], proving that linear independence is guaranteed if the T-junction extensions do not intersect (this criterion is called *analysis-suitability*, see Definition 5.1.8 in this thesis). The second issue, namely how to generate nested spline spaces, was solved in a new refinement algorithm by Michael Scott [29], also preserving linear

independence of the T-splines. Still in 2012, Beirão da Veiga, Buffa, Cho and Sangalli provided new insight on the linear independence of T-splines by introducing the more abstract concept of dual-compatibility and proving its equivalence to analysis-suitability [30], and in 2013, Beirão da Veiga, Buffa, Sangalli and Vàzquez provided the theoretical background for T-splines of arbitrary polynomial degree [31], still restricted to the two-dimensional case. At that time, Wang, Zhang, Liu and Hughes introduced techniques for the construction of 3D T-spline meshes from boundary representations [32, 33], motivating the theoretical research on T-splines in three space dimensions, but in particular the linear independence of higher-dimensional T-splines was only characterized through the dual-compatibility criterion, until in 2016, the author of this thesis introduced a definition of T-junction extensions and analysis-suitability in three dimensions [34]. The research on 2D T-splines proceeds; Li and Scott characterized analysis-suitable T-spline spaces with globally highest smoothness [35] in 2014, and a characterization of analysis-suitable T-spline spaces with locally reduced smoothness was presented by Bressan, Buffa and Sangalli [36] in 2015.

This thesis We present four mesh refinement algorithms REFINE_HB, REFINE_THB, REFINE_TS$_{2D}$ and REFINE_TS$_{nD}$ for the Adaptive Isogeometric Method using multivariate Hierarchical B-splines, multivariate Truncated Hierarchical B-splines, bivariate T-splines, and multivariate T-splines, respectively. The algorithm REFINE_THB and the related results, in particular the complexity analysis, are cited from our joint work with Buffa and Giannelli [37], and the algorithm REFINE_HB is derived thereof. The refinement algorithm REFINE_TS$_{2D}$ has been introduced in 2015 [38], and finally REFINE_TS$_{nD}$ is a new refinement procedure introduced in this thesis, based on the preliminary work on three-dimensional T-splines [34]. The presented refinement strategies preserve shape regularity of the mesh as well as linear independence and bounded overlap of the basis functions. We address, if non-trivial, boundedness of mesh overlays, nestedness of the induced spline spaces and complexity in terms of marked and refined elements. Boundedness of the overlay and linear complexity of the refinement procedure are important pillars for the theoretical rate-optimality of the Adaptive Isogeometric Method, cf. [10, Equations (2.9) and (2.10)]. The nesting of the spline spaces is crucial as well, because it implies the so-called Galerkin orthogonality, which characterizes the approximate solution as a best-approximation of the exact solution with respect to a norm that depends on the problem (see Section 2.4). Altogether, this work paves the way for a proof of rate-optimality for the Adaptive Isogeometric Method with HB-splines, THB-splines, or T-splines in any space dimension. It shall be noted that rate-optimality in IGA has been proven very recently for the application of Hierarchical B-splines [39] to elliptic PDEs in arbitrary dimension, and for the IGABEM [40], an isogeometric variant of the Boundary Element Method which only requires a discretization of the domain boundary instead of the full domain. However, the latter is a result only for 2D domains, involving one-dimensional boundary manifolds. In order to justify the proposed methods and theoretical results in this thesis, numerical experiments underline their practical relevance, showing that they are not outperformed by currently prevalent refinement strategies.

The thesis is organized as follows. Chapter 2 gives an introduction into Isogeometric Analysis and mesh-adaptive Galerkin methods, in order to explain the framework in which the subsequent refinement strategies are discussed. In Chapter 3, we address Hierarchical B-splines and the corresponding refinement routine REFINE_HB. In order to provide an easy access to the basic concepts of the refinement routine, this is done in two dimensions and with dyadic refinement in Section 3.1 and for arbitrary dimension and q-adic refinement in Section 3.2, and Chapter 4 adapts the results from Chapter 3 to Truncated Hierarchical B-splines. The main focus of this thesis is Chapter 5, which presents and discusses the refinement strategy REFINE_TS$_{\text{2D}}$ for two-dimensional T-splines that we introduced in 2015 [38] as well as a refinement strategy REFINE_TS$_{\text{nD}}$ for T-splines in arbitrary dimension. The following Chapter 6 summarizes our joint work with Paul Hennig and Markus Kästner from TU Dresden [41], where we computationally compare the THB- and T-spline refinement routines in several prototypical problems. Chapter 7 sketches basic ideas for the refinement of T-splines on unstructured meshes and for the handling of T-splines with locally reduced smoothness, and Chapter 8 concludes the thesis with final remarks.

2 The Adaptive Isogeometric Method

This chapter introduces the mesh-adaptive Galerkin method with spline ansatz spaces. The subsequent chapters will investigate different strategies for the REFINE module of this method, which is explained in Section 2.5 below. We give a very quick introduction into B-splines, in order to explain basic concepts of Isogeometric Analysis. The last two sections of this chapter outline the framework of mesh-adaptivity in Galerkin methods.

2.1 B-splines

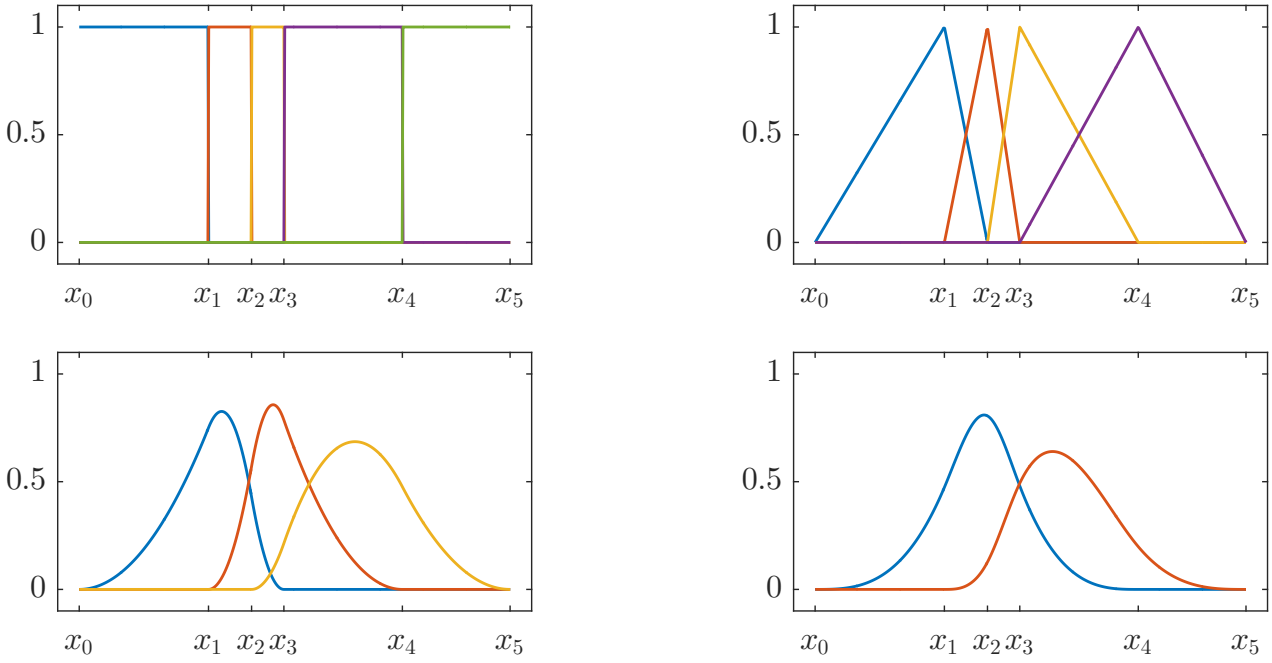

Figure 2.1: Example for B-splines of degree $p = 0, 1, 2, 3$ (upper left, upper right, lower left, lower right, resp.) for a fixed, strictly increasing knot vector. B-splines are polynomials of degree p in each segment, and they are C^{p-1}-continuous at the knots.

B-splines (where B stands for "basis") are a particular choice of basis functions for a globally continuous piecewise polynomial space. We give a one-dimensional definition below, which will later be generalized to arbitrary dimension. For a given *knot vector* $(x_0, \dots, x_m) \in \mathbb{R}^{m+1}$ with $x_0 \le \cdots \le x_m$, we call $\mathcal{Q} \coloneqq \{[x_0, x_1], \dots, [x_{m-1}, x_m]\}$ the (one-dimensional) mesh. B-splines form a basis for the piecewise p-degree polynomial space with global C^{p-1}-continuity,

$$\mathcal{B}(x_0, \dots, x_m) \coloneqq \left\{ f \in C^{p-1}([x_0, x_m]) \mid f \in P_p([x_{i-1}, x_i]) \text{ for } i = 1, \dots, m \right\}. \quad (2.1)$$

Definition 2.1.1 (B-spline)**.** Given a knot vector $(x_0, \dots, x_m) \in \mathbb{R}^{m+1}$ with $x_0 \leq \dots \leq x_m$, the i-th B-spline of degree p is defined recursively by

$$N_{i,0}(x) := \begin{cases} 1 & \text{if} \quad x_{i-1} \leq x < x_i \\ 0 & \text{otherwise} \end{cases} \qquad \text{for } i = 1, \dots, m,$$

$$N_{i,p}(x) := \frac{x - x_{i-1}}{x_{i+p-1} - x_{i-1}} N_{i,p-1}(x) + \frac{x_{i+p} - x}{x_{i+p} - x_i} N_{i+1,p-1}(x) \quad \text{for } i = 1, \dots, m-p. \tag{2.2}$$

The above definition is known as the Cox-deBoor recursion formula, see e.g. [42, p. 131]. See Figures 2.1 and 2.2 for examples. It can be seen in Figure 2.1 that for strictly increasing knot vectors, the above definition does not yield a basis of the space $\mathcal{B}(x_0, \dots, x_m)$. However, it does yield a basis for *open knot vectors*, i.e., knot vectors in which the first and last knot have multiplicity $p + 1$ (see Figure 2.2 for examples). While multiple knots at the boundary are crucial for the construction

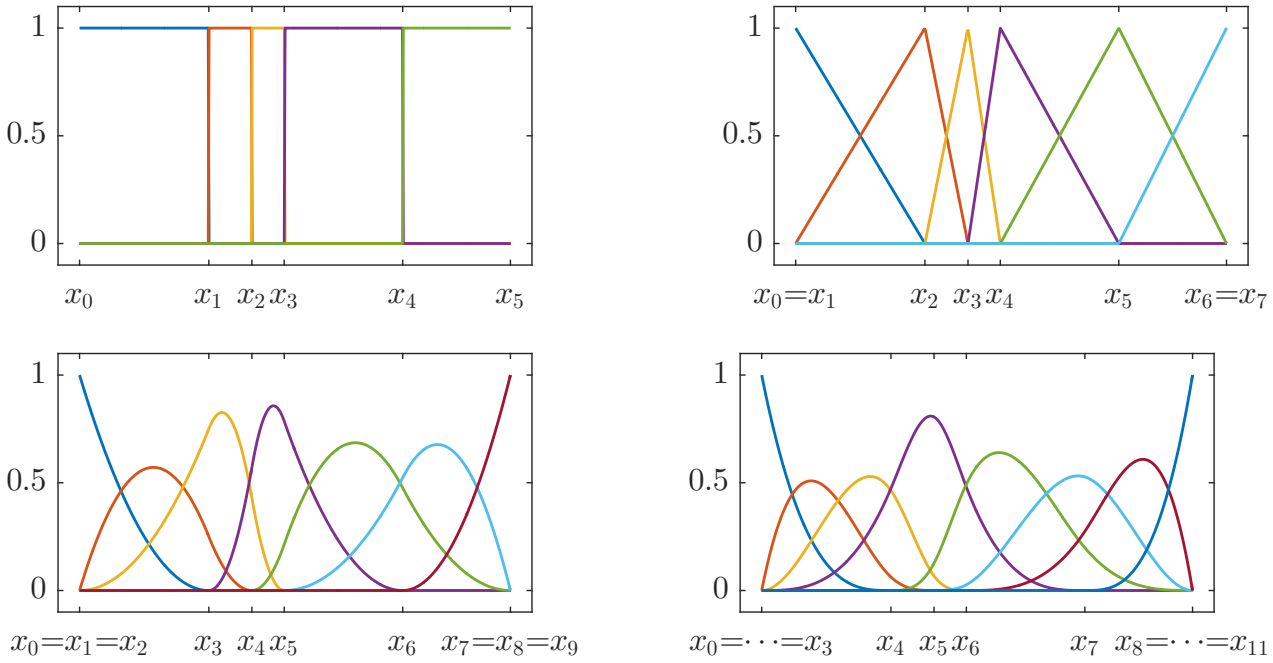

Figure 2.2: Example for B-splines of degree $p = 0, 1, 2, 3$ for open knot vectors. In that case, the B-splines form a basis of $P_p(\mathcal{Q}) \cap C^{p-1}([x_0, x_m])$.

of a spline basis, multiple knots in the interior of the domain locally reduce the continuity of the basis functions. At an interior knot with multiplicity μ, the B-splines are $C^{p-\mu}$-continuous, while "C^{-1}-continuity" means discontinuity, and "C^{-2}-continuity" means discontinuity plus the existence of a basis function that is zero everywhere except this knot.

2.2 Geometry representation

B-splines and in particular their generalization to Non-Uniform Rational B-splines (NURBS, see Section 2.3 below) are commonly used in Computer-Aided Design

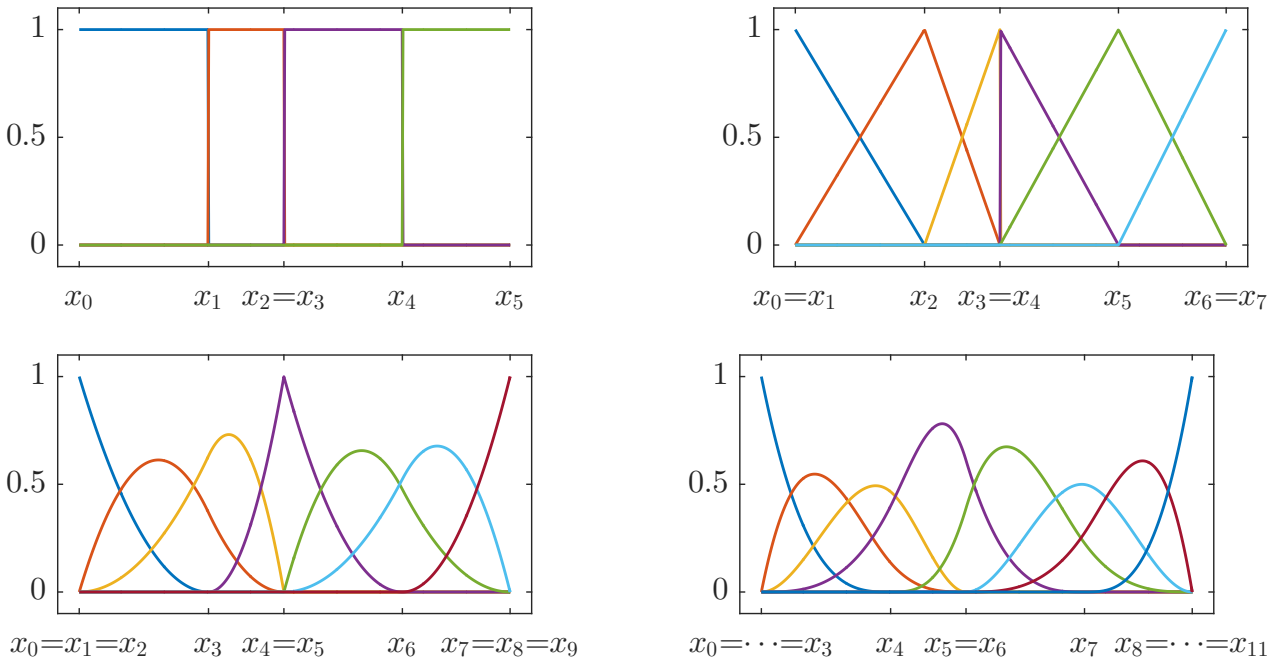

Figure 2.3: Example for B-splines of degree 0, 1, 2 and 3 for open knot vectors with a knot of multiplicity 2. In that knot, the continuity of the B-splines is reduced to C^{p-2}.

(CAD). This section explains in two examples how a spline basis is used for the representation of domains with specially curved boundaries.

We restrict our study to $p > 0$ and consider an open knot vector $(x_0, \dots, x_{m+p})$, i.e., $x_0{=}\cdots{=}x_p$, $x_m{=}\cdots{=}x_{m+p}$ and corresponding B-splines $N_{1,p}, \dots, N_{m,p}$. For a given set of *control points* $c_1, \dots, c_m \in \mathbb{R}^2$, the described *B-spline curve* is the image of a map from $[x_0, x_{m+p}]$ into $\mathbb{R}^2$,

$$M_1 : \quad [x_0, x_{m+p}] \to \mathbb{R}^2, \quad x \mapsto \sum_{i=1}^{m} N_{i,p}(x) \cdot c_i. \tag{2.3}$$

See Figure 2.4 for examples. Since all B-splines are non-negative and a partition of unity (i.e., they sum up to 1), the B-spline curve is always in the convex hull of the control points. The purpose of a CAD application is to design the shape of an object. This may be e.g. a ship hull, an airplane, or components like screws or other construction elements. The user creates and manipulates control meshes in order to design and modify the described geometry. We illustrate in a second example how this technique is applied for B-spline surfaces. We consider the knot vector $(x_0, \dots, x_{m+p})$ from Figure 2.2 and the knot vector $(\hat{x}_0, \dots, \hat{x}_{m+p})$ from Figure 2.3, and the corresponding B-splines $N_{1,p}, \dots, N_{m,p}$ and $\hat{N}_{1,p}, \dots, \hat{N}_{m,p}$, respectively. We consider the domain $\overline{\Omega} := [x_0, x_{m+p}] \times [\hat{x}_0, \hat{x}_{m+p}]$, which is partitioned by the *tensor-product mesh*

$$\mathcal{Q} = \{[x_{i-1}, x_i] \times [\hat{x}_{j-1}, \hat{x}_j] \mid i, j \in \{1, \dots, m+p\}\}. \tag{2.4}$$

We define the *tensor-product basis*

$$N_{i,j,p}(x, y) = N_{i,p}(x) \cdot \hat{N}_{j,p}(y) \quad \text{for all } i, j \in \{1, \dots, m\}. \tag{2.5}$$

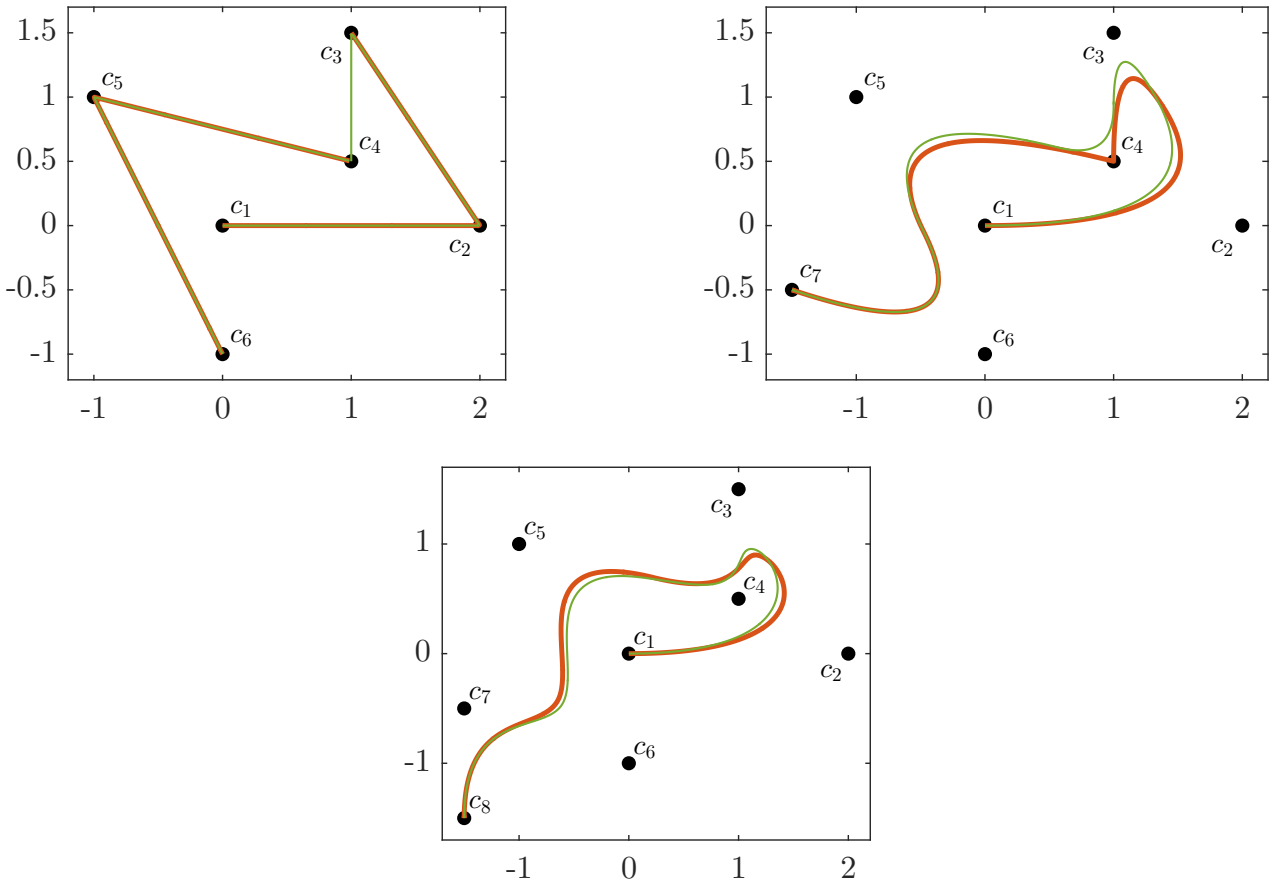

Figure 2.4: Examples for B-spline curves of degree 1, 2 and 3 for the knot vectors and B-splines from Figure 2.2 (thin, green) and for the knot vectors and B-splines from Figure 2.3 (thick, red). Reduced continuity of the basis functions leads to reduced smoothness of the curve.

We make up control points $c_{i,j}$ for all $i, j \in \{1, \dots, m\}$ and describe a free-form surface through the map

$$M_2 : \overline{\Omega} \to \mathbb{R}^3, \quad x \mapsto \sum_{i,j=1}^{m} N_{i,j,p}(x) \cdot c_{i,j}. \tag{2.6}$$

See Figure 2.5 for examples.

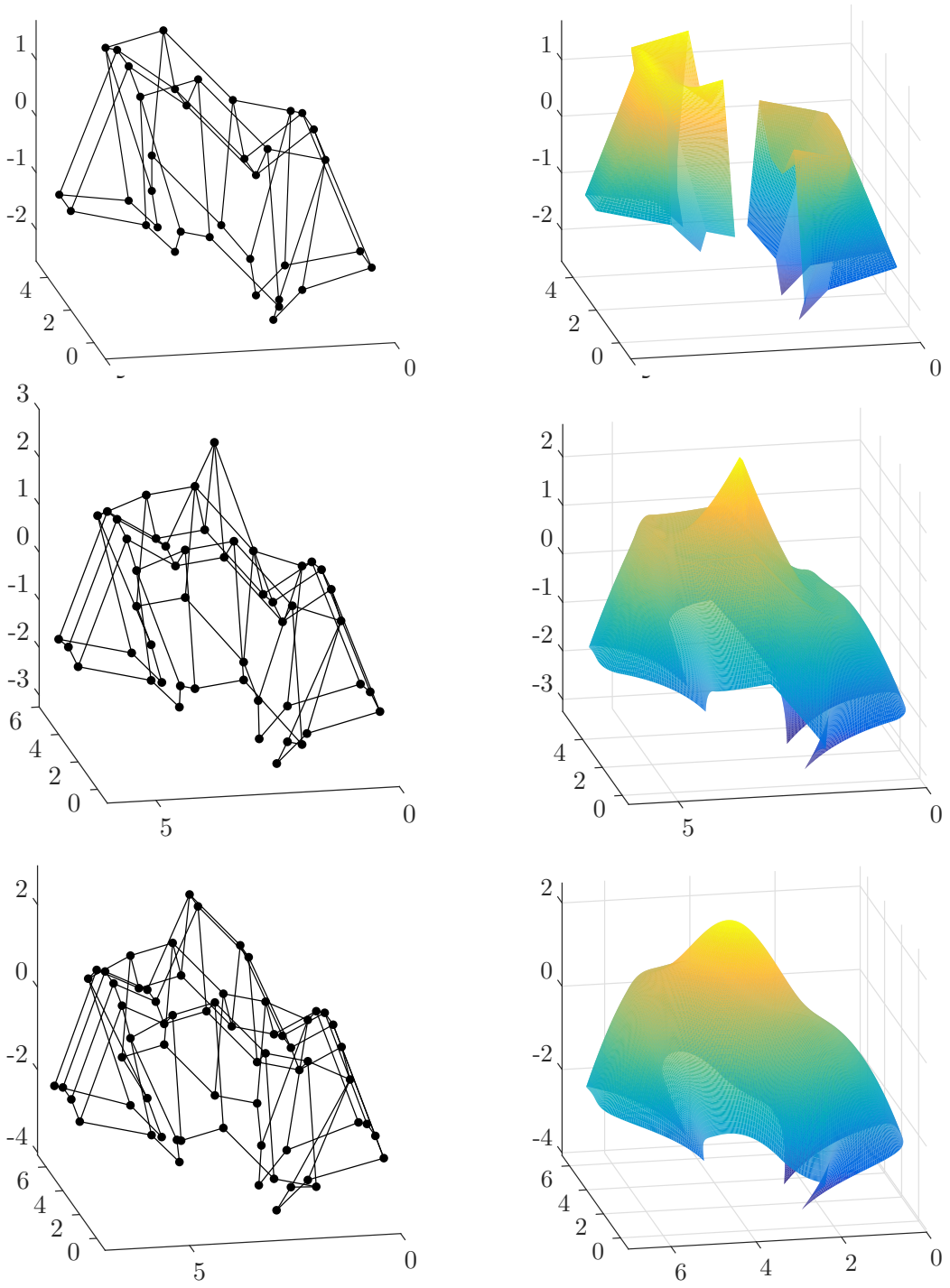

Figure 2.5: Examples for B-spline surfaces (right column) of degree 1, 2 and 3 using the B-splines from Figure 2.2 in x-direction and B-splines from Figure 2.3 in y-direction. The figures on the left show so-called *control meshes*, which are the control points connected by grid lines for visualization. As in Figure 2.4, reduced continuity of the basis functions leads to reduced (directional) smoothness of the surface.

2.3 NURBS

In order to exactly describe conic sections, in particular circles and circular arcs, Non-Uniform Rational B-Splines (NURBS) have been developed. They are obtained by multiplying the B-splines with positive weights $w_1, \dots w_m \in \mathbb{R}_{\bullet>0}$ and afterwards enforcing a partition of unity. In one space dimension, the NURBS are defined by

$$R_{i,p}(x) = \frac{w_i N_{i,p}(x)}{\sum_{j=1}^{m} w_j N_{j,p}} \quad \text{for all } i \in \{1, \dots, m+p-1\}. \tag{2.7}$$

By construction, NURBS sum up to 1, and they inherit from B-splines smoothness and linear independence, but they span a space other than piecewise polynomials, which is necessary, since classical B-spline cannot describe conic sections exactly.

Figure 2.6 shows the construction of a circle (thick red lines). It is composed of three circular arcs of 120° each. We use the setting $p = 2$ and the knot vector $(0, 0, 0, 1, 1, 2, 2, 3, 3, 3)$. The weights are $w_1 = w_3 = w_5 = w_7 = 1$ at the start and end points of the arcs, and the remaining weights are computed as

$$w_2 = w_4 = w_6 = \cos(120^\circ/2) = \tfrac{1}{2}, \tag{2.8}$$

see e.g. [12, p. 58]. For comparison, Figure 2.6 also shows the result of an analogous map applying unweighted quadratic B-splines (thin blue lines).

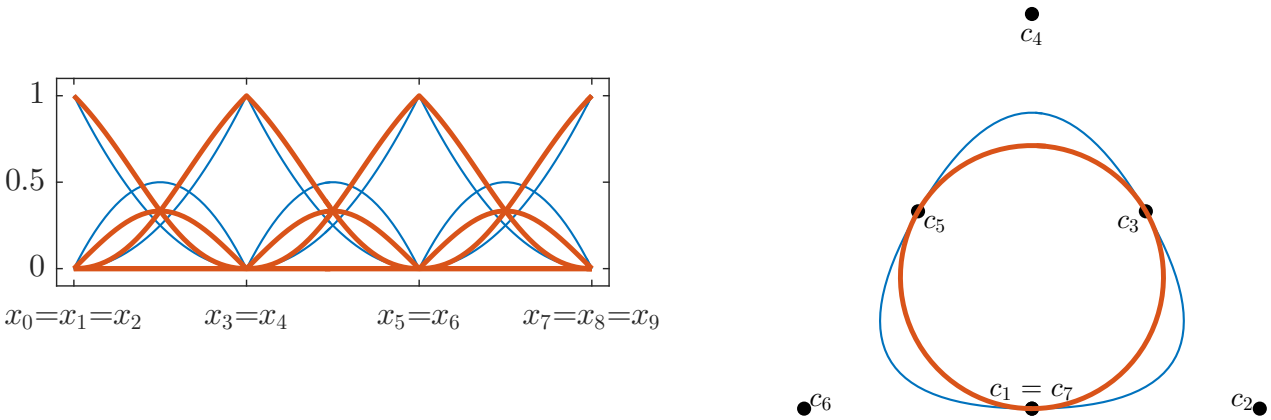

Figure 2.6: Example for a circle described through NURBS (thick, red) with $p = 2$ and weights $w_i = \begin{cases} 1 & \text{if } i \text{ even} \\ 1/2 & \text{otherwise} \end{cases}$. The analogous map with quadratic B-splines (without weights) is illustrated with thin blue lines.

2.4 Isogeometric Analysis

The design of real-world constructions rises physics questions, e.g., on the statical (elastic) behavior of the designed object under load. These questions are addressed by approximately solving partial differential equations (PDEs) that involve the designed object as the computational domain. The most common approach for the approximate solution of these problems is the *Finite Element Method (FEM)*, which is a special case of a *Galerkin method*. *Isogeometric Analysis* is an alternative realization of a Galerkin method, and it will be explained at the end of this subsection.

The Galerkin method is outlined as follows. Let $\mathcal{V}$ be a Hilbert space of real-valued functions on an open set $\Omega \subset \mathbb{R}^d$. We call Ω the *computational domain*. The problem to be solved is a weakly formulated PDE that seeks u in $\mathcal{V}$ such that

$$\forall\, v \in \mathcal{V}: \quad a(u,v) = f(v) \quad \text{a.e. in } \Omega, \tag{2.9}$$

plus conditions on the behavior of u on the boundary $\partial\Omega$. In this problem, $a(\bullet,\bullet)$ is a continuous, coercive and symmetric bilinear form and f is a bounded linear operator on $\mathcal{V}$. We consider a finite-dimensional subspace $\mathcal{V}_n$ of $\mathcal{V}$ with $\dim \mathcal{V}_n = d_n \in \mathbb{N}$. The *discrete solution* $u_n \in \mathcal{V}_n$ that satisfies $a(u_n, v_n) = f(v_n)$ a.e. in Ω for all $v_n \in \mathcal{V}_n$ is computed as follows. Given a basis $\{b_1, \ldots, b_{d_n}\}$ of $\mathcal{V}_n$, let $A = (a(b_i, b_j))_{i,j=1}^{d_n}$ be the Gramian matrix of the bilinear form $a(\bullet,\bullet)$, also called *stiffness matrix* in Numerical Analysis due to its application in elasticity problems, and $F = (f(b_i))_{i=1}^{d_n}$ the so-called *load vector*. The solution U of the linear equation system $AU = F$ is a vector that contains the coefficients of $u_n = \langle (b_1, \ldots, b_{d_n}), U \rangle$. If $a(\bullet,\bullet)$ is a scalar product (which is the case for simple problems, e.g., for all problems considered in Chapter 6), then the discrete solution u_n is the best approximation of u in $\mathcal{V}_n$ with respect to the norm $\|\bullet\|_a = \sqrt{a(\bullet,\bullet)}$ induced by $a(\bullet,\bullet)$.

The (classical, conforming) FEM is a Galerkin method in which the finite-dimensional space $\mathcal{V}_n$ from above is constructed as follows. The computational domain Ω is partitioned into a finite set (*mesh*) $\mathcal{Q}$ of cells, which are usually triangles or quadrilaterals; in higher dimension, simplices or (hyper-)cuboids. A finite-dimensional function space $\check{\mathcal{V}}$ is chosen, most common choices are, in case of triangles/simplices, spaces of polynomials up to a fixed total degree k (the resulting FEM is known as P_k-FEM), or, in case of quadrilaterals/cuboids, up to a fixed partial degree (this results in Q_k-FEM). The space $\mathcal{V}_n$ is the globally continuous piecewise $\check{\mathcal{V}}$-space,

$$\mathcal{V}_n \coloneqq \{v \in \mathcal{V} \mid v \in C(\overline{\Omega}) \wedge \forall\, \mathtt{Q} \in \mathcal{Q} : v|_{\mathtt{Q}} \in \check{\mathcal{V}}(\mathtt{Q})\}. \tag{2.10}$$

Given a domain Ω designed in a CAD application, we denote the corresponding geometry map by M, and its preimage by Ω_{param}. We call Ω_{param} the *parametric domain* and Ω the *physical domain*. The FEM requires a mesh that partitions Ω. However, the CAD representation only provides a mesh $\mathcal{Q}_{\text{param}}$, which partitions the parametric domain Ω_{param} and was used to construct the spline basis. Its image $M(\mathcal{Q}_{\text{param}})$ consists of deformed cells, which, by enforcing continuity of $\mathcal{V}_n$, leads to $\mathcal{V}_n = \{0\}$ if M cannot be described as a map with piecewise $\check{\mathcal{V}}$-functions. This is the case in general, and in particular if NURBS have been used. A common workaround is the generation of a new mesh for the FEM. The domain Ω_{FEM} partitioned by this mesh has a polygonal boundary and hence is only an approximation of Ω. This approximation error is a delicate problem since in particular elasticity problems are in general *not* well-posed with respect to the domain, which means that small perturbations in the geometry data may have unbounded effects on the exact and the approximate solution of the PDE, for example at the re-entrant corner in an L-shaped construction piece under tension. An additional drawback of the above workaround is that mesh generation may be expensive for complex geometries.

An alternative approach has been entitled *Isogeometric Analysis* and is a Galerkin method that makes use of the geometry representation. Let $\mathcal{S}$ be the set of (possibly

rational) spline functions that were used to construct the geometry map M. The discrete space $\mathcal{V}_n$ is defined as the *pullback space* of the spline space $\operatorname{span}\mathcal{S}$,

$$\mathcal{V}_n \coloneqq \operatorname{span}\{b \circ M^{-1} \mid b \in \mathcal{S}\}. \tag{2.11}$$

Provided that M^{-1} exists and is continuous, which crucially depends on the control points, the functions $M^{-1} \circ b$ inherit linear independence, positivity, the partition of unity property, and (in case of multiple inner knots, locally reduced) smoothness from $\mathcal{S}$.

2.5 A mesh-adaptive Galerkin method

The physics problems discussed above often require resolving local features of the solution (e.g., a singularity of the strain) while keeping the number of degrees of freedom (i.e., the dimension of the discrete space) as small as possible. This means for a mesh-based Galerkin method that the mesh needs to be locally fine in the environment of a certain point or lower-dimensional subdomain, while remaining coarse away from these features. This is addressed by the Adaptive Finite Element Method, which is an iterative procedure that consist of the steps

$$\circlearrowright \text{SOLVE} \to \text{ESTIMATE} \to \text{MARK} \to \text{REFINE}$$

and they are described as follows.

SOLVE: Given a finite-dimensional function space $\mathcal{V}_n$, compute a Galerkin approximation of the solution of the PDE as described above.

ESTIMATE: Compute local estimates for the error, i.e., the difference of approximate and exact solution.

MARK: Based on these local estimates, select mesh elements $\mathcal{M} \subseteq \mathcal{Q}$ for refinement.

REFINE: Refine the mesh $\mathcal{Q}$ and construct the new discrete function space $\mathcal{V}_{n+1}$. This is the focus of the thesis, and different strategies will be investigated in the subsequent chapters.

Given a fixed refinement routine with linear complexity (which will be specified later, see e.g. Theorem 3.1.12), we denote by $\mathbb{V}$ the class of function spaces that can be generated by this refinement routine. For certain problems, it has been proven that if the Adaptive FEM is applied with Dörfler marking, which is explained below, and an appropriate error estimator, the sequence of discrete solutions $u_1 \in \mathcal{V}_1 \in \mathbb{V}$, $u_2 \in \mathcal{V}_2 \in \mathbb{V}, \dots$ has the best convergence rate (with respect to degrees of freedom) that is possible in the class $\mathbb{V}$ of discrete function spaces [7, 8, 9, 10].

The error estimator

For a given mesh $\mathcal{Q}$ and corresponding discrete solution u_n, the error estimator is a functional $\eta_{\mathcal{Q}} : \mathcal{Q} \to \mathbb{R}_{\bullet \geq 0}$ that yields an estimate for the elementwise error $\|u_n|_{Q} - u|_{Q}\|_a$ on each element $Q \in \mathcal{Q}$. To satisfy the above-mentioned theory on optimal convergence rates, $\eta_{\mathcal{Q}}$ has to satisfy a set of axioms proposed in [10], which

include stability on non-refined elements, reduction on refined elements, reliability ($C \cdot \eta_{\mathcal{Q}}$ bounds the error from above) and effiency ($c \cdot \eta_{\mathcal{Q}}$ bounds the error from below), where C and c are fixed constants that may depend on the domain and the initial mesh, but not on the refinement level or the discrete solution u_n. The analysis of the error $u - u_n$ using the approximation u_n is called *a posteriori error analysis* (in contrast to *a priori error analysis*). Fundamentals and a collection of appropriate error estimators for a wide range of physical problems can be found in [43].

The marking strategy

Given the estimated local errors $\eta_{\mathcal{Q}}(\mathtt{Q})$ for $\mathtt{Q} \in \mathcal{Q}$ and a marking parameter $\theta \in [0, 1]$, which is chosen manually, the following strategies are commonly used for the step MARK.

- *Dörfler marking:* Mark $\mathcal{M} \subset \mathcal{Q}$ with minimal cardinality $\#\mathcal{M}$ while accumulating at least a θ-amount of the total error,

$$\sum_{\mathtt{Q} \in \mathcal{M}} \eta_{\mathcal{Q}}(\mathtt{Q}) \geq \theta \cdot \sum_{\mathtt{Q} \in \mathcal{Q}} \eta_{\mathcal{Q}}(\mathtt{Q}). \tag{2.12}$$

  This strategy was introduced in [5] and has particular importance for the analysis on optimal convergence rates.

- *Quantile marking:* Mark $\mathcal{M} \subset \mathcal{Q}$ with maximal accumulated error $\sum_{\mathtt{Q} \in \mathcal{M}} \eta_{\mathcal{Q}}(\mathtt{Q})$ while marking at most θ times the total number of elements,

$$\#\mathcal{M} \leq \theta \cdot \#\mathcal{Q}. \tag{2.13}$$

  This is e.g. used in [25, 44].

- *Maximum marking:* Let $\eta_{\max} = \max_{\tilde{\mathtt{Q}} \in \mathcal{Q}} \eta_{\mathcal{Q}}(\tilde{\mathtt{Q}})$ be the maximal estimated element error, and mark all elements for which at least θ times that error was estimated,

$$\mathcal{M} = \{\mathtt{Q} \in \mathcal{Q} \mid \eta_{\mathcal{Q}}(\mathtt{Q}) \geq \theta \cdot \eta_{\max}\}. \tag{2.14}$$

  This strategy was introduced in [4] and can be considered as the traditional marking strategy.

For a modified version of Maximum marking, the discrete solutions are proven to be instance-optimal [45]. This means that in each step, the error of the discrete solution $u_n \in \mathcal{V}_n \in \mathbb{V}$ is bounded by a constant times the smallest error of the discrete solutions of all function spaces $\tilde{\mathcal{V}}_n \in \mathbb{V}$ with a comparable (or smaller) number of degrees of freedom. This is an even stronger result than the rate optimality described above, however [45] accounts only for the Poisson problem with homogeneous Dirichlet boundary conditions, and the authors are only aware of a generalization for the nonconforming Crouzeix-Raviart AFEM and the Stokes equation [46].

It should be noted that all above-mentioned literature assumes that the problem data, i.e., the right-hand side f and coefficients of $a(\bullet, \bullet)$, are resolved by the mesh and sufficiently well-approximated by the discrete space. This is not the case in

general applications. In order to resolve the problem data, [6] proposes an additional marking step. In [47, 48, 49], this strategy is called *separate marking* and is equipped with a data approximation step instead of mesh refinement. If resolving the data requires a very fine mesh all over the domain, there is no use in adaptive schemes for the data approximation. The Problem is then called a *multiscale* problem, due to the interest in the macroscopic behavior of the solution given microscopicly-structured data. This kind of problem is addressed by numerical homogenization techniques, which are e.g. addressed in [50, 51].

2.6 Geometry update

The refinement of the parametric mesh updates the spline basis which also describes the geometry. Consequently, this requires an update of the geometry description, i.e., of the control points. Given a knot vector $(x_0, \dots, x_{m+p})$ and a new knot vector $(\tilde{x}_0, \dots, \tilde{x}_{n+p})$ which is a strict superset of $(x_0, \dots, x_{m+p})$, i.e., $n > m$, the new control points $\tilde{c}_1, \dots, \tilde{c}_n$ are constructed by linear combinations of the old control points $c_1, \dots, c_m$. Algorithms for the computation of these linear combinations are known as *knot insertion* routines. We cite below an algorithm from [12, p. 37].

Algorithm 2.6.1 (Knot insertion)**.**

Input: $(x_0, \dots, x_{m+p})$, $(\tilde{x}_0, \dots, \tilde{x}_{n+p})$, $c_1, \dots, c_m$

for all $i = 1, \dots, n+p$, $j = 1, \dots, m+p$ **do**

$$T_{ij}^{(0)} = \begin{cases} 1 & \text{if } \tilde{x}_i \in [x_j, x_{j+1}) \\ 0 & \text{otherwise.} \end{cases}$$

end for

for all $q = 1, \dots, p$ **do**

for all $i = 1, \dots, n+p-q$, $j = 1, \dots, m+p-q$ **do**

$$T_{ij}^{(q)} = \frac{\tilde{x}_{i+q} - x_{j-1}}{x_{j+q-1} - x_{j-1}} T_{ij}^{(q-1)} + \frac{x_{j+q} - \tilde{x}_{i+q}}{x_{j+q} - x_j} T_{i(j+1)}^{(q-1)}.$$

end for

end for

$$\begin{pmatrix} \tilde{c}_1 \\ \vdots \\ \tilde{c}_n \end{pmatrix} = \begin{pmatrix} T_{1,1}^{(p)} & \cdots & T_{1,m}^{(p)} \\ \vdots & \ddots & \vdots \\ T_{n,1}^{(p)} & \cdots & T_{n,m}^{(p)} \end{pmatrix} \cdot \begin{pmatrix} c_1 \\ \vdots \\ c_m \end{pmatrix}.$$

return $\tilde{c}_1, \dots, \tilde{c}_n$

We illustrate the algorithm in the following example. Consider the quadratic knot vector from Figure 2.3 (bottom left), $(x_0, \dots, x_9) = (0, 0, 0, 0.6, 0.95, 0.95, 1.5, 2, 2, 2)$. We insert three knots at the positions $1.2, 1.7, 1.7$ using the above algorithm, which yields the new knot vector $(x_0, \dots, x_1 2) = (0, 0, 0, 0.6, 0.95, 0.95, 1.2, 1.5, 1.7, 1.7, 2, 2, 2)$ and the transformation matrix

$$T^{(2)} = \begin{pmatrix} 1 & 0 & 0 & 0 & 0 & 0 & 0 & 0 & 0 & 0 \\ 0 & 1 & 0 & 0 & 0 & 0 & 0 & 0 & 0 & 0 \\ 0 & 0 & 1 & 0 & 0 & 0 & 0 & 0 & 0 & 0 \\ 0 & 0 & 0 & 1 & \frac{6}{11} & 0 & 0 & 0 & 0 & 0 \\ 0 & 0 & 0 & 0 & \frac{5}{11} & \frac{16}{21} & \frac{2}{7} & \frac{6}{35} & 0 & 0 \\ 0 & 0 & 0 & 0 & 0 & \frac{5}{21} & \frac{5}{7} & \frac{117}{175} & \frac{3}{5} & 0 \\ 0 & 0 & 0 & 0 & 0 & 0 & 0 & \frac{4}{25} & \frac{2}{5} & 1 \end{pmatrix}^{\top}. \tag{2.15}$$

The first four rows (columns in the transposed version above) and the last one are unit vectors, which means that the corresponding control points $c_1, \ldots, c_4$ and c_7 remain unchanged. The control points c_5 and c_6 are replaced by five new control points which are linear combinations of the old control points $c_4, \ldots, c_7$. The updated control points, which represent exactly the same curve as before, are shown in Figure 2.7.

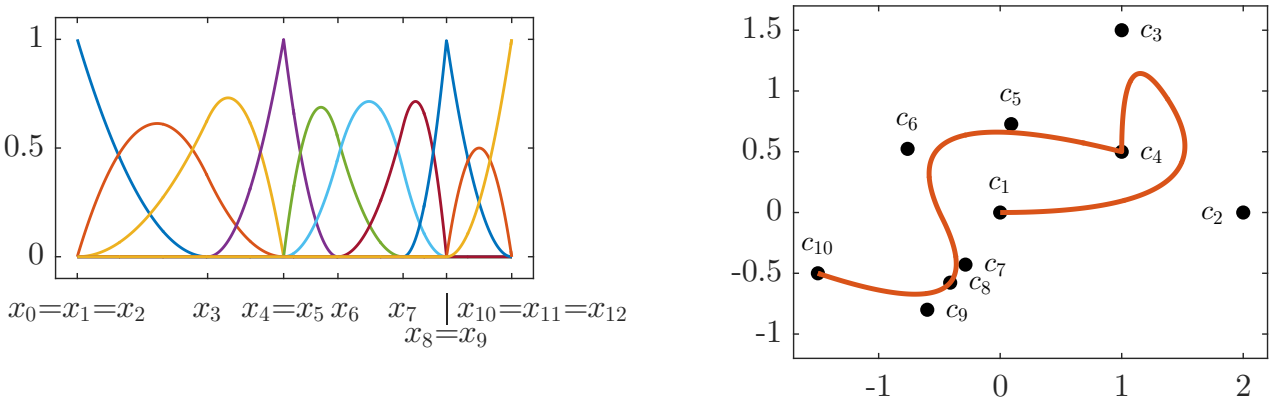

Figure 2.7: Example for the knot insertion routine. We refined the knot vector for quadratic quadratic B-splines from Figure 2.3, and updated the control points for the corresponding curve in Figure 2.4.

3 Hierarchical B-splines

Throughout the rest of this thesis, we investigate several strategies for the adaption of B-splines to non-uniform meshes and their local refinement. The spline basis corresponding to a given parametric mesh $\mathcal{Q}$ will be denoted in the style $\mathcal{B}(\mathcal{Q})$, and the mesh refinement routine by $\tilde{\mathcal{Q}} \coloneqq \textsc{refine}(\mathcal{Q}, \mathcal{M})$, with $\mathcal{M} \subseteq \mathcal{Q}$ being a set of elements to be refined, and $\tilde{\mathcal{Q}}$ the new refined mesh. This chapter introduces the basis $\mathcal{B}_{\text{HB}}$ and the REFINE_HB method as one realization of the REFINE module. The subsequent chapters introduce the alternative realizations ($\mathcal{B}_{\text{THB}}$, REFINE_THB) in Chapter 4 and ($\mathcal{B}_{\text{TS}}$, REFINE_TS) in Chapter 5.

3.1 Local dyadic refinement in 2D

For the sake of legibility, we assume the initial parametric mesh $\mathcal{Q}_{\text{param}}$ (where initial means 'before refinement') to be constructed from knot intervals of length 1. Non-uniform knot configurations can be met by a piecewise affine, globally continuous and rotation-free map from the refined mesh.

The local refinement for hierarchical splines chooses B-splines from several uniform meshes of different mesh widths and combines them to a basis of a non-uniform spline space. We introduce the notation for uniform meshes below, and we will subsequently explain the local refinement strategy. In Chapter 2, the term 'B-spline' was defined as a basis function of a spline space. However, this term is used ambigously in the literature, and often also used for any spline function generated by the B-splines. We will therefore use the term 'B-spline basis' to emphasize when the spline basis is meant.

3.1.1 Uniform meshes

We assume the *initial mesh* $\mathcal{Q}_0 = \mathcal{Q}_{\mathsf{u}[0]}$ to be a tensor product mesh, and its elements are closed squares with side length 1 (see Figure 3.1),

$$\mathcal{Q}_{\mathsf{u}[0]} \coloneqq \Big\{ [n_1 - 1, n_1] \times [n_2 - 1, n_2] \mid n_1 \in \{1, \dots, N_1\}, n_2 \in \{1, \dots, N_2\} \Big\}. \tag{3.1}$$

The corresponding spline basis $\mathcal{B}_0$ is spanned by the corresponding tensor-product B-splines. For each level $k \in \mathbb{N}_0$, we define the tensor-product mesh

$$\mathcal{Q}_{\mathsf{u}[k]} \coloneqq \Big\{ [x - 2^{-k}, x] \times [y - 2^{-k}, y] \mid 2^k x \in \{1, \dots, 2^k N_1\}, 2^k y \in \{1, \dots, 2^k N_2\} \Big\} \tag{3.2}$$

and $\mathcal{B}_k$ the corresponding set of bivariate B-spline basis functions.

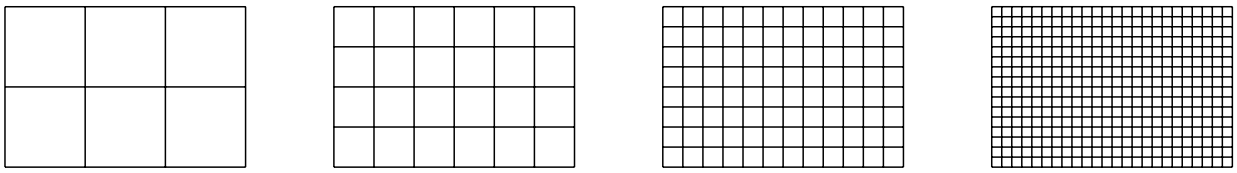

$\mathcal{Q}_{\mathsf{u}[0]}$ $\mathcal{Q}_{\mathsf{u}[1]}$ $\mathcal{Q}_{\mathsf{u}[2]}$ $\mathcal{Q}_{\mathsf{u}[3]}$

Figure 3.1 [41]: Example for the uniform meshes $\mathcal{Q}_{\mathsf{u}[0]}, \dots, \mathcal{Q}_{\mathsf{u}[3]}$ for $N_1 = 3$ and $N_2 = 2$.

Definition 3.1.1. We define the uniform refinement routine by

$$\textsc{refine\_uniform}(\mathcal{Q}_{\mathsf{u}[k]}, \mathcal{M}) \coloneqq (\mathcal{Q}_{\mathsf{u}[k+1]}, \mathcal{B}_{k+1}) \quad \text{for any } k \in \mathbb{N}_0 \text{ and } \mathcal{M} \subseteq \mathcal{Q}. \tag{3.3}$$

Note that the set of marked elements $\mathcal{M}$ enters only for formal reasons and has no effect on the refinement. We denote the class of uniform meshes by

$$\mathbb{M}_{\textsc{uniform}} \coloneqq \{\mathcal{Q}_{\mathsf{u}[n]} \mid n \in \mathbb{N}_0\}. \tag{3.4}$$

Definition 3.1.2 (Level)**.** Given $k \in \mathbb{N}$ and $\mathtt{Q} \in \mathcal{Q}_{\mathsf{u}[k]}$, we denote the *level* of $\mathtt{Q}$ by $\ell(\mathtt{Q}) \coloneqq k$.

3.1.2 Local refinement

For the use of Hierarchical B-splines (HB-splines), the underlying rectangular mesh $\mathcal{Q}$ may consist of finitely many elements from meshes in $\mathbb{M}_{\textsc{uniform}}$, such that any two elements of $\mathcal{Q}$ have disjoint interior, and the union of all elements of $\mathcal{Q}$ is the same domain $[0, N_1] \times [0, N_2]$ that is covered by uniform meshes. In particular, $\mathcal{Q}$ is meant to contain elements of different levels:

$$\mathbb{M}_{\textsc{hb}} \coloneqq \Big\{ \mathcal{Q} \subset \textstyle\bigcup_{\mathcal{Q}' \in \mathbb{M}_{\textsc{uniform}}} \mathcal{Q}' \mid \#\mathcal{Q} < \infty,\ \bigcup_{\mathtt{Q} \in \mathcal{Q}} \mathtt{Q} = [0, N_1] \times [0, N_2], \\ \forall \mathtt{Q}, \mathtt{Q}' \in \mathcal{Q} :\ \operatorname{int}(\mathtt{Q}) \cap \operatorname{int}(\mathtt{Q}') = \emptyset \Big\}. \tag{3.5}$$

Definition 3.1.3 (Subdivision)**.** For any $\mathtt{Q} \in \mathcal{Q} \in \mathbb{M}_{\textsc{hb}}$, we define

$$\textsc{subdivide}(\mathtt{Q}) \coloneqq \big\{ \mathtt{Q}' \in \mathcal{Q}_{\mathsf{u}[\ell(\mathtt{Q})+1]} \mid \mathtt{Q}' \subset \mathtt{Q} \big\} \tag{3.6}$$

and for $\mathcal{M} \subset \mathcal{Q} \in \mathbb{M}_{\textsc{hb}}$, we denote the corresponding partial subdivision by

$$\textsc{subdivide}(\mathcal{Q}, \mathcal{M}) \coloneqq \mathcal{Q} \setminus \mathcal{M} \cup \bigcup_{\mathtt{Q} \in \mathcal{M}} \textsc{subdivide}(\mathtt{Q}). \tag{3.7}$$

Definition 3.1.4 (Level-k domain)**.** Given some mesh $\mathcal{Q} \in \mathbb{M}_{\textsc{hb}}$, and $k \in \mathbb{N}_0$, we denote by $\Omega_{\mathcal{Q},k}$ the domain that is covered by "level-k or finer" elements, $\Omega_{\mathcal{Q},k} \coloneqq \bigcup \big\{ \mathtt{Q} \in \mathcal{Q} \mid \ell(\mathtt{Q}) \geq k \big\}$. See Figure 3.2 for an example.

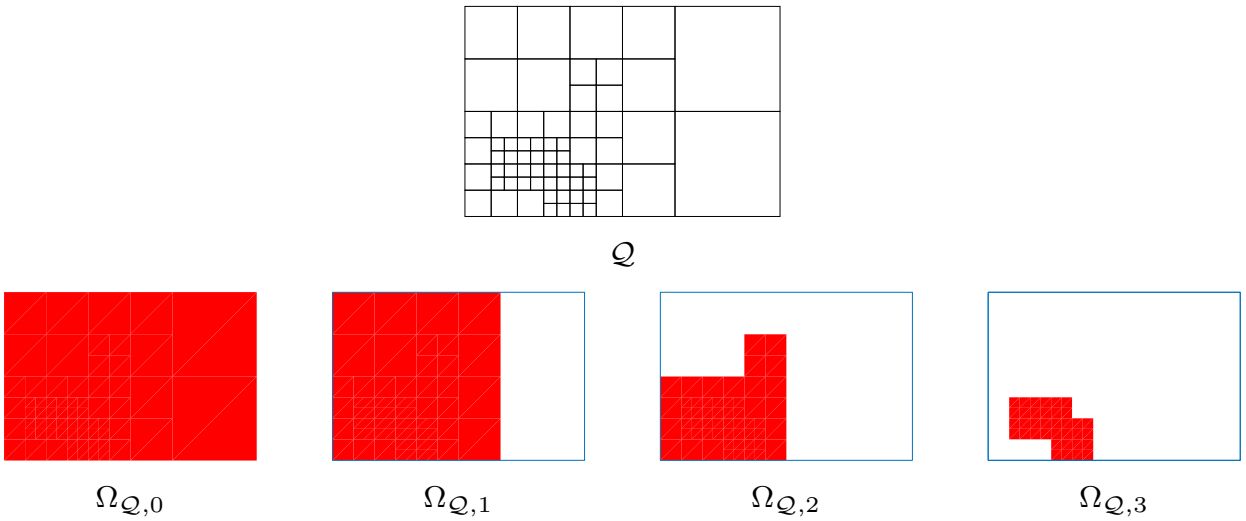

Figure 3.2 [41]: Example for level-k domains, for $k = 0, \dots, 3$. The domains $\Omega_{\mathcal{Q},0}, \dots, \Omega_{\mathcal{Q},3}$ are shaded in red.

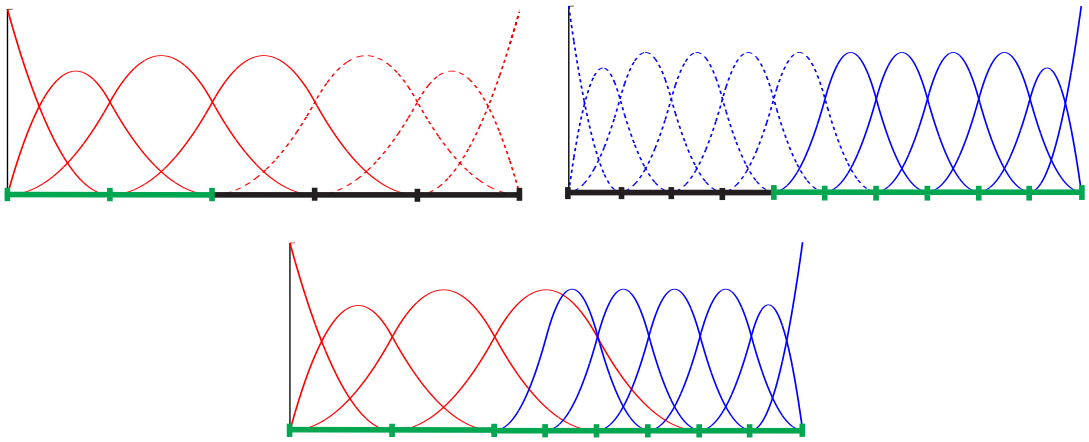

Figure 3.3 [52]: Level-1 (left) and Level-2 quadratic B-splines (right) for a one-dimensional mesh, and the hierarchical basis composed of B-splines of both levels (below).

Definition 3.1.5. The hierarchical B-spline (HB-spline) basis $\mathcal{B}_{\text{HB}}$ with respect to the mesh $\mathcal{Q}$ is defined as the set of all those B-splines whose support is entirely in the corresponding level-ℓ-domain, but not in a finer one,

$$\mathcal{B}_{\text{HB}}(\mathcal{Q}) \coloneqq \bigcup_{k \in \mathbb{N}_0} \{B \in \mathcal{B}_k \mid \operatorname{supp} B \subseteq \Omega_{\mathcal{Q},k} \wedge \operatorname{supp} B \nsubseteq \Omega_{\mathcal{Q},k+1}\}\,. \tag{3.8}$$

The refinement for HB-splines defined below is conceptionally similar to the refinement procedure described in [53] and [37]. It only differs in the construction of the neighbourhood $\mathcal{N}_{\text{HB}}$, where a different level is chosen for the B-splines whose supports are used in the construction. An example is given in Figure 3.5.

Definition 3.1.6 (Refinement for HB-Splines)**.** We define for each $Q \in \mathcal{Q}$ the *n-th ancestor* as the unique element of $\bigcup \mathbb{M}_{\text{UNIFORM}}$ which has the level $\ell(Q) - n$ and is a

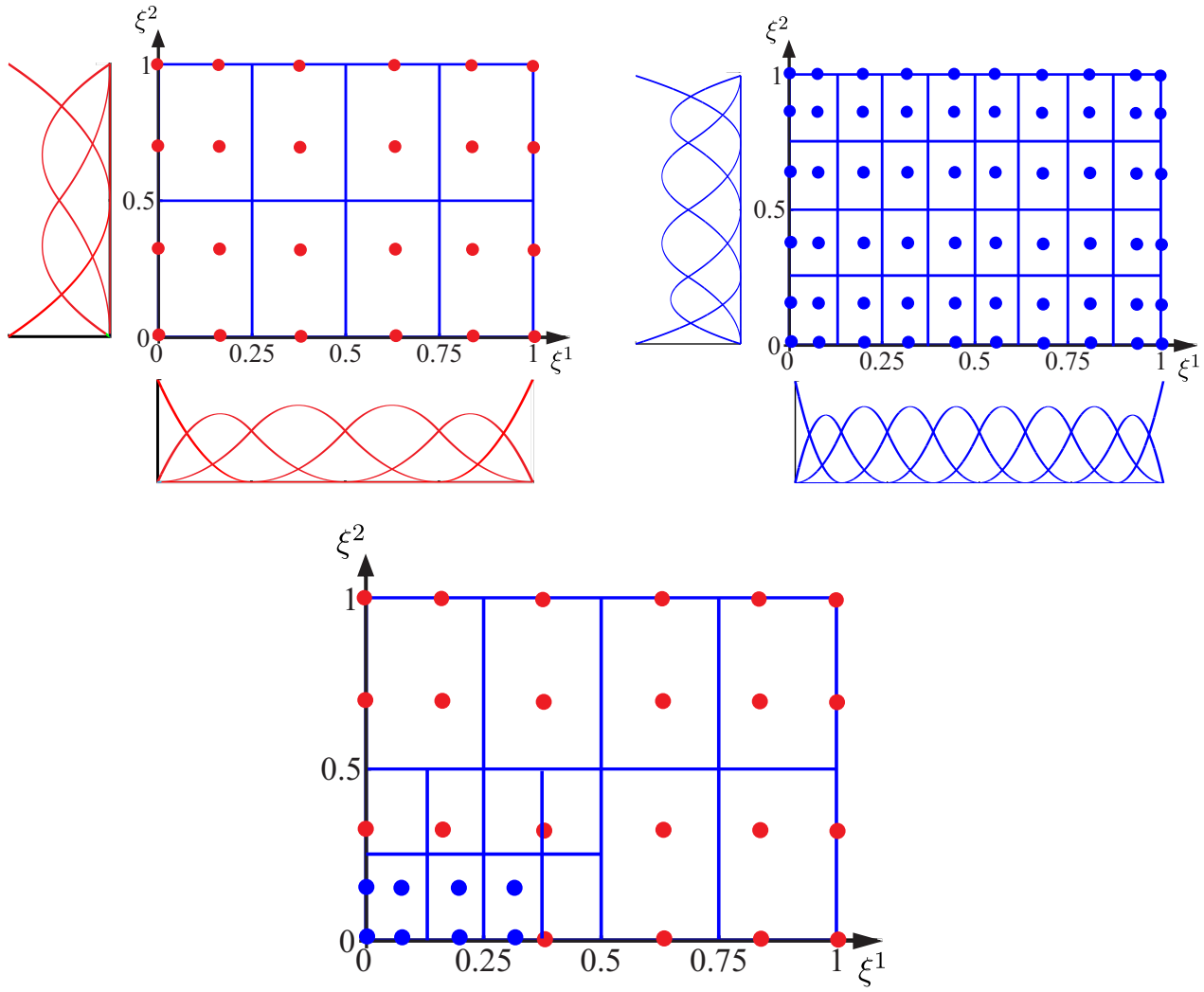

Figure 3.4 [52]: Level-1 (left) and Level-2 quadratic B-splines (right) for a two-dimensional mesh, visualised by dots at the Greville points (control points that induce the identity map, see e.g. [13]), and the hierarchical basis composed of B-splines of both levels (below).

superset of Q,

$$\operatorname{anc}^n(\mathsf{Q}) \coloneqq \mathsf{Q}' \in \mathcal{Q}_{\mathsf{u}[\ell(\mathsf{Q})-n]} \text{ such that } \mathsf{Q} \subset \mathsf{Q}' \tag{3.9}$$

If $\ell(\mathsf{Q}) < n$, we set $\operatorname{anc}^n(\mathsf{Q}) = \mathsf{Q}$. We further define the *support extension*

$$\mathcal{S}(\mathsf{Q}) \coloneqq \bigcup_{\substack{B \in \mathcal{B}_{\ell(\mathsf{Q})} \\ \mathsf{Q} \subset \operatorname{supp} B}} \operatorname{supp} B, \tag{3.10}$$

and the *coarse neighbourhood* consisting of elements with level $\ell(\mathsf{Q}) - m + 1$

$$\mathcal{N}_{\text{HB}}(\mathcal{Q}, \mathsf{Q}) \coloneqq \left\{ \mathsf{Q}' \in \mathcal{Q} \mid \ell(\mathsf{Q}') = \ell(\mathsf{Q}) - m + 1 \text{ and } \mathsf{Q}' \subset \mathcal{S}(\operatorname{anc}^{m-1}(\mathsf{Q})) \right\}, \tag{3.11}$$

with generalized notations $\mathcal{N}_{\text{HB}}(\mathcal{Q}, \mathcal{M}) \coloneqq \bigcup_{\mathsf{Q} \in \mathcal{M}} \mathcal{N}_{\text{HB}}(\mathcal{Q}, \mathsf{Q})$ and

$$\mathcal{N}^k_{\text{HB}}(\mathcal{Q}, \mathcal{M}) \coloneqq \underbrace{\mathcal{N}_{\text{HB}}(\mathcal{Q}, \dots \mathcal{N}_{\text{HB}}(\mathcal{Q}, \mathcal{M}) \dots)}_{k \text{ times}}. \tag{3.12}$$

We define the *closure*

$$\textsc{closure\_hb}(\mathcal{Q},\mathcal{M}) \coloneqq \bigcup_{k=0}^{\max \ell(\mathcal{M})} \mathcal{N}_{\mathrm{HB}}^{k}(\mathcal{Q},\mathcal{M}), \tag{3.13}$$

and the extended refinement procedure

$$\textsc{refine\_hb}(\mathcal{Q},\mathcal{M}) \coloneqq \textsc{subdivide}\big(\mathcal{Q}, \textsc{closure\_hb}(\mathcal{Q},\mathcal{M})\big). \tag{3.14}$$

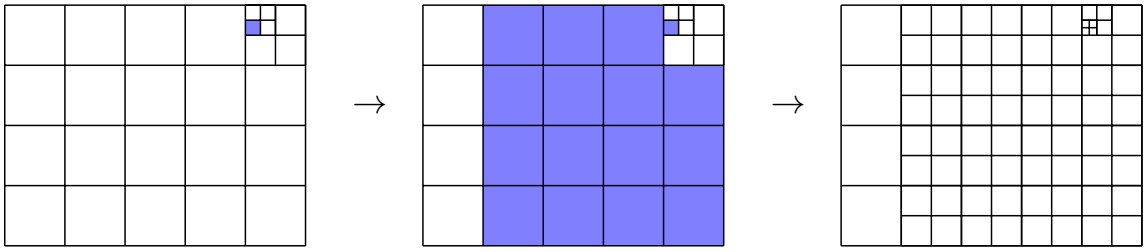

Figure 3.5: Example for the HB-spline refinement with $m = 3$. First, an element $Q \in \mathcal{Q}$ is marked (highlighted in blue), hence $\mathcal{M} = \{Q\}$. Second, $\textsc{closure\_hb}(\mathcal{Q},\mathcal{M})$ is computed (highlighted in blue). Third, all elements in $\textsc{closure\_hb}(\mathcal{Q},\mathcal{M})$ are subdivided.

3.1.3 Admissible meshes

We introduce below a class of quasi-uniform meshes, which we call *admissible* meshes. Considering the B-spline basis, an admissible mesh guarantees for an upper bound on the number of basis functions that take non-zero values on an arbitrary mesh element. This is crucial for the SOLVE step, as it guarantees the stiffness matrix A to have a bounded number of nonzero entries in each row and column. A matrix with that property is called *sparse*, and sparse linear equation systems can be solved with linear complexity. This restriction is therefore a fundamental ingredient for the theoretical analysis of adaptive isogeometric methods, see [53].

Definition 3.1.7. A mesh $\mathcal{Q} \in \mathbb{M}_{\mathrm{HB}}$ is called *admissible* if

$$\forall\, Q \in \mathcal{Q}: \quad \mathcal{S}(\mathrm{anc}^{m}(Q)) \subseteq \Omega_{\mathcal{Q},\ell(Q)-m+1}. \tag{3.15}$$

The above definition implies that any B-spline $B \in \mathcal{B}_k \cap \mathcal{B}_{\mathrm{HB}}(\mathcal{Q})$ with $Q \subset \operatorname{supp} B$ is by construction (see Definition 3.1.5) of a level k bounded by $\ell(Q)-m+1 \leq k \leq \ell(Q)$. Hence all functions from $\mathcal{B}_{\mathrm{HB}}(\mathcal{Q})$ that have support on Q are associated to at most m different levels $\ell(Q),\dots,\ell(Q)-m+1$. Note that the above-defined term "admissible" depends on m and the polynomial degree p of the B-splines. Since the case $m = 1$ refers to uniform meshes, we will from now on focus on the case $m \geq 2$.

Proposition 3.1.8. *The above-defined refinement routine* REFINE_HB *fulfills the following properties.*

(i) All meshes generated from $\mathcal{Q}_0 = \mathcal{Q}_{\mathrm{u}[0]}$ and (successive) application of REFINE_HB *are admissible.*

(ii) Any mesh $\mathcal{Q} \in \mathbb{M}_{\mathrm{HB}}$ which is admissible can be generated by $\mathcal{Q}_0$ and (successive) application of REFINE_HB*.*

3.1.4 Overlay

The *overlay* $\mathcal{Q}_*$ of two meshes $\mathcal{Q}_1, \mathcal{Q}_2$ is the mesh obtained as the coarsest common refinement of $\mathcal{Q}_1$ and $\mathcal{Q}_2$, usually denoted by

$$\mathcal{Q}_* = \mathcal{Q}_1 \otimes \mathcal{Q}_2 \tag{3.16}$$

and consist of elements from $\mathcal{Q}_1$ and $\mathcal{Q}_2$. Let $\{\Omega_{1,k}\}_{k=0,\dots,L_1}$ and $\{\Omega_{2,k}\}_{k=0,\dots,L_2}$ with $\Omega_{1,0} = \Omega_{2,0}$ be the nested sequences of domains that define the hierarchical meshes $\mathcal{Q}_1$ and $\mathcal{Q}_2$, respectively. The domain hierarchy $\{\Omega_{*,k}\}_{k=0,\dots,L_*}$, with $L_* = \max(L_1, L_2)$, associated to $\mathcal{Q}_*$ satisfies

$$\Omega_{*,k} = \Omega_{1,k} \cup \Omega_{2,k} \tag{3.17}$$

for $k = 1, \dots, L_*$, where $\Omega_{i,k} = \emptyset$ if $k \geq L_i$, for i=1,2. Using that $\mathcal{Q}_1$ and $\mathcal{Q}_2$ are admissible, we have for any element $\mathtt{Q} \in \mathcal{Q}_* \subset \mathcal{Q}_1 \cup \mathcal{Q}_2$ that

$$\mathcal{S}(\mathrm{anc}^m(\mathtt{Q})) \subseteq \Omega_{1,k} \cup \Omega_{2,k} = \Omega_{*,k}. \tag{3.18}$$

Hence, the overlay $\mathcal{Q}_*$ of two admissible meshes is an admissible mesh and can be generated by REFINE_HB.

Lemma 3.1.9. *The number of elements of the overlay $\mathcal{Q}_* = \mathcal{Q}_1 \otimes \mathcal{Q}_2$ is bounded by*

$$\#\mathcal{Q}_* = \#(\mathcal{Q}_1 \otimes \mathcal{Q}_2) \leq \#\mathcal{Q}_1 + \#\mathcal{Q}_2 - \#\mathcal{Q}_0. \tag{3.19}$$

Proof. We proceed as in [38]. The overlay is a subset of the union of the two involved meshes, i.e.,

$$\mathcal{Q}_1 \otimes \mathcal{Q}_2 \;=\; \mathrm{Min}_{\subseteq}(\mathcal{Q}_1 \cup \mathcal{Q}_2) \;\subseteq\; \mathcal{Q}_1 \cup \mathcal{Q}_2 \;. \tag{3.20}$$

Define the shorthand notation $\mathcal{Q}(\mathtt{Q}) \coloneqq \{\mathtt{Q}' \in \mathcal{Q} \mid \mathtt{Q}' \subseteq \mathtt{Q}\}$. To prove the lemma, it suffices to show

$$\forall\, \mathtt{Q} \in \mathcal{Q}_0, \quad \#(\mathcal{Q}_1 \otimes \mathcal{Q}_2)(\mathtt{Q}) + 1 \leq \#\mathcal{Q}_1(\mathtt{Q}) + \#\mathcal{Q}_2(\mathtt{Q}) \;. \tag{3.21}$$

Case 1. $\mathcal{Q}_1(\mathtt{Q}) \subseteq (\mathcal{Q}_1 \otimes \mathcal{Q}_2)(\mathtt{Q})$. This implies equality and hence

$$\#(\mathcal{Q}_1 \otimes \mathcal{Q}_2)(\mathtt{Q}) + 1 = \#\mathcal{Q}_1(\mathtt{Q}) + 1 \leq \#\mathcal{Q}_1(\mathtt{Q}) + \#\mathcal{Q}_2(\mathtt{Q}) \;. \tag{3.22}$$

Case 2. There exists $\mathtt{Q}' \in \mathcal{Q}_1(\mathtt{Q}) \setminus (\mathcal{Q}_1 \otimes \mathcal{Q}_2)(\mathtt{Q})$. Then $(\mathcal{Q}_1 \otimes \mathcal{Q}_2)(\mathtt{Q}) = (\mathcal{Q}_1 \otimes \mathcal{Q}_2)(\mathtt{Q}) \setminus \{\mathtt{Q}'\}$ and hence

$$\begin{aligned}[b]\#(\mathcal{Q}_1 \otimes \mathcal{Q}_2)(\mathtt{Q}) \;&=\; \#\left((\mathcal{Q}_1 \otimes \mathcal{Q}_2)(\mathtt{Q}) \setminus \{\mathtt{Q}'\}\right) \overset{(3.20)}{\leq} \#\left((\mathcal{Q}_1 \cup \mathcal{Q}_2)(\mathtt{Q}) \setminus \{\mathtt{Q}'\}\right) \\ &\leq\; \#(\mathcal{Q}_1 \setminus \{\mathtt{Q}\}) + \#\mathcal{Q}_2(\mathtt{Q}) \;=\; \#\mathcal{Q}_1(\mathtt{Q}) - 1 + \#\mathcal{Q}_2(\mathtt{Q}).\end{aligned} \tag{3.23}$$

□

Analogously to the adaptive finite element setting, the above inequality may be used for discussing the rate optimality of the resulting adaptive isogeometric method see e.g. [10, Equation 2.10].

3.1.5 Linear Complexity

This section is devoted to a complexity estimate in the style of a famous estimate for the Newest Vertex Bisection on triangular meshes given by Binev, Dahmen and DeVore [7] and, in an alternative version, by Stevenson [8]. Linear Complexity of the refinement procedure is an inevitable criterion for optimal convergence rates in the Adaptive Finite Element Method (see e.g. [7, 8, 10] and [53, Conclusions]). The estimate and its proof follow our own work [37].

Auxilliary results

Lemma 3.1.10. *For every pair of mesh elements $(\mathtt{Q}, \mathtt{Q}')$, let $\operatorname{dist}(\mathtt{Q}, \mathtt{Q}')$ be the Euclidean distance of their midpoints. Given a $\mathtt{Q} \in \mathcal{Q}$, all $\mathtt{Q}' \in \mathcal{N}_{\text{HB}}(\mathcal{Q}, \mathtt{Q})$ satisfy*

$$\operatorname{dist}(\mathtt{Q}, \mathtt{Q}') \leq 2^{-\ell(\mathtt{Q}')}\, C_{3.1.10} \quad \textit{with} \quad C_{3.1.10} \coloneqq \sqrt{2}\,\big(p + \tfrac{1}{2}\big). \tag{3.24}$$

Proof. The definition of $\mathcal{N}_{\text{HB}}(\mathcal{Q}, \mathtt{Q})$ yields that $\ell(\mathtt{Q}') = \ell(\mathtt{Q}) - m + 1 = \ell(\operatorname{anc}^{m-1}(\mathtt{Q}))$ and $\mathtt{Q}' \subset \mathcal{S}(\operatorname{anc}^{m-1}(\mathtt{Q}))$. The support extension $\mathcal{S}(\operatorname{anc}^{m-1}(\mathtt{Q}))$ is defined via B-splines on the level $\ell(\operatorname{anc}^{m-1}(\mathtt{Q})) = \ell(\mathtt{Q}')$. Hence, there is a B-spline $B \in \mathcal{B}_{\ell(\mathtt{Q}')}$ such that $\mathtt{Q}' \subset \operatorname{supp} B \supset \operatorname{anc}^{m-1}(\mathtt{Q}) \supset \mathtt{Q}$. Consequently, the distance between the midpoints of $\mathtt{Q}'$ and $\mathtt{Q}$ is bounded by

$$\begin{aligned}[b] \operatorname{dist}(\mathtt{Q}, \mathtt{Q}') &\leq \operatorname{diam}(\operatorname{supp} B) - \tfrac{1}{2}\operatorname{diam}(\mathtt{Q}') \\ &= 2^{1/2-\ell(\mathtt{Q}')}(p+1) - \tfrac{1}{2}\,2^{1/2-\ell(\mathtt{Q}')} = 2^{1/2-\ell(\mathtt{Q}')}\big(p + \tfrac{1}{2}\big), \end{aligned} \tag{3.25}$$

which concludes the proof. □

Lemma 3.1.11. *Let $\mathcal{Q}$ be an admissible mesh, $\mathcal{M} \subset \mathcal{Q}$ the set of elements marked for refinement, and $\hat{\mathcal{Q}} = \text{REFINE\_HB}(\mathcal{Q}, \mathcal{M})$. For any newly created $\mathtt{Q} \in \hat{\mathcal{Q}} \setminus \mathcal{Q}$, there exists a marked element $\mathtt{Q}' \in \mathcal{M}$ such that*

$$\operatorname{dist}(\mathtt{Q}, \mathtt{Q}') \leq 2^{-\ell(\mathtt{Q})} C_{3.1.11} \quad \textit{and} \quad \ell(\mathtt{Q}) \leq \ell(\mathtt{Q}') + 1, \tag{3.26}$$

where $C_{3.1.11} \coloneqq \frac{2}{1-2^{1-m}} C_{3.1.10} + 2^{-1/2}$.

Proof. The existence of $\mathtt{Q} \in \hat{\mathcal{Q}} \setminus \mathcal{Q}$ means that $\text{CLOSURE\_HB}(\mathcal{Q}, \mathcal{M})$ contains a sequence of elements $\mathtt{Q}' = \mathtt{Q}_J, \mathtt{Q}_{J-1}, \dots, \mathtt{Q}_0$ such that $\mathtt{Q}_{j-1} \in \mathcal{N}_{\text{HB}}(\mathcal{Q}, \mathtt{Q}_j)$, with $\mathtt{Q}' \in \mathcal{M}$ and $\mathtt{Q}$ being a child of $\mathtt{Q}_0$, namely $\ell(\mathtt{Q}) = \ell(\mathtt{Q}_0) + 1$. Since $\ell(\mathtt{Q}_{j-1}) = \ell(\mathtt{Q}_j) - m + 1$, it follows

$$\ell(\mathtt{Q}_j) = \ell(\mathtt{Q}_0) + j\,(m-1). \tag{3.27}$$

We have

$$\operatorname{dist}(\mathtt{Q}, \mathtt{Q}') \leq \operatorname{dist}(\mathtt{Q}, \mathtt{Q}_0) + \operatorname{dist}(\mathtt{Q}_0, \mathtt{Q}') \tag{3.28}$$

and

$$\operatorname{dist}(\mathtt{Q}, \mathtt{Q}_0) = \tfrac{1}{2}\operatorname{diam}(\mathtt{Q}) = 2^{-\ell(\mathtt{Q})-1/2}, \qquad \operatorname{dist}(\mathtt{Q}_0, \mathtt{Q}') \leq \sum_{j=0}^{J-1} \operatorname{dist}(\mathtt{Q}_{j+1}, \mathtt{Q}_j). \tag{3.29}$$

According to Lemma 3.1.10, we obtain

$$[b]\sum_{j=0}^{J-1}\operatorname{dist}(\mathtt{Q}_{j+1},\mathtt{Q}_j)\leq\sum_{j=0}^{J-1}2^{-\ell(\mathtt{Q}_j)}C_{3.1.10}\overset{(3.27)}{=}\sum_{j=0}^{J-1}2^{-\ell(\mathtt{Q}_0)-j(m-1)}C_{3.1.10}$$
$$<2^{-\ell(\mathtt{Q}_0)}C_{3.1.10}\sum_{j=0}^{\infty}2^{(1-m)\cdot j}=\frac{2^{-\ell(\mathtt{Q}_0)}C_{3.1.10}}{1-2^{1-m}}=\frac{2^{-\ell(\mathtt{Q})+1}C_{3.1.10}}{1-2^{1-m}}. \tag{3.30}$$

The combination with (3.28) and (3.29) proves the distance estimate. The application of (3.27) to the case $j=J\geq 0$, together with $\ell(\mathtt{Q})=\ell(\mathtt{Q}_0)+1$ from above, yields

$$\ell(\mathtt{Q})=\ell(\mathtt{Q}')-J\,(m-1)+1\leq\ell(\mathtt{Q}')+1, \tag{3.31}$$

which concludes the proof. □

Main result

The main result of this paper states the existence of a generic constant $C_{3.1.12}=C_{3.1.12}(p,m)<\infty$ that bounds the ratio between the number of new elements in the final mesh $\mathcal{Q}_J$ and the number of all marked elements encountered in the sequence of successive refinements from $\mathcal{Q}_0$ to $\mathcal{Q}_J$.

Theorem 3.1.12 (Complexity of REFINE_HB)**.** *Let $\mathcal{M}\coloneqq\bigcup_{j=0}^{J-1}\mathcal{M}_j$ be the set of marked elements used to generate the sequence of admissible meshes $\mathcal{Q}_0,\mathcal{Q}_1,\dots,\mathcal{Q}_J$ starting from $\mathcal{Q}_0$, namely*

$$\mathcal{Q}_j=\text{REFINE\_HB}(\mathcal{Q}_{j-1},\mathcal{M}_{j-1}),\quad \mathcal{M}_{j-1}\subseteq\mathcal{Q}_{j-1}\quad \textit{for } j\in\{1,\dots,J\}\,. \tag{3.32}$$

Then, there exists a positive constant $C_{3.1.12}$ such that

$$\#\mathcal{Q}_J-\#\mathcal{Q}_0\leq\ C_{3.1.12}\,\#\mathcal{M}. \tag{3.33}$$

Proof. Recall that $\bigcup\mathbb{M}_{\text{UNIFORM}}$ represents the set of the initial mesh elements and all elements that can be generated from their successive dyadic subdivision. For any $\mathtt{Q}\in\bigcup\mathbb{M}_{\text{UNIFORM}}$ and $\mathtt{Q}'\in\mathcal{M}$, let

$$\lambda(\mathtt{Q},\mathtt{Q}')\coloneqq\begin{cases}2^{\ell(\mathtt{Q})-\ell(\mathtt{Q}')} & \text{if } \ell(\mathtt{Q})\leq\ell(\mathtt{Q}')+1 \text{ and } \operatorname{dist}(\mathtt{Q},\mathtt{Q}')<2^{1-\ell(\mathtt{Q})}\,C_{3.1.11},\\ 0 & \text{otherwise.}\end{cases} \tag{3.34}$$

The proof consists of two main steps devoted to identify

(i) a lower bound for the sum of the λ function as $\mathtt{Q}'$ varies in $\mathcal{M}$ so that each $\mathtt{Q}\in\mathcal{Q}_J\setminus\mathcal{Q}_0$ satisfies

$$\sum_{\mathtt{Q}'\in\mathcal{M}}\lambda(\mathtt{Q},\mathtt{Q}')\ \geq\ 1\,; \tag{3.35}$$

(ii) an upper bound for the sum of the λ function as the refined element $\mathtt{Q}$ varies in $\mathcal{Q}_J\setminus\mathcal{Q}_0$ so that, for any $j=0,\dots,J-1$, each $\mathtt{Q}'\in\mathcal{M}_j$ satisfies

$$\sum_{\mathtt{Q}\in\mathcal{Q}_J\setminus\mathcal{Q}_0}\lambda(\mathtt{Q},\mathtt{Q}')\ \leq C_{3.1.12}\,. \tag{3.36}$$

If inequalities (3.35) and (3.36) hold for a certain constant $C_{3.1.12}$, we have

$$[b]\#\mathcal{Q}_J - \#\mathcal{Q}_0 \leq \#(\mathcal{Q}_J \setminus \mathcal{Q}_0) = \sum_{Q \in \mathcal{Q}_J \setminus \mathcal{Q}_0} 1$$
$$\leq \sum_{Q \in \mathcal{Q}_J \setminus \mathcal{Q}_0} \sum_{Q' \in \mathcal{M}} \lambda(Q, Q') \leq \sum_{Q' \in \mathcal{M}} C_{3.1.12} = C_{3.1.12}\, \#\mathcal{M}, \qquad (3.37)$$

and the proof of the theorem is complete. We detail below the proofs of (i) and (ii).

(i) Let $Q \in \mathcal{Q}_J \setminus \mathcal{Q}_0$ be an element generated in the refinement process from $\mathcal{Q}_0$ to $\mathcal{Q}_J$, and let $j_1 < J$ be the unique index such that $Q \in \mathcal{Q}_{j_1+1} \setminus \mathcal{Q}_{j_1}$. Lemma 3.1.11 states the existence of $Q_1 \in \mathcal{M}_{j_1}$ with

$$\operatorname{dist}(Q, Q_1) \leq 2^{-\ell(Q)}\, C_{3.1.11} \quad \text{and} \quad \ell(Q) \leq \ell(Q_1) + 1\,, \qquad (3.38)$$

and, consequently $\lambda(Q, Q_1) = 2^{\ell(Q)-\ell(Q_1)} > 0$. The repeated use of Lemma 3.1.11 yields a sequence $\{Q_2, Q_3, \dots\}$ with $Q_{i-1} \in \mathcal{Q}_{j_i+1} \setminus \mathcal{Q}_{j_i}$, for $j_1 > j_2 > j_3 > \dots$, and $Q_i \in \mathcal{M}_{j_i}$ such that

$$\operatorname{dist}(Q_{i-1}, Q_i) \leq 2^{-\ell(Q_{i-1})}\, C_{3.1.11} \quad \text{and} \quad \ell(Q_{i-1}) \leq \ell(Q_i) + 1. \qquad (3.39)$$

We iteratively apply Lemma 3.1.11 as long as

$$\lambda(Q, Q_i) > 0 \quad \text{and} \quad \ell(Q_i) > 0\,, \qquad (3.40)$$

until we reach the first index L with $\lambda(Q, Q_L) = 0$ or $\ell(Q_L) = 0$. By considering the three possible cases below, inequality (3.35) may be derived as follows.

- If $\ell(Q_L) = 0$ and $\lambda(Q, Q_L) > 0$, then

$$\sum_{Q' \in \mathcal{M}} \lambda(Q, Q') \geq \lambda(Q, Q_L) = 2^{\ell(Q)-\ell(Q_L)} > 1\,, \qquad (3.41)$$

  since $\ell(Q) > \ell(Q_L) = 0$.

- If $\lambda(Q, Q_L) = 0$ because $\ell(Q) > \ell(Q_L) + 1$, then (3.39) yields $\ell(Q_{L-1}) \leq \ell(Q_L) + 1 < \ell(Q)$ and hence

$$\sum_{Q' \in \mathcal{M}} \lambda(Q, Q') \geq \lambda(Q, Q_{L-1}) = 2^{\ell(Q)-\ell(Q_{L-1})} > 1. \qquad (3.42)$$

- If $\lambda(Q, Q_L) = 0$ because $\operatorname{dist}(Q, Q_L) \geq 2^{1-\ell(Q)}\, C_{3.1.11}$, then a triangle inequality combined with Lemma 3.1.11 leads to

$$[b]2^{1-\ell(Q)}\, C_{3.1.11} \leq \operatorname{dist}(Q, Q_1) + \sum_{i=1}^{L-1} \operatorname{dist}(Q_i, Q_{i+1})$$
$$\leq 2^{-\ell(Q)}\, C_{3.1.11} + \sum_{i=1}^{L-1} 2^{-\ell(Q_i)}\, C_{3.1.11}\,. \qquad (3.43)$$

Consequently, $2^{-\ell(\mathsf{Q})} \leq \sum_{i=1}^{L-1} 2^{-\ell(\mathsf{Q}_i)}$, and we obtain

$$1 \;\leq\; \sum_{i=1}^{L-1} 2^{\ell(\mathsf{Q})-\ell(\mathsf{Q}_i)} \;=\; \sum_{i=1}^{L-1} \lambda(\mathsf{Q},\mathsf{Q}_i) \;\leq\; \sum_{\mathsf{Q}'\in\mathcal{M}} \lambda(\mathsf{Q},\mathsf{Q}'). \tag{3.44}$$

(ii) Inequality (3.36) can be derived as follows. For any $0 \leq j \leq J-1$, we consider the set of elements of level j whose distance from Q' is less than $2^{1-j}C_{3.1.11}$, defined as

$$A(\mathsf{Q}',j) \coloneqq \left\{\mathsf{Q} \in \mathcal{Q}_{\mathsf{u}[j]} \mid \operatorname{dist}(\mathsf{Q},\mathsf{Q}') < 2^{1-j}C_{3.1.11}\right\}. \tag{3.45}$$

According to the definition of λ, the set $A(\mathsf{Q}',j)$ contains all elements at level j that satisfy $\lambda(\mathsf{Q},\mathsf{Q}') > 0$. We have

$$[b] \sum_{\mathsf{Q}\in\mathcal{Q}_J\setminus\mathcal{Q}_0} \lambda(\mathsf{Q},\mathsf{Q}') \leq \sum_{\mathsf{Q}\in\bigcup\mathbb{M}_{\text{UNIFORM}}\setminus\mathcal{Q}_0} \lambda(\mathsf{Q},\mathsf{Q}') = \sum_{j=1}^{\ell(\mathsf{Q}')+1} 2^{j-\ell(\mathsf{Q}')}\,\#A(\mathsf{Q}',j). \tag{3.46}$$

Since the diameter of an element Q of level j is $2^{1/2-j}$, the diameter of the domain composed by the union of all elements in $A(\mathsf{Q}',j)$ is bounded by

$$\operatorname{diam}(A(\mathsf{Q}',j)) \leq 2\cdot 2^{1-j}C_{3.1.11} + 2^{1/2-j}, \tag{3.47}$$

and hence the volume of that domain is bounded from above by

$$\left|\bigcup A(\mathsf{Q}',j)\right| \leq \tfrac{\pi}{4}\left(2^{2-j}C_{3.1.11} + 2^{1/2-j}\right)^2. \tag{3.48}$$

Since the volume of each element in $A(\mathsf{Q}',j)$ is 2^{-2j}, the number of elements in $A(\mathsf{Q}',j)$ can be bounded by

$$\begin{aligned}\#A(\mathsf{Q}',j) &\leq 2^{2j}\left|\bigcup A(\mathsf{Q}',j)\right| \\ &\leq 2^{2j}\,\tfrac{\pi}{4}\left(2^{4-2j}C_{3.1.11}^2 + 2^{1-2j}\right) = \pi\left(4C_{3.1.11}^2 + \tfrac{1}{2}\right).\end{aligned} \tag{3.49}$$

Finally, the index substitution $k \coloneqq 1 - j + \ell(\mathsf{Q}')$ reduces (3.46) to

$$\begin{aligned}\sum_{\mathsf{Q}\in\mathcal{Q}_J\setminus\mathcal{Q}_0} \lambda(\mathsf{Q},\mathsf{Q}') &\leq \sum_{j=1}^{\ell(\mathsf{Q}')+1} 2^{j-\ell(\mathsf{Q}')}\#A(\mathsf{Q}',j) = \sum_{k=0}^{\ell(\mathsf{Q}')} 2^{1-k}\#A(\mathsf{Q}',j) \\ &< 2\sum_{k=0}^{\infty} 2^{-k}\#A(\mathsf{Q}',j) = 4\,\#A(\mathsf{Q}',j) \leq C_{3.1.12}\,,\end{aligned} \tag{3.50}$$

with $C_{3.1.12} = 4\pi\left(4C_{3.1.11}^2 + \frac{1}{2}\right)$. □

3.2 Local q-adic refinement in nD

Definition 3.2.1. Given $q, N_1, N_2, \dots, N_d \in \mathbb{N}$, we generalize the preceeding section as follows. We still assume the *initial mesh* $\mathcal{Q}_0$ to be a tensor product mesh, and its elements are closed hypercubes with side length 1 (regard Figure 3.1 as a 2D example with $q = 2$),

$$\mathcal{Q}_0 \coloneqq \Big\{ [n_1 - 1, n_1] \times \cdots \times [n_d - 1, n_d] \mid n_1 \in \{1, \dots, N_1\}, \dots, n_d \in \{1, \dots, N_d\} \Big\}. \tag{3.51}$$

The corresponding spline basis $\mathcal{B}_0$ is spanned by the corresponding tensor-product B-splines. For each level $k \in \mathbb{N}_0$, we define the tensor-product mesh

$$\mathcal{Q}_k \coloneqq \Big\{ [x_1 - q^{-k}, x_1] \times \cdots \times [x_d - q^{-k}, x_d] \mid q^k x_1 \in \{1, \dots, q^k N_1\}, \dots, q^k x_d \in \{1, \dots, q^k N_d\} \Big\} \tag{3.52}$$

and the corresponding spline space $\mathcal{B}_k$ of tensor-product B-spline basis functions of degree $\mathbf{p} = (p_1, \dots, p_d)$, i.e., the polynomial degree of the univariate B-splines that are used for constructing the multivariate B-splines may differ between the dimensions.

The uniform refinement, the class $\mathbb{M}_{\text{UNIFORM}}$, and element levels are defined exactly as in Definitions 3.1.1 and 3.1.2. For the use of HB-splines with these generalized meshes, the underlying rectangular mesh $\mathcal{Q}$ may, as before, consist of finitely many elements from meshes in $\mathbb{M}_{\text{UNIFORM}}$, such that any two elements of $\mathcal{Q}$ have disjoint interior, and the union of all elements of $\mathcal{Q}$ is the same domain $[0, N_1] \times \cdots \times [0, N_d]$ that is covered by uniform meshes.

$$\mathbb{M}_{\text{HB}} \coloneqq \Big\{ \mathcal{Q} \subset \textstyle\bigcup_{\mathcal{Q}' \in \mathbb{M}_{\text{UNIFORM}}} \mathcal{Q}' \mid \#\mathcal{Q} < \infty,\ \bigcup \mathcal{Q} = [0, N_1] \times \cdots \times [0, N_d], \ \forall \mathtt{Q}, \mathtt{Q}' \in \mathcal{Q} :\ \operatorname{int}(\mathtt{Q}) \cap \operatorname{int}(\mathtt{Q}') = \emptyset \Big\}. \tag{3.53}$$

The Definitions 3.1.3 to 3.1.7 apply analogously to this setting, in particular the definition of the refinement routine, the class of admissible meshes, and the overlay, including the stated results.

We rewrite below Subsection 3.1.5, accounting for the above generalizations.

Definition 3.2.2. We define the distance between two mesh elements as the componentwise distance of their midpoints,

$$\operatorname{Dist}(\mathtt{Q}, \mathtt{Q}') = \operatorname{abs}\big(\operatorname{mid}(\mathtt{Q}) - \operatorname{mid}(\mathtt{Q}')\big) \in \mathbb{R}^d. \tag{3.54}$$

Lemma 3.2.3. *For every pair of mesh elements $(\mathtt{Q}, \mathtt{Q}')$, let $\operatorname{Dist}(\mathtt{Q}, \mathtt{Q}')$ be the Euclidean distance of their midpoints. Given a $\mathtt{Q} \in \mathcal{Q}$, all $\mathtt{Q}' \in \mathcal{N}_{\text{HB}}(\mathcal{Q}, \mathtt{Q})$ satisfy*

$$\operatorname{Dist}(\mathtt{Q}, \mathtt{Q}') \leq q^{-\ell(\mathtt{Q}')}\, C_{3.2.3} \tag{3.55}$$

with $C_{3.2.3} \coloneqq \mathbf{p} + \frac{1}{2} \in \mathbb{R}^d$, and "$\mathbf{p} + \frac{1}{2}$" indicating an increment of $\mathbf{p}$ by $\frac{1}{2}$ in each component.

Proof. The definition of $\mathcal{N}_{\text{HB}}(\mathcal{Q}, \mathtt{Q})$ yields that $\ell(\mathtt{Q}') = \ell(\mathtt{Q}) - m + 1 = \ell(\text{anc}^{m-1}(\mathtt{Q}))$ and $\mathtt{Q}' \subset \mathcal{S}(\text{anc}^{m-1}(\mathtt{Q}))$. The support extension $\mathcal{S}(\text{anc}^{m-1}(\mathtt{Q}))$ is defined via B-splines on the level $\ell(\text{anc}^{m-1}(\mathtt{Q})) = \ell(\mathtt{Q}')$. Hence, there is a B-spline $B \in \mathcal{B}_{\ell(\mathtt{Q}')}$ such that $\mathtt{Q}' \subset$ and $\mathtt{Q} \subset \text{anc}^{m-1}(\mathtt{Q}) \subset \operatorname{supp} B$. Using the notation $\mathbf{1} \coloneqq (1, \dots, 1) \in \mathbb{R}^d$ and

$$\operatorname{size}\big([a_1, b_1] \times \cdots \times [a_d, b_d]\big) \coloneqq \big(b_1 - a_1, \dots, b_d - a_d\big) \quad \in \mathbb{R}^d, \tag{3.56}$$

the distance between the midpoints of $\mathtt{Q}'$ and $\mathtt{Q}$ is bounded by

$$\begin{aligned} \operatorname{Dist}(\mathtt{Q}, \mathtt{Q}') &\leq \operatorname{size}(\operatorname{supp} B) - \tfrac{1}{2} \operatorname{size}(\mathtt{Q}') \\ &= q^{-\ell(\mathtt{Q}')}(\mathbf{p} + \mathbf{1}) - \tfrac{1}{2}\, q^{-\ell(\mathtt{Q}')}\mathbf{1} = q^{-\ell(\mathtt{Q}')}\big(\mathbf{p} + \tfrac{1}{2}\mathbf{1}\big), \end{aligned} \tag{3.57}$$

which concludes the proof. □

Lemma 3.2.4. *Let $\mathcal{Q}$ be an admissible mesh, $\mathcal{M} \subset \mathcal{Q}$ the set of elements marked for refinement, and $\hat{\mathcal{Q}} = \text{REFINE\_HB}(\mathcal{Q}, \mathcal{M})$. For any newly created $\mathtt{Q} \in \hat{\mathcal{Q}} \setminus \mathcal{Q}$, there exists a marked element $\mathtt{Q}' \in \mathcal{M}$ such that*

$$\operatorname{Dist}(\mathtt{Q}, \mathtt{Q}') \leq q^{-\ell(\mathtt{Q})} C_{3.2.4} \quad \textit{and} \quad \ell(\mathtt{Q}) \leq \ell(\mathtt{Q}') + 1, \tag{3.58}$$

where $C_{3.2.4} \coloneqq \frac{q}{1-q^{1-m}} C_{3.2.3} + \frac{q}{2}\mathbf{1}$.

Proof. The existence of $\mathtt{Q} \in \hat{\mathcal{Q}} \setminus \mathcal{Q}$ means that $\text{CLOSURE\_HB}(\mathcal{Q}, \mathcal{M})$ contains a sequence of elements $\mathtt{Q}' = \mathtt{Q}_J, \mathtt{Q}_{J-1}, \dots, \mathtt{Q}_0$ such that $\mathtt{Q}_{j-1} \in \mathcal{N}_{\text{HB}}(\mathcal{Q}, \mathtt{Q}_j)$, with $\mathtt{Q}' \in \mathcal{M}$ and $\mathtt{Q}$ being a child of $\mathtt{Q}_0$, namely $\ell(\mathtt{Q}) = \ell(\mathtt{Q}_0) + 1$. Since $\ell(\mathtt{Q}_{j-1}) = \ell(\mathtt{Q}_j) - m + 1$, it follows

$$\ell(\mathtt{Q}_j) = \ell(\mathtt{Q}_0) + j\,(m-1). \tag{3.59}$$

We have

$$\operatorname{Dist}(\mathtt{Q}, \mathtt{Q}') \leq \operatorname{Dist}(\mathtt{Q}, \mathtt{Q}_0) + \operatorname{Dist}(\mathtt{Q}_0, \mathtt{Q}') \tag{3.60}$$

and

$$\operatorname{Dist}(\mathtt{Q}, \mathtt{Q}_0) \leq \tfrac{1}{2} \operatorname{size}(\mathtt{Q}_0) = \tfrac{1}{2}\, q^{-\ell(\mathtt{Q}_0)}\mathbf{1}, \tag{3.61}$$

$$\operatorname{Dist}(\mathtt{Q}_0, \mathtt{Q}') \leq \sum_{j=0}^{J-1} \operatorname{Dist}(\mathtt{Q}_{j+1}, \mathtt{Q}_j). \tag{3.62}$$

According to Lemma 3.2.3, we obtain

$$\begin{aligned} \sum_{j=0}^{J-1} \operatorname{Dist}(\mathtt{Q}_{j+1}, \mathtt{Q}_j) &\leq \sum_{j=0}^{J-1} q^{-\ell(\mathtt{Q}_j)} C_{3.2.3} \overset{(3.59)}{=} \sum_{j=0}^{J-1} q^{-\ell(\mathtt{Q}_0) - j(m-1)} C_{3.2.3} \\ &< q^{-\ell(\mathtt{Q}_0)} C_{3.2.3} \sum_{j=0}^{\infty} q^{(1-m)\cdot j} = \frac{q^{-\ell(\mathtt{Q}_0)} C_{3.2.3}}{1 - q^{1-m}} = \frac{q^{-\ell(\mathtt{Q})+1} C_{3.2.3}}{1 - q^{1-m}}. \end{aligned} \tag{3.63}$$

The combination with (3.60), (3.61) and (3.62) proves the distance estimate. The application of (3.59) to the case $j = J \geq 0$, together with $\ell(\mathtt{Q}) = \ell(\mathtt{Q}_0) + 1$ from above, yields

$$\ell(\mathtt{Q}) = \ell(\mathtt{Q}') - J\,(m-1) + 1 \leq \ell(\mathtt{Q}') + 1, \tag{3.64}$$

which concludes the proof. □

Theorem 3.2.5 (Complexity of REFINE_HB)**.** *Let $\mathcal{M} \coloneqq \bigcup_{j=0}^{J-1} \mathcal{M}_j$ be the set of marked elements used to generate the sequence of admissible meshes $\mathcal{Q}_0, \mathcal{Q}_1, \dots, \mathcal{Q}_J$ starting from $\mathcal{Q}_0$, namely*

$$\mathcal{Q}_j = \text{REFINE\_HB}(\mathcal{Q}_{j-1}, \mathcal{M}_{j-1}), \quad \mathcal{M}_{j-1} \subseteq \mathcal{Q}_{j-1} \quad \text{for } j \in \{1, \dots, J\}. \tag{3.65}$$

Then, there exists a positive constant $C_{3.2.5}$ such that

$$\#\mathcal{Q}_J - \#\mathcal{Q}_0 \leq C_{3.2.5}\, \#\mathcal{M}. \tag{3.66}$$

Proof. We redefine the function

$$\lambda(\mathtt{Q}, \mathtt{Q}') \coloneqq \begin{cases} q^{\ell(\mathtt{Q})-\ell(\mathtt{Q}')} & \text{if } \ell(\mathtt{Q}) \leq \ell(\mathtt{Q}') + 1 \text{ and } \operatorname{Dist}(\mathtt{Q}, \mathtt{Q}') < 2\, q^{-\ell(\mathtt{Q})}\, C_{3.2.4}, \\ 0 & \text{otherwise} \end{cases} \tag{3.67}$$

and rewrite the proof parts (i) and (ii) from Theorem 3.2.5.

(i) Let $\mathtt{Q} \in \mathcal{Q}_J \setminus \mathcal{Q}_0$ be an element generated in the refinement process from $\mathcal{Q}_0$ to $\mathcal{Q}_J$, and let $j_1 < J$ be the unique index such that $\mathtt{Q} \in \mathcal{Q}_{j_1+1} \setminus \mathcal{Q}_{j_1}$. Lemma 3.2.4 states the existence of $\mathtt{Q}_1 \in \mathcal{M}_{j_1}$ with

$$\operatorname{Dist}(\mathtt{Q}, \mathtt{Q}_1) \leq q^{-\ell(\mathtt{Q})}\, C_{3.2.4} \quad \text{and} \quad \ell(\mathtt{Q}) \leq \ell(\mathtt{Q}_1) + 1\,, \tag{3.68}$$

and, consequently $\lambda(\mathtt{Q}, \mathtt{Q}_1) = q^{\ell(\mathtt{Q})-\ell(\mathtt{Q}_1)} > 0$. The repeated use of Lemma 3.2.4 yields a sequence $\{\mathtt{Q}_2, \mathtt{Q}_3, \dots\}$ with $\mathtt{Q}_{i-1} \in \mathcal{Q}_{j_i+1} \setminus \mathcal{Q}_{j_i}$, for $j_1 > j_2 > j_3 > \dots$, and $\mathtt{Q}_i \in \mathcal{M}_{j_i}$ such that

$$\operatorname{Dist}(\mathtt{Q}_{i-1}, \mathtt{Q}_i) \leq q^{-\ell(\mathtt{Q}_{i-1})}\, C_{3.2.4} \quad \text{and} \quad \ell(\mathtt{Q}_{i-1}) \leq \ell(\mathtt{Q}_i) + 1. \tag{3.69}$$

We iteratively apply Lemma 3.2.4 as long as

$$\lambda(\mathtt{Q}, \mathtt{Q}_i) > 0 \quad \text{and} \quad \ell(\mathtt{Q}_i) > 0\,, \tag{3.70}$$

until we reach the first index L with $\lambda(\mathtt{Q}, \mathtt{Q}_L) = 0$ or $\ell(\mathtt{Q}_L) = 0$. This yields the following three cases.

- If $\ell(\mathtt{Q}_L) = 0$ and $\lambda(\mathtt{Q}, \mathtt{Q}_L) > 0$, then

$$\sum_{\mathtt{Q}' \in \mathcal{M}} \lambda(\mathtt{Q}, \mathtt{Q}') \geq \lambda(\mathtt{Q}, \mathtt{Q}_L) = q^{\ell(\mathtt{Q})-\ell(\mathtt{Q}_L)} > 1\,, \tag{3.71}$$

  since $\ell(\mathtt{Q}) > \ell(\mathtt{Q}_L) = 0$.

- If $\lambda(\mathtt{Q}, \mathtt{Q}_L) = 0$ because $\ell(\mathtt{Q}) > \ell(\mathtt{Q}_L) + 1$, then (3.69) yields $\ell(\mathtt{Q}_{L-1}) \leq \ell(\mathtt{Q}_L) + 1 < \ell(\mathtt{Q})$ and hence

$$\sum_{\mathtt{Q}' \in \mathcal{M}} \lambda(\mathtt{Q}, \mathtt{Q}') \geq \lambda(\mathtt{Q}, \mathtt{Q}_{L-1}) = q^{\ell(\mathtt{Q})-\ell(\mathtt{Q}_{L-1})} > 1. \tag{3.72}$$

- If $\lambda(\mathtt{Q}, \mathtt{Q}_L) = 0$ because $\mathrm{Dist}(\mathtt{Q}, \mathtt{Q}_L) \not< 2\, q^{-\ell(\mathtt{Q})}\, C_{3.2.4}$, then there exists an index $k \in \{1, \dots, d\}$ with $\mathrm{Dist}_k(\mathtt{Q}, \mathtt{Q}_L) \geq 2\, q^{-\ell(\mathtt{Q})}\, (C_{3.2.4})_k$ (the subscript k indicates the k-th component), and a triangle inequality combined with Lemma 3.2.4 leads to

$$\begin{aligned} 2\, q^{-\ell(\mathtt{Q})}\, (C_{3.2.4})_k &\leq \mathrm{Dist}_k(\mathtt{Q}, \mathtt{Q}_1) + \sum_{i=1}^{L-1} \mathrm{Dist}_k(\mathtt{Q}_i, \mathtt{Q}_{i+1}) \\ &\leq q^{-\ell(\mathtt{Q})}\, (C_{3.2.4})_k + \sum_{i=1}^{L-1} q^{-\ell(\mathtt{Q}_i)}\, (C_{3.2.4})_k\,. \end{aligned} \tag{3.73}$$

Consequently, $q^{-\ell(\mathtt{Q})} \leq \sum_{i=1}^{L-1} q^{-\ell(\mathtt{Q}_i)}$, and we obtain

$$1 \;\leq\; \sum_{i=1}^{L-1} q^{\ell(\mathtt{Q})-\ell(\mathtt{Q}_i)} \;=\; \sum_{i=1}^{L-1} \lambda(\mathtt{Q}, \mathtt{Q}_i) \;\leq\; \sum_{\mathtt{Q}' \in \mathcal{M}} \lambda(\mathtt{Q}, \mathtt{Q}'). \tag{3.74}$$

(ii) For any $0 \leq j \leq J-1$, we consider the set of elements of level j whose distance from $\mathtt{Q}'$ is less than $q^{1-j} C_{3.2.4}$, defined as

$$A(\mathtt{Q}', j) \coloneqq \big\{ \mathtt{Q} \in \mathcal{Q}_j \mid \mathrm{Dist}(\mathtt{Q}, \mathtt{Q}') < q^{1-j} C_{3.2.4} \big\}. \tag{3.75}$$

According to the definition of λ, the set $A(\mathtt{Q}', j)$ contains all elements at level j that satisfy $\lambda(\mathtt{Q}, \mathtt{Q}') > 0$. We have

$$\sum_{\mathtt{Q} \in \mathcal{Q}_J \setminus \mathcal{Q}_0} \lambda(\mathtt{Q}, \mathtt{Q}') \leq \sum_{\mathtt{Q} \in \bigcup \mathbb{M}_{\text{UNIFORM}} \setminus \mathcal{Q}_0} \lambda(\mathtt{Q}, \mathtt{Q}') = \sum_{j=1}^{\ell(\mathtt{Q}')+1} q^{j-\ell(\mathtt{Q}')}\, \#A(\mathtt{Q}', j). \tag{3.76}$$

Since the size of an element $\mathtt{Q}$ of level j is $q^{-j}\mathbf{1}$, the bounding box of all elements in $A(\mathtt{Q}', j)$ has a size bounded by

$$\mathrm{size}(A(\mathtt{Q}', j)) \leq 2 \cdot q^{1-j} C_{3.2.4} + q^{-j}\mathbf{1}, \tag{3.77}$$

and hence the volume of that domain is bounded by

$$\begin{aligned} |\bigcup A(\mathtt{Q}', j)| &\leq \mathrm{prod}\big(q^{1-j} C_{3.2.4} + q^{-j}\mathbf{1}\big) \\ &\coloneqq \prod_{k=1}^{d} \big(q^{1-j} (C_{3.2.4})_k + q^{-j}\big) \\ &= q^{-dj} \prod_{k=1}^{d} \big(q\, (C_{3.2.4})_k + 1\big). \end{aligned} \tag{3.78}$$

Since the volume of each element in $A(\mathtt{Q}', j)$ is q^{-dj}, the number of elements in $A(\mathtt{Q}', j)$ can be bounded by

$$\#A(\mathtt{Q}', j) \leq q^{dj}\, |\bigcup A(\mathtt{Q}', j)| \leq \prod_{k=1}^{d} \big(q\, (C_{3.2.4})_k + 1\big). \tag{3.79}$$

Finally, the index substitution $k \coloneqq 1 - j + \ell(\mathtt{Q}')$ reduces (3.76) to

$$\sum_{\mathtt{Q} \in \mathcal{Q}_J \setminus \mathcal{Q}_0} \lambda(\mathtt{Q}, \mathtt{Q}') \leq \sum_{j=1}^{\ell(\mathtt{Q}')+1} q^{j-\ell(\mathtt{Q}')} \# A(\mathtt{Q}', j) = \sum_{k=0}^{\ell(\mathtt{Q}')} q^{1-k} \# A(\mathtt{Q}', j)$$

$$< q \sum_{k=0}^{\infty} q^{-k} \# A(\mathtt{Q}', j) = \tfrac{q}{1-q^{-1}} \, \# A(\mathtt{Q}', j) \leq C_{3.2.5} \,, \tag{3.80}$$

with $C_{3.2.5} = \frac{q^{d+1}}{q-1} \, \mathrm{prod}(C_{3.2.4} + \mathbf{1})$. □

4 Truncated Hierarchical B-splines

This chapter introduces Truncated Hierarchical B-splines (THB-splines), which are defined for the same mesh class that has been adressed in the previous chapter, $\mathbb{M}_{\text{THB}} = \mathbb{M}_{\text{HB}}$, with $\mathbb{M}_{\text{HB}}$ in the generalized setting from Section 3.2. THB-splines are an alternative choice of basis functions, and they span the same spline space as the HB-splines, $\operatorname{span}\mathcal{B}_{\text{THB}}(\mathcal{Q}) = \operatorname{span}\mathcal{B}_{\text{HB}}(\mathcal{Q})$, for all $\mathcal{Q} \in \mathbb{M}_{\text{HB}}$. THB-splines have been introduced in [19] and aim at reducing the overlap of basis functions by choosing a spline basis with smaller supports. The reduced overlap yields a sparser stiffness matrix for the Galerkin method, which results in less time required for its assembly, less memory to store it, and potentially less time for solving the discrete problem. We will below define the THB-spline basis, and subsequently adapt the definitions and results from Chapter 3 to this basis, which in essence results in smaller neighbourhoods to be marked in the refinement procedure, and consequently allows for more local refinement in the sense that the class of admissible meshes is larger, and the complexity constant in Theorem 4.2.6 is smaller than $C_{4.2.6}$ from the estimate in Section 3.2.

4.1 Truncating the B-spline basis

The following definition introduces the truncation mechanism, the key concept used to define the truncated basis for hierarchical splines [19].

Definition 4.1.1 (One-level truncation)**.** Let $s \in \operatorname{span}\mathcal{B}_k$ for some $k \in \mathbb{N}_0$. There exist unique coefficients $\{c_{B,s} \mid B \in \mathcal{B}_{k+1}\} \subset \mathbb{R}$ such that s is represented by the spline basis $\mathcal{B}_{k+1}$,

$$s = \sum_{B \in \mathcal{B}_{k+1}} c_{B,s} B. \tag{4.1}$$

The *truncation* of s with respect to $\mathcal{B}_{k+1}$ is defined by omitting all those functions $B \in \mathcal{B}_{k+1}$ that can be represented by functions from $\mathcal{B}_{\text{HB}}(\mathcal{Q})$,

$$\operatorname{trunc}_{k+1}(s) \coloneqq \sum_{\substack{B \in \mathcal{B}_{k+1} \\ \operatorname{supp} B \not\subseteq \Omega_{\mathcal{Q},k+1}}} c_{B,s} B. \tag{4.2}$$

The above-defined truncation discards the contribution of those B-splines in $\mathcal{B}_{k+1}$ whose support is contained in the refined domain $\Omega_{\mathcal{Q},k+1}$. The iterative application of this truncation among the levels of the hierarchy leads to the following definition.

Definition 4.1.2 (Truncated spline basis)**.** The *truncated hierarchical B-spline (THB-spline) basis* $\mathcal{B}_{\text{THB}}(\mathcal{Q})$ with respect to the mesh $\mathcal{Q}$ is defined as

$$\begin{aligned}&\mathcal{B}_{\text{THB}}(\mathcal{Q}) \coloneqq \{\text{Trunc}(B) \mid B \in \mathcal{B}_{\text{HB}}(\mathcal{Q})\},\\ &\text{where}\\ &\text{Trunc}(B) \coloneqq \text{trunc}^{N}(\dots(\text{trunc}^{k+1}(B))\dots)\end{aligned} \tag{4.3}$$

for any $B \in \mathcal{B}_k \cap \mathcal{B}_{\text{HB}}(\mathcal{Q})$ and $N = \max\{n \in \mathbb{N}_0 \mid \mathcal{B}_n \cap \mathcal{B}_{\text{HB}}(\mathcal{Q}) \neq \emptyset\}$.

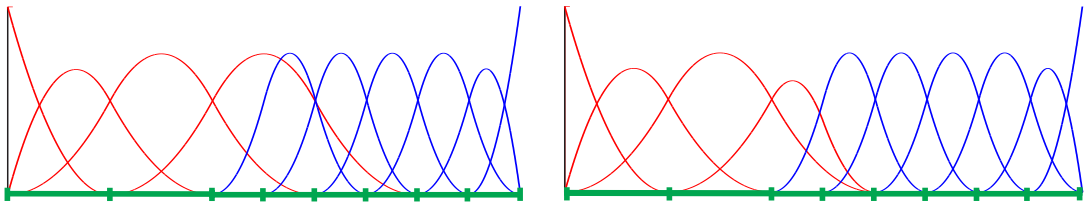

Figure 4.1 [52]: HB-splines (left) and THB-splines (right) for a one-dimensional mesh. Note that a B-spline is truncated only if its support contains the entire support of a finer (higher-level) function.

THB-splines inherit from the HB-splines linear independence, non-negativity, nested spline spaces and the partition of unity. Moreover, being defined in terms of the truncation mechanism, each THB-spline $\tilde{B} = \text{Trunc}(B)$ is characterized by a support that is either equal or smaller than the support of the HB-spline B. For details on the properties of the truncated basis, we refer to [19, 54].

4.2 Local q-adic refinement in nD

As explained at the beginning of the chapter, we consider below the mesh class $\mathbb{M}_{\text{THB}} \coloneqq \mathbb{M}_{\text{HB}}$ in the sense of Definition 3.2.1. The refinement for THB-splines defined below is, up to notation, cited from [53] and [37].

Definition 4.2.1 (Refinement for THB-Splines)**.** We define for each $Q \in \mathcal{Q}$ the *coarse neighbourhood* consisting of elements with level $\ell(Q) - m + 1$

$$\begin{aligned}\mathcal{N}_{\text{THB}}(\mathcal{Q}, Q) \coloneqq \big\{&Q' \in \mathcal{Q} \mid \ell(Q') = \ell(Q) - m + 1 \qquad (4.4)\\ &\text{and } \exists\, Q'' \in \text{SUBDIVIDE}(Q') : \ Q'' \subset \mathcal{S}(\text{anc}^{m-2}(Q))\big\}, \qquad (4.5)\end{aligned}$$

with generalized notations $\mathcal{N}_{\text{THB}}(\mathcal{Q}, \mathcal{M}) \coloneqq \bigcup_{Q \in \mathcal{M}} \mathcal{N}_{\text{THB}}(\mathcal{Q}, Q)$ and

$$\mathcal{N}^k_{\text{THB}}(\mathcal{Q}, \mathcal{M}) \coloneqq \underbrace{\mathcal{N}_{\text{THB}}(\mathcal{Q}, \dots \mathcal{N}_{\text{THB}}(\mathcal{Q}, \mathcal{M})\dots)}_{k \text{ times}}. \tag{4.6}$$

We define the *closure*

$$\text{CLOSURE\_THB}(\mathcal{Q}, \mathcal{M}) \coloneqq \bigcup_{k=0}^{\max \ell(\mathcal{M})} \mathcal{N}^k_{\text{THB}}(\mathcal{Q}, \mathcal{M}), \tag{4.7}$$

and the extended refinement procedure

$$\text{REFINE\_THB}(\mathcal{Q}, \mathcal{M}) \coloneqq \text{SUBDIVIDE}\big(\mathcal{Q}, \text{CLOSURE\_THB}(\mathcal{Q}, \mathcal{M})\big). \tag{4.8}$$

Note that compared to the HB-splines, the above-defined neighbourhood makes use of $\mathcal{S}(\mathrm{anc}^{m-2}(\square))$ instead of $\mathcal{S}(\mathrm{anc}^{m-1}(\square))$, which yields a neighbourhood which is by a factor q smaller in each dimension and hence yields substantially more localized refinement.

4.2.1 Admissible meshes and overlay

Similar to the framework for HB-splines, we define admissibility by an upper bound on the overlap of basis functions.

Definition 4.2.2. A mesh $\mathcal{Q} \in \mathbb{M}_{\mathrm{THB}}$ is called *admissible* if

$$\forall\, \square \in \mathcal{Q}: \quad \mathcal{S}(\mathrm{anc}^{m-1}(\square)) \subseteq \Omega_{\mathcal{Q},\ell(\square)-m+1}. \tag{4.9}$$

This definition is equivalent to the definition of *strict admissibility* from [37]. It is used below to characterize the mesh class generated by the refinement procedure REFINE_THB. Same as for the HB-spline setting, this definition guarantees for bounded overlap of the THB-splines. Note again that the above-defined term "admissible" depends on m and the polynomial degree p of the B-splines. Since $m = 1$ refers to uniform meshes, we focus on the case $m \geq 2$.

The overlay of admissible meshes and its properties are completely analogue to the HB-spline case, with $\mathcal{Q}_* \coloneqq \mathcal{Q}_1 \otimes \mathcal{Q}_2$ being admissible for any admissible meshes $\mathcal{Q}_1$ and $\mathcal{Q}_2$.

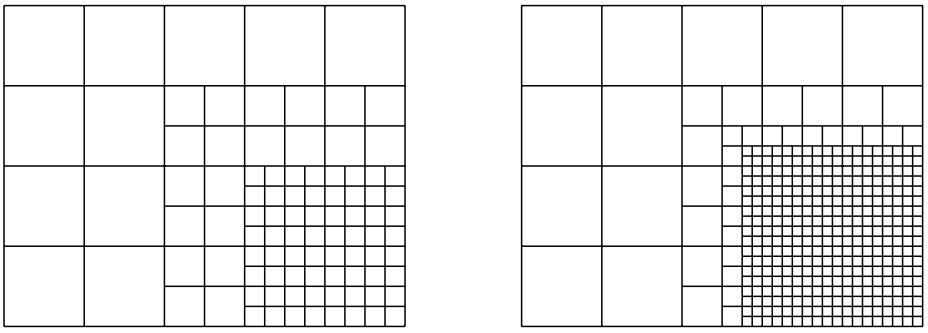

(a) (b)

Figure 4.2 [37]: Two examples on m-admissible meshes. The left mesh (a) is 2-admissible for $\mathbf{p} \leq 2$. It is *not* 2-admissible if $p_1 > 2$ or $p_2 > 2$, but it is 3-admissible for any $\mathbf{p}$. The mesh on the right-hand side (b) is 2-admissible only if $\mathbf{p} = (1, 1)$, and 4-admissible for all other $\mathbf{p}$.

Proposition 4.2.3. *The above-defined refinement routine* REFINE_THB *fulfills the following properties.*

(i) All meshes generated from $\mathcal{Q}_0$ and (successive) application of REFINE_THB *are admissible.*

(ii) Any mesh $\mathcal{Q} \in \mathbb{M}_{\mathrm{THB}}$ which is admissible can be generated by $\mathcal{Q}_0$ and (successive) application of REFINE_THB*.*

4.2.2 Linear complexity

In this Section, we prove that REFINE_THB has linear complexity with respect to the number of marked and generated elements. The proofs are very similar to those in Section 3.1.5, and consequently we only prove two Lemmas below, and for Theorem 4.2.6 we refer the reader to the proof of Theorem 3.1.12. The following Lemma is similar to Lemma 3.2.3 and makes use of the distance operator defined in Definition 3.2.2. The subsequent Lemma 4.2.5 is an adaption of Lemma 3.1.11 to the THB-spline setting.

Lemma 4.2.4. *For every pair of mesh elements (Q, Q'), let $\mathrm{Dist}(Q, Q')$ be the Euclidean distance of their midpoints. Given a $Q \in \mathcal{Q}$, all $Q' \in \mathcal{N}_{\mathrm{THB}}(\mathcal{Q}, Q)$ satisfy*

$$\mathrm{Dist}(Q, Q') \leq q^{-\ell(Q')-1}\, C_{4.2.4} \tag{4.10}$$

with $C_{4.2.4} \coloneqq \mathbf{p} + \frac{q}{2} + 1 \in \mathbb{R}^d$, and "$\mathbf{p} + \frac{q}{2} + 1$" indicating an increment of $\mathbf{p}$ by $\frac{q}{2} + 1$ in each component.

Proof. The definition of $\mathcal{N}_{\mathrm{THB}}(\mathcal{Q}, Q)$ yields that

$$\ell(Q') = \ell(Q) - m + 1 = \ell(\mathrm{anc}^{m-2}(Q)) - 1 \tag{4.11}$$

and $Q'' \in \mathrm{SUBDIVIDE}(Q')$ such that $Q' \supset Q'' \subset \mathcal{S}(\mathrm{anc}^{m-2}(Q))$. The support extension $\mathcal{S}(\mathrm{anc}^{m-2}(Q))$ is defined via B-splines on the level $\ell(\mathrm{anc}^{m-2}(Q)) = \ell(Q'')$. Hence, there is a B-spline $B \in \mathcal{B}_{\ell(Q'')}$ such that $Q' \supset Q'' \subset \operatorname{supp} B$ and $Q \subset \mathrm{anc}^{m-2}(Q) \subset \operatorname{supp} B$. Using the notation $\mathbf{1} \coloneqq (1, \ldots, 1) \in \mathbb{R}^d$ and

$$\mathrm{size}\big([a_1, b_1] \times \cdots \times [a_d, b_d]\big) \coloneqq \big(b_1 - a_1, \ldots, b_d - a_d\big) \quad \in \mathbb{R}^d, \tag{4.12}$$

the distance between the midpoints of Q' and Q is bounded by

$$\begin{aligned} \mathrm{Dist}(Q, Q') &\leq \mathrm{size}(\operatorname{supp} B) + \tfrac{1}{2}\,\mathrm{size}(Q') \\ &= q^{-\ell(Q'')}(\mathbf{p} + \mathbf{1}) + \tfrac{1}{2}\, q^{-\ell(Q')}\mathbf{1} = q^{-\ell(Q')-1}\big(\mathbf{p} + (\tfrac{q}{2} + 1)\mathbf{1}\big), \end{aligned} \tag{4.13}$$

which concludes the proof. □

Lemma 4.2.5. *Let $\mathcal{Q}$ be an admissible mesh, $\mathcal{M} \subset \mathcal{Q}$ the set of elements marked for refinement, and $\hat{\mathcal{Q}} = \mathrm{REFINE\_THB}(\mathcal{Q}, \mathcal{M})$. For any newly created $Q \in \hat{\mathcal{Q}} \setminus \mathcal{Q}$, there exists a marked element $Q' \in \mathcal{M}$ such that*

$$\mathrm{Dist}(Q, Q') \leq q^{-\ell(Q)} C_{4.2.5} \quad \text{and} \quad \ell(Q) \leq \ell(Q') + 1, \tag{4.14}$$

where $C_{4.2.5} \coloneqq \frac{1}{1-q^{1-m}} C_{4.2.4} + \frac{q}{2}\mathbf{1}$.

Proof. The existence of $Q \in \hat{\mathcal{Q}} \setminus \mathcal{Q}$ means that $\mathrm{CLOSURE\_THB}(\mathcal{Q}, \mathcal{M})$ contains a sequence of elements $Q' = Q_J, Q_{J-1}, \ldots, Q_0$ such that $Q_{j-1} \in \mathcal{N}_{\mathrm{THB}}(\mathcal{Q}, Q_j)$, with $Q' \in \mathcal{M}$ and Q being a child of Q_0, namely $\ell(Q) = \ell(Q_0)+1$. Since $\ell(Q_{j-1}) = \ell(Q_j) - m + 1$, it follows

$$\ell(Q_j) = \ell(Q_0) + j\,(m-1). \tag{4.15}$$

We have

$$\mathrm{Dist}(\mathtt{Q},\mathtt{Q}') \le \mathrm{Dist}(\mathtt{Q},\mathtt{Q}_0) + \mathrm{Dist}(\mathtt{Q}_0,\mathtt{Q}') \tag{4.16}$$

and

$$\mathrm{Dist}(\mathtt{Q},\mathtt{Q}_0) \le \tfrac{1}{2}\,\mathrm{size}(\mathtt{Q}_0) = \tfrac{1}{2}\,q^{-\ell(\mathtt{Q}_0)}\mathbf{1}, \tag{4.17}$$

$$\mathrm{Dist}(\mathtt{Q}_0,\mathtt{Q}') \le \sum_{j=0}^{J-1} \mathrm{Dist}(\mathtt{Q}_{j+1},\mathtt{Q}_j). \tag{4.18}$$

According to Lemma 4.2.4, we obtain

$$\begin{aligned}\sum_{j=0}^{J-1} \mathrm{Dist}(\mathtt{Q}_{j+1},\mathtt{Q}_j) &\le \sum_{j=0}^{J-1} q^{-\ell(\mathtt{Q}_j)-1} C_{4.2.4} \overset{(4.15)}{=} \sum_{j=0}^{J-1} q^{-\ell(\mathtt{Q}_0)-j(m-1)-1} C_{4.2.4} \\ &< q^{-\ell(\mathtt{Q}_0)-1} C_{4.2.4} \sum_{j=0}^{\infty} q^{(1-m)\cdot j} = \frac{q^{-\ell(\mathtt{Q}_0)-1} C_{4.2.4}}{1-q^{1-m}} = \frac{q^{-\ell(\mathtt{Q})} C_{4.2.4}}{1-q^{1-m}}.\end{aligned} \tag{4.19}$$

The combination with (4.16), (4.17) and (4.18) proves the distance estimate. The application of (4.15) to the case $j = J \ge 0$, together with $\ell(\mathtt{Q}) = \ell(\mathtt{Q}_0) + 1$ from above, yields

$$\ell(\mathtt{Q}) = \ell(\mathtt{Q}') - J\,(m-1) + 1 \le \ell(\mathtt{Q}') + 1, \tag{4.20}$$

which concludes the proof. □

Theorem 4.2.6 (Complexity of REFINE_THB)**.** *Let $\mathcal{M} := \bigcup_{j=0}^{J-1} \mathcal{M}_j$ be the set of marked elements used to generate the sequence of admissible meshes $\mathcal{Q}_0, \mathcal{Q}_1, \dots, \mathcal{Q}_J$ starting from $\mathcal{Q}_0$, namely*

$$\mathcal{Q}_j = \mathrm{REFINE\_THB}(\mathcal{Q}_{j-1}, \mathcal{M}_{j-1}), \quad \mathcal{M}_{j-1} \subseteq \mathcal{Q}_{j-1} \quad \textit{for } j \in \{1,\dots,J\}. \tag{4.21}$$

Then, there exists a positive constant $C_{4.2.6}$ such that

$$\#\mathcal{Q}_J - \#\mathcal{Q}_0 \le\ C_{4.2.6}\,\#\mathcal{M}. \tag{4.22}$$

The proof is the same as the proof of Theorem 3.2.5, with $C_{3.2.4}$ replaced by $C_{4.2.5}$, and consequently $C_{4.2.6} = \frac{q^{d+1}}{q-1}\ \mathrm{prod}(C_{4.2.5} + \mathbf{1})$, with "prod" from (3.46).

5 Analysis-Suitable T-splines

This chapter investigates the local refinement for T-splines. Introduced for purposes of computer graphics and modeling, they are designed to allow for a local refinement of NURBS (see Section 2.3) while preserving smoothness and local support of each basis function as well as the partition of unity. As pointed out in the introduction, Isogeometric Analysis was established later than T-splines, and algorithmic difficulties arise when T-splines are applied in a Galerkin method. First, for general box meshes, they do not form a basis due to linear dependencies. Second, T-splines that correspond to (partially) nested meshes, in the sense that one is a refinement of the other, may span spline spaces that are not nested. Both difficulties have been addressed and solved in the refinement procedure proposed by Scott et al. [29], which supports zero knot intervals as well as the manifold-like structure of more complex geometry representations, see e.g. [22]. Since the algorithm is based on analysis-suitability in the sense of Definition 5.1.8 below, it is limited to the two-dimensional case, and we are not aware of any complexity analysis (comparable to Section 3.1.5) for this algorithm, which is necessary for the theoretical analysis of convergence rates of the Adaptive Isogeometric Method, see e.g. [10, Equation 2.9]. This chapter introduces an alternative refinement procedure for T-splines which allows for the desired complexity analysis as well as a generalization to higher dimensions. We will explain T-splines and analysis-suitability in Section 5.1 below, and present the refinement algorithm for the two dimensional setting, uniform polynomial degree and dyadic refinement in Section 5.2. We investigate linear independence of the T-splines, nestedness of the spanned spline spaces, the overlay of two meshes, and the complexity of the refinement procedure. Sections 5.3 and 5.4 generalize the results to higher dimensions, polynomial degrees that differ between the dimensions, and element subdivision with more than two children.

5.1 AST-splines in 2D

This section defines bivariate T-splines and analysis-suitability, which is a sufficient condition for linear independence of the T-splines. We introduce the mesh class $\mathbb{M}_{\mathrm{TS}}$ below, and subsequently explain the construction of T-splines for a given mesh and odd polynomial degree p. For even p we refer the reader to [31].

Definition 5.1.1 (Intermediate uniform meshes)**.** For each level $k \in \mathbb{N}$, we define the tensor-product mesh

$$\mathcal{Q}_{\mathsf{u}[k+1/2]} \coloneqq \left\{ [x-2^{-k-1}, x]\times[y-2^{-k}, y] \mid 2^{k+1}x \in \{1,\dots,2^{k+1}M\}, 2^k y \in \{1,\dots,2^k N\} \right\}. \tag{5.1}$$

The class of uniform meshes, including the above-defined intermediate uniform

meshes, is denoted by

$$\mathbb{M}^{1/2}_{\text{UNIFORM}} \coloneqq \{\mathcal{Q}_{\mathsf{u}[k]} \mid 2k \in \mathbb{N}_0\} \supset \mathbb{M}_{\text{UNIFORM}}. \tag{5.2}$$

For the use of T-splines, the underlying rectangular mesh $\mathcal{Q}$ may, similarly to the preceeding chapters, consist of finitely many elements from meshes in $\mathbb{M}^{1/2}_{\text{UNIFORM}}$, such that any two elements of $\mathcal{Q}$ have disjoint interior, and the union of all elements of $\mathcal{Q}$ is the same domain $[0, M] \times [0, N]$ that is covered by uniform meshes.

$$\mathbb{M}_{\text{TS}} \coloneqq \Big\{ \mathcal{Q} \subset \bigcup\nolimits_{\mathcal{Q}' \in \mathbb{M}^{1/2}_{\text{UNIFORM}}} \mathcal{Q}' \mid \#\mathcal{Q} < \infty,\ \bigcup \mathcal{Q} = [0, M] \times [0, N], \\ \forall \mathsf{Q}, \mathsf{Q}' \in \mathcal{Q} :\ \operatorname{int}(\mathsf{Q}) \cap \operatorname{int}(\mathsf{Q}') = \emptyset \Big\}. \tag{5.3}$$

Definition 5.1.2 (Skeleton)**.** Given a mesh $\mathcal{Q} \in \mathbb{M}_{\text{TS}}$ and $\mathsf{Q} = [x, x+\tilde{x}] \times [y, y+\tilde{y}] \in \mathcal{Q}$, we denote the union of all vertical (resp. horizontal) element sides by

$$\begin{aligned} \mathsf{vSk}(\mathsf{Q}) &\coloneqq \{x, x + \tilde{x}\} \times [y, y + \tilde{y}], \\ \mathsf{hSk}(\mathsf{Q}) &\coloneqq [x, x + \tilde{x}] \times \{y, y + \tilde{y}\}, \\ \mathsf{vSk}(\mathcal{Q}) &\coloneqq \bigcup_{\mathsf{Q} \in \mathcal{Q}} \mathsf{vSk}(\mathsf{Q}), \quad \mathsf{hSk}(\mathcal{Q}) \coloneqq \bigcup_{\mathsf{Q} \in \mathcal{Q}} \mathsf{hSk}(\mathsf{Q}). \end{aligned} \tag{5.4}$$

We call $\mathsf{vSk}(\mathcal{Q})$ the *vertical skeleton* and $\mathsf{hSk}(\mathcal{Q})$ the *horizontal skeleton*, and if only one mesh $\mathcal{Q}$ is considered in the context, we will use the shortcut notation vSk and hSk, respectively.

Definition 5.1.3 (Vertices and T-junctions)**.** For any mesh $\mathcal{Q} \in \mathbb{M}_{\text{TS}}$ and element $\mathsf{Q} = [x, x + \tilde{x}] \times [y, y + \tilde{y}] \in \mathcal{Q}$, we define the set of *nodes*

$$\mathsf{N}(\mathsf{Q}) \coloneqq \{x, x + \tilde{x}\} \times \{y, y + \tilde{y}\}, \text{ and } \mathsf{N}(\mathcal{Q}) \coloneqq \bigcup_{\mathsf{Q} \in \mathcal{Q}} \mathsf{N}(\mathsf{Q}). \tag{5.5}$$

We denote as *T-junction* each vertex that is in an element without being a vertex of it,

$$\mathsf{T}(\mathsf{Q}) \coloneqq \mathsf{N}(\mathcal{Q}) \cap \mathsf{Q} \setminus \mathsf{N}(\mathsf{Q}), \text{ and } \mathsf{T}(\mathcal{Q}) \coloneqq \bigcup_{\mathsf{Q} \in \mathcal{Q}} \mathsf{T}(\mathsf{Q}). \tag{5.6}$$

Note that the above union is disjoint, i.e., for any T-junction $v \in \mathsf{T}(\mathcal{Q})$ there is a *unique* element $\mathsf{Q}_v \in \mathcal{Q}$ such that $v \in \mathsf{T}(\mathsf{Q}_v)$. We distinguish horizontal and vertical T-junctions. A T-junction is called *horizontal* if it is in a vertical side of the corresponding element, and *vertical* if it is in a horizontal side,

$$\begin{aligned} \mathsf{T}_{\mathsf{h}}(\mathsf{Q}) &\coloneqq \big\{ v \in \mathsf{T}(\mathsf{Q}) \mid v \in \mathsf{vSk}(\mathsf{Q}) \big\}, \\ \mathsf{T}_{\mathsf{v}}(\mathsf{Q}) &\coloneqq \big\{ v \in \mathsf{T}(\mathsf{Q}) \mid v \in \mathsf{hSk}(\mathsf{Q}) \big\}, \\ \mathsf{T}_{\mathsf{h}}(\mathcal{Q}) &\coloneqq \bigcup_{\mathsf{Q} \in \mathcal{Q}} \mathsf{T}_{\mathsf{h}}(\mathsf{Q}), \quad \mathsf{T}_{\mathsf{v}}(\mathcal{Q}) \coloneqq \bigcup_{\mathsf{Q} \in \mathcal{Q}} \mathsf{T}_{\mathsf{v}}(\mathsf{Q}). \end{aligned} \tag{5.7}$$

Note that $\mathsf{T}_{\mathsf{h}}(\mathcal{Q})$ and $\mathsf{T}_{\mathsf{v}}(\mathcal{Q})$ are disjoint and $\mathsf{T}_{\mathsf{h}}(\mathcal{Q}) \cup \mathsf{T}_{\mathsf{v}}(\mathcal{Q}) = \mathsf{T}(\mathcal{Q})$.

Definition 5.1.4 (Global index vectors)**.** For any $v = (v_1, v_2) \in [0, M] \times [0, N]$, we define

$$\mathsf{X}(v) \coloneqq \Big\{(\underbrace{\tbinom{0}{v_2}, \dots, \tbinom{0}{v_2}}_{\lceil \frac{p}{2} \rceil \text{ times}})\Big\} \times \operatorname{sort}_{\mathrm{x}}\Big(\{\tbinom{z_1}{z_2} \in \mathsf{vSk} \mid z_2 = v_2\}\Big) \times \Big\{(\underbrace{\tbinom{M}{v_2}, \dots, \tbinom{M}{v_2}}_{\lceil \frac{p}{2} \rceil \text{ times}})\Big\},$$

$$\mathsf{Y}(v) \coloneqq \Big\{(\underbrace{\tbinom{v_1}{0}, \dots, \tbinom{v_1}{0}}_{\lceil \frac{p}{2} \rceil \text{ times}})\Big\} \times \operatorname{sort}_{\mathrm{y}}\Big(\{\ \tbinom{z_1}{z_2} \in \mathsf{hSk} \mid z_1 = v_1\}\Big) \times \Big\{(\underbrace{\tbinom{v_1}{N}, \dots, \tbinom{v_1}{N}}_{\lceil \frac{p}{2} \rceil \text{ times}})\Big\} \tag{5.8}$$

where $\operatorname{sort}_{\mathrm{x}}(S)$ (resp. $\operatorname{sort}_{\mathrm{y}}(S)$) returns a vector of which the components are the elements of S in ascending order with respect to their x-components (resp. y-components).

Remark. The entries of the above-defined vectors $\mathsf{X}(v)$ and $\mathsf{Y}(v)$ are points. The term 'global index vector' follows the literature, where global index vectors are defined as sets or vectors of indices and referred to as "global index sets" [38] or "global index vectors" [29].

Definition 5.1.5 (B-spline for a given knot vector)**.** Recall the construction of B-splines from Definition 2.1.1. For a given knot vector $(x_0, \dots, x_m)$ we introduce the notation $N_{(x_1,\dots,x_m)} \coloneqq N_{1,m-1}$ for the unique B-spline that involves all knots $x_0, \dots, x_m$.

Definition 5.1.6 (T-splines)**.** To each vertex $v = (v_1, v_2) \in \mathsf{N}(\mathcal{Q})$, we associate a local index vector $\mathsf{x}(v) \in \mathbb{R}^{p+2}$, which consists of the x-components of the unique $p + 2$ consecutive elements in $\mathsf{X}(v)$ having v_1 as their $\frac{p+3}{2}$-th (this is, the middle) entry. We analogously define $\mathsf{y}(v) \in \mathbb{R}^{p+2}$. We associate to each vertex $v \in \mathsf{N}(\mathcal{Q})$ a bivariate B-spline function defined as the product of the one-dimensional B-spline functions on the corresponding local index vectors,

$$B_v(x, y) \coloneqq N_{\mathsf{x}(v)}(x) \cdot N_{\mathsf{y}(v)}(y). \tag{5.9}$$

Given a mesh $\mathcal{Q} \in \mathbb{M}_{\mathrm{TS}}$, the associated set of T-splines is defined by

$$\mathcal{B}_{\mathrm{TS}}(\mathcal{Q}) \coloneqq \{B_v \mid v \in \mathsf{N}(\mathcal{Q})\}. \tag{5.10}$$

We give a brief review on the concept of analysis-suitability below, using the notation from [31]. At the end of this section, we will prove that all meshes generated by REFINE_TS2D (see Definition 5.2.3 below) are analysis-suitable and hence provide linearly independent T-splines.

Definition 5.1.7 (T-junction extensions)**.** For any T-junction $v \in \mathsf{T}(\mathcal{Q})$, we define the *T-junction extension* as follows. We denote by $\mathsf{x}_{\mathsf{ext}}(v)$ the unique set of $p + 1$ consecutive elements of $\mathsf{X}(v)$ having the two elements of $\mathsf{X}(v) \cap \mathcal{Q}_v$ as the two middle entries. We denote by $\operatorname{conv}(\mathsf{x}_{\mathsf{ext}}(v))$ the convex hull of these points. Analogously, let $\mathsf{y}_{\mathsf{ext}}(v)$ be the unique set of $p + 1$ elements of $\mathsf{Y}(v)$ having the two elements of $\mathsf{Y}(v) \cap \mathcal{Q}_v$ as the two middle entries, and $\operatorname{conv}(\mathsf{y}_{\mathsf{ext}}(v))$ the convex hull of these points. The *T-junction extension* of v is defined as

$$\operatorname{ext}_{\mathcal{Q}}(v) \coloneqq \begin{cases} \operatorname{conv}(\mathsf{x}_{\mathsf{ext}}(v)) & \text{if } v \in \mathsf{T}_{\mathsf{h}}(\mathcal{Q}), \\ \operatorname{conv}(\mathsf{y}_{\mathsf{ext}}(v)) & \text{if } v \in \mathsf{T}_{\mathsf{v}}(\mathcal{Q}). \end{cases} \tag{5.11}$$

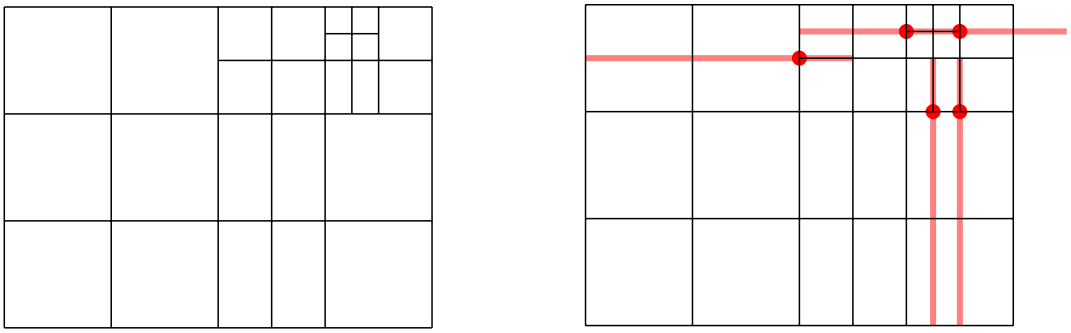

Figure 5.1: Example for T-junction extensions. The left figure show the considered mesh, and the right figure shows the same mesh with indicated T-junctions (red bullets) and the corresponding T-junction extensions (light red thick lines).

Definition 5.1.8 (Analysis-Suitability [31, Definition 2.5])**.** A mesh is *analysis-suitable* if horizontal T-junction extensions do not intersect vertical T-junction extensions.

It is known from the literature that for an analysis-suitable mesh $\mathcal{Q}$, the corresponding T-splines are linearly independent [30, 28]. Moreover, given a mesh $\mathcal{Q} \in \mathbb{M}_{\text{TS}}$ and a refinement $\tilde{\mathcal{Q}}$ thereof, the corresponding spline spaces are only nested if each T-junction extension is either eliminated or unchanged [35].

5.2 Local dyadic refinement in 2D

We introduce below a local refinement routine for T-splines in two dimensions. Similar to REFINE_HB and REFINE_THB, the refinement is defined through the subdivision of a superset (the closure) of the marked elements, and the closure is, as before, defined as a higher-order neighbourhood of the marked elements. Unlike REFINE_HB and REFINE_THB, the (first-order) neighbourhood of a mesh element is defined through a distance criterion, instead of the support extensions used in the previous chapters.

Definition 5.2.1 (Intermediate children)**.** For $Q \in \mathcal{Q}_{\mathsf{u}[k]}$ and $2k \in \mathbb{N}_0$, we define

$$\text{SUBDIVIDE}^{1/2}(Q) \coloneqq \left\{ Q' \in \mathcal{Q}_{\mathsf{u}[k+1/2]} \mid Q' \subset Q \right\}. \tag{5.12}$$

For $\mathcal{M} \subset \mathcal{Q} \in \mathbb{M}_{\text{HB}}$, we denote the corresponding partial subdivision by

$$\text{SUBDIVIDE}^{1/2}(\mathcal{Q}, \mathcal{M}) \coloneqq \mathcal{Q} \setminus \mathcal{M} \cup \bigcup_{Q \in \mathcal{M}} \text{SUBDIVIDE}^{1/2}(Q). \tag{5.13}$$

Definition 5.2.2 (Vector-valued distance)**.** Given $x \in \overline{\Omega}$ and an element Q, we define their distance as the componentwise absolute value of the difference between x and the midpoint of Q,

$$\text{Dist}(Q, x) \coloneqq \text{abs}\big(\text{mid}(Q) - x\big) \ \in \mathbb{R}^2. \tag{5.14}$$

For two elements Q_1, Q_2, we define the shorthand notation

$$\text{Dist}(Q_1, Q_2) \coloneqq \text{abs}\big(\text{mid}(Q_1) - \text{mid}(Q_2)\big). \tag{5.15}$$

Definition 5.2.3 (Refinement for bivariate T-splines)**.** We define for each $\mathtt{Q} \in \mathcal{Q}$ the *coarse neighbourhood*

$$\mathcal{N}_{\mathrm{TS}}(\mathcal{Q}, \mathtt{Q}) \coloneqq \left\{ \mathtt{Q}' \in \mathcal{Q} \cap \mathcal{Q}_{\mathsf{u}[\ell(\mathtt{Q})-1/2]} \mid \mathrm{Dist}(\mathtt{Q}, \mathtt{Q}') \leq \mathbf{D}(\ell(\mathtt{Q})) \right\}, \tag{5.16}$$

with

$$\mathbf{D}(k) = \begin{cases} 2^{-k} \left(\left\lfloor \frac{p}{2} \right\rfloor + \frac{1}{2}, \left\lceil \frac{p}{2} \right\rceil + \frac{1}{2} \right) & \text{if } k \in \mathbb{N}_0, \\ 2^{-k-1/2} \left(\left\lceil \frac{p}{2} \right\rceil + \frac{1}{2}, 2\left\lfloor \frac{p}{2} \right\rfloor + 1 \right) & \text{otherwise,} \end{cases} \tag{5.17}$$

where p is the polynomial degree of the B-splines in x- and y-direction. Moreover, we define the *closure*

$$\textsc{closure\_ts}(\mathcal{Q}, \mathcal{M}) \coloneqq \bigcup_{k=0}^{2 \cdot \max \ell(\mathcal{M})} \mathcal{N}_{\mathrm{TS}}^k(\mathcal{Q}, \mathcal{M}), \tag{5.18}$$

and the extended refinement procedure

$$\textsc{refine\_ts}_{\mathrm{2D}}(\mathcal{Q}, \mathcal{M}) \coloneqq \textsc{subdivide}^{1/2}\big(\mathcal{Q}, \textsc{closure\_ts}(\mathcal{Q}, \mathcal{M})\big). \tag{5.19}$$

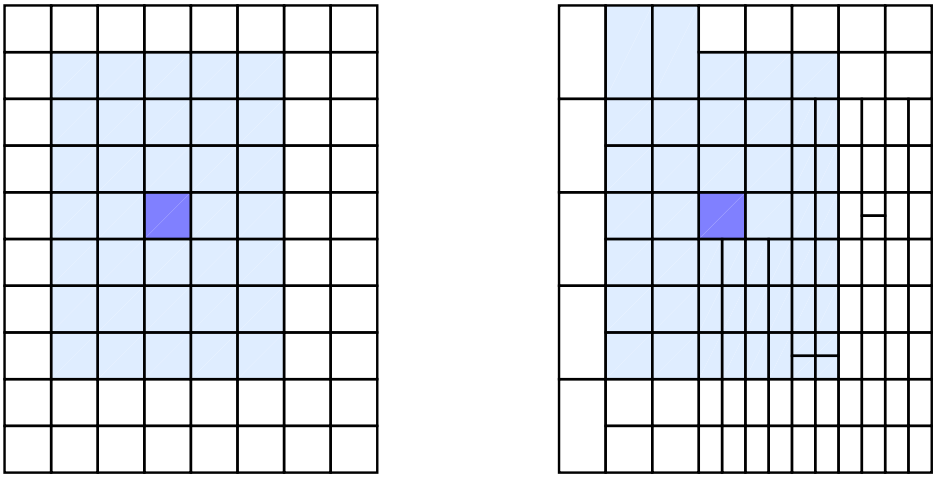

Figure 5.2 [38]: Example of the neighbourhood in a uniform mesh (right) and in a non-uniform mesh (left) for integer $\ell(\mathtt{Q})$ and $\mathbf{p} = (5, 5)$. $\mathtt{Q}$ is marked in blue, and the neighbourhood $\mathcal{Q} \cap U(\mathtt{Q})$ defined in (5.25) is highlighted in light blue. In the uniform mesh (right), the coarse neighbourhood $\mathcal{N}_{\mathrm{TS}}(\mathcal{Q}, \mathtt{Q})$ is empty, and in the non-uniform mesh (left), it consists of two coarser elements.

5.2.1 Admissible meshes

In contrast to the preceeding chapters, we define admissible meshes for T-splines inductively over elementary refinement steps. We will show below that this class of admissible meshes equals the mesh class generated by $\textsc{refine\_ts}_{\mathrm{2D}}$, and, to the end of the section, that all these meshes are analysis-suitable.

Definition 5.2.4 (Admissible bisections)**.** Given a mesh $\mathcal{Q}$ and an element $\mathtt{Q} \in \mathcal{Q}$, the bisection of $\mathtt{Q}$ is called *admissible* if the coarse neighbourhood $\mathcal{N}_{\mathrm{TS}}(\mathcal{Q}, \mathtt{Q})$ is empty. In the case of several elements $\mathcal{M} = \{\mathtt{Q}_1, \ldots, \mathtt{Q}_J\} \subseteq \mathcal{Q}$, the bisection

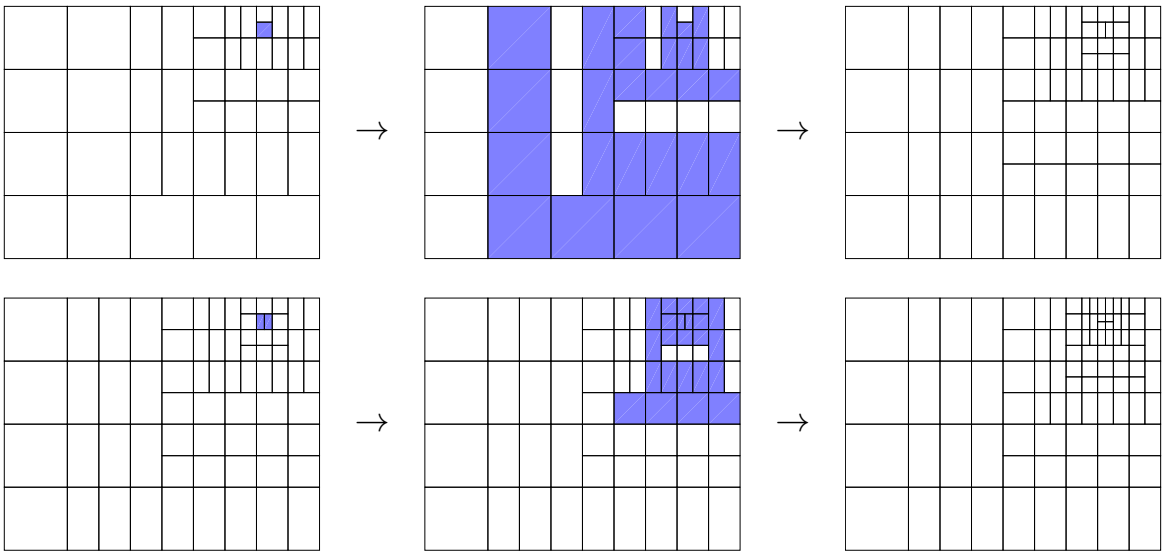

Figure 5.3 [41]: Example for the T-spline refinement. In order to subdivide the marked element as for the THB-spline refinement, the refinement routine REFINE_TS$_{2D}$ is applied twice.

SUBDIVIDE$^{1/2}(\mathcal{Q},\mathcal{M})$ is admissible if there is an order $(\sigma(1),\dots,\sigma(J))$ (this is, if there is a permutation σ of $\{1,\dots,J\}$) such that

$$\text{SUBDIVIDE}^{1/2}(\mathcal{Q},\mathcal{M}) = \text{SUBDIVIDE}^{1/2}(\dots\text{SUBDIVIDE}^{1/2}(\mathcal{Q},\mathcal{Q}_{\sigma(1)}),\dots,\mathcal{Q}_{\sigma(J)}) \tag{5.20}$$

is a concatenation of admissible bisections.

Definition 5.2.5 (Admissible mesh)**.** A refinement $\mathcal{Q}$ of $\mathcal{Q}_0$ is *admissible* if there is a sequence of meshes $\mathcal{Q}_1,\dots,\mathcal{Q}_J=\mathcal{Q}$ and markings $\mathcal{M}_j\subseteq\mathcal{Q}_j$ for $j=0,\dots,J-1$, such that $\mathcal{Q}_{j+1}=\text{SUBDIVIDE}^{1/2}(\mathcal{Q}_j,\mathcal{M}_j)$ is an admissible bisection for all $j=0,\dots,J-1$. The set of all admissible meshes is the initial mesh and its admissible refinements.

Proposition 5.2.6. *For any admissible mesh $\mathcal{Q}$ and any set of marked elements $\mathcal{M}\subseteq\mathcal{Q}$, the refinement* REFINE_TS$_{2D}(\mathcal{Q},\mathcal{M})$ *is also admissible.*

The proof of Proposition 5.2.6 given at the end of this section relies on the subsequent results.

Lemma 5.2.7 (Local quasi-uniformity)**.** *Given an admissible mesh $\mathcal{Q}$ and $\square\in\mathcal{Q}$, any $\square'\in\mathcal{Q}$ with* $\operatorname{Dist}(\square,\square')\le\mathbf{D}(\ell(\square))$ *satisfies* $\ell(\square')\ge\ell(\square)-\frac{1}{2}$.

Proof. For $\ell(\square)=0$, the assertion is always true. For $\ell(\square)>0$, consider the parent $\hat\square$ of $\square$ (i.e., the unique element $\hat\square\in\bigcup\mathbb{M}_{\text{TS}}$ with $\square\in\operatorname{child}(\hat\square)$). Since $\square$ results from the bisection of $\hat\square$, we have

$$\begin{aligned} d(\square) \coloneqq \operatorname{Dist}(\square,\hat\square) &= \begin{cases} (2^{-\ell(\hat\square)-2},0) & \text{if } \ell(\hat\square)\in\mathbb{N}_0,\\ (0,2^{-\ell(\hat\square)-3/2}) & \text{otherwise.}\end{cases}\\ &= \begin{cases} (0,2^{-\ell(\square)-1}) & \text{if } \ell(\square)\in\mathbb{N}_0,\\ (2^{-\ell(\square)-3/2},0) & \text{otherwise.}\end{cases} \end{aligned} \tag{5.21}$$

Since $\mathcal{Q}$ is admissible, there are admissible meshes $\mathcal{Q}_0, \dots, \mathcal{Q}_J = \mathcal{Q}$ and some $j \in \{0, \dots, J-1\}$ such that $Q \in \mathcal{Q}_{j+1} = \text{SUBDIVIDE}^{1/2}(\mathcal{Q}_j, \{\hat{Q}\})$. The admissibility of $\mathcal{Q}_{j+1}$ implies that $\mathcal{N}_{\text{TS}}(\mathcal{Q}_j, \hat{Q})$ is empty. It follows that all $Q' \in \mathcal{Q}_j$ with $\text{Dist}(Q', \hat{Q}) \leq \mathbf{D}(\ell(\hat{Q}))$ satisfies $\ell(Q') \geq \ell(\hat{Q}) = \ell(Q) - \frac{1}{2}$. (If otherwise there was Q'' with $\ell(Q'') < \ell(\hat{Q})$, then there would be an ancestor $\text{anc}^k(Q)$ and a refinement step $\tilde{\jmath}$ such that $Q'' \in \mathcal{N}_{\text{TS}}(\mathcal{Q}_{\tilde{\jmath}}, \text{anc}^k(Q))$, and hence $\mathcal{Q}_j$ would not be admissible.) Since levels do not decrease during refinement, we get

$$\begin{aligned}
\ell(Q) - \tfrac{1}{2} &\leq \min\big\{\ell(Q') \mid Q' \in \mathcal{Q}_j \text{ and } \text{Dist}(\hat{Q}, Q') \leq \mathbf{D}(\ell(\hat{Q}))\big\} \\
&\leq \min\big\{\ell(Q') \mid Q' \in \mathcal{Q} \text{ and } \text{Dist}(\hat{Q}, Q') \leq \mathbf{D}(\ell(\hat{Q}))\big\} \\
&= \min\big\{\ell(Q') \mid Q' \in \mathcal{Q} \text{ and } \text{Dist}(\hat{Q}, Q') \leq \mathbf{D}(\ell(Q) - \tfrac{1}{2})\big\} \\
&\leq \min\big\{\ell(Q') \mid Q' \in \mathcal{Q} \text{ and } \text{Dist}(Q, Q') + d(Q) \leq \mathbf{D}(\ell(Q) - \tfrac{1}{2})\big\}. \qquad (5.22)
\end{aligned}$$

One easily computes $\mathbf{D}(\ell(Q) - \frac{1}{2}) - d(Q) > \mathbf{D}(\ell(Q))$, which concludes the proof. □

Corollary 5.2.8. *Let $\mathcal{Q}$ be admissible, $Q \in \mathcal{Q}$ and*

$$U(Q) := \{x \in \overline{\Omega} \mid \text{Dist}(Q, x) < \mathbf{D}(\ell(Q))\}, \qquad (5.23)$$

then

$$\big\{Q' \in \mathcal{Q} \mid \text{Dist}(Q, Q') \leq \mathbf{D}(\ell(Q))\big\} = \{Q' \in \mathcal{Q} \mid Q' \cap U(Q) \neq \emptyset\}. \qquad (5.24)$$

Proof. This is a consequence of Lemma 5.2.7 in the strong version (5.22) that involves a bigger patch of Q. □

Throughout the rest of this chapter, for a given mesh $\mathcal{Q}$ and an element $Q \in \mathcal{Q}$, we will use the shortcut notation

$$\mathcal{Q} \cap U(Q) := \{Q' \in \mathcal{Q} \mid Q' \cap U(Q) \neq \emptyset\}. \qquad (5.25)$$

Proof of Proposition 5.2.6. Given the admissible mesh $\mathcal{Q}$ and marked elements $\mathcal{M} \subseteq \mathcal{Q}$ to be bisected, we have to show that there is a sequence of meshes that are subsequent admissible bisections, with $\mathcal{Q}$ being the first and $\text{REFINE\_TS}_{\text{2D}}(\mathcal{Q}, \mathcal{M})$ the last mesh in that sequence. Set $\widetilde{\mathcal{M}} := \text{CLOSURE\_TS}(\mathcal{Q}, \mathcal{M})$ and

$$\begin{aligned}
\overline{L} &:= 2 \max \ell(\widetilde{\mathcal{M}}), \quad \underline{L} := 2 \min \ell(\widetilde{\mathcal{M}}) \\
\mathcal{M}_j &:= \big\{Q \in \widetilde{\mathcal{M}} \mid 2\,\ell(Q) = j\big\} \qquad \text{for } j = \underline{L}, \dots, \overline{L} \\
\mathcal{Q}_{\underline{L}} &:= \mathcal{Q}, \quad \mathcal{Q}_{j+1} := \text{SUBDIVIDE}^{1/2}(\mathcal{Q}_j, \mathcal{M}_j) \text{ for } j = \underline{L}, \dots, \overline{L}. \qquad (5.26)
\end{aligned}$$

It follows that $\text{REFINE\_TS}_{\text{2D}}(\mathcal{Q}, \mathcal{M}) = \mathcal{Q}_{\overline{L}+1}$. We will show by induction over j that all bisections in (5.26) are admissible.

For the first step $j = \underline{L}$, we know $\{Q' \in \widetilde{\mathcal{M}} \mid 2\,\ell(Q') < \underline{L}\} = \emptyset$, and by construction of $\widetilde{\mathcal{M}}$ that for each $Q \in \mathcal{M}_{\underline{L}}$ holds $\{Q' \in \mathcal{Q} \cap U(Q) \mid \ell(Q') < \ell(Q)\} \subseteq \widetilde{\mathcal{M}}$. Together with $2\,\ell(Q) = \underline{L}$ follows for any $Q \in \mathcal{M}_{\underline{L}}$ that there is no $Q' \in \mathcal{Q} \cap U(Q)$ with $\ell(Q') < \ell(Q)$. This is, the bisections of all $Q \in \mathcal{M}_{\underline{L}}$ are admissible independently of their order and hence $\text{SUBDIVIDE}^{1/2}(\mathcal{Q}_{\underline{L}}, \mathcal{M}_{\underline{L}})$ is admissible.

Consider an arbitrary step $j \in \{\underline{L}, \dots, \overline{L}\}$ and assume that $\mathcal{Q}_{\underline{L}}, \dots, \mathcal{Q}_j$ are admissible meshes. Assume for contradiction that there is $\mathtt{Q} \in \mathcal{M}_j$ of which the bisection is not admissible, i.e., there exists $\mathtt{Q}' \in \mathcal{Q}_j \cap U(\mathtt{Q})$ with $\ell(\mathtt{Q}') < \ell(\mathtt{Q})$ and consequently $\mathtt{Q}' \notin \widetilde{\mathcal{M}}$, because $\mathtt{Q}'$ has not been bisected yet. It follows from the definition of CLOSURE_TS in Definition 5.2.3 that $\mathtt{Q}' \notin \mathcal{Q}$. Hence, there is $\hat{\mathtt{Q}} \in \mathcal{Q}$ such that $\mathtt{Q}' \subset \hat{\mathtt{Q}}$. We have $\ell(\hat{\mathtt{Q}}) < \ell(\mathtt{Q}') < \ell(\mathtt{Q})$, which implies $\ell(\hat{\mathtt{Q}}) < \ell(\mathtt{Q}) - \frac{1}{2}$. Note that $\mathtt{Q} \in \mathcal{Q}$ because $\mathcal{M}_j \subseteq \widetilde{\mathcal{M}} \subseteq \mathcal{Q}$. Moreover, from $\mathtt{Q}' \subset \hat{\mathtt{Q}}$ and $\mathtt{Q}' \in \mathcal{Q}_j \cap U(\mathtt{Q})$ it follows that $\hat{\mathtt{Q}} \in \mathcal{Q} \cap U(\mathtt{Q})$. Together with $\ell(\hat{\mathtt{Q}}) < \ell(\mathtt{Q}) - \frac{1}{2}$, Lemma 5.2.7 implies that $\mathcal{Q}$ is not admissible, which contradicts the assumption. □

Remark. Since for admissible bisections $\textsc{subdivide}^{1/2}(\mathcal{Q}, \{\mathtt{Q}\})$ holds

$$\textsc{subdivide}^{1/2}(\mathcal{Q}, \{\mathtt{Q}\}) = \textsc{refine\_ts}_{\text{2D}}(\mathcal{Q}, \{\mathtt{Q}\}), \tag{5.27}$$

all admissible meshes can be generated by $\textsc{refine\_ts}_{\text{2D}}$. This and Proposition 5.2.6 yield that the mesh class generated by $\textsc{refine\_ts}_{\text{2D}}$ is exactly the class of admissible meshes from Definition 5.2.5.

Theorem 5.2.9. *All admissible meshes (in the sense of Definition 5.2.5) are analysis-suitable.*

Proof. We prove the theorem by induction over admissible bisections. We know that the initial mesh $\mathcal{Q}_0$ is analysis-suitable because it is a tensor-product mesh without any T-junctions. Consider a sequence $\mathcal{Q}_0, \dots, \mathcal{Q}_J$ of successive admissible bisections such that $\mathcal{Q}_0, \dots, \mathcal{Q}_{J-1}$ are analysis-suitable. Without loss of generality we shall assume that elements are refined in ascending order with respect to their level, i.e., for $\mathcal{Q}_{j+1} = \textsc{subdivide}^{1/2}(\mathcal{Q}_j, \mathtt{Q}_j)$, we assume that $0 = \ell(\mathtt{Q}_0) \leq \dots \leq \ell(\mathtt{Q}_{J-1})$. There is such a sequence for any admissible mesh; see the proof of Proposition 5.2.21. We have to show that $\mathcal{Q}_J$ is analysis-suitable as well.

We denote $\mathtt{Q} \coloneqq \mathtt{Q}_{J-1} = [x, x+\tilde{x}] \times [y, y+\tilde{y}] \in \mathcal{Q}_{J-1}$, and we assume without loss of generality that $\ell(\mathtt{Q}) \in \mathbb{N}_0$. The assumption that elements are refined in ascending order with respect to their level implies that no element finer than $\mathtt{Q}$ has been bisected yet, i.e.,

$$\max \ell(\mathcal{Q}_J) = \ell(\mathtt{Q}) + \tfrac{1}{2}. \tag{5.28}$$

The uniform mesh $\mathcal{Q}_{\mathsf{u}[\ell(\mathtt{Q})+1/2]}$ is a refinement of $\mathcal{Q}_J$, in particular

$$\mathsf{hSk}(\mathcal{Q}_J) \;\subseteq\; \mathsf{hSk}(\mathcal{Q}_{\mathsf{u}[\ell(\mathtt{Q})+1/2]}) \;=\; \mathsf{hSk}(\mathcal{Q}_{\mathsf{u}[\ell(\mathtt{Q})]}), \tag{5.29}$$

since $\ell(\mathtt{Q}) \in \mathbb{N}_0$. Since $\mathcal{Q}_J$ is admissible, all elements in $\mathcal{Q}_J \cap U(\mathtt{Q})$ are at least of level $\ell(\mathtt{Q})$ and hence

$$\mathsf{hSk}(\mathcal{Q}_J) \cap U(\mathtt{Q}) \;\supseteq\; \mathsf{hSk}(\mathcal{Q}_{\mathsf{u}[\ell(\mathtt{Q})]}) \cap U(\mathtt{Q}). \tag{5.30}$$

and

$$\forall\, \tilde{\mathtt{Q}} \in \mathcal{Q}_J \cap U(\mathtt{Q}): \quad \operatorname{size}(\ell(\tilde{\mathtt{Q}})) \leq \operatorname{size}(\ell(\mathtt{Q})) \tag{5.31}$$

with the level-dependent size $\operatorname{size}(\ell(\mathtt{Q})) \coloneqq (\tilde{x}, \tilde{y}) = (2^{-\ell(\mathtt{Q})}, 2^{-\ell(\mathtt{Q})})$ since $\ell(\mathtt{Q}) \in \mathbb{N}_0$. If $\ell(\mathtt{Q})$ was non-integer, then the size would be $(2^{-\ell(\mathtt{Q})-1/2}, 2^{-\ell(\mathtt{Q})+1/2})$. Together, (5.29) and (5.30) read

$$\mathsf{hSk}(\mathcal{Q}_J) \cap U(\mathtt{Q}) \;=\; \mathsf{hSk}(\mathcal{Q}_{\mathsf{u}[\ell(\mathtt{Q})]}) \cap U(\mathtt{Q}). \tag{5.32}$$

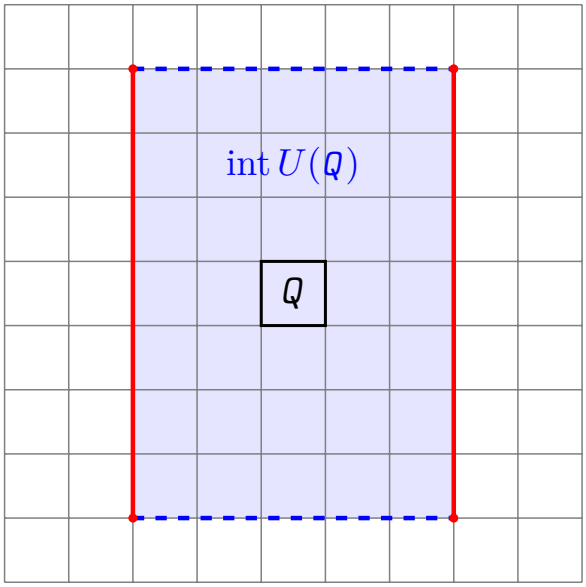

Figure 5.4: Example of the patch in a uniform mesh for $p = q = 5$. The horizontal T-junction $\tilde{T}$ may be on a solid red line or outside of $U(Q)$, but not in the interior of $U(Q)$ (shaded area) or on the dashed blue lines, which are open at their endpoints.

Consider a T-junction $T \in \mathcal{T}_J \setminus \mathcal{T}_{J-1}$ that is generated by the bisection of Q. Then T is a vertical T-junction on the boundary of Q, and with (5.31) follows

$$\operatorname{ext}(T) \subseteq \left\{x + \tilde{x}/2\right\} \times \left[y - 2^{-\ell(Q)}\left\lceil \tfrac{q}{2} \right\rceil,\ y + \tilde{y} + 2^{-\ell(Q)}\left\lceil \tfrac{q}{2} \right\rceil\right]. \tag{5.33}$$

Consider an arbitrary horizontal T-junction $\tilde{T} = (t_1, t_2) \in \mathcal{T}$. We will prove that $\operatorname{ext}(\tilde{T})$ does not intersect $\operatorname{ext}(T)$. From (5.29) we conclude that $\operatorname{ext}(\tilde{T}) \subseteq \mathsf{hSk}(\mathcal{Q}_{\mathrm{u}[\ell(Q)]})$, and (5.32) implies that the vertex $\tilde{T}$ is not in the interior of the patch of Q and not on its top or bottom boundary, i.e.

$$\tilde{T} \notin \left]x - 2^{-\ell(Q)}\left\lfloor \tfrac{p}{2} \right\rfloor,\ x + \tilde{x} + 2^{-\ell(Q)}\left\lfloor \tfrac{p}{2} \right\rfloor\right[\times \left[y - 2^{-\ell(Q)}\left\lceil \tfrac{q}{2} \right\rceil,\ y + \tilde{y} + 2^{-\ell(Q)}\left\lceil \tfrac{q}{2} \right\rceil\right]. \tag{5.34}$$

See Figure 5.4 for a sketch. Assume without loss of generality that $\tilde{T}$ is on the left side of Q, this is,

$$t_1 \leq x - 2^{-\ell(Q)}\left\lfloor \tfrac{p}{2} \right\rfloor. \tag{5.35}$$

If the element $Q_{\tilde{T}}$ (cf. Definition 5.1.3) is on the left side of $\tilde{T}$, then the edge-extension $\operatorname{ext}_e(\tilde{T})$ points towards Q in the sense that

$$\begin{aligned} & \forall\ (x, t_2) \in \operatorname{ext}(\tilde{T}) :\ \ x - t_1 \leq 2^{-\ell(Q)}\left\lfloor \tfrac{p}{2} \right\rfloor \overset{(5.35)}{\leq} x - t_1 \\ \Leftrightarrow\quad & \forall\ (x, t_2) \in \operatorname{ext}(\tilde{T}) :\ \ x \leq x < x + \tilde{x}/2. \end{aligned} \tag{5.36}$$

This means that $\operatorname{ext}(\tilde{T})$ does not intersect $\operatorname{ext}(T)$. See Figure 5.5a for an illustration.

If $Q_{\tilde{T}}$ is on the right side of $\tilde{T}$, then there are two finer elements with levels in $\mathbb{N}_0$ on the left side. Since there are no elements in $\mathcal{Q}_J$ with a level higher than $\ell(Q) + \frac{1}{2}$, which is non-integer, the two elements on the left side of $\tilde{T}$ have at most level

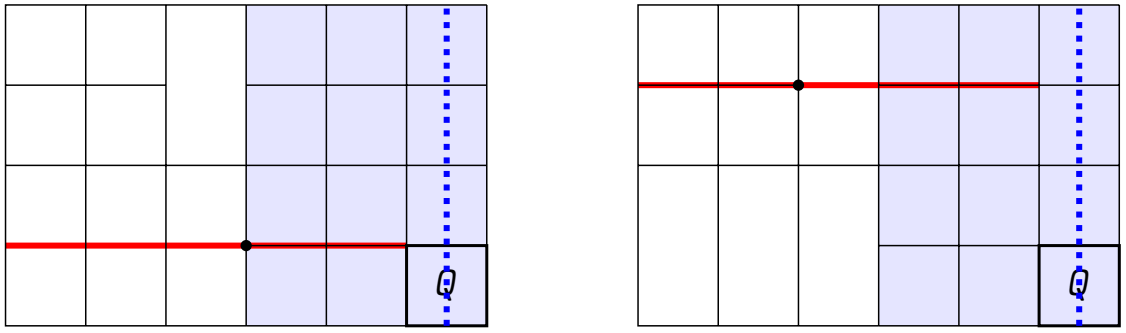

(a) (b)

Figure 5.5: In both cases, the T-junction extension $\mathrm{ext}(\tilde{T})$ (thick red line) does not intersect the set $\left\{x+\tilde{x}/2\right\} \times \left[y-2^{-\ell(Q)}\lceil\frac{q}{2}\rceil,\ y+\tilde{y}+2^{-\ell(Q)}\lceil\frac{q}{2}\rceil\right]$ (dotted blue line), which includes $\mathrm{ext}(T)$. The patch $\mathcal{Q}_J \cap U(Q)$ is shaded in light blue.

$\ell(Q)$, and hence $\ell(Q_{\tilde{T}}) \leq \ell(Q) - \frac{1}{2}$. Consequently, $Q' \notin \mathcal{Q}_J \cap U(Q)$, and the length of the intersection of the face extension $\mathrm{ext}_f(\tilde{T})$ with the patch of Q is at most $2^{-\ell(Q)}\left(\lceil\frac{p}{2}\rceil - 1\right) \leq 2^{-\ell(Q)}\left\lfloor\frac{p}{2}\right\rfloor$. This leads to the same result as the previous case and is illustrated in Figure 5.5b. Since $\tilde{T}$ was chosen arbitrary, $\mathcal{Q}_J$ is analysis-suitable. This concludes the proof. □

Corollary 5.2.10. *All admissible meshes provide T-splines that are non-negative, linearly independent, and form a partition of unity [31, 13]. Moreover, on each element $Q \in \mathcal{Q}$ in an admissible mesh $\mathcal{Q}$, there are not more than $2(p+1)(q+1)$ T-splines that have support on Q [13, Proposition 7.6].*

This means that on each element, each T-spline communicates only with a finite number of other T-splines, independent of the total number of functions. This is an important requirement for sparsity of the linear system to be solved in Finite Element Analysis, in the sense that every row and every column of a corresponding stiffness or mass matrix has at most $2(p+1)^2$ non-zero entries.

5.2.2 Nestedness

This section investigates the nesting behavior of the T-spline spaces corresponding to admissible meshes. In order to prove that nested admissible meshes induce nested spline spaces, we make use of Theorem 6.1 from [35]. Before presenting the Theorem, we briefly introduce necessary notations.

Definition 5.2.11 (Refinement relation)**.** For any partitions $\mathcal{Q}_1, \mathcal{Q}_2$ of $\overline{\Omega}$, we introduce the refinement relation "$\preceq$", which is defined using the overlay (see Section 5.2.3),

$$\mathcal{Q}_1 \preceq \mathcal{Q}_2 \quad \Leftrightarrow \quad \mathcal{Q}_1 \otimes \mathcal{Q}_2 = \mathcal{Q}_2. \tag{5.37}$$

Corollary 5.2.12. *Denote the* skeleton *of a mesh $\mathcal{Q}$ by $\mathsf{Sk}(\mathcal{Q}) := \mathsf{hSk}(\mathcal{Q}) \cup \mathsf{vSk}(\mathcal{Q})$. Then for rectangular partitions $\mathcal{Q}_1, \mathcal{Q}_2$ of $\overline{\Omega}$ holds the equivalence*

$$\mathcal{Q}_1 \preceq \mathcal{Q}_2 \quad \Leftrightarrow \quad \mathsf{Sk}(\mathcal{Q}_1) \subseteq \mathsf{Sk}(\mathcal{Q}_2). \tag{5.38}$$

Definition 5.2.13 (Extended mesh)**.** Given a rectangular partition $\mathcal{Q}$ of $\overline{\Omega}$, denote by $\mathrm{ext}(\mathcal{Q})$ the union of all T-junction extensions in the mesh $\mathcal{Q}$. Then the *extended mesh* $\mathcal{Q}^{\mathrm{ext}}$ is defined as the unique rectangular partition of $\overline{\Omega}$ such that

$$\mathsf{Sk}(\mathcal{Q}^{\mathrm{ext}}) = \mathsf{Sk}(\mathcal{Q}) \cup \mathrm{ext}(\mathcal{Q}). \tag{5.39}$$

Definition 5.2.14 (Mesh perturbation)**.** Given a partition $\mathcal{Q}$ of $\overline{\Omega}$ into axis-aligned rectangles, we define by $\mathrm{Ptb}(\mathcal{Q})$ the set of all continuous and invertible mappings $\delta : \overline{\Omega} \to \overline{\Omega}$ such that the corners $(0,0)$, $(M,0)$, (M,N), $(0,N)$ are fixed points of δ and

$$\delta(\mathcal{Q}) = \left\{ \delta(\mathtt{Q}) \mid \mathtt{Q} \in \mathcal{Q} \right\} \tag{5.40}$$

is also a partition of $\overline{\Omega}$ into axis-aligned rectangles.

This definition differs from the definition of pertubations given in [35], which we found difficult to reproduce in a formal manner. The subsequent Proposition 5.2.15 shows that our definition includes the understanding of perturbations from [35].

Remark. For $\delta \in \mathrm{Ptb}(\mathcal{Q})$, the perturbed mesh $\delta(\mathcal{Q})$ has the skeleton $\mathsf{Sk}(\delta(\mathcal{Q})) = \delta(\mathsf{Sk}(\mathcal{Q}))$. Hence, global index vectors can be defined according to Definition 5.1.4, and since all T-junctions in $\delta(\mathcal{Q})$ are of axis-parallel types ($\vdash, \perp, \dashv$, or $\top$), we can also apply Definition 5.1.7 for T-junction extensions in the perturbed mesh. Note in particular that the perturbation δ does not in general map T-junction extensions to the corresponding extensions in the perturbed mesh, i.e., if T is a T-junction in $\mathcal{Q}$, then

$$\mathrm{ext}_{\delta(\mathcal{Q})}(\delta(T)) \;\neq\; \delta(\mathrm{ext}_{\mathcal{Q}}(T)). \tag{5.41}$$

Proposition 5.2.15. *For any rectangular partition $\mathcal{Q}$ of $\overline{\Omega}$, there is some $\delta^* \in \mathrm{Ptb}(\mathcal{Q})$ such that any two T-junction face extensions in $\delta^*(\mathcal{Q})$ are disjoint.*

In the context of [35], this means that $\delta^*(\mathcal{Q})$ has no crossing vertices and no overlap vertices.

Proof. If all T-junction extensions in $\mathcal{Q}$ are pairwise disjoint, then δ^* is the identity map. If there exist T-junctions T_1, T_2 in $\mathcal{Q}$ with intersecting face extensions, then T_1 and T_2 are either both vertical or both horizontal T-junctions. Assume without loss of generality that T_1 and T_2 are vertical T-junctions. Since their (vertical) face extensions overlap, both T-junctions have the same x-coordinate t_0. Let $T_1 = (t_0, t_1)$ and $T_2 = (t_0, t_2)$, and assume $t_1 < t_2$. There exists $t_{1.5}$ with $t_1 \le t_{1.5} \le t_2$ such that at least one of the open segments $\{t_0\} \times (t_1, t_{1.5})$ and $\{t_0\} \times (t_{1.5}, t_2)$ does not intersect with the vertical skeleton $\mathsf{vSk}(\mathcal{Q})$. Assume that $\{t_0\} \times (t_1, t_{1.5}) \cap \mathsf{vSk}(\mathcal{Q}) = \emptyset$ and define

$$\begin{aligned} \overline{\Omega}_{x=t_0} &\coloneqq \left\{ (x,y) \in \overline{\Omega} \mid x = t_0 \right\} \\ \text{and } \mathcal{Q}_{x=t_0} &\coloneqq \left\{ \mathtt{Q} \in \mathcal{Q} \mid \mathtt{Q} \cap \overline{\Omega}_{x=t_0} \neq \emptyset \right\}. \end{aligned} \tag{5.42}$$

Let h be the length of the shortest edge in $\mathcal{Q}$, and set $\varepsilon \coloneqq h/2$. We define $\delta_{T_1 T_2}$ by

$$\delta_{T_1 T_2}(x,y) = \begin{cases} (x,y) & \text{if } (x,y) \in \bigcup(\mathcal{Q} \setminus \mathcal{Q}_{x=t_0}) \\ (x-\varepsilon, y) & \text{if } x = t_0 \text{ and } y < t_1 \\ (x+\varepsilon, y) & \text{if } x = t_0 \text{ and } y > t_{1.5} \\ \left(x + \frac{\varepsilon\,(2y - t_1 - t_{1.5})}{t_{1.5} - t_1}, y\right) & \text{if } x = t_0 \text{ and } t_1 \le y \le t_{1.5} \end{cases} \tag{5.43}$$

and elsewhere by horizontal linear interpolation, which is illustrated in Figure 5.6. The map $\delta_{T_1T_2}$ then satisfies the following properties.

1. $\delta_{T_1T_2}$ is in $\mathrm{Ptb}(\mathcal{Q})$.
2. The T-junction extensions of $\delta_{T_1T_2}(T_1)$ and $\delta_{T_1T_2}(T_2)$ do not intersect.
3. $\delta_{T_1T_2}$ does not lead to intersecting of T-junction extensions that did not intersect in the unperturbed mesh $\mathcal{Q}$.

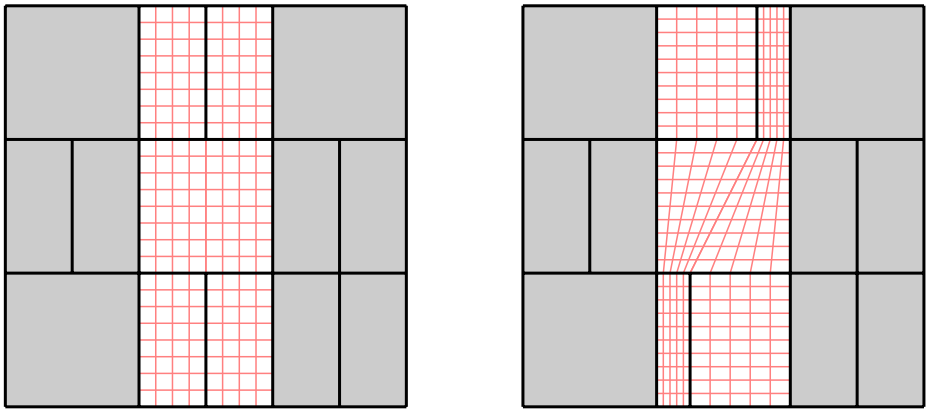

(a) The unperturbed mesh $\mathcal{Q}$. (b) The perturbed mesh $\delta_{T_1T_2}(\mathcal{Q})$.

Figure 5.6 [38]: Example for a perturbation $\delta_{T_1T_2}$. In the shaded area, $\delta_{T_1T_2}$ equals the identity map. In the non-shaded region, we underlaid a red grid to illustrate the behavior of $\delta_{T_1T_2}$.

A straight-forward proof shows that perturbations can be concatenated in the sense that

$$\delta_1 \in \mathrm{Ptb}(\mathcal{Q}),\ \delta_2 \in \mathrm{Ptb}(\delta_1(\mathcal{Q})) \ \Rightarrow\ \delta_2 \circ \delta_1 \in \mathrm{Ptb}(\mathcal{Q}). \tag{5.44}$$

This allows for the subsequent conclusion of the proof. Given the mesh $\mathcal{Q}_0 \coloneqq \mathcal{Q}$ choose an arbitrary pair (T_0, T_0') of T-junctions in $\mathcal{Q}$ such that their face extensions intersect, and set $\mathcal{Q}_1 \coloneqq \delta_{T_0T_0'}(\mathcal{Q}_0)$. Then choose (T_1, T_1') such that T_1 and T_1' are T-junctions with intersecting face extensions in $\mathcal{Q}_1$, construct $\delta_{T_1T_1'}$ as above, accounting that h and ε may have changed. Set $\mathcal{Q}_2 \coloneqq \delta_{T_1T_1'}(\mathcal{Q}_1)$. Repeat this until in a mesh $\mathcal{Q}_n$, there are no intersecting T-junction face extensions. Then $\delta^* \coloneqq \delta_{T_{n-1}T_{n-1}'} \circ \cdots \circ \delta_{T_0T_0'}$ is in $\mathrm{Ptb}(\mathcal{Q})$ and satisfies that all T-junction face extensions in $\delta^*(\mathcal{Q})$ are pairwise disjoint. □

Theorem 5.2.16 ([35, Theorem 6.1])**.** *Given two analysis-suitable meshes $\mathcal{Q}_1$ and $\mathcal{Q}_2$, if for all $\delta \in \mathrm{Ptb}(\mathcal{Q}_2)$ holds*

$$\big(\delta(\mathcal{Q}_1)\big)^{\mathrm{ext}} \preceq \big(\delta(\mathcal{Q}_2)\big)^{\mathrm{ext}}, \tag{5.45}$$

then the T-spline spaces corresponding to $\mathcal{Q}_1$ and $\mathcal{Q}_2$ are nested.

The main result of this section is the following.

Theorem 5.2.17. *Any two admissible meshes $\mathcal{Q}_1, \mathcal{Q}_2$ that are nested in the sense $\mathcal{Q}_1 \preceq \mathcal{Q}_2$ satisfy for all $\delta \in \mathrm{Ptb}(\mathcal{Q}_2)$*

$$\big(\delta(\mathcal{Q}_1)\big)^{\mathrm{ext}} \preceq \big(\delta(\mathcal{Q}_2)\big)^{\mathrm{ext}}. \tag{5.46}$$

Proof. According to Corollary 5.2.12, we have to show that

$$\mathrm{ext}\big(\delta(\mathcal{Q}_1)\big) \cup \mathsf{Sk}\big(\delta(\mathcal{Q}_1)\big) \;\subseteq\; \mathrm{ext}\big(\delta(\mathcal{Q}_2)\big) \cup \mathsf{Sk}\big(\delta(\mathcal{Q}_2)\big). \tag{5.47}$$

We prove this for $\mathcal{Q}_2$ being an admissible bisection of $\mathcal{Q}_1$. The claim then follows inductively for all admissible refinements of $\mathcal{Q}_1$. Let $\square \in \mathcal{Q}_1$ and let $\mathcal{Q}_2 \coloneqq \textsc{subdivide}^{1/2}(\mathcal{Q}_1, \square)$ be admissible. Since "$\preceq$" denotes an elementwise subset relation, it is preserved under the mapping δ. Thus, from $\mathcal{Q}_1 \preceq \mathcal{Q}_2$ follows $\delta(\mathcal{Q}_1) \preceq \delta(\mathcal{Q}_2)$ and consequently $\mathsf{Sk}\big(\delta(\mathcal{Q}_1)\big) \subseteq \mathsf{Sk}\big(\delta(\mathcal{Q}_2)\big)$. It remains to prove that

$$\mathrm{ext}\big(\delta(\mathcal{Q}_1)\big) \;\subseteq\; \mathrm{ext}\big(\delta(\mathcal{Q}_2)\big) \cup \mathsf{Sk}\big(\delta(\mathcal{Q}_2)\big). \tag{5.48}$$

Denote by $\mathcal{T}_1$ and $\mathcal{T}_2$ the set of T-junctions in $\mathcal{Q}_1$ and $\mathcal{Q}_2$, respectively. Assume without loss of generality that $\ell(\square) \in \mathbb{N}_0$, and consider an arbitrary T-junction T^δ in the mesh $\delta(\mathcal{Q}_1)$. Since δ is continuous and invertible, there is a one-to-one correspondence between the T-junctions in $\mathcal{Q}_1$ and $\delta(\mathcal{Q}_1)$, i.e., there is $T \in \mathcal{T}_1$ with $\delta(T) = T^\delta$, and T and T^δ are of the same type ($\vdash$, $\perp$, $\dashv$, or $\top$).

Case 1. $T \notin \square$. Then T is still a T-junction after bisecting $\square$, i.e., $T \in \mathcal{T}_2$. Consequently, T^δ is also a T-junction in $\delta(\mathcal{Q}_2)$.

Case 1a. T is a vertical T-junction. Since $\ell(\square)$ is assumed to be integer, its bisection does not affect the horizontal skeleton, i.e., $\mathsf{hSk}(\mathcal{Q}_1) = \mathsf{hSk}(\mathcal{Q}_2)$ and hence $\mathsf{hSk}(\delta(\mathcal{Q}_1)) = \mathsf{hSk}(\delta(\mathcal{Q}_2))$. Consquently, the T-junction extensions of T and T^δ are preserved,

$$\mathrm{ext}_{\mathcal{Q}_1}(T) = \mathrm{ext}_{\mathcal{Q}_2}(T) \;\text{ and }\; \mathrm{ext}_{\delta(\mathcal{Q}_1)}(T^\delta) = \mathrm{ext}_{\delta(\mathcal{Q}_2)}(T^\delta) \subseteq \mathrm{ext}\,\big(\delta(\mathcal{Q}_2)\big). \tag{5.49}$$

Case 1b. T is a horizontal T-junction. We will show that the corresponding T-junction extension in the pertubed mesh is preserved, i.e.,

$$\mathrm{ext}_{\delta(\mathcal{Q}_1)}(T^\delta) = \mathrm{ext}_{\delta(\mathcal{Q}_2)}(T^\delta). \tag{5.50}$$

Assume for contradiction that $\mathrm{ext}_{\delta(\mathcal{Q}_1)}(T^\delta) \neq \mathrm{ext}_{\delta(\mathcal{Q}_2)}(T^\delta)$. The bisection of $\square$ generates a vertical edge $E_\square \supseteq \mathsf{vSk}(\mathcal{Q}_2) \setminus \mathsf{vSk}(\mathcal{Q}_1)$, and we denote

$$E_\square^\delta \coloneqq \delta(E_\square) \supseteq \mathsf{vSk}(\delta(\mathcal{Q}_2)) \setminus \mathsf{vSk}(\delta(\mathcal{Q}_1)). \tag{5.51}$$

Obviously, $E_\square^\delta$ intersects with $\mathrm{ext}_{\delta(\mathcal{Q}_1)}(T^\delta)$, otherwise the T-junction extension would be the same in $\delta(\mathcal{Q}_2)$. Given $\square = [x, x+\tilde{x}] \times [y, y+\tilde{y}]$, we define the half-open domain $\square_{\mathrm{ho}} \coloneqq]x, x+\tilde{x}[\times [y, y+\tilde{y}]$, which is the rectangle $\square$ without its vertical edges. Then $E_\square \subset \square_{\mathrm{ho}}$ and hence $E_\square^\delta \subset \square_{\mathrm{ho}}^\delta \coloneqq \delta(\square_{\mathrm{ho}})$. Together, we have that $\mathrm{ext}_{\delta(\mathcal{Q}_1)}(T^\delta)$ intersects with $\square_{\mathrm{ho}}^\delta$. Since the bisection of $\square$ is admissible, we know from the proof of Theorem 5.2.9 that $\mathrm{ext}_{\mathcal{Q}_1}(T)$ does not intersect with $\square_{\mathrm{ho}}$ in the unperturbed mesh $\mathcal{Q}_1$. Define the T-environment

$$U(T) \coloneqq \bigcup_{\substack{\square' \in \mathcal{Q}_1 \\ \square'_{\mathrm{ho}} \cap \mathrm{ext}(T) \neq \emptyset}} \square', \tag{5.52}$$

as the union of all $\mathtt{Q}' \in \mathcal{Q}_1$ such that $\mathrm{ext}(T)$ intersects the corresponding half-open ${\mathtt{Q}'}_{\mathrm{ho}}$. Then $U(T)$ is a rectangular domain that does not intersect with $\mathtt{Q}_{\mathrm{ho}}$. Since for each $\mathtt{Q}' \subseteq U(T)$, the image $\delta(\mathtt{Q}')$ is a rectangle and since δ is continuous, $\delta\big(U(T)\big)$ is a rectangular domain that does not intersect with $\mathtt{Q}^\delta_{\mathrm{ho}}$. Moreover, since all edges and vertices in $U(T)$ are continuously mapped into $\delta\big(U(T)\big)$, we have $U(T^\delta) \subseteq \delta\big(U(T)\big)$. Together, we get that $U(T^\delta)$ does not intersect with $\mathtt{Q}^\delta_{\mathrm{ho}}$, hence $\mathrm{ext}_{\delta(\mathcal{Q}_1)}(T^\delta)$ does not intersect with $\mathtt{Q}^\delta_{\mathrm{ho}}$, which is the desired contradiction.

Case 2. $T \in \mathtt{Q}$. In Section 5.2, we assumed that $\mathbf{p} \geq 2$. This implies that all neighbors of $\mathtt{Q}$ are in $\mathcal{Q}_1 \cap U(\mathtt{Q})$ and that $\mathtt{Q}$ is in the patch of all those neighbors as well. Since $\mathcal{Q}_1$ is admissible, the level of a neighbor of $\mathtt{Q}$ is either $\ell(\mathtt{Q})$ or $\ell(\mathtt{Q}) + \frac{1}{2}$. Since $\ell(\mathtt{Q}) \in \mathbb{N}_0$, the T-junction T is vertical, and T^δ is a vertical T-junction as well. Since T is on the boundary of $\mathtt{Q}$, and the bisection of $\mathtt{Q}$ generates a vertical edge, T is not a T-junction anymore in $\mathcal{Q}_2$. Hence T^δ is a vertex, but not a T-junction in $\delta(\mathcal{Q}_2)$. The T-junction extension $\mathrm{ext}(T^\delta)$ hence only exists in $\delta(\mathcal{Q}_1)$. Consider the edge extension of T^δ.

Case 2a. $\mathrm{ext}_e(T^\delta) \subseteq \mathsf{vSk}(\delta(\mathcal{Q}_2))$. There is no problem with that.

Case 2b. $\mathrm{ext}_e(T^\delta) \not\subseteq \mathsf{vSk}(\delta(\mathcal{Q}_2))$. Then there exists some $\tilde{T}^\delta \in \mathrm{ext}_e(T^\delta)$ which is a T-junction in $\delta(\mathcal{Q}_2)$, such that

$$\mathrm{ext}_e(T^\delta) \subset \mathrm{ext}_{\delta(\mathcal{Q}_2)}(\tilde{T}^\delta) \subseteq \mathrm{ext}(\delta(\mathcal{Q}_2)). \tag{5.53}$$

The Cases 2a and 2b hold analogously for the face extension $\mathrm{ext}_f(T^\delta)$. Together, we have

$$\mathrm{ext}(T^\delta) \subseteq \mathrm{ext}(\delta(\mathcal{Q}_2)) \cup \mathsf{vSk}(\delta(\mathcal{Q}_2)), \tag{5.54}$$

which concludes the proof. □

The combination of Theorem 5.2.16 and 5.2.17 reads as follows.

Corollary 5.2.18. *For any two admissible meshes $\mathcal{Q}_1, \mathcal{Q}_2$ that are nested in the sense $\mathcal{Q}_1 \preceq \mathcal{Q}_2$, the corresponding T-spline spaces are also nested.*

5.2.3 Overlay

This section discusses the coarsest common refinement of two admissible meshes $\mathcal{Q}_1, \mathcal{Q}_2$, called *overlay* and denoted by $\mathcal{Q}_1 \otimes \mathcal{Q}_2$. We prove that the overlay of two admissible meshes is also admissible and has bounded cardinality in terms of the involved meshes. This is a classical result in the context of adaptive simplicial meshes and will be crucial for further analysis of adaptive algorithms (cf. Assumption (2.10) in [10]).

Definition 5.2.19 (Overlay)**.** We define the operator $\mathrm{Min}_\subseteq$ which yields all minimal elements of a set that is partially ordered by "$\subseteq$",

$$\mathrm{Min}_\subseteq(\mathcal{M}) \coloneqq \big\{ \mathtt{Q} \in \mathcal{M} \mid \forall \mathtt{Q}' \in \mathcal{M} : \mathtt{Q}' \subseteq \mathtt{Q} \Rightarrow \mathtt{Q}' = \mathtt{Q} \big\}. \tag{5.55}$$

The *overlay* of two admissible meshes $\mathcal{Q}_1, \mathcal{Q}_2$ is defined by

$$\mathcal{Q}_1 \otimes \mathcal{Q}_2 \coloneqq \mathrm{Min}_\subseteq\big(\mathcal{Q}_1 \cup \mathcal{Q}_2 \big). \tag{5.56}$$

Proposition 5.2.20. *$\mathcal{Q}_1 \otimes \mathcal{Q}_2$ is the coarsest refinement of $\mathcal{Q}_1$ and $\mathcal{Q}_2$ in the sense that for any $\hat{\mathcal{Q}}$ being a refinement of $\mathcal{Q}_1$ and $\mathcal{Q}_2$, and $\mathcal{Q}_1 \otimes \mathcal{Q}_2$ being a refinement of $\hat{\mathcal{Q}}$, it follows that $\hat{\mathcal{Q}} = \mathcal{Q}_1 \otimes \mathcal{Q}_2$.*

Proof. $\mathcal{Q}_1$ is a refinement of $\mathcal{Q}_2$ if and only if for each $\mathtt{Q}_1 \in \mathcal{Q}_1$, there is $\mathtt{Q}_2 \in \mathcal{Q}_2$ with $\mathtt{Q}_1 \subseteq \mathtt{Q}_2$, which is equivalent to $\mathcal{Q}_1 = \mathcal{Q}_1 \otimes \mathcal{Q}_2$. Given that $\mathcal{Q}_1 \otimes \hat{\mathcal{Q}} = \hat{\mathcal{Q}} = \mathcal{Q}_2 \otimes \hat{\mathcal{Q}}$ and $\mathcal{Q}_1 \otimes \mathcal{Q}_2 = (\mathcal{Q}_1 \otimes \mathcal{Q}_2) \otimes \hat{\mathcal{Q}}$, we have

$$\begin{aligned}\mathcal{Q}_1 \otimes \mathcal{Q}_2 &= (\mathcal{Q}_1 \otimes \mathcal{Q}_2) \otimes \hat{\mathcal{Q}} = \operatorname{Min}_{\subseteq}(\mathcal{Q}_1 \otimes \mathcal{Q}_2 \cup \hat{\mathcal{Q}}) \\ &= \operatorname{Min}_{\subseteq}(\operatorname{Min}_{\subseteq}(\mathcal{Q}_1 \cup \mathcal{Q}_2) \cup \hat{\mathcal{Q}}) = \operatorname{Min}_{\subseteq}(\mathcal{Q}_1 \cup \mathcal{Q}_2 \cup \hat{\mathcal{Q}}) \\ &= \operatorname{Min}_{\subseteq}(\mathcal{Q}_1 \cup \operatorname{Min}_{\subseteq}(\mathcal{Q}_2 \cup \hat{\mathcal{Q}})) = \operatorname{Min}_{\subseteq}(\mathcal{Q}_1 \cup \mathcal{Q}_2 \otimes \hat{\mathcal{Q}}) \\ &= \operatorname{Min}_{\subseteq}(\mathcal{Q}_1 \cup \hat{\mathcal{Q}}) = \mathcal{Q}_1 \otimes \hat{\mathcal{Q}} = \hat{\mathcal{Q}}. \end{aligned} \tag{5.57}$$

□

Proposition 5.2.21. *For any admissible meshes $\mathcal{Q}_1, \mathcal{Q}_2$, the overlay $\mathcal{Q}_1 \otimes \mathcal{Q}_2$ is also admissible.*

Proof. Consider the set of admissible elements which are coarser than elements of the overlay,

$$\mathcal{M} \coloneqq \Big\{ \mathtt{Q} \in \bigcup \mathbb{M}_{\text{TS}} \mid \exists \mathtt{Q}' \in \mathcal{Q}_1 \otimes \mathcal{Q}_2 : \mathtt{Q}' \subsetneq \mathtt{Q} \Big\}. \tag{5.58}$$

Then $\mathcal{Q}_1 \otimes \mathcal{Q}_2$ is the coarsest partition of $[0, M] \times [0, N]$ into elements from $\bigcup \mathbb{M}_{\text{TS}}$ that refines all elements occuring in $\mathcal{M}$. Note also that $\mathcal{M}$ satisfies

$$\forall\, \mathtt{Q}, \mathtt{Q}' \in \bigcup \mathbb{M}_{\text{TS}} : \quad \mathtt{Q} \in \mathcal{M} \wedge \mathtt{Q} \subseteq \mathtt{Q}' \Rightarrow \mathtt{Q}' \in \mathcal{M}. \tag{5.59}$$

For $j = 0, \dots, J = 2 \max \ell(\mathcal{M})$ and $\bar{\mathcal{Q}}_0 \coloneqq \mathcal{Q}_0$, set

$$\begin{aligned} \mathcal{M}_j &\coloneqq \{\mathtt{Q} \in \mathcal{M} \mid 2\,\ell(\mathtt{Q}) = j\} \\ \text{and} \quad \bar{\mathcal{Q}}_{j+1} &\coloneqq \textsc{subdivide}^{1/2}(\bar{\mathcal{Q}}_j, \mathcal{M}_j). \end{aligned} \tag{5.60}$$

Claim 1. For all $j \in \{0, \dots, J\}$ holds $\mathcal{M}_j \subseteq \bar{\mathcal{Q}}_j$. This is shown by induction over j. For $j = 0$, the claim is true because all elements of $\bigcup \mathbb{M}_{\text{TS}}$ with zero level are in $\mathcal{Q}_0$. Assume the claim to be true for $0, \dots, j-1$ and assume for contradiction that there exists $\mathtt{Q} \in \mathcal{M}_j \setminus \bar{\mathcal{Q}}_j$.

Since $\mathtt{Q}$ has not been bisected yet, $\bar{\mathcal{Q}}_j$ does not contain any $\mathtt{Q}'$ with $\mathtt{Q}' \subset \mathtt{Q}$. Consequently, there exists $\mathtt{Q}' \in \bar{\mathcal{Q}}_j$ with $\mathtt{Q} \subset \mathtt{Q}'$ and hence $\ell(\mathtt{Q}') < \ell(\mathtt{Q}) = \frac{j}{2}$. From (5.59) follows $\mathtt{Q}' \in \mathcal{M}_{\ell(\mathtt{Q}')} \in \mathcal{M}$, and $\ell(\mathtt{Q}') < \frac{j}{2}$ implies that $\mathtt{Q}'$ has been refined in a previous step. This yields $\mathtt{Q}' \notin \bar{\mathcal{Q}}_j$, which is the desired contradiction.

Claim 2. For all $j \in \{0, \dots, J\}$, the bisection (5.60) *is admissible.* Consider $\mathtt{Q} \in \mathcal{M}_j$ for an arbitrary j. By definition of $\mathcal{M}$, there exists $\mathtt{Q}' \in \mathcal{Q}_1 \otimes \mathcal{Q}_2 \subseteq \mathcal{Q}_1 \cup \mathcal{Q}_2$ with $\mathtt{Q}' \subsetneq \mathtt{Q}$. Without loss of generality, we assume $\mathtt{Q}' \in \mathcal{Q}_1$. Since $\mathcal{Q}_1$ is admissible, there is a sequence of admissible meshes $\mathcal{Q}_0 = \mathcal{Q}_{1|0}, \mathcal{Q}_{1|1}, \dots, \mathcal{Q}_{1|\mathcal{I}} = \mathcal{Q}_1$ and $i \in \{0, \dots, \mathcal{I}-1\}$ such that $\mathcal{Q}_{1|i+1} = \textsc{subdivide}^{1/2}(\mathcal{Q}_{1|i}, \{\mathtt{Q}\})$. The fact that $\mathcal{Q}_{1|i+1}$ is admissible (and that levels do not decrease during refinement) implies

$$\min \ell(\mathcal{Q}_1 \cap U(\mathtt{Q})) \geq \min \ell(\mathcal{Q}_{1|i} \cap U(\mathtt{Q})) \geq \ell(\mathtt{Q}) = \tfrac{j}{2}. \tag{5.61}$$

Assume for contradiction that there is $\tilde{\mathtt{Q}} \in \mathcal{Q}_j \cap U(\mathtt{Q})$ with $\ell(\tilde{\mathtt{Q}}) < \ell(\mathtt{Q}) = \frac{j}{2}$. This implies $\tilde{\mathtt{Q}} \notin \mathcal{M}$ (otherwise $\tilde{\mathtt{Q}}$ would have been bisected in a previous step). Moreover, (5.61) and Corollary 5.2.8 yield that there is $\tilde{\mathtt{Q}}' \in \mathcal{Q}_1 \cap U(\mathtt{Q})$ with $\tilde{\mathtt{Q}}' \subset \tilde{\mathtt{Q}}$ and hence $\tilde{\mathtt{Q}} \in \mathcal{M}$ in contradiction to $\tilde{\mathtt{Q}} \notin \mathcal{M}$ from before. This proves Claim 2.

The proven claims show $\mathcal{M}_j = \bar{\mathcal{Q}}_j \setminus \bar{\mathcal{Q}}_{j+1}$ for all $j = 0, \dots, J$ and hence for the admissible mesh $\bar{\mathcal{Q}}_{J+1}$ that there is no coarser partition of $[0, M] \times [0, N]$ into elements from $\bigcup \mathbb{M}_{\mathrm{TS}}$ that refines all elements in $\mathcal{M}$. This property defines a unique partition and hence $\mathcal{Q}_1 \otimes \mathcal{Q}_2 = \bar{\mathcal{Q}}_{J+1}$ is admissible. □

Lemma 5.2.22. *For all admissible meshes $\mathcal{Q}_1, \mathcal{Q}_2$ holds*

$$\#(\mathcal{Q}_1 \otimes \mathcal{Q}_2) + \#\mathcal{Q}_0 \leq \#\mathcal{Q}_1 + \#\mathcal{Q}_2 \ . \tag{5.62}$$

Proof. By definition, the overlay is a subset of the union of the two involved meshes, i.e.,

$$\mathcal{Q}_1 \otimes \mathcal{Q}_2 \ = \ \mathrm{Min}_{\subseteq}(\mathcal{Q}_1 \cup \mathcal{Q}_2) \ \subseteq \ \mathcal{Q}_1 \cup \mathcal{Q}_2 \ . \tag{5.63}$$

Define the shorthand notation $\mathcal{Q}(\mathtt{Q}) \coloneqq \{\mathtt{Q}' \in \mathcal{Q} \mid \mathtt{Q}' \subseteq \mathtt{Q}\}$. To prove the lemma, it suffices to show

$$\forall\ \mathtt{Q} \in \mathcal{Q}_0, \quad \#(\mathcal{Q}_1 \otimes \mathcal{Q}_2)(\mathtt{Q}) + 1 \leq \#\mathcal{Q}_1(\mathtt{Q}) + \#\mathcal{Q}_2(\mathtt{Q}) \ . \tag{5.64}$$

Case 1. $\mathcal{Q}_1(\mathtt{Q}) \subseteq (\mathcal{Q}_1 \otimes \mathcal{Q}_2)(\mathtt{Q})$. This implies equality and hence

$$\#(\mathcal{Q}_1 \otimes \mathcal{Q}_2)(\mathtt{Q}) + 1 = \#\mathcal{Q}_1(\mathtt{Q}) + 1 \leq \#\mathcal{Q}_1(\mathtt{Q}) + \#\mathcal{Q}_2(\mathtt{Q}) \ . \tag{5.65}$$

Case 2. There exists $\mathtt{Q}' \in \mathcal{Q}_1(\mathtt{Q}) \setminus (\mathcal{Q}_1 \otimes \mathcal{Q}_2)(\mathtt{Q})$. Then $(\mathcal{Q}_1 \otimes \mathcal{Q}_2)(\mathtt{Q}) = (\mathcal{Q}_1 \otimes \mathcal{Q}_2)(\mathtt{Q}) \setminus \{\mathtt{Q}'\}$ and hence

$$\begin{aligned} \#(\mathcal{Q}_1 \otimes \mathcal{Q}_2)(\mathtt{Q}) \ &= \ \#\big((\mathcal{Q}_1 \otimes \mathcal{Q}_2)(\mathtt{Q}) \setminus \{\mathtt{Q}'\}\big) \overset{(5.63)}{\leq} \ \#\big((\mathcal{Q}_1 \cup \mathcal{Q}_2)(\mathtt{Q}) \setminus \{\mathtt{Q}'\}\big) \\ &\leq \ \#(\mathcal{Q}_1 \setminus \{\mathtt{Q}\}) + \#\mathcal{Q}_2(\mathtt{Q}) \ = \ \#\mathcal{Q}_1(\mathtt{Q}) - 1 + \#\mathcal{Q}_2(\mathtt{Q}). \end{aligned} \tag{5.66}$$

□

5.2.4 Linear Complexity

This section is devoted to a complexity estimate in the style of a famous estimate for the Newest Vertex Bisection on triangular meshes given by Binev, Dahmen and DeVore [7] and, in an alternative version, by Stevenson [8]. The estimate reads as follows.

Theorem 5.2.23. *Any sequence of admissible meshes $\mathcal{Q}_0, \mathcal{Q}_1, \dots, \mathcal{Q}_J$ with*

$$\mathcal{Q}_j = \textsc{refine\_ts}_{2\mathrm{D}}(\mathcal{Q}_{j-1}, \mathcal{M}_{j-1}), \quad \mathcal{M}_{j-1} \subseteq \mathcal{Q}_{j-1} \quad \textit{for } j \in \{1, \dots, J\} \tag{5.67}$$

satisfies

$$|\mathcal{Q}_J \setminus \mathcal{Q}_0| \ \leq \ C_{5.2.23} \sum_{j=0}^{J-1} |\mathcal{M}_j| \ , \tag{5.68}$$

with $C_{5.2.23} = (2 + 2\sqrt{2})(4C_{5.2.26i} + 1)(4C_{5.2.26ii} + \sqrt{2})$ and $C_{5.2.26i}, C_{5.2.26ii}$ from Lemma 5.2.26 below.

Remark. Theorem 5.2.23 shows that, with regard to possible mesh gradings, the refinement algorithm is as flexible as successive bisection without the closure step. However, this result is non-trivial. Given an admissible mesh $\mathcal{Q}$ and an element $\mathtt{Q} \in \mathcal{Q}$ to be bisected, there is no uniform bound on the number of generated elements $\#(\textsc{refine\_ts}_{2\mathrm{D}}(\mathcal{Q}, \{\mathtt{Q}\}) \setminus \mathcal{Q})$. This is illustrated by the following example.

Example 5.2.24. Consider the case $p = 1$ and the initial mesh $\mathcal{Q}_0$ given through $M = 3$ and $N = 4$. Mark the element in the lower left corner of the mesh and compute the corresponding refinement $\mathcal{Q}_1$; repeat this step k times. Then there exists an element $\mathtt{Q}_k$ in $\mathcal{Q}_k$ such that $\#(\textsc{refine\_ts}_{2\mathrm{D}}(\mathcal{Q}_k, \mathtt{Q}_k) \setminus \mathcal{Q}_k) \geq k$. This is illustrated in Figure 5.7.

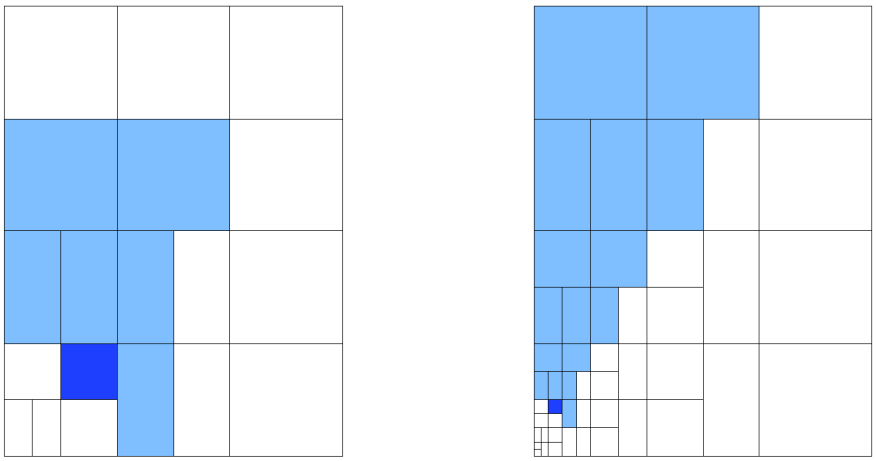

Figure 5.7 [38]: The mesh $\mathcal{Q}_3$ and the mesh $\mathcal{Q}_8$ from Example 5.2.24. The rectangles $\mathtt{Q}_3$ and $\mathtt{Q}_8$ are marked blue. The closures $\textsc{closure\_ts}(\mathcal{Q}_3, \{\mathtt{Q}_3\})$ and $\textsc{closure\_ts}(\mathcal{Q}_8, \{\mathtt{Q}_8\})$ are marked in light blue. Since the closure of $\mathtt{Q}_3$ consists of 7 elements, 14 elements will be generated if $\mathtt{Q}_3$ is bisected. Analogously, marking $\mathtt{Q}_8$ would cause the generation of 34 new elements.

Example 5.2.25. The large constant $C_{5.2.23}$ is not observed in practise. For $p = 3$, we constructed for each $J \in \{1, \dots, 2000\}$ a sequence $\mathcal{Q}_0, \mathcal{Q}_1, \dots, \mathcal{Q}_J$ with $\mathcal{Q}_{j+1} = \textsc{subdivide}^{1/2}(\mathcal{Q}_j, \mathtt{Q}_j)$ and $\mathtt{Q}_j \in \mathcal{Q}_j$ of uniform random choice. The ratio $|\mathcal{Q}_J| / J$ was below 6 (see Figure 5.8), instead of the theoretical upper bound $C_{5.2.23}|_{p=3} \approx 6\,042$ from Theorem 5.2.23. We applied this procedure for $p = 2, \dots, 9$. The results are listed in Table 5.1. In Table 5.2, we listed similar results for $J \in \{1, \dots, 100\}$, always marking the element in the lower left corner. In that case, the observed ratios are higher, but still orders of magnitude below the corresponding theoretical bounds.

We devote the rest of this section to proving Theorem 5.2.23.

Lemma 5.2.26. *Given an admissible mesh $\mathcal{Q}$, $\mathcal{M} \subseteq \mathcal{Q}$ and $\mathtt{Q} \in \textsc{refine\_ts}_{2\mathrm{D}}(\mathcal{Q}, \mathcal{M}) \setminus \mathcal{Q}$, there exists $\mathtt{Q}' \in \mathcal{M}$ such that $\ell(\mathtt{Q}) \leq \ell(\mathtt{Q}') + \frac{1}{2}$ and*

$$\operatorname{Dist}(\mathtt{Q}, \mathtt{Q}') \leq 2^{-\ell(\mathtt{Q})}(C_{5.2.26i}, C_{5.2.26ii}), \tag{5.69}$$

with "$\leq$" understood componentwise and constants

$$C_{5.2.26i} := \left(1 + 2^{-1/2}\right) p + 1 + \tfrac{5}{4}\sqrt{2}, \quad C_{5.2.26ii} := \left(1 + \sqrt{2}\right) p + \tfrac{3}{2} + \sqrt{2}. \tag{5.70}$$

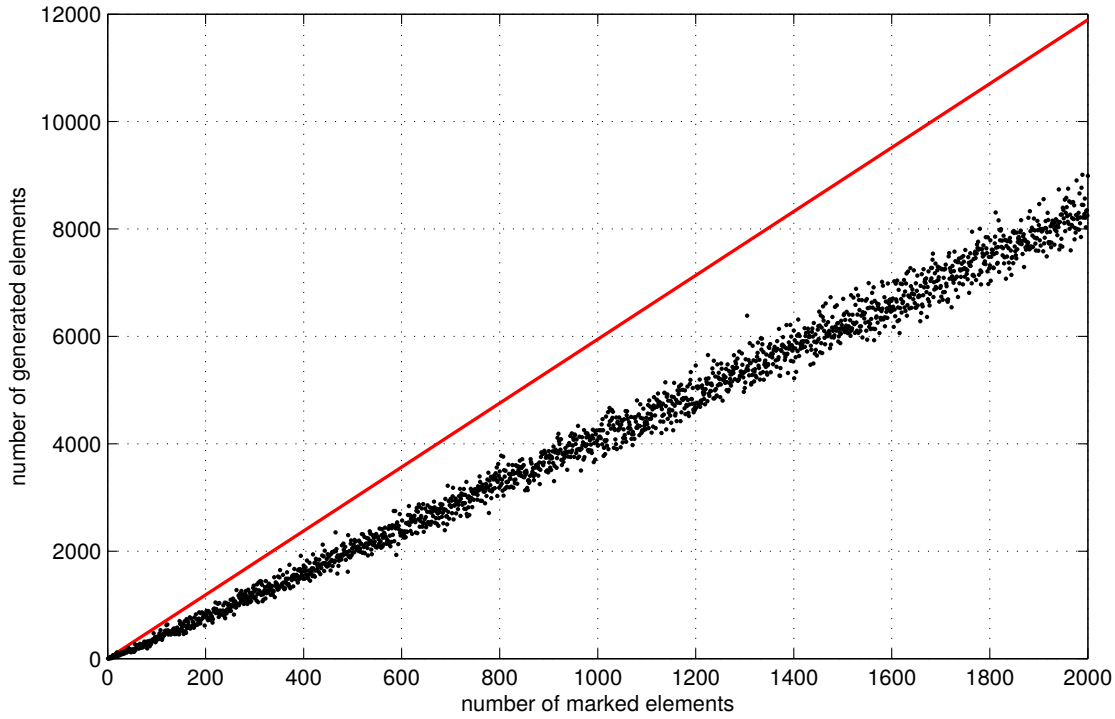

Figure 5.8 [38]: Generated and marked elements for randomly refined admissible meshes for $p = 3$. Each black dot corresponds to a sequence of random admissible refinements. The red line depicts the highest observed ratio (≈ 5.95). The median of the observed ratios is ≈ 4.09.

Table 5.1: Maximal observed ratios of generated and marked elements for random refinement.

p	2	3	4	5	6	7	8	9
$\tilde{C}$	6	8	9	10	12	13	16	23

Proof. The coefficient $\mathbf{D}(k)$ from Definition 5.2.3 is bounded by

$$\mathbf{D}(k) \leq \left((p+\sqrt{2})\,2^{-k-1},\ (p+\sqrt{2})\,2^{-k-1/2}\right) \quad \text{for all } k \in \mathbb{N}. \tag{5.71}$$

Hence for $\tilde{\mathtt{Q}} \in \mathcal{Q}$, any $\tilde{\mathtt{Q}}' \in \mathcal{Q} \cap U(\tilde{\mathtt{Q}})$ satisfies

$$\operatorname{Dist}(\tilde{\mathtt{Q}}, \tilde{\mathtt{Q}}') \leq 2^{-\ell(\tilde{\mathtt{Q}})} \left(\tfrac{p+\sqrt{2}}{2},\ \tfrac{p}{\sqrt{2}} + 1\right). \tag{5.72}$$

The existence of $\mathtt{Q} \in \textsc{refine\_ts}_{2\mathrm{D}}(\mathcal{Q}, \mathcal{M}) \setminus \mathcal{Q}$ means that $\textsc{refine\_ts}_{2\mathrm{D}}$ bisects $\mathtt{Q}' = \mathtt{Q}_J, \mathtt{Q}_{J-1}, \ldots, \mathtt{Q}_0$ such that $\mathtt{Q}_{j-1} \in \mathcal{Q} \cap U(\mathtt{Q}_j)$ and $\ell(\mathtt{Q}_{j-1}) < \ell(\mathtt{Q}_j)$ for $j = J, \ldots, 1$, having $\mathtt{Q}' \in \mathcal{M}$ and $\mathtt{Q} \in \textsc{subdivide}^{1/2}(\mathtt{Q}_0)$. Lemma 5.2.7 yields $\ell(\mathtt{Q}_{j-1}) = \ell(\mathtt{Q}_j) - 1$

Table 5.2: Maximal observed ratios of generated and marked elements when refining the lower left corner.

p	2	3	4	5	6	7	8	9
$\tilde{C}$	24	46	91	132	202	260	355	431

for $j = J, \dots, 1$, which allows for the estimate

$$\begin{aligned}
\operatorname{Dist}(\mathtt{Q}', \mathtt{Q}_0) &\leq \sum_{j=1}^{J} \operatorname{Dist}(\mathtt{Q}_j, \mathtt{Q}_{j-1}) \overset{(5.72)}{\leq} \sum_{j=1}^{J} 2^{-\ell(\mathtt{Q}_j)} \left(\tfrac{p+\sqrt{2}}{2},\ \tfrac{p}{\sqrt{2}} + 1\right) \\
&= \sum_{j=1}^{J} 2^{-(\ell(\mathtt{Q}_0)+j)} \left(\tfrac{p+\sqrt{2}}{2},\ \tfrac{p}{\sqrt{2}} + 1\right) \\
&< 2^{-\ell(\mathtt{Q}_0)} \left(\tfrac{p+\sqrt{2}}{2},\ \tfrac{p}{\sqrt{2}} + 1\right) \sum_{j=1}^{\infty} 2^{-j} \\
&= (1+\sqrt{2})\, 2^{-\ell(\mathtt{Q}_0)} \left(\tfrac{p+\sqrt{2}}{2},\ \tfrac{p}{\sqrt{2}} + 1\right) \\
&= (2+\sqrt{2})\, 2^{-\ell(\mathtt{Q})} \left(\tfrac{p+\sqrt{2}}{2},\ \tfrac{p}{\sqrt{2}} + 1\right). \qquad (5.73)
\end{aligned}$$

The estimate $\operatorname{Dist}(\mathtt{Q}_0, \mathtt{Q}) \leq 2^{-2-\ell(\mathtt{Q}_0)} \left(1, \sqrt{2}\right)$ and a triangle inequality conclude the proof. □

Proof of Theorem 5.2.23.
(1) For $\mathtt{Q} \in \bigcup \mathbb{M}_{\mathrm{TS}}$ and $\mathtt{Q}' \in \mathcal{M} \coloneqq \mathcal{M}_0 \cup \cdots \cup \mathcal{M}_{J-1}$, define $\lambda(\mathtt{Q}, \mathtt{Q}')$ by

$$\lambda(\mathtt{Q}, \mathtt{Q}') \coloneqq \begin{cases} 2^{(\ell(\mathtt{Q}) - \ell(\mathtt{Q}'))} & \text{if } \ell(\mathtt{Q}) \leq \ell(\mathtt{Q}') + \frac{1}{2} \\ & \quad \text{and } \operatorname{Dist}(\mathtt{Q}, \mathtt{Q}') < 2^{1-\ell(\mathtt{Q})}(C_{5.2.26i}, C_{5.2.26ii}), \\ 0 & \text{otherwise.} \end{cases} \qquad (5.74)$$

(2) *Main idea of the proof.*

$$\begin{aligned}
|\mathcal{Q}_J \setminus \mathcal{Q}_0| = \sum_{\mathtt{Q} \in \mathcal{Q}_J \setminus \mathcal{Q}_0} 1 &\overset{(3)}{\leq} \sum_{\mathtt{Q} \in \mathcal{Q}_J \setminus \mathcal{Q}_0} \sum_{\mathtt{Q}' \in \mathcal{M}} \lambda(\mathtt{Q}, \mathtt{Q}') \\
&\overset{(4)}{\leq} \sum_{\mathtt{Q}' \in \mathcal{M}} C_{5.2.23} = C_{5.2.23} \sum_{j=0}^{J-1} |\mathcal{M}_j|. \qquad (5.75)
\end{aligned}$$

(3) *Each* $\mathtt{Q} \in \mathcal{Q}_J \setminus \mathcal{Q}_0$ *satisfies*

$$\sum_{\mathtt{Q}' \in \mathcal{M}} \lambda(\mathtt{Q}, \mathtt{Q}') \ \geq\ 1. \qquad (5.76)$$

Consider $\mathsf{Q} \in \mathcal{Q}_J \setminus \mathcal{Q}_0$. Set $j_1 < J$ such that $\mathsf{Q} \in \mathcal{Q}_{j_1+1} \setminus \mathcal{Q}_{j_1}$. Lemma 5.2.26 states the existence of $\mathsf{Q}_1 \in \mathcal{M}_{j_1}$ with $\mathrm{Dist}(\mathsf{Q}, \mathsf{Q}_1) \leq 2^{-\ell(\mathsf{Q})}(C_{5.2.26i}, C_{5.2.26ii})$ and $\ell(\mathsf{Q}) \leq \ell(\mathsf{Q}_1) + \frac{1}{2}$. Hence $\lambda(\mathsf{Q}, \mathsf{Q}_1) = 2^{\ell(\mathsf{Q})-\ell(\mathsf{Q}_1)} > 0$. The repeated use of Lemma 5.2.26 yields $j_1 > j_2 > j_3 > \dots$ and $\mathsf{Q}_2, \mathsf{Q}_3, \dots$ with $\mathsf{Q}_{i-1} \in \mathcal{Q}_{j_i+1} \setminus \mathcal{Q}_{j_i}$ and $\mathsf{Q}_i \in \mathcal{M}_{j_i}$ such that

$$\mathrm{Dist}(\mathsf{Q}_{i-1}, \mathsf{Q}_i) \leq 2^{-\ell(\mathsf{Q}_{i-1})}(C_{5.2.26i}, C_{5.2.26ii}) \text{ and } \ell(\mathsf{Q}_{i-1}) \leq \ell(\mathsf{Q}_i) + \tfrac{1}{2}. \tag{5.77}$$

We repeat applying Lemma 5.2.26 as $\lambda(\mathsf{Q}, \mathsf{Q}_i) > 0$ and $\ell(\mathsf{Q}_i) > 0$, and we stop at the first index L with $\lambda(\mathsf{Q}, \mathsf{Q}_L) = 0$ or $\ell(\mathsf{Q}_L) = 0$. If $\ell(\mathsf{Q}_L) = 0$ and $\lambda(\mathsf{Q}, \mathsf{Q}_L) > 0$, then

$$\sum_{\mathsf{Q}' \in \mathcal{M}} \lambda(\mathsf{Q}, \mathsf{Q}') \geq \lambda(\mathsf{Q}, \mathsf{Q}_L) = 2^{(\ell(\mathsf{Q})-\ell(\mathsf{Q}_L))} \geq \sqrt{2}. \tag{5.78}$$

If $\lambda(\mathsf{Q}, \mathsf{Q}_L) = 0$ because $\ell(\mathsf{Q}) > \ell(\mathsf{Q}_L) + \frac{1}{2}$, then (5.77) yields $\ell(\mathsf{Q}_{L-1}) \leq \ell(\mathsf{Q}_L) + \frac{1}{2} < \ell(\mathsf{Q})$ and hence

$$\sum_{\mathsf{Q}' \in \mathcal{M}} \lambda(\mathsf{Q}, \mathsf{Q}') \geq \lambda(\mathsf{Q}, \mathsf{Q}_{L-1}) = 2^{(\ell(\mathsf{Q})-\ell(\mathsf{Q}_{L-1}))} \geq \sqrt{2}. \tag{5.79}$$

If $\lambda(\mathsf{Q}, \mathsf{Q}_L) = 0$ because $\mathrm{Dist}(\mathsf{Q}, \mathsf{Q}_L) \not< 2^{1-\ell(\mathsf{Q})}(C_{5.2.26i}, C_{5.2.26ii})$, then $\mathrm{Dist}_1(\mathsf{Q}, \mathsf{Q}_L) \geq 2^{1-\ell(\mathsf{Q})}C_{5.2.26i}$ or $\mathrm{Dist}_2(\mathsf{Q}, \mathsf{Q}_L) \geq 2^{1-\ell(\mathsf{Q})}C_{5.2.26ii}$. We assume without loss of generality the first, and a triangle inequality shows

$$2^{1-\ell(\mathsf{Q})}C_{5.2.26i} \;\leq\; \mathrm{Dist}_1(\mathsf{Q}, \mathsf{Q}_1) + \sum_{i=1}^{L-1} \mathrm{Dist}_1(\mathsf{Q}_i, \mathsf{Q}_{i+1}) \;\leq\; 2^{-\ell(\mathsf{Q})}C_{5.2.26i} + \sum_{i=1}^{L-1} 2^{-\ell(\mathsf{Q}_i)}C_{5.2.26i}, \tag{5.80}$$

and hence $2^{-\ell(\mathsf{Q})} \leq \sum_{i=1}^{L-1} 2^{-\ell(\mathsf{Q}_i)}$. The proof is concluded with

$$1 \;\leq\; \sum_{i=1}^{L-1} 2^{(\ell(\mathsf{Q})-\ell(\mathsf{Q}_i))} \;=\; \sum_{i=1}^{L-1} \lambda(\mathsf{Q}, \mathsf{Q}_i) \;\leq\; \sum_{\mathsf{Q}' \in \mathcal{M}} \lambda(\mathsf{Q}, \mathsf{Q}'). \tag{5.81}$$

(4) *For all $j \in \{0, \dots, J-1\}$ and $\mathsf{Q}' \in \mathcal{M}_j$ holds*

$$\sum_{\mathsf{Q} \in \mathcal{Q}_J \setminus \mathcal{Q}_0} \lambda(\mathsf{Q}, \mathsf{Q}') \;\leq\; (2 + 2\sqrt{2})(4C_{5.2.26i} + 1)(4C_{5.2.26ii} + \sqrt{2}) \;=\; C_{5.2.23}\,. \tag{5.82}$$

This is shown as follows. By definition of λ, we have

$$\sum_{\mathsf{Q} \in \mathcal{Q}_J \setminus \mathcal{Q}_0} \lambda(\mathsf{Q}, \mathsf{Q}') \leq \sum_{\mathsf{Q} \in \bigcup \mathbb{M}_{\mathrm{TS}} \setminus \mathcal{Q}_0} \lambda(\mathsf{Q}, \mathsf{Q}')$$

$$= \sum_{j=1}^{2\cdot\ell(\mathsf{Q}')+1} 2^{j/2-\ell(\mathsf{Q}')} \, \#\underbrace{\left\{\mathsf{Q} \in \bigcup \mathbb{M}_{\mathrm{TS}} \mid \ell(\mathsf{Q}) = \tfrac{j}{2} \text{ and } \mathrm{Dist}(\mathsf{Q}, \mathsf{Q}') < 2^{1-j/2}(C_{5.2.26i}, C_{5.2.26ii})\right\}}_{B}. \tag{5.83}$$

Since we know by definition of the level that $\ell(\mathtt{Q}) = \frac{j}{2}$ implies $|\mathtt{Q}| = 2^{-j}$, we know that $2^j \left|\bigcup B\right|$ is an upper bound of $\#B$. The rectangular set $\bigcup B$ is the union of all admissible elements of level $\frac{j}{2}$ having their midpoints inside a rectangle of size

$$2^{2-j/2} C_{5.2.26i} \times 2^{2-j/2} C_{5.2.26ii}. \tag{5.84}$$

An admissible element of level $\frac{j}{2}$ is not bigger than $2^{-j/2} \times 2^{(-j-1/2)}$. Together, we have

$$\left|\bigcup B\right| \leq 2^{-j}(4C_{5.2.26i} + 1)(4C_{5.2.26ii} + \sqrt{2}), \tag{5.85}$$

and hence $\#B \leq (4C_{5.2.26i} + 1)(4C_{5.2.26ii} + \sqrt{2})$. An index substitution $k \coloneqq 1 - j + 2{\cdot}\ell(\mathtt{Q}')$ proves the claim with

$$\sum_{j=1}^{2\cdot\ell(\mathtt{Q}')+1} 2^{j/2-\ell(\mathtt{Q}')} = \sum_{k=0}^{2\cdot\ell(\mathtt{Q}')} 2^{(1-k)/2} < \sqrt{2} + \sum_{k=0}^{\infty} 2^{-k/2} = \sqrt{2} + \tfrac{\sqrt{2}}{\sqrt{2}-1} = 2 + 2\sqrt{2}. \tag{5.86}$$

□

5.3 AST-splines in nD

In this section, we generalize the mesh class $\mathbb{M}_{\text{TS}}$ to higher dimension d, a polynomial degree $\mathbf{p} = (p_1, \dots, p_d)$ that may vary between dimensions, as well as an arbitrary (but fixed) number q of children in each element's subdivision. We will call q the *grading parameter*. Subsequently, we define multivariate T-splines corresponding to these generalized meshes, and introduce an abstract version of analysis-suitability. We will stick closely to the structure of the preceding sections.

Definition 5.3.1 (Intermediate uniform meshes)**.** For each level $k \in \mathbb{N}$ and $j \in \{1, \dots, d\}$, we define the tensor-product mesh

$$\begin{aligned}\mathcal{Q}_{\mathtt{u}[k+j/d]} \coloneqq \Big\{ &[x_1 - q^{-k-1}, x_1] \times \cdots \times [x_j - q^{-k-1}, x_j] \times \\ &\times [x_{j+1} - q^{-k}, x_{j+1}] \times \cdots \times [x_d - q^{-k}, x_d] \\ &\mid q^{k+1} x_i \in \{1, \dots, q^{k+1} N_i\} \text{ for } i = 1, \dots, j \\ &\text{and } \; q^k x_i \in \{1, \dots, q^k N_i\} \quad \text{for } i = j+1, \dots, d \Big\}. \end{aligned} \tag{5.87}$$

The class of uniform meshes, including the above-defined intermediate uniform meshes, is denoted by

$$\mathbb{M}^{1/d}_{\text{UNIFORM}} \coloneqq \{\mathcal{Q}_{\mathtt{u}[k]} \mid d{\cdot}k \in \mathbb{N}_0\} \supset \mathbb{M}_{\text{UNIFORM}}. \tag{5.88}$$

For the use of T-splines, the underlying rectangular mesh $\mathcal{Q}$ may, similiarly to the preceeding chapters, consist of finitely many elements from meshes in $\mathbb{M}^{1/d}_{\text{UNIFORM}}$, such

that any two elements of $\mathcal{Q}$ have disjoint interior, and the union of all elements of $\mathcal{Q}$ is the same domain $[0, N_1] \times \cdots \times [0, N_d]$ that is covered by uniform meshes.

$$\mathbb{M}_{\text{TS}} \coloneqq \Big\{ \mathcal{Q} \subset \bigcup_{\mathcal{Q}' \in \mathbb{M}^{1/d}_{\text{UNIFORM}}} \mathcal{Q}' \mid \#\mathcal{Q} < \infty,\ \bigcup \mathcal{Q} = [0, N_1] \times \cdots \times [0, N_d], \\ \forall Q, Q' \in \mathcal{Q} :\ \operatorname{int}(Q) \cap \operatorname{int}(Q') = \emptyset \Big\}. \tag{5.89}$$

Definition 5.3.2 (Nodes)**.** For each element $Q = [x_1, x_1 + \tilde{x}_1] \times \cdots \times [x_d, x_d + \tilde{x}_d]$, the corresponding set of *nodes* is denoted by

$$\mathsf{N}(Q) \coloneqq \{x_1, x_1 + \tilde{x}_1\} \times \cdots \times \{x_d, x_d + \tilde{x}_d\}. \tag{5.90}$$

Given a mesh $\mathcal{Q}$, we set $\mathsf{N}(\mathcal{Q}) \coloneqq \bigcup_{Q \in \mathcal{Q}} \mathsf{N}(Q)$, if only one mesh $\mathcal{Q}$ is considered in the context, we abbreviate $\mathsf{N} \coloneqq \mathsf{N}(\mathcal{Q})$.

Definition 5.3.3 (Skeleton)**.** Given a mesh $\mathcal{Q}$, denote the union of all (closed) element faces that are orthogonal to the first dimension by $\mathsf{Sk}_1(\mathcal{Q}) \coloneqq \bigcup_{Q \in \mathcal{Q}} \mathsf{Sk}_1(Q)$, with

$$\mathsf{Sk}_1(Q) \coloneqq \{x_1, x_1 + \tilde{x}_1\} \times [x_2, x_2 + \tilde{x}_2] \times \cdots \times [x_d, x_d + \tilde{x}_d] \\ \text{for any } Q = [x_1, x_1 + \tilde{x}_1] \times \cdots \times [x_d, x_d + \tilde{x}_d] \in \mathcal{Q}. \tag{5.91}$$

We call $\mathsf{Sk}_1(\mathcal{Q})$ the *1-orthogonal skeleton*. Analogously, we denote the *j-orthogonal skeleton* by $\mathsf{Sk}_j(\mathcal{Q})$ for all $j = 1, \ldots, d$. Similarly to the above Definition, we abbreviate $\mathsf{Sk}_j \coloneqq \mathsf{Sk}_J(\mathcal{Q})$ if only one mesh $\mathcal{Q}$ is considered in the context. Note that $\mathsf{Sk}_1 \cap \cdots \cap \mathsf{Sk}_d = \mathsf{N}$.

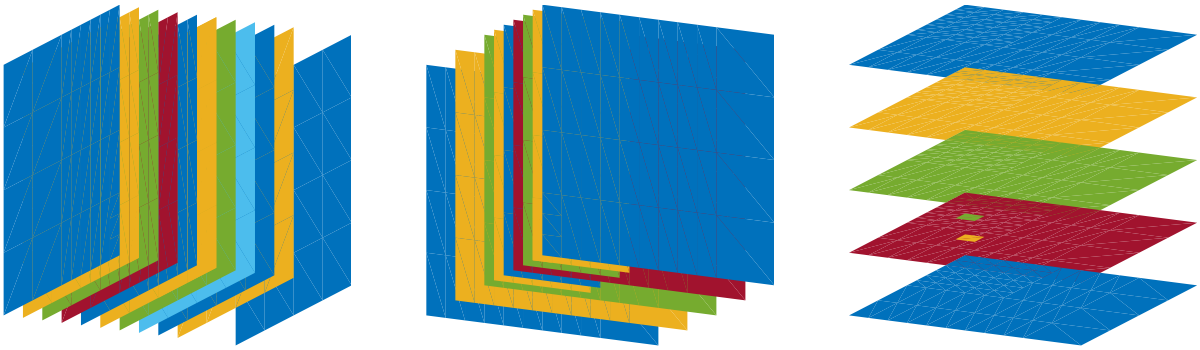

Figure 5.9 [34]: 1-orthogonal, 2-orthogonal and 3-orthogonal skeleton of the 3D mesh from Figure 5.15.

Definition 5.3.4 (Global index sets)**.** For any $v = (v_1, \ldots, v_d) \in \mathbb{R}^d$ and $j \in \{1, \ldots, d\}$, we define

$$\mathsf{K}_j(v) \coloneqq \big\{ z \in [0, N_j] \mid (v_1, \ldots, v_{j-1}, z, v_{j+1}, \ldots, v_d) \in \mathsf{Sk}_j \big\} \\ \cup \big\{ -\lceil \tfrac{p_j}{2} \rceil, \ldots, -1, N_j + 1, \ldots, N_j + \lceil \tfrac{p_j}{2} \rceil \big\}. \tag{5.92}$$

Definition 5.3.5 (Local index vectors)**.** To each node $v \in \mathsf{N}$ and each dimension $j = 1, \dots, d$, we associate a *local index vector* $\mathsf{k}_j(v) \in \mathbb{R}^{p_j+2}$, which is obtained by taking the unique $p_j + 2$ consecutive elements in $\mathsf{K}_j(v)$ having v_j as their $\frac{p_j+3}{2}$-th (this is, the middle) entry.

Definition 5.3.6 (T-spline)**.** We associate to each node $v \in \mathsf{N}$ a multivariate B-spline, referred as *T-spline*, defined as the product of the B-splines on the corresponding local index vectors,

$$B_v(x_1, \dots, x_d) \coloneqq N_{\mathsf{k}_1(v)}(x_1) \cdots N_{\mathsf{k}_d(v)}(x_d). \tag{5.93}$$

We define analysis-suitability in the multidimensional setting below. Similarly to the 2D case before, we construct T-junction extensions, and define analysis-suitability as the absence of intersections of these T-junction extensions. In contrast to the 2D case, we will not differentiate between possible kinds of T-junctions, but we will give an abstract definition of T-junction extensions as the intersection of domain slices with particular T-spline supports. Subsequent to these definitions, we explain dual-compatibility in nD and show that all analysis-suitable meshes are dual-compatible, which is sufficient for linear independence.

Definition 5.3.7 (T-junction extensions)**.** For $z \in \mathbb{R}$ and $j = 1, \dots, d$, we define the slices

$$\mathsf{S}_j(z) \coloneqq \{(x_1, \dots, x_d) \in [0, N_1] \times \cdots \times [0, N_d] \mid x_j = z\}. \tag{5.94}$$

Moreover, we denote by

$$\mathsf{N}_j(z) \coloneqq \{v \in \mathsf{N} \mid z \in \mathsf{K}_j(v)\} \tag{5.95}$$

the set of all nodes that have z in their j-orthogonal global index vector, i.e., all nodes of which the projection on the slice $\mathsf{S}_j(z)$ lies in some element's face. Based on $\mathsf{S}_j(z)$ and $\mathsf{N}_j(z)$, we define slicewise T-junction extensions

$$\mathsf{TJ}_j(z) \coloneqq \mathsf{S}_j(z) \cap \bigcup_{v \in \mathsf{N}_j(z)} \operatorname{supp} B_v \;\cap \bigcup_{v \in \mathsf{N} \setminus \mathsf{N}_j(z)} \operatorname{supp} B_v. \tag{5.96}$$

For $j = 1, \dots, d$, the *global j-orthogonal T-junction extension* TJ_j is defined by

$$\mathsf{TJ}_j \coloneqq \bigcup_{z \in \mathbb{R}} \mathsf{TJ}_j(z). \tag{5.97}$$

In a uniform mesh, the global T-junction extensions are empty. In a non-uniform mesh, the T-junction extensions are a superset of all hanging hyperfaces (this is, all kinds of T-junctions in the nD setting). See Figure 5.10 for a 2D visualization of these definitions.

Definition 5.3.8 (Analysis-suitability)**.** A given mesh $\mathcal{Q}$ is *analysis-suitable* if the above-defined T-junction extensions do not intersect, i.e. if $\mathsf{TJ}_i \cap \mathsf{TJ}_j = \emptyset$ for any $i, j \in \{1, \dots, d\}$ with $i \neq j$.

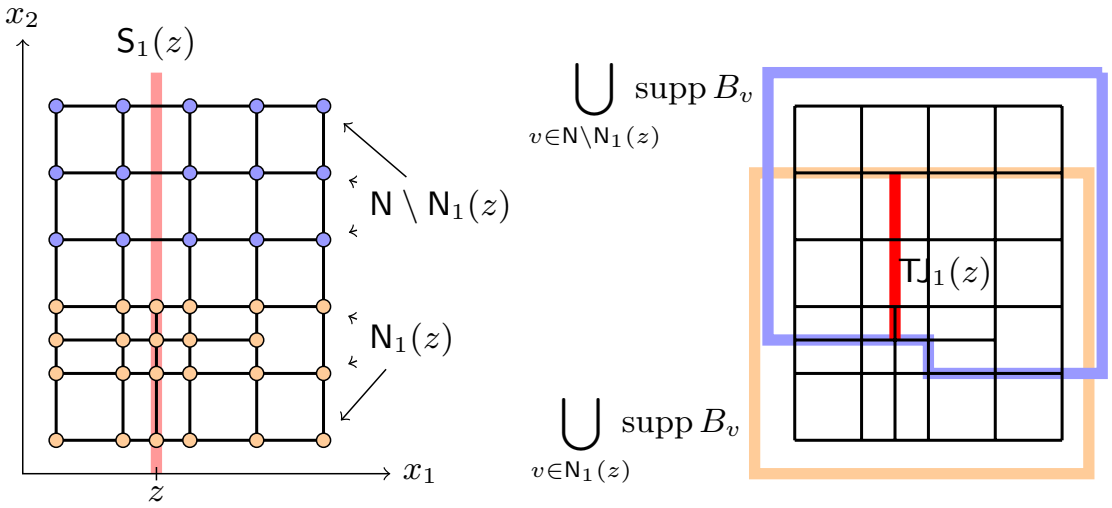

Figure 5.10: Example for the construction of the T-junction extension $\mathsf{TJ}_1(z)$ in an analysis-suitable mesh. The left figure illustrates the construction of $\mathsf{N}_1(z)$ and its complement $\mathsf{N} \setminus \mathsf{N}_1(z)$, and the right figure shows the resulting T-junction extension, which coincides with the corresponding classical T-junction extension.

We will recall below the concept of dual-compatibility, which is a sufficient criterion for linear independence of the T-splines, based on dual functionals. We follow the ideas of [13] for the definitions and for the proof of linear independence. In addition, we prove that all analysis-suitable meshes are dual-compatible.

Proposition 5.3.9 (Dual functional, [55, Theorem 4.41])**.** *Given the local index vector $X = (x^1, \dots, x^{p+2})$, there exists an L^2-functional λ_X with $\operatorname{supp} \lambda_X = \operatorname{supp} N_X$ such that for any $\tilde{X} = (\tilde{x}^1, \dots, \tilde{x}^{p+2})$ satisfying*

$$\begin{aligned} &\forall\, x \in \{x^1, \dots, x^{p+2}\} : \quad \tilde{x}^1 \le x \le \tilde{x}^{p+2} \Rightarrow x \in \{\tilde{x}^1, \dots, \tilde{x}^{p+2}\} \\ \textit{and} \quad &\forall\, \tilde{x} \in \{\tilde{x}^1, \dots, \tilde{x}^{p+2}\} : \quad x^1 \le \tilde{x} \le x^{p+2} \Rightarrow \tilde{x} \in \{x^1, \dots, x^{p+2}\}, \end{aligned} \tag{5.98}$$

follows $\lambda_X(N_{\tilde{X}}) = \delta_{X\tilde{X}}$.

Proof. Following [55], we construct a dual functional on the same local index vector X which we denote by $\lambda_X : L^2\big([0,1]\big) \to \mathbb{R}$. For details, see [55, Theorem 4.34, 4.37, and 4.41]. Let $y_j = \cos\big(\frac{p-j+1}{p+1}\pi\big)$ for $j = 0, \dots, p+1$. Using divided differences, the perfect B-spline of order $p+1$ is defined by

$$B^*_{p+1}(x) \coloneqq (p+1)\,(-1)^{p+1}\big[y_0, \dots, y_{p+1}\big]\,((x - \bullet)_+)^p \tag{5.99}$$

and satisfies (amongst other things) $\int_{-1}^{1} B^*_{p+1}(x)\,\mathrm{d}x = 1$ as depicted in Figure 5.12. Set

$$G_X(x) \coloneqq \int_{-1}^{2x - x^1 - x^{p+2}/x^{p+2} - x^1} B^*_{p+1}(t)\,\mathrm{d}t \quad \text{for } x^1 \le x \le x^{p+2} \tag{5.100}$$

and

$$\phi_X(x) = \tfrac{1}{p!}\left(x - x^2\right) \cdots \left(x - x^{p+1}\right). \tag{5.101}$$

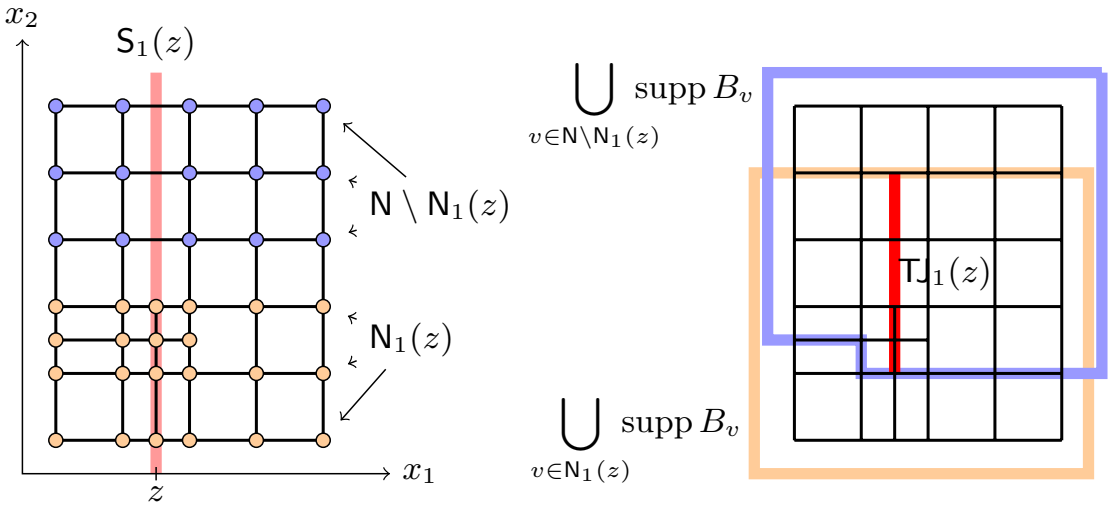

Figure 5.11: Example for the construction of the T-junction extension $\mathsf{TJ}_1(z)$ in a mesh that is not analysis-suitable. The left figure illustrates the construction of $\mathsf{N}_1(z)$ and its complement $\mathsf{N} \setminus \mathsf{N}_1(z)$, and the right figure shows the resulting T-junction extension, which is strictly larger than the corresponding classical T-junction extension.

We define the dual functional by

$$\lambda_X(f) = \int_{x^1}^{x^{p+2}} f\, D^{p+1}(G_X\, \phi_X)\, \mathrm{d}x \quad \text{for all } f \in L^2\big([0,1]\big). \tag{5.102}$$

Note in particular that for all $f \in L^2(\mathbb{R})$ with $f|_{[x^1, x^{p+2}]} = 0$ follows $\lambda_X(f) = 0$. If (5.98) holds then the claim follows by construction, see [55, Theorem 4.41]. □

We say that two index vectors verifying (5.98) *overlap*. In order to define the set of T-splines of which we desire linear independence, we construct local index vectors for each node.

Definition 5.3.10. We define the functional λ_v by

$$\lambda_v(B_w) \coloneqq \lambda_{\mathsf{k}_1(v)}(N_{\mathsf{k}_1(w)}) \cdots \lambda_{\mathsf{k}_d(v)}(N_{\mathsf{k}_d(w)}) \tag{5.103}$$

using the one-dimensional functional λ_X defined in (5.102).

Definition 5.3.11. We say that two nodes $v, w \in \mathsf{N}$ *partially overlap* if their index vectors overlap in at least all but one dimension; this is, if (at least) $d-1$ of the pairs

$$\big(\mathsf{k}_1(v), \mathsf{k}_1(w)\big), \ldots, \big(\mathsf{k}_d(v), \mathsf{k}_d(w)\big) \tag{5.104}$$

overlap in the sense of Proposition 5.3.9.

Definition 5.3.12. A mesh $\mathcal{Q}$ is *dual-compatible* if any two nodes $v, w \in \mathsf{N}$ with $\big|\operatorname{supp} B_v \cap \operatorname{supp} B_w\big| > 0$ partially overlap.

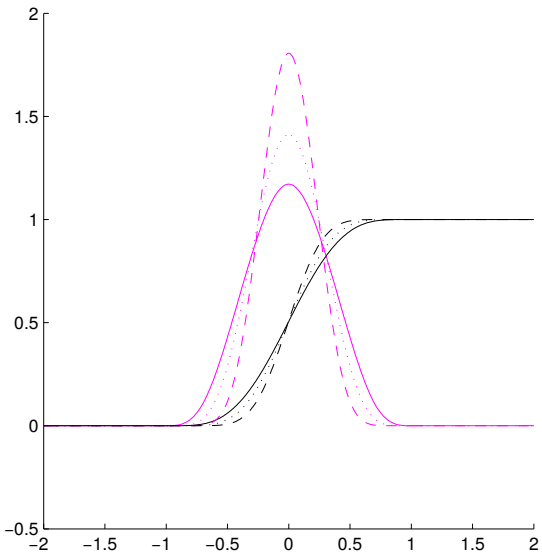

Figure 5.12 [34]: Plot of the perfect B-splines B_4^* (solid), B_6^* (dotted), B_{10}^* (dashed) and the corresponding antiderivatives.

Remark. The above Definition 5.3.11 fulfills the definition of *partial overlap* given in [13, Def. 7.1], which is not equivalent. The definition given in [13] is more general, and the corresponding mesh classes are nested in the sense that the class defined above is a subset of the one defined in [13]. However, we do have equivalence of these definitions in the two-dimensional setting.

The following lemma states that the T-junction extensions from Definition 5.3.7 indicate non-overlapping knot vectors, and it is applied in the proof of Theroem 5.3.14 below.

Lemma 5.3.13. *Let* $z \in [0, \tilde{X}_j]$ *and* $v, w \in \mathsf{N}$. *If* $v \in \mathsf{N}_j(z) \not\ni w$ *and* $\mathsf{S}_j(z) \cap \operatorname{supp} B_v \cap \operatorname{supp} B_w \neq \emptyset$, *then* $\mathsf{k}_j(v)$ *and* $\mathsf{k}_j(w)$ *do not overlap in the sense of* (5.98).

Proof. Let $v = (v_1, \ldots, v_d)$. From $v \in \mathsf{N}_j(z) \not\ni w$ and Definition 5.3.7, we conclude that

$$\mathsf{K}_j(v) \ni z \notin \mathsf{K}_j(w). \tag{5.105}$$

Let $\mathsf{k}_j(v) = (x_1^{v,j}, \ldots, x_{p_j+2}^{v,j})$ be the local index vector associated to v in direction j, then $\operatorname{supp} B_v \cap \mathsf{S}_j(z) \neq \emptyset$ implies that $x_1^{v,j} \leq z \leq x_{p_j+2}^{v,j}$, and hence $z \in \mathsf{k}_j(v)$. With $z \notin \mathsf{K}_j(w)$, we have in particular $z \notin \mathsf{k}_j(w)$. Let $\mathsf{k}_j(w) = (x_1^{w,j}, \ldots, x_{p_j+2}^{w,j})$ be the local index vector associated to w, then $\operatorname{supp} B_w \cap \mathsf{S}_j(z) \neq \emptyset$ implies that $x_1^{w,j} \leq z \leq x_{p_j+2}^{w,j}$. Together with $\mathsf{k}_j(v) \ni z \notin \mathsf{k}_j(w)$, we see that v and w do not overlap. □

Theorem 5.3.14. *Analysis-suitability is equivalent to dual-compatibility.*

Proof. (i) All analysis-suitable meshes are dual-compatible. Assume for contradiction a mesh $\mathcal{Q}$ which is not DC, hence there exist nodes $v, w \in \mathsf{N}$ with $\left|\operatorname{supp} B_v \cap \operatorname{supp} B_w\right| > 0$ that do not overlap in two dimensions, without loss

of generality the first and the second dimension. We will show that there exist two T-junction extensions $\mathsf{TJ}_1(z_1)$ and $\mathsf{TJ}_2(z_2)$ with nonempty intersection. We denote $v = (v_1, \dots, v_d)$, $w = (w_1, \dots, w_d)$, $\mathsf{k}_j(v) = (x_1^{v,j}, \dots, x_{p_j+2}^{v,j})$ and analogously $\mathsf{k}_j(w)$ for $j = 1, \dots, d$. Moreover, we define

$$x_{\mathrm{m}}^j \coloneqq \max(x_1^{v,j}, x_1^{w,j}) \text{ and } x_{\mathrm{M}}^j \coloneqq \min(x_{p_j+2}^{v,j}, x_{p_j+2}^{w,j}) \text{ for } j = 1, \dots, d \quad (5.106)$$

and note that since the supports of B_v and B_w are axis-aligned hypercuboids, their intersection is also an axis-aligned hypercuboid,

$$\operatorname{supp} B_v \cap \operatorname{supp} B_w = [x_{\mathrm{m}}^1, x_{\mathrm{M}}^1] \times \cdots \times [x_{\mathrm{m}}^d, x_{\mathrm{M}}^d]. \quad (5.107)$$

Since $\mathsf{k}_1(v)$ and $\mathsf{k}_1(w)$ do not overlap, there exists $z_1 \in [x_{\mathrm{m}}^1, x_{\mathrm{M}}^1]$ with either $\mathsf{k}_1(v) \ni z_1 \notin \mathsf{k}_1(w)$ or $\mathsf{k}_1(v) \not\ni z_1 \in \mathsf{k}_1(w)$. Without loss of generality we assume $\mathsf{k}_1(v) \ni z_1 \notin \mathsf{k}_1(w)$. From $z_1 \in [x_{\mathrm{m}}^1, x_{\mathrm{M}}^1]$ we deduct

$$\{z_1\} \cap \mathsf{K}_1(w) \subseteq [x_{\mathrm{m}}^1, x_{\mathrm{M}}^1] \cap \mathsf{K}_1(w) \subseteq \mathsf{k}_1(w) \not\ni z_1, \quad (5.108)$$

and consequently $z_1 \notin \mathsf{K}_1(w)$. Together, this is $\mathsf{K}_1(v) \ni z_1 \notin \mathsf{K}_1(w)$ and Definition 5.3.7 yields $v \in \mathsf{N}_1(z_1) \not\ni w$. It follows that

$$\begin{aligned}
\mathsf{TJ}_1(z_1) &= \mathsf{S}_1(z_1) \cap \bigcup_{v' \in \mathsf{N}_1(z_1)} \operatorname{supp} B_{v'} \cap \bigcup_{v' \in \mathsf{N} \setminus \mathsf{N}_1(z_1)} \operatorname{supp} B_{v'} \\
&\supseteq \mathsf{S}_1(z_1) \cap \operatorname{supp} B_v \cap \operatorname{supp} B_w \\
&= \{z_1\} \times [x_{\mathrm{m}}^2, x_{\mathrm{M}}^2] \times \cdots \times [x_{\mathrm{m}}^d, x_{\mathrm{M}}^d].
\end{aligned}$$

Analogously, we have

$$\mathsf{TJ}_2(z_2) \supseteq [x_{\mathrm{m}}^1, x_{\mathrm{M}}^1] \times \{z_2\} \times [x_{\mathrm{m}}^3, x_{\mathrm{M}}^3] \cdots \times [x_{\mathrm{m}}^d, x_{\mathrm{M}}^d]$$

and hence

$$\mathsf{TJ}_1(z_1) \cap \mathsf{TJ}_2(z_2) \supseteq \{z_1\} \times \{z_2\} \times [x_{\mathrm{m}}^3, x_{\mathrm{M}}^3] \times \cdots \times [x_{\mathrm{m}}^d, x_{\mathrm{M}}^d] \neq \emptyset, \quad (5.109)$$

which means that the mesh $\mathcal{Q}$ is not analysis-suitable.

(ii) All dual-compatible meshes are analysis-suitable. Assume for contradiction that the mesh is not analysis-suitable, and w.l.o.g. that there is $w = (w_1, \dots, w_d) \in \mathbb{R}^d$ such that $\mathsf{TJ}_1 \cap \mathsf{TJ}_2 \supseteq \{w\} \neq \emptyset$. Definition 5.3.7 implies that there exist $v^1, v^2, v^3, v^4 \in \mathsf{N}$ with $v^1 \in \mathsf{N}_1(w_1) \not\ni v^2$ and $v^3 \in \mathsf{N}_2(w_2) \not\ni v^4$ such that

$$w \in \mathsf{S}_1(w_1) \cap \mathsf{S}_2(w_2) \cap \operatorname{supp} B_{v^1} \cap \operatorname{supp} B_{v^2} \cap \operatorname{supp} B_{v^3} \cap \operatorname{supp} B_{v^4}. \quad (5.110)$$

Lemma 5.3.13 yields that $\mathsf{k}_1(v^1)$ and $\mathsf{k}_1(v^2)$ do not overlap, and that $\mathsf{k}_2(v^3)$ and $\mathsf{k}_2(v^4)$ do not overlap.

Case 1. If $v^1 \in \mathsf{N}_2(w_2) \not\ni v^2$, or $v^1 \notin \mathsf{N}_2(w_2) \ni v^2$, then v^1 and v^2 do not partially overlap.

Case 2. If $v^1 \in \mathsf{N}_2(w_2)$ and $v^4 \notin \mathsf{N}_1(w_1)$, then v^1 and v^4 do not partially overlap.

Case 3. If $v^1 \notin \mathsf{N}_2(w_2)$ and $v^3 \notin \mathsf{N}_1(w_1)$, then v^1 and v^3 do not partially overlap.

Case 4. If $v^2 \in \mathsf{N}_2(w_2)$ and $v^4 \in \mathsf{N}_1(w_1)$, then v^2 and v^4 do not partially overlap.

Case 5. If $v^2 \notin \mathsf{N}_2(w_2)$ and $v^3 \in \mathsf{N}_1(w_1)$, then v^2 and v^3 do not partially overlap.

In all cases (see Table 5.3), the mesh is not dual-compatible.
This concludes the proof. □

Table 5.3: The five cases considered in the proof of Theorem 5.3.14 cover all possible configurations.

$v_1 \in \mathsf{N}_\mathrm{y}(r)$	$v_2 \in \mathsf{N}_\mathrm{y}(r)$	$v_3 \in \mathsf{N}_\mathrm{y}(r)$	$v_4 \in \mathsf{N}_\mathrm{y}(r)$	case(s)
true	true	true	true	4
true	true	true	false	2
true	true	false	true	4
true	true	false	false	2
true	false	true	true	1, 5
true	false	true	false	1, 2, 5
true	false	false	true	1
true	false	false	false	1, 2
false	true	true	true	1, 4
false	true	true	false	1
false	true	false	true	1, 3, 4
false	true	false	false	1, 3
false	false	true	true	5
false	false	true	false	5
false	false	false	true	3
false	false	false	false	3

Theorem 5.3.15. *Let $\mathcal{Q}$ be a DC T-mesh. Then the set of functionals $\{\lambda_v \mid v \in \mathsf{N}\}$ is a set of dual functionals for the set $\{B_v \mid v \in \mathsf{N}\}$.*

The proof below follows the ideas of [30, Proposition 5.1] and [13, Proposition 7.3].

Proof. Let $v, w \in \mathsf{N}$. We need to show that

$$\lambda_v(B_w) = \delta_{vw}, \tag{5.111}$$

with δ representing the Kronecker symbol.

If $\operatorname{supp} B_v$ and $\operatorname{supp} B_w$ are disjoint (or have an intersection of empty interior), then at least one of the pairs

$$\big(\operatorname{supp}(N_{\mathsf{k}_1(v)}), \operatorname{supp}(N_{\mathsf{k}_1(w)})\big), \ldots, \big(\operatorname{supp}(N_{\mathsf{k}_d(v)}), \operatorname{supp}(N_{\mathsf{k}_d(w)})\big) \tag{5.112}$$

has an intersection with empty interior.

Assume w.l.o.g. that $\left|\operatorname{supp}(N_{\mathsf{k}_1(v)}) \cap \operatorname{supp}(N_{\mathsf{k}_1(w)})\right| = 0$, then

$$\lambda_v(B_w) = \underbrace{\lambda_{\mathsf{k}_1(v)}(N_{\mathsf{k}_1(w)})}_{0} \cdot \lambda_{\mathsf{k}_2(v)}(N_{\mathsf{k}_2(w)}) \cdots \lambda_{\mathsf{k}_d(v)}(N_{\mathsf{k}_d(w)}) = 0. \tag{5.113}$$

Assume that $\operatorname{supp} B_v$ and $\operatorname{supp} B_w$ have an intersection with nonempty interior. Since the mesh $\mathcal{Q}$ is DC, the two nodes overlap in at least all but one dimension. Without loss of generality we may assume that the index vectors

$$\big(\mathsf{k}_1(v), \mathsf{k}_1(w)\big), \ldots, \big(\mathsf{k}_{d-1}(v), \mathsf{k}_{d-1}(w)\big)$$

overlap. Proposition 5.3.9 yields

$$\lambda_{\mathsf{k}_j(v)}(N_{\mathsf{k}_j(w)}) = \delta_{v_j w_j} \quad \text{for } j = 1, \ldots, d-1. \tag{5.114}$$

The above identities immediately prove (5.111) if $v_j \neq w_j$ for some $j \in \{1, \ldots, d-1\}$. If on the contrary, $v_j = w_j$ fro all $j = 1, \ldots, d-1$, then v and w are aligned in d-th dimension, this is, $\mathsf{k}_d(v)$ and $\mathsf{k}_d(w)$ are both vectors of $p_d + 2$ consecutive indices from the same index set $\mathsf{K}_d(v) = \mathsf{K}_d(w)$. Hence v and w must overlap also in d-th dimension. Again, Proposition 5.3.9 yields

$$\lambda_{\mathsf{k}_d(v)}(N_{\mathsf{k}_d(w)}) = \delta_{v_d w_d}, \tag{5.115}$$

which concludes the proof. □

5.4 Local q-adic refinement in nD

In the subsequent definitions, we will give a detailed description of the elementary subdivision steps.

Definition 5.4.1 (Intermediate children)**.** For $\mathfrak{Q} \in \mathcal{Q}_{\mathrm{u}[k]}$ and $d{\cdot}k \in \mathbb{N}_0$, we define

$$\textsc{subdivide}^{1/d}(\mathfrak{Q}) \coloneqq \big\{ \mathfrak{Q}' \in \mathcal{Q}_{\mathrm{u}[k+1/d]} \mid \mathfrak{Q}' \subset \mathfrak{Q} \big\}. \tag{5.116}$$

For $\mathcal{M} \subset \mathcal{Q} \in \mathbb{M}_{\mathrm{HB}}$, we denote the corresponding partial subdivision by

$$\textsc{subdivide}^{1/d}(\mathcal{Q}, \mathcal{M}) \coloneqq \mathcal{Q} \setminus \mathcal{M} \cup \bigcup_{\mathfrak{Q} \in \mathcal{M}} \textsc{subdivide}^{1/d}(\mathfrak{Q}). \tag{5.117}$$

See Figure 5.13 for an example.

Definition 5.4.2 (Vector-valued distance)**.** Given $z \in \overline{\Omega}$ and an element $\mathfrak{Q}$, we define their distance as the componentwise absolute value of the difference between z and the midpoint of $\mathfrak{Q} = [x_1, x_1 + \tilde{x}_1] \times \cdots \times [x_d, x_d + \tilde{x}_d]$,

$$\begin{aligned} \operatorname{Dist}(\mathfrak{Q}, z) &\coloneqq \operatorname{abs}\big(\operatorname{mid}(\mathfrak{Q}) - z\big) \ \in \mathbb{R}^d, \\ \text{with} \quad \operatorname{abs}(z) &\coloneqq \big(|z_1|, \ldots, |z_d|\big) \\ \text{and} \quad \operatorname{mid}(\mathfrak{Q}) &\coloneqq \big(x_1 + \tfrac{\tilde{x}_1}{2}, \ldots, x_d + \tfrac{\tilde{x}_d}{2}\big). \end{aligned} \tag{5.118}$$

For two elements $\mathfrak{Q}_1, \mathfrak{Q}_2$, we define the shorthand notation

$$\operatorname{Dist}(\mathfrak{Q}_1, \mathfrak{Q}_2) \coloneqq \operatorname{abs}\big(\operatorname{mid}(\mathfrak{Q}_1) - \operatorname{mid}(\mathfrak{Q}_2)\big). \tag{5.119}$$

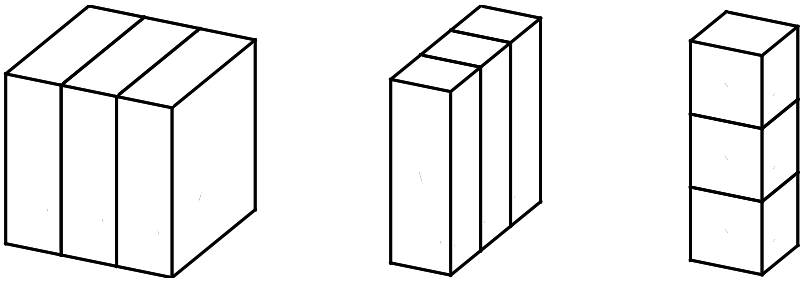

Figure 5.13 [34]: Elementary subdivision routines for $d = 3$ and $q = 3$: subdivision of an element with level 0 orthogonal to the 1st dimension (left), subdivision of an element with level $\frac{1}{3}$ orthogonal to the 2nd dimension (middle), and subdivision of an element with level $\frac{2}{3}$ orthogonal to the 3rd dimension (right). The subdivision of an element with level 1 is again orthogonal to the 1st dimension (left).

Definition 5.4.3. Since we will stick to the above subdivision rules, the size of an element $\mathtt{Q}$ depends on the grading parameter q and the level $\ell(\mathtt{Q})$ only, and we denote

$$\operatorname{size}(\ell(\mathtt{Q})) \coloneqq q^{-\lfloor \ell(\mathtt{Q}) \rfloor} \Big(\underbrace{\tfrac{1}{q}, \dots, \tfrac{1}{q}}_{\substack{d \cdot \ell(\mathtt{Q}) \bmod d \\ \text{times}}}, 1, \dots, 1 \Big) \in \mathbb{R}^d. \tag{5.120}$$

Definition 5.4.4 (Refinement for multivariate T-splines)**.** Given an element $\mathtt{Q}$, a grading parameter $q \geq 2$ and the polynomial degree $\mathbf{p}$, we define the open environment

$$U(\mathtt{Q}) \coloneqq \{ z \in \mathbb{R}^d \mid \operatorname{Dist}(\mathtt{Q}, z) < \operatorname{size}(\ell(\mathtt{Q})) \circ (\mathbf{p} + \tfrac{3}{2}) \}, \tag{5.121}$$

where $\circ$ denotes the componentwise (Hadamard) product, such that

$$\operatorname{size}(\ell(\mathtt{Q})) \circ (\mathbf{p} + \tfrac{3}{2}) = q^{-\lfloor \ell(\mathtt{Q}) \rfloor} \big(\tfrac{p_1 + 3/2}{q}, \dots, \tfrac{p_i + 3/2}{q}, p_{i+1} + \tfrac{3}{2}, \dots, p_d + \tfrac{3}{2} \big) \tag{5.122}$$

with $i = d \cdot \ell(\mathtt{Q}) \bmod d$. We define for each $\mathtt{Q} \in \mathcal{Q}$ the *coarse neighbourhood*

$$\mathcal{N}_{\text{TS}}(\mathcal{Q}, \mathtt{Q}) \coloneqq \big\{ \mathtt{Q}' \in \mathcal{Q} \cap \mathcal{Q}_{\mathrm{u}\lfloor \ell(\mathtt{Q}) - 1/d \rfloor} \mid \mathtt{Q}' \cap U(\mathtt{Q}) \neq \emptyset \big\}.$$

Moreover, we define the *closure*

$$\text{CLOSURE\_TS}(\mathcal{Q}, \mathcal{M}) \coloneqq \bigcup_{k=0}^{d \cdot \max \ell(\mathcal{M})} \mathcal{N}_{\text{TS}}^k(\mathcal{Q}, \mathcal{M}),$$

and the extended refinement procedure

$$\text{REFINE\_TS}_{\text{nD}}(\mathcal{Q}, \mathcal{M}) \coloneqq \text{SUBDIVIDE}^{1/d}\big(\mathcal{Q}, \text{CLOSURE\_TS}(\mathcal{Q}, \mathcal{M})\big). \tag{5.123}$$

Note as a technical detail that this definition does *not* require that $\mathtt{Q} \in \mathcal{Q}$. See also Figure 5.14 for examples.

Remark. By definition, the size of the environment $U(\mathtt{Q})$ of an element $\mathtt{Q}$ scales linearly with the size of $\mathtt{Q}$ and with the polynomial degree $\mathbf{p}$. Since $\operatorname{size}(k)$ is decreasing in q, choosing q large will cause small environments and hence more localized refinement. This is illustrated in Example 5.4.5 below.

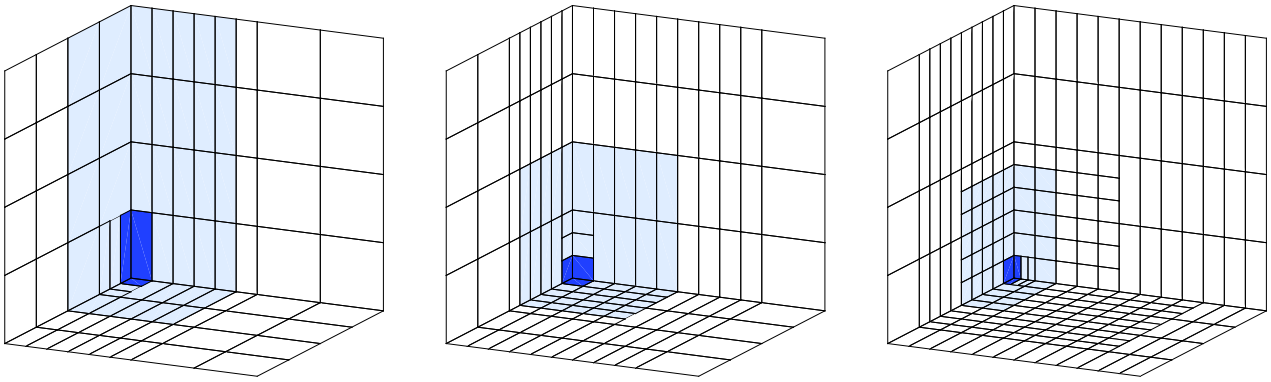

Figure 5.14 [34]: Examples for the neighbourhood $\mathcal{Q} \cap U(\mathtt{Q})$ of an element $\mathtt{Q}$, for $\mathbf{p} = (3,3,3)$, $q = 3$ and $\ell(\mathtt{Q}) = \frac{2}{3}, 1, \frac{4}{3}$.

Example 5.4.5. Consider an initial mesh that consists of $4 \times 5 \times 8$ cubes of size $1\times1\times1$. We refine the mesh by marking the lower left front corner element repeatedly until it is of the size $\frac{1}{16} \times \frac{1}{16} \times \frac{1}{16}$. The resulting meshes for different choices of q are illustrated in Figure 5.16, and the results are listed in Table 5.4.

Table 5.4: Number of refinement steps vs. number of new elements for the meshes in Figure 5.16.

Figure	q	number of refinement steps	number of new elements
5.16a	2	12	10728
5.16b	4	6	3175
5.16c	16	3	1030

5.4.1 Admissible meshes

In the subsequent definitions, we introduce a class of admissible meshes. We will then prove that this class coindices with the meshes generated by REFINE_TS$_{\mathrm{nD}}$. Throughout the rest of this chapter, for a given a mesh $\mathcal{Q}$ and an element $\mathtt{Q} \in \mathcal{Q}$, we will use the shortcut notation

$$\mathcal{Q} \cap U(\mathtt{Q}) \coloneqq \{\mathtt{Q}' \in \mathcal{Q} \mid \mathtt{Q}' \cap U(\mathtt{Q}) \neq \emptyset\}. \tag{5.124}$$

Definition 5.4.6 (Admissible subdivisions in nD)**.** Given a mesh $\mathcal{Q}$ and an element $\mathtt{Q} \in \mathcal{Q}$, the subdivision of $\mathtt{Q}$ is called *admissible* if all $\mathtt{Q}' \in \mathcal{Q} \cap U(\mathtt{Q})$ satisfy $\ell(\mathtt{Q}') \geq \ell(\mathtt{Q})$. In the case of several elements $\mathcal{M} = \{\mathtt{Q}_1, \dots, \mathtt{Q}_J\} \subseteq \mathcal{Q}$, the subdivision $\mathrm{SUBDIVIDE}^{1/d}(\mathcal{Q}, \mathcal{M})$ is admissible if there is an ordering $(\sigma(1), \dots, \sigma(J))$ (this is, if there is a permutation σ of $\{1, \dots, J\}$) such that

$$\mathrm{SUBDIVIDE}^{1/d}(\mathcal{Q}, \mathcal{M}) = \mathrm{SUBDIVIDE}^{1/d}(\dots \mathrm{SUBDIVIDE}^{1/d}(\mathcal{Q}, \mathtt{Q}_{\sigma(1)}), \dots, \mathtt{Q}_{\sigma(J)}) \tag{5.125}$$

is a concatenation of admissible subdivisions.

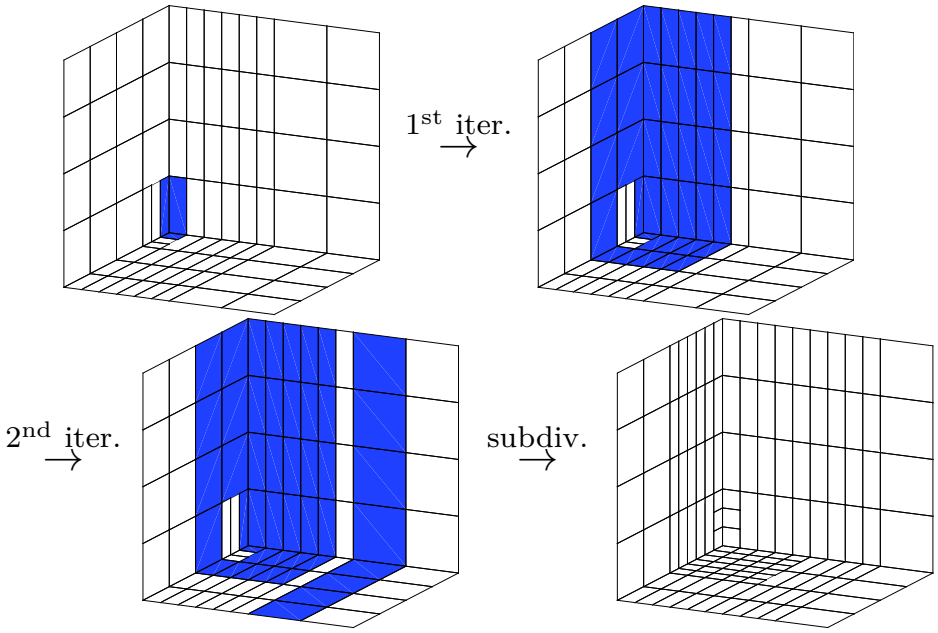

Figure 5.15 [34]: Example for REFINE_TS$_{\text{nD}}$, with $\mathbf{p} = (3,3,3)$, $q = 3$ and $\mathcal{M} = \mathcal{N}^0_{\text{TS}}(\mathcal{M}) = \{\mathsf{Q}\}$ with $\ell(\mathsf{Q}) = \max \ell(\mathcal{M}) = \frac{2}{3}$. The first iteration of the construction of CLOSURE_TS computes $\mathcal{N}_{\text{TS}}(\mathcal{Q}, \mathcal{M})$, which consists of all level-$\frac{1}{3}$-elements intersecting $U(\mathsf{Q})$. In the second iteration, all level-0-"neighbours" of those elements form $\mathcal{N}^2_{\text{TS}}(\mathcal{Q}, \mathcal{M})$. Finally, all marked elements CLOSURE_TS$(\mathcal{Q}, \mathcal{M}) = \mathcal{M} \cup \mathcal{N}_{\text{TS}}(\mathcal{Q}, \mathcal{M}) \cup \mathcal{N}^2_{\text{TS}}(\mathcal{Q}, \mathcal{M})$ are subdivided in the directions that correspond to their levels.

Definition 5.4.7 (Admissible mesh)**.** A refinement $\mathcal{Q}$ of $\mathcal{Q}_0$ is admissible if there is a sequence of meshes $\mathcal{Q}_1, \dots, \mathcal{Q}_J = \mathcal{Q}$ and markings $\mathcal{M}_j \subseteq \mathcal{Q}_j$ for $j = 0, \dots, J-1$, such that $\mathcal{Q}_{j+1} = \text{SUBDIVIDE}^{1/d}(\mathcal{Q}_j, \mathcal{M}_j)$ is an admissible subdivision for all $j = 0, \dots, J-1$. The set of all admissible meshes is the initial mesh and its admissible refinements.

Theorem 5.4.8. *For any admissible mesh $\mathcal{Q}$ and any set of marked elements $\mathcal{M} \subseteq \mathcal{Q}$, the refinement* REFINE_TS$_{\text{nD}}(\mathcal{Q}, \mathcal{M})$ *is admissible.*

The proof of Theorem 5.4.8 is exactly the same as for Proposition 5.2.6 using Definition 5.4.4 instead of Corollary 5.2.8, and Lemma 5.4.10 below instead of Lemma 5.2.7.

Lemma 5.4.9. *Given an admissible mesh $\mathcal{Q}$ and two nested elements $\mathsf{Q} \subseteq \hat{\mathsf{Q}}$ with $\mathsf{Q}, \hat{\mathsf{Q}} \in \bigcup \mathbb{M}_{\text{TS}}$, the corresponding neighbourhoods are nested in the sense $U(\mathsf{Q}) \subseteq U(\hat{\mathsf{Q}})$.*

Proof. If $\mathsf{Q} = \hat{\mathsf{Q}}$, the claim is trivially fulfilled. If otherwise $\mathsf{Q} \subsetneq \hat{\mathsf{Q}}$, we consider the following two cases.

Case 1. Assume that $\ell(\mathsf{Q}) = \ell(\hat{\mathsf{Q}}) + \frac{1}{d}$. We denote $\mathsf{Q} = [x, x+\tilde{x}] \times \cdots \times [x_d, x_d + \tilde{x}_d]$ and recall from Definition 5.4.3 that

$$\operatorname{size}(\ell(\mathsf{Q})) = q^{-\lfloor \ell(\mathsf{Q}) \rfloor} \Big(\underbrace{\tfrac{1}{q}, \dots, \tfrac{1}{q}}_{\substack{d \cdot \ell(\mathsf{Q}) \bmod d \\ \text{times}}}, 1, \dots, 1 \Big) \in \mathbb{R}^d. \tag{5.126}$$

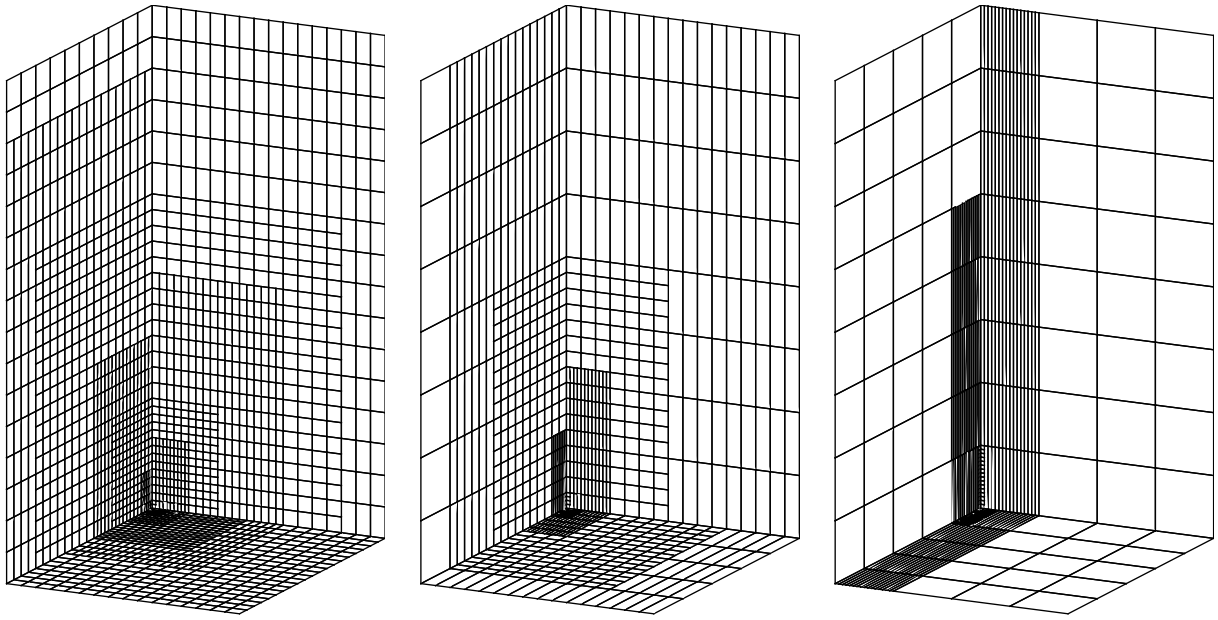

(a) $q = 2$ (b) $q = 4$ (c) $q = 16$

Figure 5.16 [34]: Refinement examples for $\mathbf{p} = (3, 3, 3)$ and different choices of q. In all cases, the initial mesh consists of $4 \times 5 \times 8$ cubes of size $1 \times 1 \times 1$, and is refined by marking the lower left front corner element repeatedly until it is of the size $\frac{1}{16} \times \frac{1}{16} \times \frac{1}{16}$.

Since $\mathtt{Q}$ results from the subdivision of $\hat{\mathtt{Q}}$, we also have

$$\begin{aligned}\operatorname{size}(\ell(\hat{\mathtt{Q}})) &= q^{-\lfloor \ell(\hat{\mathtt{Q}}) \rfloor} \big(\underbrace{\tfrac{1}{q}, \dots, \tfrac{1}{q}}_{\substack{d\cdot\ell(\hat{\mathtt{Q}}) \bmod d \\ \text{times}}}, 1, \dots, 1 \big) \in \mathbb{R}^d. \\ &= q^{-\lfloor \ell(\mathtt{Q}) - 1/d \rfloor} \big(\underbrace{\tfrac{1}{q}, \dots, \tfrac{1}{q}}_{\substack{(d\cdot\ell(\mathtt{Q})-1) \bmod d \\ \text{times}}}, 1, \dots, 1 \big) \in \mathbb{R}^d. \end{aligned} \tag{5.127}$$

Moreover, the distance between $\mathtt{Q}$ and $\hat{\mathtt{Q}}$ is bounded by

$$\operatorname{Dist}(\mathtt{Q}, \hat{\mathtt{Q}}) \leq \tfrac{q-1}{2q} q^{-\lfloor \ell(\hat{\mathtt{Q}}) \rfloor} \cdot e_{d\cdot\ell(\mathtt{Q}) \bmod d}, \tag{5.128}$$

where $e_{d\cdot\ell(\mathtt{Q}) \bmod d}$ denotes the $(d\cdot\ell(\mathtt{Q}) \bmod d)$-th unit vector. A straightforward verification shows that

$$\begin{aligned}\operatorname{size}(\ell(\mathtt{Q})) \circ (\tfrac{\mathbf{p}}{2} + 1) + \operatorname{Dist}(\mathtt{Q}, \hat{\mathtt{Q}}) &\leq \operatorname{size}(\ell(\mathtt{Q}) - \tfrac{1}{d}) \circ (\tfrac{\mathbf{p}}{2} + 1) \\ &= \operatorname{size}(\ell(\hat{\mathtt{Q}})) \circ (\tfrac{\mathbf{p}}{2} + 1). \end{aligned} \tag{5.129}$$

The case 1 is concluded with

$$\begin{aligned} U(\mathtt{Q}) &= \{x \in \mathbb{R}^d \mid \operatorname{Dist}(\mathtt{Q}, x) \leq \operatorname{size}(\ell(\mathtt{Q})) \circ (\tfrac{\mathbf{p}}{2} + 1)\} \\ &\subseteq \{x \in \mathbb{R}^d \mid \operatorname{Dist}(\hat{\mathtt{Q}}, x) \leq \operatorname{size}(\ell(\mathtt{Q})) \circ (\tfrac{\mathbf{p}}{2} + 1) + \operatorname{Dist}(\mathtt{Q}, \hat{\mathtt{Q}})\} \\ &\subseteq U(\hat{\mathtt{Q}}). \end{aligned} \tag{5.130}$$

Case 2. Consider $\mathtt{Q} \subset \hat{\mathtt{Q}}$ with $\ell(\mathtt{Q}) > \ell(\hat{\mathtt{Q}}) + \frac{1}{d}$, then there is a sequence

$$\mathtt{Q} = \mathtt{Q}_0 \subset \mathtt{Q}_1 \subset \cdots \subset \mathtt{Q}_J = \hat{\mathtt{Q}} \tag{5.131}$$

such that $\mathtt{Q}_{j-1} \in \textsc{subdivide}^{1/d}(\mathtt{Q}_j)$ for $j = 1, \dots, L$. Case 1 yields

$$U(\mathtt{Q}) \subseteq U(\mathtt{Q}_1) \subseteq \cdots \subseteq U(\hat{\mathtt{Q}}). \tag{5.132}$$

□

Lemma 5.4.10 (Local quasi-uniformity)**.** *Given an admissible mesh $\mathcal{Q}$ and $\mathtt{Q} \in \mathcal{Q}$, any $\mathtt{Q}' \in \mathcal{Q} \cap U(\mathtt{Q})$ satisfies $\ell(\mathtt{Q}') \geq \ell(\mathtt{Q}) - \frac{1}{d}$.*

Proof. For $\ell(\mathtt{Q}) = 0$, the assertion is always true. For $\ell(\mathtt{Q}) > 0$, consider the parent $\hat{\mathtt{Q}}$ of $\mathtt{Q}$ (i.e., the unique element $\hat{\mathtt{Q}} \in \bigcup \mathbb{M}_{\mathrm{TS}}$ with $\mathtt{Q} \in \textsc{subdivide}^{1/d}(\hat{\mathtt{Q}})$). Since $\mathcal{Q}$ is admissible, there are admissible meshes $\mathcal{Q}_0, \dots, \mathcal{Q}_J = \mathcal{Q}$ and some $j \in \{0, \dots, J-1\}$ such that $\mathtt{Q} \in \mathcal{Q}_{j+1} = \textsc{subdivide}^{1/d}(\mathcal{Q}_j, \{\hat{\mathtt{Q}}\})$. The admissibility of $\mathcal{Q}_{j+1}$ implies that any $\mathtt{Q}' \in \mathcal{Q}_j \cap U(\hat{\mathtt{Q}})$ satisfies $\ell(\mathtt{Q}') \geq \ell(\hat{\mathtt{Q}}) = \ell(\mathtt{Q}) - \frac{1}{d}$. Since levels do not decrease during refinement, we get

$$\begin{aligned} \ell(\mathtt{Q}) - \tfrac{1}{d} &\leq \min \ell(\mathcal{Q}_j \cap U(\hat{\mathtt{Q}})) \leq \min \ell(\mathcal{Q} \cap U(\hat{\mathtt{Q}})) \\ &\overset{\text{Lemma 5.4.9}}{\leq} \min \ell(\mathcal{Q} \cap U(\mathtt{Q})). \end{aligned} \tag{5.133}$$

□

Theorem 5.4.11. *For any $q \geq 2$, all admissible meshes are analysis-suitable.*

Proof. We prove the claim by induction over admissible subdivisions. Assume that the mesh $\mathcal{Q}$ is admissible and analysis-suitable, and let $\mathtt{Q} \in \mathcal{Q}$ such that $\hat{\mathcal{Q}} \coloneqq \textsc{subdivide}^{1/d}(\mathcal{Q}, \mathtt{Q})$ is an admissible subdivision of $\mathcal{Q}$. We have to show that $\hat{\mathcal{Q}}$ is analysis-suitable. We assume without loss of generality that $d \cdot \ell(\mathtt{Q}) = 0 \bmod d$. Hence subdividing $\mathtt{Q}$ adds $q-1$ hyperfaces to the mesh, which are orthogonal to the first dimension. We denote $\mathtt{Q} =: [x_1, x_1 + \tilde{x}_1] \times \cdots \times [x_d, x_d + \tilde{x}_d]$ and $\Xi \coloneqq \{x_1 + \frac{j}{q}\tilde{x}_1 \mid j \in \{1, \dots, q-1\}\}$. The skeletons of $\hat{\mathcal{Q}}$ satisfy

$$\widehat{\mathsf{Sk}}_1 = \mathsf{Sk}_1 \cup \big(\Xi \times [x_2, x_2 + \tilde{x}_2] \times \cdots \times [x_d, x_d + \tilde{x}_d]\big), \quad \widehat{\mathsf{Sk}}_j = \mathsf{Sk}_j \text{ for } j = 2, \dots, d. \tag{5.134}$$

Let $\hat{v} \in \mathsf{N}(\hat{\mathcal{Q}}) \backslash \mathsf{N}$ be a new node. Using the local quasi-uniformity from Lemma 5.4.10, it can be verified for $j = 2, \dots, d$ that for all $z \in \mathsf{K}_j(\hat{v})$ follows $\mathsf{TJ}_j(z) \cap \operatorname{supp} B_{\hat{v}} = \emptyset$. Consequently, $\widehat{\mathsf{TJ}}_j = \mathsf{TJ}_j$. Moreover, $\widehat{\mathsf{TJ}}_1(z) = \mathsf{TJ}_1(z)$ if $z \notin \Xi$. It remains to characterize

$$\widehat{\mathsf{TJ}}_1(z) = \mathsf{S}_1(z) \cap \bigcup_{v \in \hat{\mathsf{N}}_1(z)} \operatorname{supp} B_v \cap \bigcup_{v \in \mathsf{N}(\hat{\mathcal{Q}}) \backslash \hat{\mathsf{N}}_1(z)} \operatorname{supp} B_v \tag{5.135}$$

for $z \in \Xi$. With

$$\begin{aligned} \hat{\mathsf{N}}_1(z) &= \mathsf{N}_1(z) \cup \mathsf{N}(\hat{\mathcal{Q}}) \setminus \mathsf{N} \\ \text{and } \mathsf{N}(\hat{\mathcal{Q}}) \setminus \hat{\mathsf{N}}_1(z) &= \mathsf{N} \setminus \hat{\mathsf{N}}_1(z) = \mathsf{N} \setminus \mathsf{N}_1(z), \end{aligned} \tag{5.136}$$

it follows

$$\begin{aligned}\widehat{\mathsf{TJ}}_1(z) &= \mathsf{S}_1(z) \cap \bigcup_{v\in\hat{\mathsf{N}}_1(z)} \operatorname{supp} B_v \;\cap \bigcup_{v\in\mathsf{N}(\hat{\mathcal{Q}})\setminus\hat{\mathsf{N}}_1(z)} \operatorname{supp} B_v,\\ &\overset{(5.136)}{=} \mathsf{S}_1(z) \cap \Big(\bigcup_{v\in\mathsf{N}_1(z)} \operatorname{supp} B_v \cup \bigcup_{v\in\mathsf{N}(\hat{\mathcal{Q}})\setminus\mathsf{N}} \operatorname{supp} B_v\Big) \cap \bigcup_{v\in\mathsf{N}\setminus\mathsf{N}_1(z)} \operatorname{supp} B_v\\ &= \mathsf{TJ}_1(z) \cup \Big(\underbrace{\mathsf{S}_1(z) \;\cap \bigcup_{\hat{v}\in\mathsf{N}(\hat{\mathcal{Q}})\setminus\mathsf{N}} \operatorname{supp} B_{\hat{v}}}_{\Sigma} \;\cap \bigcup_{v\in\mathsf{N}\setminus\mathsf{N}_1(z)} \operatorname{supp} B_v\Big). \qquad (5.137)\end{aligned}$$

We will prove below that $\Sigma \cap \widehat{\mathsf{TJ}}_j = \emptyset$ for $j \neq 1$. See Figures 5.17 and 5.18 for an example with $\ell(\mathtt{Q}) = 1$ and $q = 2$. Assume for contradiction that there is $s \in \mathbb{R}$ and $j \in \{2, \dots, d\}$ such that $\widehat{\mathsf{TJ}}_j(s) \cap \Sigma \neq \emptyset$. Definition 5.3.7 yields the existence of $v \in \hat{\mathsf{N}}_j(s)$ and $w \in \mathsf{N}(\hat{\mathcal{Q}}) \setminus \hat{\mathsf{N}}_j(s)$ such that

$$\mathsf{S}_j(s) \cap \operatorname{supp} B_v \cap \operatorname{supp} B_w \cap \Sigma \neq \emptyset. \qquad (5.138)$$

We define for $z, R \in \mathbb{R}^d$ the componentwise bounded box

$$B(z, R) \coloneqq \left\{ y \in \mathbb{R}^d \mid |z_i - y_i| < R_i \text{ for all } i \in \{1, \dots, d\} \right\}. \qquad (5.139)$$

and for sets $A \in \mathbb{R}^d$ the generalized notation $B(A, R) \coloneqq \bigcup_{z\in A} B(z, R)$. We will show below for $R \coloneqq \operatorname{size}(\ell(\mathtt{Q})) \circ \frac{\mathbf{p}+1}{2}$ that $w \in \overline{B}(\Sigma, R)$, and subsequently that $w \notin \overline{B}(\Sigma, R)$. This will be the desired contradiction.

Since the subdivision of $\mathtt{Q}$ is admissible, we know that all elements $\mathtt{Q}' \in \mathcal{Q} \cap U(\mathtt{Q})$ are at least of level $\ell(\mathtt{Q})$. This implies that all those elements are of equal or smaller size than $\mathtt{Q}$. It follows

$$\Sigma \subseteq \overline{U(\mathtt{Q})} \subseteq \bigcup(\mathcal{Q} \cap U(\mathtt{Q})), \qquad (5.140)$$

and with $\Sigma \subset \mathsf{S}_1(z)$, we get more precisely

$$\begin{aligned}\Sigma &\subseteq \mathsf{S}_1(z) \cap \overline{B}(\operatorname{mid}(\mathtt{Q}), \operatorname{size}(\ell(\mathtt{Q})) \circ (\tfrac{\mathbf{p}}{2} + 1))\\ &\subseteq \overline{B}(\Sigma, \operatorname{size}(\ell(\mathtt{Q})) \circ \tfrac{\mathbf{p}+1}{2}) && = \overline{B}(\Sigma, R)\\ &\subseteq \overline{B}(\operatorname{mid}(\mathtt{Q}), \operatorname{size}(\ell(\mathtt{Q})) \circ (\mathbf{p} + \tfrac{3}{2})) && = \overline{U(\mathtt{Q})}. \qquad (5.141)\end{aligned}$$

Equation (5.138) implies $\operatorname{supp} B_w \cap \Sigma \neq \emptyset$, and we conclude from (5.141) that $w \in B(\Sigma, R) \subseteq \overline{U(\mathtt{Q})}$.

In order to show $w \notin B(\Sigma, R)$, we assume that there is no element in $\mathcal{Q}$ with level higher than $\ell(\mathtt{Q}) + \frac{1}{d}$. This is an eligible assumption, since every admissible mesh can be reproduced by a sequence of level-increasing admissible subdivisions; see the proof of Proposition 5.2.21 for a detailed construction. This assumption implies that the j-orthogonal skeleton Sk_j is a subset of the j-orthogonal skeleton of a uniform $(\ell(\mathtt{Q}) + \frac{1}{d})$-leveled mesh,

$$\mathsf{Sk}_j(\mathcal{Q}) \subseteq \mathsf{Sk}_j(\mathcal{Q}_{\mathsf{u}[\ell(\mathtt{Q})+1/d]}), \qquad (5.142)$$

and with $\min \ell(\mathcal{Q} \cap U(\mathsf{Q})) = \ell(\mathsf{Q})$, we have even equality on the neighbourhood $\mathcal{Q} \cap U(\mathsf{Q})$,

$$\mathsf{Sk}_j(\mathcal{Q} \cap U(\mathsf{Q})) = \mathsf{Sk}_j(\mathcal{Q}_{\mathsf{u}[\ell(\mathsf{Q})]} \cap U(\mathsf{Q})) = \mathsf{Sk}_j(\mathcal{Q}_{\mathsf{u}[\ell(\mathsf{Q})+1/d]} \cap U(\mathsf{Q})), \tag{5.143}$$

using the notation $\mathsf{Sk}_j(\mathcal{Q} \cap U(\mathsf{Q})) \coloneqq \bigcup_{\mathsf{Q}' \in \mathcal{Q} \cap U(\mathsf{Q})} \mathsf{Sk}_j(\mathsf{Q}')$. Since $v \in \hat{\mathsf{N}}_j(s)$, we know that $\hat{\mathsf{N}}_j(s) \neq \emptyset$, which means that there are elements in $\mathcal{Q}$ that have j-orthogonal faces at the x_j-coordinate s, i.e., $\mathsf{S}_j(s) \cap \mathsf{Sk}_j(\mathcal{Q}) \neq \emptyset$. With (5.142) we get $\mathsf{S}_j(s) \cap \mathsf{Sk}_j(\mathcal{Q}_{\mathsf{u}[\ell(\mathsf{Q})+1/d]}) \neq \emptyset$. Since $\mathcal{Q}_{\mathsf{u}[\ell(\mathsf{Q})+1/d]}$ is a tensor-product mesh, its j-orthogonal skeleton consists of end-to-end slices, which yields $\mathsf{S}_j(s) \subseteq \mathsf{Sk}_j(\mathcal{Q}_{\mathsf{u}[\ell(\mathsf{Q})+1/d]})$. The restriction to the neighbourhood $\mathcal{Q} \cap U(\mathsf{Q})$ yields

$$\mathsf{S}_j(s) \cap \bigcup(\mathcal{Q} \cap U(\mathsf{Q})) \subseteq \mathsf{Sk}_j\left(\mathcal{Q}_{\mathsf{u}[\ell(\mathsf{Q})+1/d]} \cap U(\mathsf{Q})\right) \overset{(5.143)}{=} \mathsf{Sk}_j(\mathcal{Q} \cap U(\mathsf{Q})) \subseteq \mathsf{Sk}_j(\mathcal{Q}). \tag{5.144}$$

Since $w \notin \hat{\mathsf{N}}_j(s)$, we know by definition that

$$(w_1, \dots, w_{j-1}, s, w_{j+1}, \dots, w_d) \notin \mathsf{Sk}_j(\mathcal{Q}) \overset{(5.144)}{\supseteq} \mathsf{S}_j(s) \cap \bigcup(\mathcal{Q} \cap U(\mathsf{Q})) \supseteq \mathsf{S}_j(s) \cap \overline{U(\mathsf{Q})}. \tag{5.145}$$

Equation (5.138) implies that $\mathsf{S}_j(s) \cap \Sigma \neq \emptyset$, and with (5.140) we get that $\mathsf{S}_j(s) \cap \overline{U(\mathsf{Q})} \neq \emptyset$. Since $\overline{U(\mathsf{Q})}$ is an axis-aligned box, and the projection of w to the slice $\mathsf{S}_j(s)$ is not in $\mathsf{S}_j(s) \cap \overline{U(\mathsf{Q})}$, we conclude that $w \notin \overline{U(\mathsf{Q})} \supseteq \overline{B}(\Sigma, R)$.

This proves that $\widehat{\mathsf{TJ}}_j \cap \Sigma = \emptyset$. Since j was chosen arbitrary, this concludes the proof. □

Theorem 5.4.12. *For any two admissible meshes with one being a refinement of the other, the corresponding spline spaces are nested.*

Proof. We will prove the Theorem by induction over admissible subdivisions. Let $\mathcal{Q}$ be an admissible mesh, and let $\mathsf{Q}^* \in \mathcal{Q}$ such that the subdivision $\hat{\mathcal{Q}} \coloneqq \textsc{subdivide}^{1/d}(\mathcal{Q}, \mathsf{Q}^*)$ is admissible in the sense of Definition 5.4.6. We have to show that the spline spaces $\operatorname{span}(\mathcal{T})$ and $\operatorname{span}(\hat{\mathcal{T}})$ associated to the meshes $\mathcal{Q}$ and $\hat{\mathcal{Q}}$ are nested. They are defined by

$$\begin{aligned} \mathcal{T} &\coloneqq \{B_v \mid v \in \mathsf{N}(\mathcal{Q})\} \\ \text{and} \quad \hat{\mathcal{T}} &\coloneqq \{\hat{B}_v \mid v \in \mathsf{N}(\hat{\mathcal{Q}})\}, \end{aligned} \tag{5.146}$$

where $\hat{B}_v$ is the spline function associated to the local index vectors of v in the refined mesh $\hat{\mathcal{Q}}$.

We set $j_* \coloneqq (d \cdot \ell(\mathsf{Q}^*) \bmod d) + 1$ and observe that Q^* is subdivided in the j_*-th dimension. This means that all new hyperfaces in the mesh are j_*-orthogonal, and hence only the global knot vectors $\mathsf{K}_{j_*}(v)$ for $v \in \mathsf{N}(\mathcal{Q}) \cap \mathsf{Q}^*$ are updated. All other global knot vectors remain unchanged, in particular all non-j_*-orthogonal local index vectors.

$$\forall j \in \{1, \dots, d\} \setminus \{j_*\},\ \forall w \in \mathsf{N}(\mathcal{Q}): \quad \mathsf{k}_j(w) = \hat{\mathsf{k}}_j(w) \tag{5.147}$$

We consider an arbitrary new node $v = (v_1, \dots, v_d) \in \mathsf{N}(\hat{\mathcal{Q}}) \setminus \mathsf{N}(\mathcal{Q})$. We denote by

$$\underline{\hat{\mathsf{k}}}_j(v) \coloneqq \left\{(v_1, \dots, v_{j-1})\right\} \times \hat{\mathsf{k}}_i(v) \times \left\{(v_{j+1}, \dots, v_d)\right\} \tag{5.148}$$

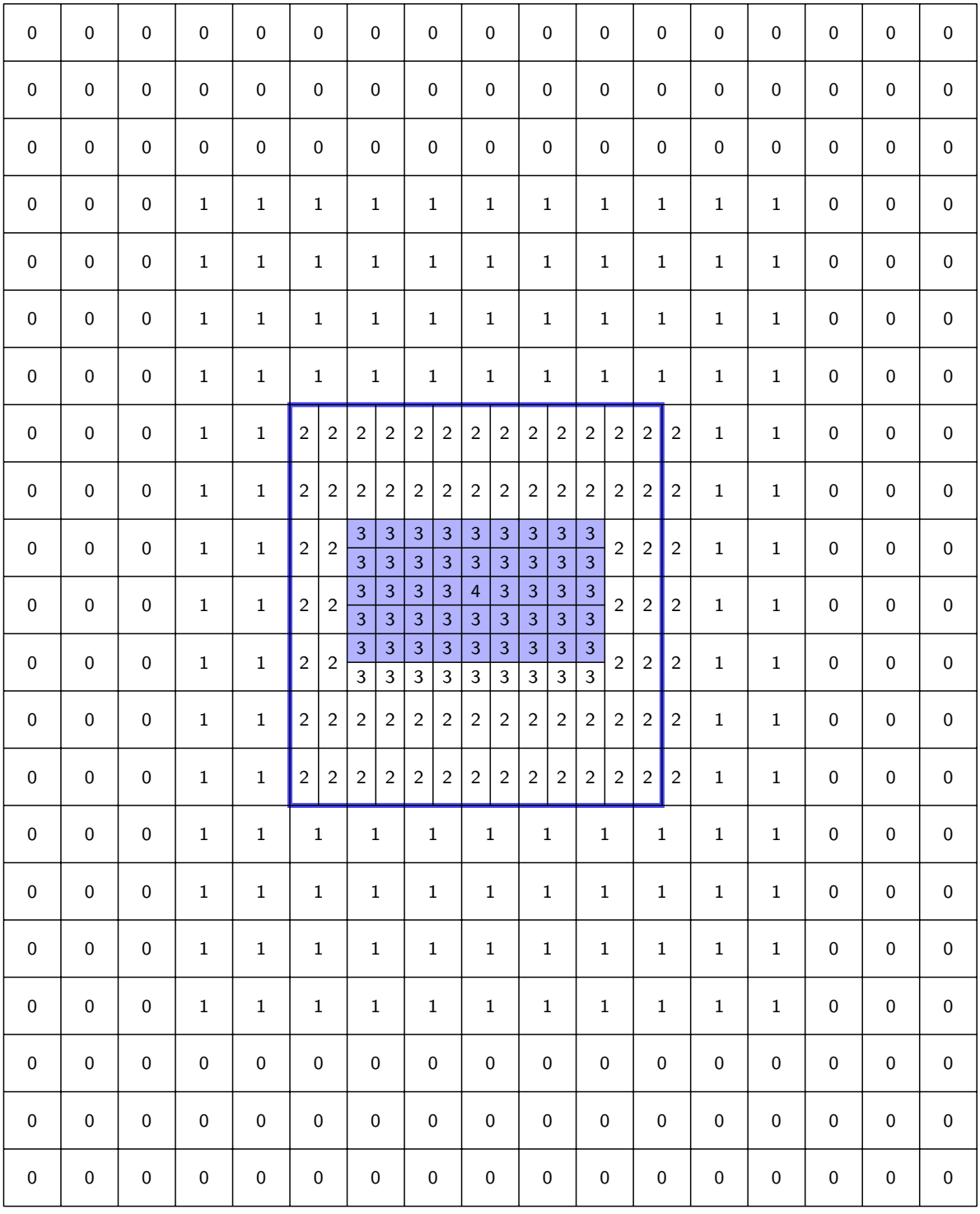

Figure 5.17 [34]: x_2x_3-view on the slice $\mathsf{S}_1(z)$. The numbers denote tripled element levels (i.e. 2 represents the level $\frac{2}{3}$), and the element in the center with level $\frac{4}{3}$ is a child of $\mathtt{Q}$. The patch $\hat{\mathcal{Q}} \cap U(\mathtt{Q})$ is highlighted in blue, and the second-order patch $\hat{\mathcal{Q}} \cap \bigcup_{\mathtt{Q}' \in \hat{\mathcal{Q}} \cap U(\mathtt{Q})} U(\mathtt{Q}')$ is indicated by a thick blue line.

the representation of the local index vector $\hat{\mathsf{k}}_i(v)$ in $\mathbb{R}^d$.For those points in $\underline{\hat{\mathsf{k}}}_j(v)$ that are also nodes, we observe the symmetry

$$\forall w, v \in \mathsf{N}(\hat{\mathcal{Q}}): \quad w \in \underline{\hat{\mathsf{k}}}_j(v) \Leftrightarrow v \in \underline{\hat{\mathsf{k}}}_j(w), \tag{5.149}$$

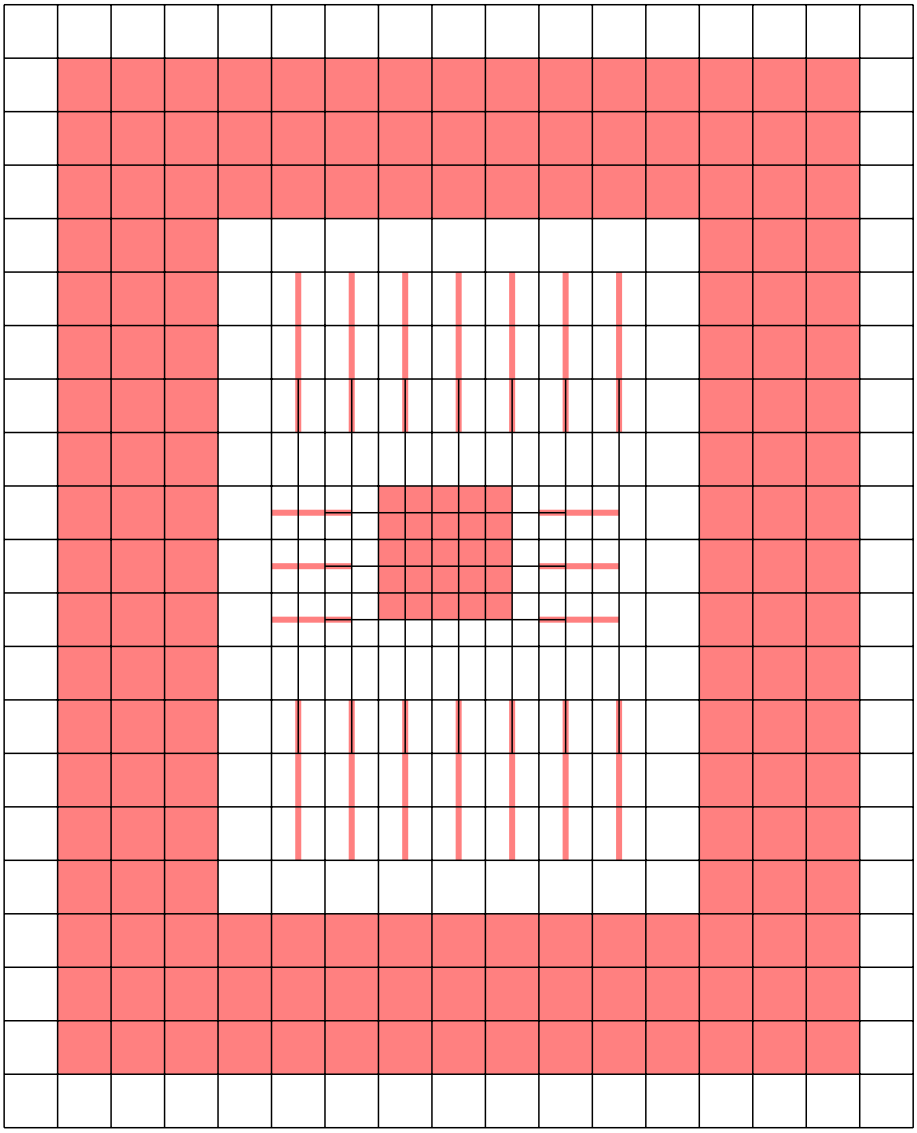

Figure 5.18 [34]: x_2x_3-view on the slice $\mathsf{S}_1(z)$. TJ_1 is indicated by red areas. TJ_2 is depicted by horizontal red lines, TJ_3 are vertical red lines. At the same time, the squared red area in the center coincides with Σ.

which implies that $\hat{\underline{\mathsf{k}}}_j(v) \cap \mathsf{N}(\hat{\mathcal{Q}})$ is the set of all nodes that are aligned with v in j-th dimension and have the j-th component of v in their new local index vector,

$$\hat{\underline{\mathsf{k}}}_j(v) \cap \mathsf{N}(\hat{\mathcal{Q}}) = \left\{ w \in \mathsf{N}(\hat{\mathcal{Q}}) \mid w_j \in \hat{\mathsf{k}}_j(v),\ \forall i \neq j :\ w_i = v_i \right\}. \tag{5.150}$$

The union of the sets $\hat{\underline{\mathsf{k}}}_{j_*}(v) \cap \mathsf{N}(\hat{\mathcal{Q}})$ over all new nodes $v \in \mathsf{N}(\hat{\mathcal{Q}}) \setminus \mathsf{N}(\mathcal{Q})$ contains *all* nodes of which the local index vectors have changed, and all new nodes,

$$\mathsf{N}(\hat{\mathcal{Q}}) \cap \bigcup_{v \in \mathsf{N}(\hat{\mathcal{Q}}) \setminus \mathsf{N}(\mathcal{Q})} \hat{\underline{\mathsf{k}}}_{j_*}(v) = \mathsf{N}(\hat{\mathcal{Q}}) \setminus \mathsf{N}(\mathcal{Q}) \cup \left\{ w \in \mathsf{N}(\mathcal{Q}) \mid \hat{B}_w \neq B_w \right\}. \tag{5.151}$$

In particular, each node $w \in \mathsf{N}(\mathcal{Q})$ of which the associated basis function has changed, i.e. $\hat{B}_w \neq B_w \in \mathcal{T} \setminus \hat{\mathcal{T}}$, is in the local index vector $\underline{\mathsf{k}}_{j_*}(v)$ of some new node $v \in \mathsf{N}(\hat{\mathcal{Q}}) \setminus \mathsf{N}(\mathcal{Q})$. It hence suffices to show that for all affected nodes, the

corresponding old T-spline is in the new spline space,

$$\forall\, v \in \mathsf{N}(\hat{\mathcal{Q}}) \setminus \mathsf{N}(\mathcal{Q})\ \forall\, w \in \hat{\underline{\mathsf{k}}}_{j_*}(v) \cap \mathsf{N}(\mathcal{Q}) : \quad B_w \in \operatorname{span}(\hat{\mathcal{T}}), \tag{5.152}$$

which is fullfilled if we prove for any $v \in \mathsf{N}(\hat{\mathcal{Q}}) \setminus \mathsf{N}(\mathcal{Q})$ that

$$\operatorname{span}\{B_w \mid w \in \hat{\underline{\mathsf{k}}}_{j_*}(v) \cap \mathsf{N}(\mathcal{Q})\} \subseteq \operatorname{span}\{\hat{B}_w \mid w \in \hat{\underline{\mathsf{k}}}_{j_*}(v) \cap \mathsf{N}(\hat{\mathcal{Q}})\}. \tag{5.153}$$

The main part of this proof below is to show that for any $v \in \mathsf{N}(\hat{\mathcal{Q}}) \setminus \mathsf{N}(\mathcal{Q})$ and any two new or affected nodes $w, z \in \hat{\underline{\mathsf{k}}}_{j_*}(v) \cap \mathsf{N}(\hat{\mathcal{Q}})$, the non-$j_*$-directional local index vectors of w and z coiincide,

$$\forall w, z \in \hat{\underline{\mathsf{k}}}_{j_*}(v) \cap \mathsf{N}(\hat{\mathcal{Q}})\ \forall j \in \{1, \dots, d\}, j \neq j_* : \quad \hat{\mathsf{k}}_j(w) = \hat{\mathsf{k}}_j(z). \tag{5.154}$$

In the one-dimensional case, T-splines coiincide with B-splines, and the spline spaces that correspond to nested (j_*-directional) knot vectors are always nested. Together, these arguments conclude the proof.

In order to show that (5.154) holds, we need to control the knot interval lengths in the local index vectors that correspond to the involved spline functions. Hence for any new node v and $w \in \hat{\underline{\mathsf{k}}}_j(v) \cap \mathsf{N}(\hat{\mathcal{Q}})$, we need to control the size or, equivalently, the level of each element Q' that includes two points that correspond to entries of a local index vector of w,

$$\mathcal{E}(\mathsf{Q}^*) \coloneqq \bigcup_{v \in \mathsf{N}(\hat{\mathcal{Q}}) \setminus \mathsf{N}(\hat{\mathcal{Q}})} \big\{ \mathsf{Q}' \in \mathcal{Q} \mid \exists w \in \hat{\underline{\mathsf{k}}}_{j_*}(v) \cap \mathsf{N}(\hat{\mathcal{Q}}),\ j \neq j_* :\ \#(\mathsf{Q}' \cap \hat{\underline{\mathsf{k}}}_j(w)) \geq 2 \big\}. \tag{5.155}$$

Note that $\mathcal{E}(\mathsf{Q}^*) \subseteq \mathcal{Q}$, and $\mathcal{Q} \setminus \hat{\mathcal{Q}} = \{\mathsf{Q}^*\}$ as well as $\hat{\mathcal{Q}} \setminus \mathcal{Q} = \textsc{subdivide}^{1/d}(\mathsf{Q}^*)$. Since the size of the children of Q^* differ only in j_*-direction from the size of Q, the definition

$$\hat{\mathcal{E}}(\mathsf{Q}^*) \coloneqq \bigcup_{v \in \mathsf{N}(\hat{\mathcal{Q}}) \setminus \mathsf{N}(\hat{\mathcal{Q}})} \big\{ \mathsf{Q}' \in \hat{\mathcal{Q}} \mid \exists w \in \hat{\underline{\mathsf{k}}}_{j_*}(v) \cap \mathsf{N}(\hat{\mathcal{Q}}),\ j \neq j_* :\ \#(\mathsf{Q}' \cap \hat{\underline{\mathsf{k}}}_j(w)) \geq 2 \big\} \tag{5.156}$$

yields $\mathcal{E}(\mathsf{Q}^*) \setminus \hat{\mathcal{E}}(\mathsf{Q}^*) = \{\mathsf{Q}\}$ and $\hat{\mathcal{E}}(\mathsf{Q}^*) \setminus \mathcal{E}(\mathsf{Q}^*) = \textsc{subdivide}^{1/d}(\mathsf{Q}^*)$. We will control the element levels in $\mathcal{E}(\mathsf{Q}^*)$ by proving *(i)* that $\mathcal{E}(\mathsf{Q}^*) \subseteq \mathcal{Q} \cap U(\mathsf{Q}^*)$, and subsequently *(ii)* that each element $\mathsf{Q}' \in \mathcal{E}(\mathsf{Q}^*)$ has an element of level $\ell(\mathsf{Q}^*)$ in its neighbourhood $\mathcal{Q} \cap U(\mathsf{Q}')$. This will yield a lower and an upper bound on the element levels in $\mathcal{E}(\mathsf{Q}^*)$.

(i). We assumed the subdivision $\textsc{subdivide}^{1/d}(\mathcal{Q}, \mathsf{Q}^*)$ to be admissible, which means by Definition 5.4.6 that

$$\forall \mathsf{Q}' \in \mathcal{Q} \cap U(\mathsf{Q}^*) : \quad \ell(\mathsf{Q}') \geq \ell(\mathsf{Q}^*). \tag{5.157}$$

With Definition 5.4.3 and $d \cdot \ell(\mathsf{Q}^*) \bmod d = j_* - 1$, this implies that all elements in $U(\mathsf{Q}^*)$ are at most of the size

$$q^{-\lfloor \ell(\mathsf{Q}^*) \rfloor} \big(\underbrace{\tfrac{1}{q}, \dots, \tfrac{1}{q}}_{(j_*-1) \text{ times}}, 1, \dots, 1 \big). \tag{5.158}$$

We denote $\mathsf{Q}^* = [x_1, x_1+\tilde{x}_1] \times \cdots \times [x_d, x_d+\tilde{x}_d]$ and consider an arbitrary new node $v \in \mathsf{N}(\hat{\mathcal{Q}}) \setminus \mathsf{N}(\mathcal{Q})$, and observe

$$\operatorname{size}(\ell(\mathsf{Q}^*)) = (\tilde{x}_1, \ldots, \tilde{x}_d), \tag{5.159}$$

$$x_j \leq v_j \leq x_j + \tilde{x}_j \quad \text{for all } j \in \{1, \ldots, d\} \tag{5.160}$$

$$\text{and} \quad x_{j_*} < v_{j_*} < x_{j_*} + \tilde{x}_{j_*}. \tag{5.161}$$

Consider some arbitrary $w \in \underline{\hat{\mathsf{k}}}_{j_*}(v) \cap \mathsf{N}(\hat{\mathcal{Q}})$. The definition of $\underline{\hat{\mathsf{k}}}_{j_*}(v)$ (5.148) implies that w and v are connected by a chain of at most $\frac{p_{j_*}+1}{2}$ elements, this is, one child of Q^* which has the j_*-directional size $q^{-\lfloor \ell(\mathsf{Q}^*)\rfloor - 1}$, and $\frac{p_{j_*}-1}{2}$ more elements with yet unbounded sizes. We want to show that

$$w \in U(\mathsf{Q}^*), \tag{5.162}$$

with $U(\mathsf{Q}^*)$ from Definition 5.4.4. Assume for contradiction that $w \notin U(\mathsf{Q}^*)$, which means that there is some dimension $\tilde{\jmath} \in \{1, \ldots, d\}$ such that

$$\underbrace{\left| x_{\tilde{\jmath}} + \tfrac{\tilde{x}_{\tilde{\jmath}}}{2} - w_{\tilde{\jmath}} \right|}_{\substack{\tilde{\jmath}\text{-th entry of} \\ \operatorname{Dist}(\mathsf{Q}^*, w)}} \geq \tilde{x}_{\tilde{\jmath}} \cdot (p_{\tilde{\jmath}} + \tfrac{3}{2}). \tag{5.163}$$

Together, (5.160) and (5.150) yield $x_j \leq w_j = v_j \leq x_j + \tilde{x}_j$ for all $j \neq j_*$, and hence

$$\left| x_j + \tfrac{\tilde{x}_j}{2} - w_j \right| \leq \tfrac{\tilde{x}_j}{2} < \tilde{x}_j \cdot (p_j + \tfrac{3}{2}) \quad \text{for all } j \neq j_*. \tag{5.164}$$

This implies that $\tilde{\jmath} = j_*$ and hence

$$\left| x_{j_*} + \tfrac{\tilde{x}_{j_*}}{2} - w_{j_*} \right| \geq \underbrace{q^{-\lfloor \ell(\mathsf{Q}^*)\rfloor}}_{\substack{j_*\text{-th entry of} \\ \operatorname{size}(\ell(\mathsf{Q}^*))}} \cdot (p_{j_*} + \tfrac{3}{2}). \tag{5.165}$$

We know from above that the j_*-directional sizes of all elements in $\mathcal{Q} \cap U(\mathsf{Q}^*)$ are smaller or equal to $q^{-\lfloor \ell(\mathsf{Q}^*)\rfloor}$. Without loss of generality, we assume equality in (5.165), which means that w is in the boundary of the open box $U(\mathsf{Q}^*)$ and hence that all j_*-direction edges between w and v are in the environment $U(\mathsf{Q}^*)$. This implies that the number of elements between w and v is at least $|w_{j_*} - v_{j_*}| \cdot q^{\lfloor \ell(\mathsf{Q}^*)\rfloor}$. We conclude from (5.161) that

$$\left| x_{j_*} + \tfrac{\tilde{x}_{j_*}}{2} - v_{j_*} \right| < \tfrac{\tilde{x}_{j_*}}{2} = \tfrac{1}{2} q^{-\lfloor \ell(\mathsf{Q}^*)\rfloor}, \tag{5.166}$$

and hence

$$\begin{aligned} |w_{j_*} - v_{j_*}| \cdot q^{\lfloor \ell(\mathsf{Q}^*)\rfloor} &\geq \left(\left| x_{j_*} + \tfrac{\tilde{x}_{j_*}}{2} - w_{j_*} \right| - \left| x_{j_*} + \tfrac{\tilde{x}_{j_*}}{2} - v_{j_*} \right| \right) \cdot q^{\lfloor \ell(\mathsf{Q}^*)\rfloor} \\ &\overset{\substack{(5.165)\\(5.166)}}{>} \left((p_{j_*} + \tfrac{3}{2}) q^{-\lfloor \ell(\mathsf{Q}^*)\rfloor} - \tfrac{1}{2} q^{-\lfloor \ell(\mathsf{Q}^*)\rfloor} \right) \cdot q^{\lfloor \ell(\mathsf{Q}^*)\rfloor} = p_{j_*} + 1, \end{aligned} \tag{5.167}$$

which means that the number of elements between w and v is greater than $p_{j_*}+1 > \frac{p_{j_*}+1}{2}$. This contradicts our knowledge from above that w and v are connected by a chain of at most $\frac{p_{j_*}+1}{2}$ elements, and proves (5.162).

We have proven for arbitrary $w \in \hat{\underline{\mathsf{k}}}_{j_*}(v) \cap \mathsf{N}(\hat{\mathcal{Q}})$ that $w \in U(\mathsf{Q}^*)$, and we want to show below that $\mathcal{E}(\mathsf{Q}^*) \subseteq \mathcal{Q} \cap U(\mathsf{Q}^*)$. We consider $j \neq j_*$ and denote $\hat{\underline{\mathsf{k}}}_j(w) = \{\tilde{w}_1, \dots, \tilde{w}_{p_j+2}\} \subset \overline{\Omega}$, assuming that the points $\tilde{w}_1, \dots, \tilde{w}_{p_j+2}$ are ordered with respect to their j-th component. Consider $\tilde{w} \in \{\tilde{w}_2, \dots, \tilde{w}_{p_j+1}\}$. We want to show that

$$\tilde{w} \in U(\mathsf{Q}^*). \tag{5.168}$$

From Definition 5.3.5 we know that w_j is the middle entry of $\hat{\mathsf{k}}_j(w) \subseteq \hat{\mathsf{K}}_j(w)$. This and the definition of $\hat{\mathsf{K}}_j(w)$ imply that w and $\tilde{w}$ are connected by a chain of at most $\frac{p_j-1}{2}$ elements,

$$\exists\, \mathsf{Q}_1, \dots, \mathsf{Q}_{(p_j-1)/2} \in \mathcal{Q}: \quad [w, \tilde{w}] \coloneqq \{tw + (1-t)\tilde{w} \mid t \in [0,1]\} \subset \mathsf{Q}_1 \cup \dots \cup \mathsf{Q}_{(p_j-1)/2}. \tag{5.169}$$

Recall from above that $j \neq j_*$, and that $\tilde{w}_i = w_i$ for all $i \neq j$. Hence the points w and $\tilde{w}$ differ only in j-direction. We know from (5.164) that $\left| x_j + \frac{\tilde{x}_j}{2} - w_j \right| \leq \frac{\tilde{x}_j}{2}$. Similarly to the proof above, the assumption $\tilde{w} \notin U(\mathsf{Q}^*)$ yields that any set of elements $\mathcal{M} \subset \hat{\mathcal{Q}}$ satisfying $[w, \tilde{w}] \subset \bigcup \mathcal{M}$ contains at least $p_j + 1$ elements, in contradiction to the existence of $\{\mathsf{Q}_1, \dots, \mathsf{Q}_{(p_j-1)/2}\}$ which contains only $\frac{p_j-1}{2}$ elements. This proves (5.168).

We have proven $\tilde{w} \in U(\mathsf{Q}^*)$, which implies that all elements neighboring $\tilde{w}$ are in $U(\mathsf{Q}^*)$. Note that if a mesh element contains two points that correspond to the same local index vector, then at most one of these two points corresponds to the first or last entry of that local index vector. This and the fact that w and $\tilde{w}$ were chosen arbitrary yield that all elements of which we want to control the size are in the neighbourhood of Q^*,

$$\mathcal{E}(\mathsf{Q}^*) \subseteq \mathcal{Q} \cap U(\mathsf{Q}^*). \tag{5.170}$$

(ii). In order to get an upper bound on the level of elements from $\mathcal{E}(\mathsf{Q}^*)$, we want to show that each of those elements has an element of level $\ell(\mathsf{Q}^*)$ in its environment,

$$\forall \mathsf{Q}' \in \mathcal{E}(\mathsf{Q}^*)\ \exists \mathsf{Q}'' \in U(\mathsf{Q}'): \quad \ell(\mathsf{Q}'') = \ell(\mathsf{Q}^*). \tag{5.171}$$

Assume for contradiction that there is some $\mathsf{Q}' \in \mathcal{E}(\mathsf{Q}^*)$ such that

$$\forall \mathsf{Q}'' \in U(\mathsf{Q}'): \quad \ell(\mathsf{Q}'') \neq \ell(\mathsf{Q}^*). \tag{5.172}$$

The combination of $\mathsf{Q}' \in \mathcal{E}(\mathsf{Q}^*)$ and (5.170) yields $\mathsf{Q}' \in U(\mathsf{Q}^*)$. With (5.157), we have $\ell(\mathsf{Q}') \geq \ell(\mathsf{Q}^*)$. Since $\mathsf{Q}' \in U(\mathsf{Q}')$, the assumption (5.172) yields $\ell(\mathsf{Q}') \neq \ell(\mathsf{Q}^*)$ and hence $\ell(\mathsf{Q}') > \ell(\mathsf{Q}^*)$, or equivalently $\ell(\mathsf{Q}') \geq \ell(\mathsf{Q}^*) + \frac{1}{d}$. Lemma 5.4.10 states that

$$\forall\ \mathsf{Q}'' \in U(\mathsf{Q}'): \quad \ell(\mathsf{Q}'') \geq \ell(\mathsf{Q}') - \tfrac{1}{d} \geq \ell(\mathsf{Q}^*), \tag{5.173}$$

and together with (5.172),

$$\forall\ \mathsf{Q}'' \in U(\mathsf{Q}'): \quad \ell(\mathsf{Q}'') > \ell(\mathsf{Q}^*). \tag{5.174}$$

This means that all j_*-direction edges in $U(\mathtt{Q}')$ are at most of the length $q^{-\lfloor \ell(\mathtt{Q}^*)\rfloor -1}$. From $\mathtt{Q}' \in \mathcal{E}(\mathtt{Q}^*)$ we conclude that there exist $v \in \mathsf{N}(\hat{\mathcal{Q}}) \setminus \mathsf{N}(\mathcal{Q})$ and $w \in \hat{\underline{\mathsf{k}}}_{j_*}(v)$, $j \neq j_*$ with $\hat{\underline{\mathsf{k}}}_j(w) = (\tilde{w}_1, \ldots, \tilde{w}_{p_j+2})$, as well as $\tilde{w} \in \mathtt{Q}' \cap \{\tilde{w}_2, \ldots, \tilde{w}_{p_j+1}\}$.

Case 1. If $\ell(\mathtt{Q}') > \ell(\mathtt{Q}^*) + \frac{1}{d}$, then $\mathtt{Q}'$ has an ancestor $\hat{\mathtt{Q}}'$ with $\ell(\hat{\mathtt{Q}}') = \ell(\mathtt{Q}^*) + \frac{1}{d}$. Since $v \in \mathtt{Q}^*$, the assumption (5.172) implies that $v \notin U(\mathtt{Q}')$. From $w \in \hat{\underline{\mathsf{k}}}_{j_*}(v)$ follows that w and v are connected by a chain of at most $\frac{p_{j_*}+1}{2}$ elements. We follow exactly the proofs of (5.162) and (5.168) above, only exchanging v and $\tilde{w}$ and replacing $\mathtt{Q}^*$ by $\hat{\mathtt{Q}}'$. Similarly to the proof of (5.162), we get the contradiction that w and v are connected by more than $p_{j_*} + 1$ elements.

Case 2. If $\ell(\mathtt{Q}') = \ell(\mathtt{Q}^*) + \frac{1}{d}$, then Lemma 5.4.10 yields for arbitrary $\mathtt{Q}'' \in U(\mathtt{Q}')$ that $\ell(\mathtt{Q}^*) + \frac{1}{d} = \ell(\mathtt{Q}') \leq \ell(\mathtt{Q}'') + 1$, which means $\ell(\mathtt{Q}^*) \leq \ell(\mathtt{Q}'')$. Together with (5.172), we have $\ell(\mathtt{Q}^*) < \ell(\mathtt{Q}'')$ and hence $\ell(\mathtt{Q}^*) + \frac{1}{d} \leq \ell(\mathtt{Q}'')$ for any $\mathtt{Q}'' \in U(\mathtt{Q}')$. We set $\hat{\mathtt{Q}}' \coloneqq \mathtt{Q}'$ and proceed as in Case 1, deriving the same desired contradiction. This concludes the proof of (5.171).

We have proven that each element in $\mathcal{E}(\mathtt{Q}^*)$ has an element of level $\ell(\mathtt{Q}^*)$ in its environment. Hence, Lemma 5.4.10 implies that these elements are at most of level $\ell(\mathtt{Q}^*) + \frac{1}{d}$. This and (5.170) together read

$$\forall \mathtt{Q}' \in \mathcal{E}(\mathtt{Q}^*): \quad \ell(\mathtt{Q}^*) \leq \ell(\mathtt{Q}') \leq \ell(\mathtt{Q}^*) + \tfrac{1}{d}, \tag{5.175}$$

which proves (5.154). Equations (5.147) and (5.154) together, expressed in terms of the associated 1D B-spline functions, yield

$$\forall w, z \in \hat{\underline{\mathsf{k}}}_{j_*}(v)\ \forall j \in \{1, \ldots, d\}, j \neq j_*: \quad N_{\hat{\mathsf{k}}_j(w)} = N_{\hat{\mathsf{k}}_j(z)}, \tag{5.176}$$

$$\forall w, z \in \hat{\underline{\mathsf{k}}}_{j_*}(v) \cap \mathsf{N}(\mathcal{Q})\ \forall j \in \{1, \ldots, d\}, j \neq j_*: \quad N_{\hat{\mathsf{k}}_j(w)} = N_{\mathsf{k}_j(w)} = N_{\mathsf{k}_j(z)} = N_{\hat{\mathsf{k}}_j(z)}. \tag{5.177}$$

We define $N_v^{\neq j_*} \coloneqq \prod_{\substack{j \in \{1,\ldots,d\} \\ j \neq j_*}} N_{\hat{\mathsf{k}}_j(v)}$ and conclude with (5.177) and (5.176) that

$$\forall w \in \hat{\underline{\mathsf{k}}}_{j_*}(v) \cap \mathsf{N}(\mathcal{Q}): \quad B_w = N_v^{\neq j_*} \cdot N_{\mathsf{k}_{j_*}(w)} \tag{5.178}$$

$$\text{and} \quad \forall w \in \hat{\underline{\mathsf{k}}}_{j_*}(v): \quad \hat{B}_w = N_v^{\neq j_*} \cdot N_{\hat{\mathsf{k}}_{j_*}(w)}. \tag{5.179}$$

We know that in the case of knot insertion in 1D, the corresponding 1D B-spline spaces are nested:

$$\operatorname{span}\{N_{\mathsf{k}_{j_*}(w)} \mid w \in \hat{\underline{\mathsf{k}}}_{j_*}(v) \cap \mathsf{N}(\mathcal{Q})\} \subseteq \operatorname{span}\{N_{\hat{\mathsf{k}}_{j_*}(w)} \mid w \in \hat{\underline{\mathsf{k}}}_{j_*}(v)\}. \tag{5.180}$$

The combination of (5.178), (5.179) and (5.180) shows that Equation (5.153) holds. This concludes the proof. □

5.4.2 Linear Complexity

This section is devoted to a complexity estimate in the style of a famous estimate for the Newest Vertex Bisection on triangular meshes given by Binev, Dahmen and DeVore [7] and, in an alternative version, by Stevenson [8]. Linear Complexity of the refinement procedure is an inevitable criterion for optimal convergence rates in

the Adaptive Finite Element Method (see e.g. [7, 8, 10] and [53, Conclusions]). The estimate and its proof follow our own work [38, 37], which we generalize now to three dimensions and q-graded refinement. The estimate reads as follows.

Theorem 5.4.13. *Any sequence of admissible meshes $\mathcal{Q}_0, \mathcal{Q}_1, \dots, \mathcal{Q}_J$ with*

$$\mathcal{Q}_j = \text{REFINE\_TS}_{\text{nD}}(\mathcal{Q}_{j-1}, \mathcal{M}_{j-1}), \quad \mathcal{M}_{j-1} \subseteq \mathcal{Q}_{j-1} \quad \text{for } j \in \{1, \dots, J\} \tag{5.181}$$

satisfies

$$|\mathcal{Q}_J \setminus \mathcal{Q}_0| \;\leq\; C_{5.4.13} \sum_{j=0}^{J-1} |\mathcal{M}_j| \,, \tag{5.182}$$

with

$$C_{5.4.13} = \tfrac{q^{1/d}}{1-q^{-1/d}} \operatorname{prod}\big(4C_{5.4.14} + (1, q^{1/d}, \dots, q^{(d-1)/d})\big) \tag{5.183}$$

and $C_{5.4.14}$ from Lemma 5.4.14 below.

Lemma 5.4.14. *Given an admissible mesh $\mathcal{Q}$, a set of marked elements $\mathcal{M} \subseteq \mathcal{Q}$, and $\mathtt{Q} \in \text{REFINE\_TS}_{\text{nD}}(\mathcal{Q}, \mathcal{M}) \setminus \mathcal{Q}$, there exists $\mathtt{Q}' \in \mathcal{M}$ such that $\ell(\mathtt{Q}) \leq \ell(\mathtt{Q}') + 1$ and*

$$\operatorname{Dist}(\mathtt{Q}, \mathtt{Q}') \leq q^{-\ell(\mathtt{Q})}\, C_{5.4.14}, \tag{5.184}$$

with "$\leq$" understood componentwise and

$$C_{5.4.14} \coloneqq \tfrac{1}{1-q^{-1/d}} \left(1, q^{1/d}, \dots, q^{(d-1)/d}\right) \circ (\mathbf{p} + \tfrac{3+q^{1/d}}{2}) + \left(\tfrac{q^{1/d}}{2}, \tfrac{q^{2/d}}{2}, \dots, \tfrac{q}{2}\right). \tag{5.185}$$

Proof. The function $\operatorname{size}(k)$ from Definition 5.4.3 is decreasing in k and bounded by

$$\operatorname{size}(k) \leq q^{-k}\left(1, q^{1/d}, \dots, q^{(d-1)/d}\right) \quad \text{for all } k \in \mathbb{N}_0. \tag{5.186}$$

Consequently, the term $\operatorname{size}(\ell(\mathtt{Q})) \circ (\mathbf{p} + \frac{3}{2})$ from Definition 5.4.4 is also decreasing in $\ell(\mathtt{Q})$ and bounded by

$$\operatorname{size}(\ell(\mathtt{Q})) \circ (\mathbf{p} + \tfrac{3}{2}) \leq q^{-\ell(\mathtt{Q})} \underbrace{\left(1, q^{1/d}, \dots, q^{(d-1)/d}\right) \circ (\mathbf{p} + \tfrac{3}{2})}_{\tilde{\mathbf{p}}}. \tag{5.187}$$

Hence for any $\tilde{\mathtt{Q}} \in \mathcal{Q}$ and $\tilde{\mathtt{Q}}' \in \mathcal{Q} \cap U(\tilde{\mathtt{Q}})$, there exists $x \in \tilde{\mathtt{Q}}' \cap U(\tilde{\mathtt{Q}})$ and hence

$$\begin{aligned}
\operatorname{Dist}(\tilde{\mathtt{Q}}, \tilde{\mathtt{Q}}') &\leq \operatorname{Dist}(\tilde{\mathtt{Q}}, x) + \operatorname{Dist}(\tilde{\mathtt{Q}}', x) \\
&\leq \operatorname{Dist}(\tilde{\mathtt{Q}}, x) + \tfrac{1}{2} \operatorname{size}(\ell(\tilde{\mathtt{Q}}')) \\
&\overset{\text{Lemma } 5.4.10}{\leq} \operatorname{Dist}(\tilde{\mathtt{Q}}, x) + \tfrac{1}{2} \operatorname{size}(\ell(\tilde{\mathtt{Q}}) - \tfrac{1}{d}) \\
&\overset{(5.186)}{\underset{(5.187)}{\leq}} q^{-\ell(\tilde{\mathtt{Q}})}\, \tilde{\mathbf{p}} + q^{-\ell(\tilde{\mathtt{Q}})} \underbrace{\left(\tfrac{q^{1/d}}{2}, \tfrac{q^{2/d}}{2}, \dots, \tfrac{q}{2}\right)}_{\mathbf{s}} \\
&\leq q^{-\ell(\tilde{\mathtt{Q}})} \left(\tilde{\mathbf{p}} + \mathbf{s}\right).
\end{aligned} \tag{5.188}$$

The existence of $\mathtt{Q} \in \text{REFINE\_TS}_{\text{nD}}(\mathcal{Q}, \mathcal{M}) \setminus \mathcal{Q}$ means that $\text{REFINE\_TS}_{\text{nD}}$ subdivides $\mathtt{Q}' = \mathtt{Q}_J, \mathtt{Q}_{J-1}, \dots, \mathtt{Q}_0$ such that $\mathtt{Q}_{j-1} \in \mathcal{Q} \cap U(\mathtt{Q}_j)$ and $\ell(\mathtt{Q}_{j-1}) < \ell(\mathtt{Q}_j)$ for $j =$

$J,\dots,1$, having $\square' \in \mathcal{M}$ and $\square \in \text{SUBDIVIDE}^{1/d}(\square_0)$. Lemma 5.4.10 yields $\ell(\square_{j-1}) = \ell(\square_j) - \frac{1}{d}$ for $j = J,\dots,1$, which yields the estimate

$$\begin{aligned}\text{Dist}(\square',\square_0) &\le \sum_{j=1}^{J} \text{Dist}(\square_j,\square_{j-1}) \overset{(5.188)}{\le} \sum_{j=1}^{J} q^{-\ell(\square_j)}\,(\tilde{\mathbf{p}}+\mathbf{s}) \\ &= \sum_{j=1}^{J} q^{-(\ell(\square_0)+j)}\,(\tilde{\mathbf{p}}+\mathbf{s}) < q^{-\ell(\square_0)}\,(\tilde{\mathbf{p}}+\mathbf{s}) \sum_{j=1}^{\infty} q^{-j/d} \\ &= \frac{q^{-1/d-\ell(\square_0)}}{1-q^{-1/d}}\,(\tilde{\mathbf{p}}+\mathbf{s}) = \frac{q^{-\ell(\square)}}{1-q^{-1/d}}\,(\tilde{\mathbf{p}}+\mathbf{s}). \end{aligned} \tag{5.189}$$

The distance between $\square$ and its parent element $\square_0$ is bounded by

$$\text{Dist}(\square,\square_0) \le \tfrac{1}{2}\,\text{size}(\ell(\square_0)) \le q^{-\ell(\square)}\mathbf{s}. \tag{5.190}$$

This and a triangle inequality conclude the proof. □

Proof of Theorem 5.4.13.
(1) For $\square \in \bigcup \mathbb{M}_{\text{TS}}$ and $\square' \in \mathcal{M} \coloneqq \mathcal{M}_0 \cup \dots \cup \mathcal{M}_{J-1}$, define $\lambda(\square,\square')$ by

$$\lambda(\square,\square') \coloneqq \begin{cases} q^{\ell(\square)-\ell(\square')} & \text{if } \ell(\square) \le \ell(\square') + \frac{1}{d} \\ & \quad \text{and } \text{Dist}(\square,\square') < 2q^{-\ell(\square)}\,C_{5.4.14}, \\ 0 & \text{otherwise.} \end{cases} \tag{5.191}$$

(2) *Main idea of the proof.*

$$\begin{aligned}|\mathcal{Q}_J \setminus \mathcal{Q}_0| = \sum_{\square\in\mathcal{Q}_J\setminus\mathcal{Q}_0} 1 &\overset{(3)}{\le} \sum_{\square\in\mathcal{Q}_J\setminus\mathcal{Q}_0} \sum_{\square'\in\mathcal{M}} \lambda(\square,\square') \\ &\overset{(4)}{\le} \sum_{\square'\in\mathcal{M}} C_{5.4.13} = C_{5.4.13} \sum_{j=0}^{J-1} |\mathcal{M}_j|. \end{aligned} \tag{5.192}$$

(3) *Each* $\square \in \mathcal{Q}_J \setminus \mathcal{Q}_0$ *satisfies*

$$\sum_{\square'\in\mathcal{M}} \lambda(\square,\square') \ge 1. \tag{5.193}$$

Consider $\square \in \mathcal{Q}_J \setminus \mathcal{Q}_0$. Set $j_1 < J$ such that $\square \in \mathcal{Q}_{j_1+1} \setminus \mathcal{Q}_{j_1}$. Lemma 5.4.14 states the existence of $\square_1 \in \mathcal{M}_{j_1}$ with $\text{Dist}(\square,\square_1) \le q^{-\ell(\square)}\,C_{5.4.14}$ and $\ell(\square) \le \ell(\square_1) + \frac{1}{d}$. Hence $\lambda(\square,\square_1) = q^{\ell(\square)-\ell(\square_1)} > 0$. The repeated use of Lemma 5.4.14 yields $j_1 > j_2 > j_3 > \dots$ and $\square_2,\square_3,\dots$ with $\square_{i-1} \in \mathcal{Q}_{j_i+1} \setminus \mathcal{Q}_{j_i}$ and $\square_i \in \mathcal{M}_{j_i}$ such that

$$\text{Dist}(\square_{i-1},\square_i) \le q^{-\ell(\square_{i-1})}\,C_{5.4.14} \text{ and } \ell(\square_{i-1}) \le \ell(\square_i) + \tfrac{1}{d}. \tag{5.194}$$

We repeat applying Lemma 5.4.14 as $\lambda(\square,\square_i) > 0$ and $\ell(\square_i) > 0$, and we stop at the first index L with $\lambda(\square,\square_L) = 0$ or $\ell(\square_L) = 0$. If $\ell(\square_L) = 0$ and $\lambda(\square,\square_L) > 0$, then

$$\sum_{\square'\in\mathcal{M}} \lambda(\square,\square') \ge \lambda(\square,\square_L) = q^{\ell(\square)-\ell(\square_L)} \ge q^{1/d}. \tag{5.195}$$

If $\lambda(\mathfrak{Q}, \mathfrak{Q}_L) = 0$ because $\ell(\mathfrak{Q}) > \ell(\mathfrak{Q}_L) + \frac{1}{d}$, then (5.194) yields $\ell(\mathfrak{Q}_{L-1}) \le \ell(\mathfrak{Q}_L) + \frac{1}{d} < \ell(\mathfrak{Q})$ and hence

$$\sum_{\mathfrak{Q}' \in \mathcal{M}} \lambda(\mathfrak{Q}, \mathfrak{Q}') \ge \lambda(\mathfrak{Q}, \mathfrak{Q}_{L-1}) = q^{\ell(\mathfrak{Q}) - \ell(\mathfrak{Q}_{L-1})} > q^{1/d}. \tag{5.196}$$

If $\lambda(\mathfrak{Q}, \mathfrak{Q}_L) = 0$ because $\mathrm{Dist}(\mathfrak{Q}, \mathfrak{Q}_L) \not< 2q^{-\ell(\mathfrak{Q})} C_{5.4.14}$, then there exists an index $k \in \{1, \dots, d\}$ with $\mathrm{Dist}_k(\mathfrak{Q}, \mathfrak{Q}_L) \ge 2q^{-\ell(\mathfrak{Q})} (C_{5.4.14})_k$, and a triangle inequality shows

$$\begin{aligned} 2q^{-\ell(\mathfrak{Q})} (C_{5.4.14})_k &\le \mathrm{Dist}_k(\mathfrak{Q}, \mathfrak{Q}_1) + \sum_{i=1}^{L-1} \mathrm{Dist}_k(\mathfrak{Q}_i, \mathfrak{Q}_{i+1}) \\ &\le q^{-\ell(\mathfrak{Q})} (C_{5.4.14})_k + \sum_{i=1}^{L-1} q^{-\ell(\mathfrak{Q}_i)} (C_{5.4.14})_k, \end{aligned} \tag{5.197}$$

and hence $q^{-\ell(\mathfrak{Q})} \le \sum_{i=1}^{L-1} q^{-\ell(\mathfrak{Q}_i)}$. The proof is concluded with

$$1 \le \sum_{i=1}^{L-1} q^{\ell(\mathfrak{Q}) - \ell(\mathfrak{Q}_i)} = \sum_{i=1}^{L-1} \lambda(\mathfrak{Q}, \mathfrak{Q}_i) \le \sum_{\mathfrak{Q}' \in \mathcal{M}} \lambda(\mathfrak{Q}, \mathfrak{Q}'). \tag{5.198}$$

(4) *For all $j \in \{0, \dots, J-1\}$ and $\mathfrak{Q}' \in \mathcal{M}_j$ holds*

$$\sum_{\mathfrak{Q} \in \mathcal{Q}_J \setminus \mathcal{Q}_0} \lambda(\mathfrak{Q}, \mathfrak{Q}') \le \tfrac{q^{1/d}}{1 - q^{-1/d}} \operatorname{prod}\big(4C_{5.4.14} + (1, q^{1/d} \dots, q^{(d-1)/d})\big) = C_{5.4.13}. \tag{5.199}$$

This is shown as follows. By definition of λ, we have

$$\begin{aligned} \sum_{\mathfrak{Q} \in \mathcal{Q}_J \setminus \mathcal{Q}_0} \lambda(\mathfrak{Q}, \mathfrak{Q}') &\le \sum_{\mathfrak{Q} \in \bigcup \mathbb{M}_{\mathrm{TS}} \setminus \mathcal{Q}_0} \lambda(\mathfrak{Q}, \mathfrak{Q}') \\ &= \sum_{j=1}^{d \cdot \ell(\mathfrak{Q}') + 1} q^{j - \ell(\mathfrak{Q}')} \underbrace{\#\Big\{\mathfrak{Q} \in \bigcup \mathbb{M}_{\mathrm{TS}} \mid \ell(\mathfrak{Q}) = \tfrac{j}{d},\ \mathrm{Dist}(\mathfrak{Q}, \mathfrak{Q}') < 2q^{-j/d} C_{5.4.14}\Big\}}_{B}. \end{aligned} \tag{5.200}$$

Since we know by Definition 5.4.3 that $\ell(\mathfrak{Q}) = \frac{j}{d}$ implies $|\mathfrak{Q}| = \operatorname{prod}\operatorname{size}(\ell(\mathfrak{Q})) = q^{-j}$, we know that $q^j \left|\bigcup B\right|$ is an upper bound of $\#B$. The cuboidal set $\bigcup B$ is the union of all admissible elements of level $\frac{j}{d}$ having their midpoints inside a cuboid of size $4q^{-j/d} C_{5.4.14}$. An admissible element of level j is not bigger than $q^{-j/d} \times q^{(1-j)/d} \times \dots \times q^{(d-1-j)/d}$. Together, we have

$$\left|\bigcup B\right| \le q^{-j} \operatorname{prod}\big(4C_{5.4.14} + (1, q^{1/d} \dots, q^{(d-1)/d})\big), \tag{5.201}$$

and hence $\#B \le \operatorname{prod}\big(4C_{5.4.14} + (1, q^{1/d} \dots, q^{(d-1)/d})\big)$. An index substitution $k := 1 - j + d \cdot \ell(\mathfrak{Q}')$ proves the claim with

$$\sum_{j=1}^{d \cdot \ell(\mathfrak{Q}') + 1} q^{j - \ell(\mathfrak{Q}')} = \sum_{k=0}^{d \cdot \ell(\mathfrak{Q}')} q^{(1-k)/d} < q^{1/d} \sum_{k=0}^{\infty} q^{-k/d} = \tfrac{q^{1/d}}{1 - q^{-1/d}}. \tag{5.202}$$ □

An experiment on $C_{5.4.13}$

The constant $C_{5.4.13}$ arising from this theory is very large, however we observed much smaller ratios of refined and marked elements in an experiment with $d = 3$ and $\mathbf{p} = (3, 3, 3)$. Starting from a $5 \times 5 \times 5$ mesh, we applied the refinement algorithm with only one corner element marked, always sticking to the same corner. This is realistic when resolving a singularity of the solution of a discretized PDE. In all cases the experimental constant was below $\frac{C_{5.4.13}}{3000}$, see Figure 5.19. The advantage of greater grading parameters could not be seen in random refinement all over the domain.

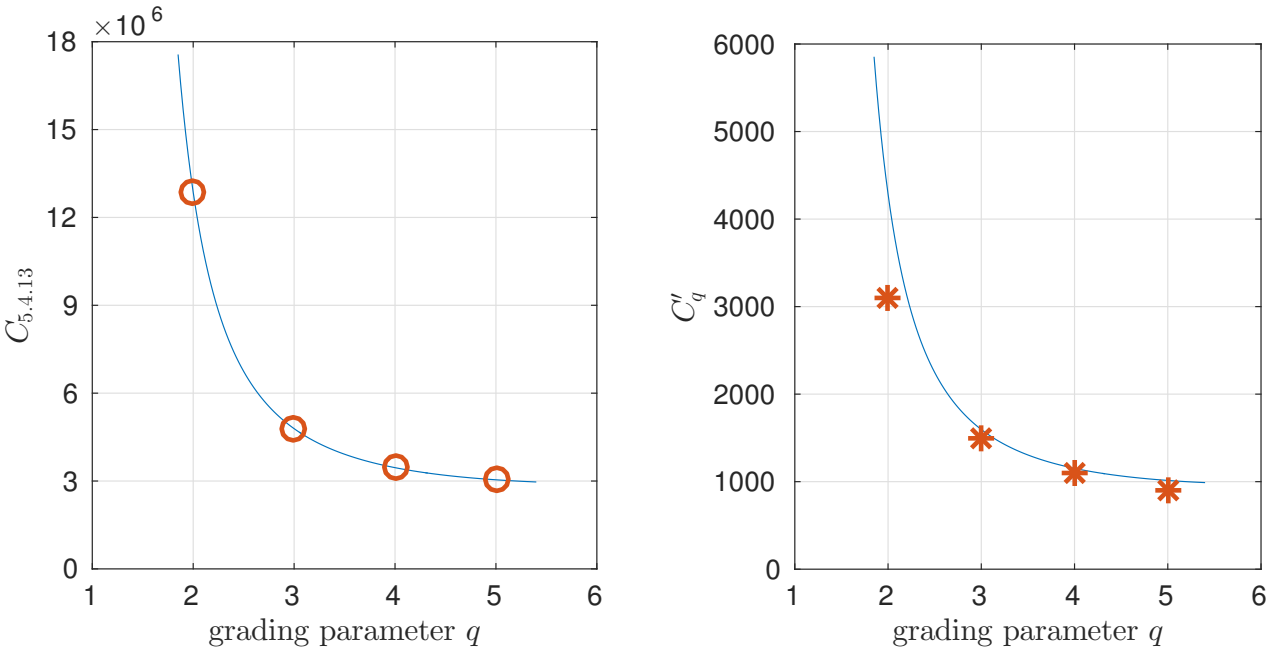

Figure 5.19 [34]: The complexity constant $C_{5.4.13}$ in theory (left) and experiment (right). The values of C'_q were taken from an experiment illustrated in Figure 5.20.

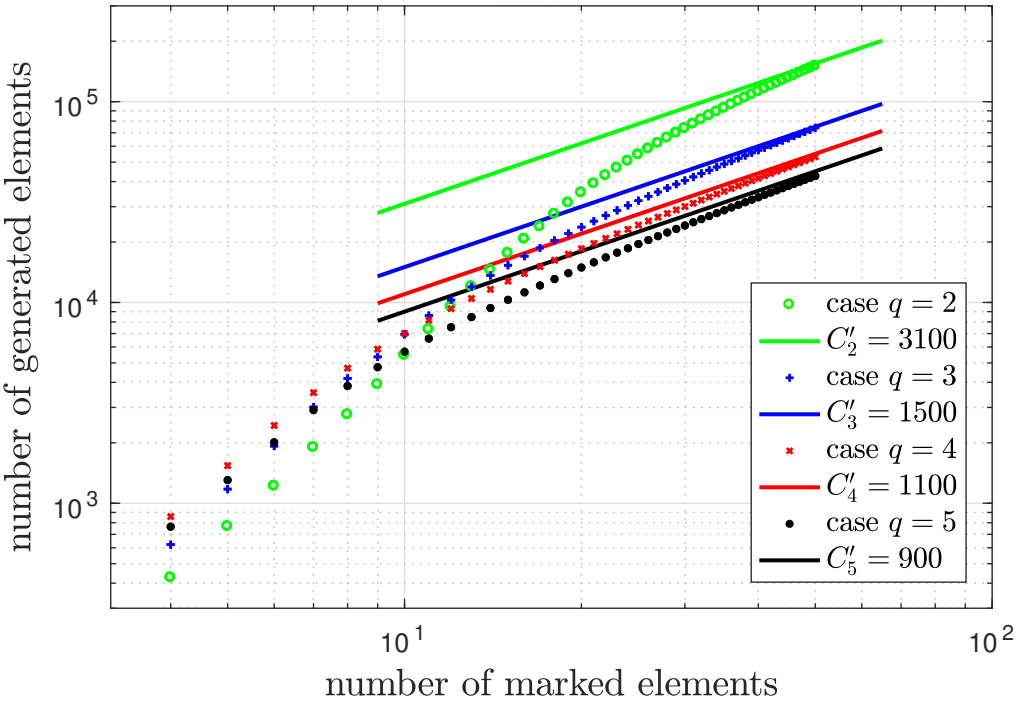

Figure 5.20 [34]: Estimation of the experimental constants C'_q for $q = 2, \ldots, 5$.

6 Numerical Experiments

This chapter summarizes [41], where the refinement strategies proposed in Chapters 4 and 5 are compared to the refinement for AST-splines proposed in [29] and a more naive refinement strategy for THB-splines. In addition to achievable convergence rates and the mesh grading, the comparison includes numerical properties of the stiffness matrix as its sparsity and condition number. To clearly point out differences between the refinement strategies, the first example is designed as a worst case scenario and does not correspond to a physical problem. The second and third example are well-established benchmark problems in the context of Adaptive Finite Element Methods [25, 17, 56], including the Poisson problem and linear elasticity with given analytical solutions. In all examples and for all refinement strategies, cubic B-spline basis functions are used.

6.1 Alternative refinement strategies

This section introduces a naive refinement strategy $\text{REFINE\_THB}_{\text{NN}}$ for THB-splines as well as the refinement routine $\text{REFINE\_TS}_{[29]}$ proposed in [29] for analysis-suitable T-splines. Both strategies are considered in the numerical experiments below and represent low-cost alternatives to REFINE_THB and $\text{REFINE\_TS}_{\text{2D}}$, respectively.

6.1.1 Nearest neighbor refinement for THB-splines

The nearest neighbor refinement serves as a cheap alternative to REFINE_THB from Chapter 4 and is defined through a more naive choice of the coarse neighbourhood $\mathcal{N}_{\text{THB\_NN}}(\mathcal{Q}, \mathcal{M})$ as described below.

Definition 6.1.1 (Nearest neighbor refinement for THB-Splines)**.** We define for each $\mathtt{Q} \in \mathcal{Q}$ the *coarse neighbourhood* consisting of elements with level $\ell(\mathtt{Q}) - m + 1$

$$\mathcal{N}_{\text{THB\_NN}}(\mathcal{Q}, \mathtt{Q}) \coloneqq \left\{ \mathtt{Q}' \in \mathcal{Q} \mid \ell(\mathtt{Q}') = \ell(\mathtt{Q}) - m + 1 \text{ and } \mathtt{Q}' \cap \mathtt{Q} \neq \emptyset \right\} \tag{6.1}$$

$$= \mathcal{Q}_{\mathsf{u}[\ell(\mathtt{Q})-m+1]} \cap (\mathcal{Q} \cap \mathtt{Q}), \tag{6.2}$$

with generalized notations $\mathcal{N}_{\text{THB\_NN}}(\mathcal{Q}, \mathcal{M}) \coloneqq \bigcup_{\mathtt{Q} \in \mathcal{M}} \mathcal{N}_{\text{THB\_NN}}(\mathcal{Q}, \mathtt{Q})$ and

$$\mathcal{N}^k_{\text{THB\_NN}}(\mathcal{Q}, \mathcal{M}) \coloneqq \underbrace{\mathcal{N}_{\text{THB\_NN}}(\mathcal{Q}, \dots \mathcal{N}_{\text{THB\_NN}}(\mathcal{Q},}_{k \text{ times}} \mathcal{M}) \dots). \tag{6.3}$$

We define the *closure*

$$\text{CLOSURE\_THB}_{\text{NN}}(\mathcal{Q}, \mathcal{M}) \coloneqq \bigcup_{k=0}^{\max \ell(\mathcal{M})} \mathcal{N}^k_{\text{THB\_NN}}(\mathcal{Q}, \mathcal{M}), \tag{6.4}$$

and the extended refinement procedure

$$\text{REFINE\_THB}_{\text{NN}}(\mathcal{Q}, \mathcal{M}) \coloneqq \text{SUBDIVIDE}\big(\mathcal{Q}, \text{CLOSURE\_THB}_{\text{NN}}(\mathcal{Q}, \mathcal{M})\big). \tag{6.5}$$

6.1.2 Scott refinement for T-splines

We explain below the refinement routine proposed in [29]. This strategy is not based on element hierarchies, but solely on T-junction extensions. It is suitable for meshes with multiple edges and requires only local information on the edges' orientations, which is an important feature for the application to unstructured meshes. However, it is limited to the two-dimensional case, the overlay of two generated meshes may not be analysis-suitable and its (expected) complexity has not been analyzed yet, hence the theoretical analysis of convergence rates using this algorithm may not be solved in the near future.

Definition 6.1.2 (Bisection with parameters)**.** For any rectangle $\mathtt{Q} = [x, x+\tilde{x}] \times [y, y+\tilde{y}]$ and parameters $j \in \{1,2\}$, $0 < q < 1$, we define the refinement

$$\textsc{bisect}_{j,q}(\mathtt{Q}) \coloneqq \begin{cases} \big\{[x, x+q\tilde{x}] \times [y, y+\tilde{y}],\ [x+q\tilde{x}, x+\tilde{x}] \times [y, y+\tilde{y}]\big\} & \text{if } j = 1, \\ \big\{[x, x+\tilde{x}] \times [y, y+q\tilde{y}],\ [x, x+\tilde{x}] \times [y+q\tilde{y}, y+\tilde{y}]\big\} & \text{if } j = 2. \end{cases} \tag{6.6}$$

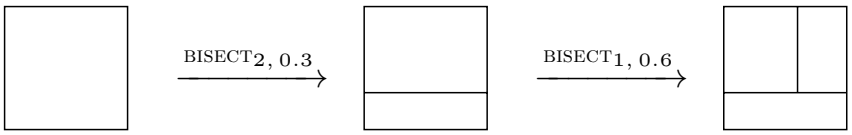

Figure 6.1 [41]: Example for $\textsc{bisect}_{j,q}$.

Definition 6.1.3 (Mesh class $\mathbb{M}_{[29]}$)**.** We define the mesh class $\mathbb{M}_{[29]}$ inductively through the $\textsc{bisect}_{j,q}$ routine;

$$\begin{aligned} &\mathcal{Q}_0 \in \mathbb{M}_{[29]}, \text{ and} \\ &\forall \mathcal{Q} \in \mathbb{M}_{[29]}\ \forall \mathtt{Q} \in \mathcal{Q},\ j \in \{1,2\},\ 0 < q < 1 : \quad \big(\mathcal{Q} \setminus \{\mathtt{Q}\} \cup \textsc{bisect}_{j,q}(\mathtt{Q})\big) \in \mathbb{M}_{[29]}. \end{aligned} \tag{6.7}$$

Definition 6.1.4 (Bézier mesh)**.** Recall the Definition 5.1.7 for T-junction extensions. Given a mesh $\mathcal{Q} \in \cup\mathbb{M}_{[29]}$, adding all T-junction extensions as actual edges to $\mathcal{Q}$ yields the *Bézier mesh*, also called *extended T-mesh*. It represents the lowest-dimensional piecewise polynomial space that contains $\mathcal{B}^{\mathcal{Q}}_{\mathrm{TS}}$ and is used for mesh comparisons in this chapter, see e.g. Figure 6.4.

Definition 6.1.5 (T-junction refinement)**.** For any T-junction $v \in \mathsf{T}(\mathcal{Q})$, we denote by

$$\textsc{refine\_tjunc}(\mathcal{Q}, v) \coloneqq \mathcal{Q} \setminus \{\mathtt{Q}_v\} \cup \textsc{bisect}_{j,q}(\mathtt{Q}_v) \tag{6.8}$$

the single-element refinement such that $v \notin \mathsf{T}(\textsc{refine\_tjunc}(\mathcal{Q}, v))$, i.e., such that v is not a T-junction anymore.

Remark. This refinement exists and is unique, and it is constructed as follows. The definition of T-junctions states that there is exactly one element $\mathtt{Q}_v \in \mathcal{Q}$ such that $v \in \mathsf{T}(\mathtt{Q}_v)$. The location of v on the boundary of $\mathtt{Q}_v$ uniquely defines bisection parameters j and q such that v is a vertex of each children $\mathtt{Q}' \in \textsc{bisect}_{j,q}(\mathtt{Q}_v)$.

Definition 6.1.6 (Extension crossing, extension incompatibility)**.** For any mesh $\mathcal{Q} \in \mathbb{M}_{[29]}$, we denote the set of *extension-crossing T-junction pairs* by

$$\mathsf{E}(\mathcal{Q}) \coloneqq \{(v,w) \in \mathsf{T}_{\mathsf{h}}(\mathcal{Q}) \times \mathsf{T}_{\mathsf{v}}(\mathcal{Q}) \mid \operatorname{ext}_{\mathcal{Q}}(v) \cap \operatorname{ext}_{\mathcal{Q}}(w) \neq \emptyset\}\,. \tag{6.9}$$

For any mesh $\mathcal{Q} \in \mathbb{M}_{[29]}$ and refinement $\tilde{\mathcal{Q}} \in \mathbb{M}_{[29]}$, we define the set of *extension-incompatible T-junctions* by

$$\mathsf{C}(\mathcal{Q}, \tilde{\mathcal{Q}}) \coloneqq \left\{v \in \mathsf{T}(\mathcal{Q}) \cap \mathsf{T}(\tilde{\mathcal{Q}}) \mid \operatorname{ext}_{\tilde{\mathcal{Q}}}(v) \subsetneq \operatorname{ext}_{\mathcal{Q}}(v)\right\}. \tag{6.10}$$

Algorithm 6.1.7 (Scott refinement for T-splines, [29])**.**

Input: mesh $\mathcal{Q} \in \mathbb{M}_{[29]}$, marked elements $\mathcal{M} \subset \mathcal{Q}$

$\tilde{\mathcal{Q}} \coloneqq \textsc{refine\_thb}(\mathcal{Q}, \mathcal{M})$

repeat

$$v_{\text{refine}} \coloneqq \operatorname*{argmin}_{v \in \mathsf{T}(\tilde{\mathcal{Q}})} \Big(\#\mathsf{E}(\textsc{refine\_tjunc}(\tilde{\mathcal{Q}}, v)) + \#\mathsf{C}(\mathcal{Q}, \textsc{refine\_tjunc}(\tilde{\mathcal{Q}}, v)) \Big)$$

$$\tilde{\mathcal{Q}} \coloneqq \textsc{refine\_tjunc}(\tilde{\mathcal{Q}}, v_{\text{refine}})$$

until $\mathsf{E}(\tilde{\mathcal{Q}}) = \emptyset$ **and** $\mathsf{C}(\mathcal{Q}, \tilde{\mathcal{Q}}) = \emptyset$

return $\textsc{refine\_ts}_{[29]}(\mathcal{Q}, \mathcal{M}) \coloneqq \big(\tilde{\mathcal{Q}}, \mathcal{B}_{\text{TS}}^{\tilde{\mathcal{Q}}}\big)$

Remark. The above algorithm does always terminate, in the worst case yielding a tensor-product mesh.

6.2 Model Problems and Discretization

This section describes the two model problems that are used for our tests. We will formulate both problems in the weak (variational) form and skip their derivation from the original PDEs. The latter are, for the Poisson problem, seeking $u \in C^2(\overline{\Omega})$ such that

$$-\Delta u = f \text{ in } \Omega, \quad \tfrac{\partial u}{\partial \nu_{\mathrm{N}}} = g \text{ on } \Gamma_{\mathrm{N}} \quad \text{and} \quad u|_{\Gamma_{\mathrm{D}}} = u_{\mathrm{D}} \text{ on } \Gamma_{\mathrm{D}}, \tag{6.11}$$

and for the problem of linear elasticity, seeking $u \in C^2(\overline{\Omega})$ such that

$$-\operatorname{div}\sigma(u) = f \text{ in } \Omega, \quad \langle \nu_{\mathrm{N}}, \sigma(u)\rangle = g \text{ on } \Gamma_{\mathrm{N}} \quad \text{and} \quad u|_{\Gamma_{\mathrm{D}}} = u_{\mathrm{D}} \text{ on } \Gamma_{\mathrm{D}}, \tag{6.12}$$

using the notation explained below.

6.2.1 Poisson problem

Data Let $\Omega \subset \mathbb{R}^2$ be an open, connected and bounded Lipschitz domain. Let the Dirichlet boundary $\Gamma_{\mathrm{D}} \subset \partial\Omega$ be closed and let each connectivity component of Γ_{D} be of positive measure. Set the Neumann boundary $\Gamma_{\mathrm{N}} \coloneqq \partial\Omega \setminus \Gamma_{\mathrm{D}}$ and the corresponding outer normal vector $\nu_{\mathrm{N}} : \Gamma_{\mathrm{N}} \to \mathbb{R}^2$. Let $u_{\mathrm{D}} \in L^2(\Gamma_{\mathrm{D}})$ and

$$H_0^1(\Omega) \coloneqq \left\{w \in H^1(\Omega) \mid w|_{\Gamma_{\mathrm{D}}} = 0 \text{ a.e. in } \Gamma_{\mathrm{D}}\right\}. \tag{6.13}$$

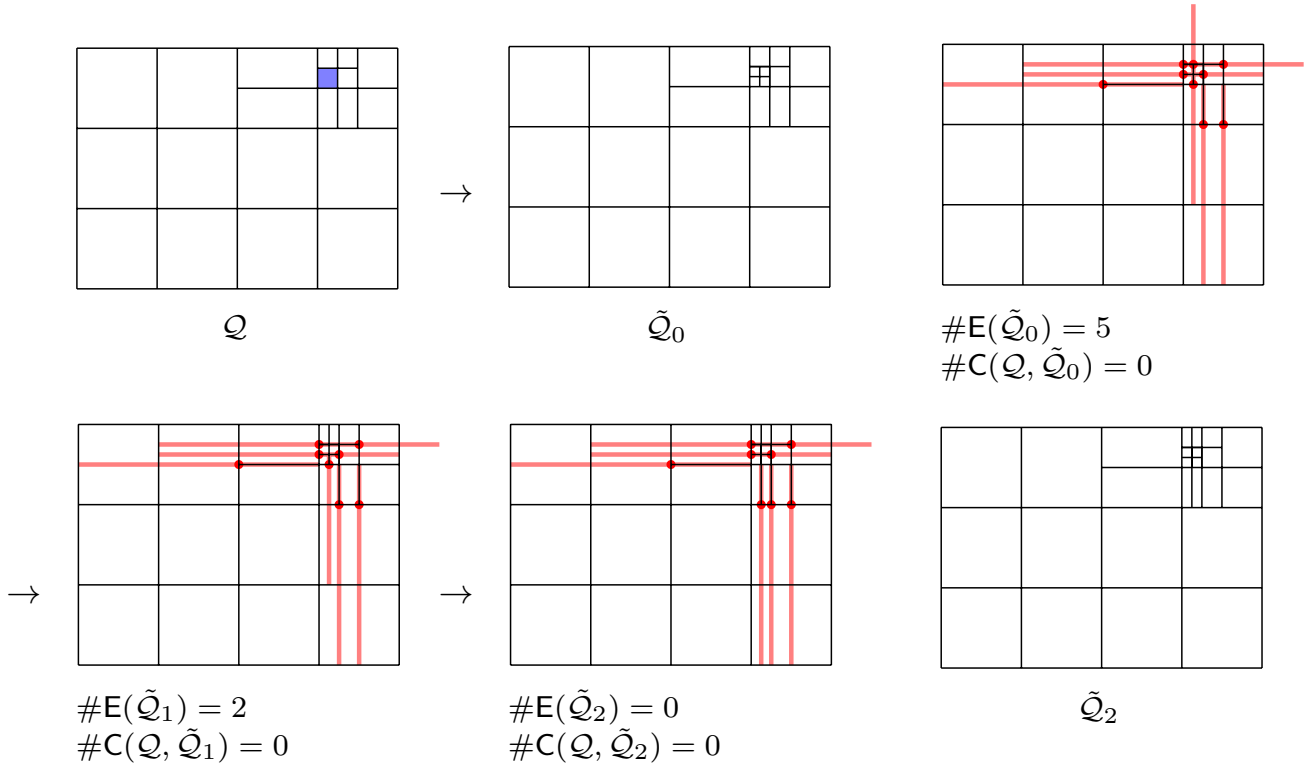

Figure 6.2 [41]: Example for the Scott T-spline refinement. In the first step, the marked element is subdivided as for the HB-spline refinement. Second, the intersections of horizontal and vertical T-junction extensions are counted. Third, REFINE_TJUNC is applied to a T-junction for which the number of extension crossings in the resulting mesh (elements of $\mathsf{E}(\tilde{\mathcal{Q}})$) is smallest, plus the term $\#\mathsf{C}(\mathcal{Q}, \tilde{\mathcal{Q}})$ to ensure nesting of the resulting spline spaces. This third step is repeated until the sets $\mathsf{E}(\tilde{\mathcal{Q}})$ and $\mathsf{C}(\mathcal{Q}, \tilde{\mathcal{Q}})$ are empty.

Problem Find $u \in H^1(\Omega)$ such that

$$\begin{aligned} \int_\Omega \langle \nabla u, \nabla v \rangle \,\mathrm{d}x = \int_\Omega f v \,\mathrm{d}x + \int_{\Gamma_\mathrm{N}} g v \,\mathrm{d}s \quad \text{for all } v \in H^1_0, \\ u|_{\Gamma_\mathrm{D}} = u_\mathrm{D} \quad \text{a.e. on } \Gamma_\mathrm{D}. \end{aligned} \tag{6.14}$$

Discretization Given a basis $\mathcal{B}$ of a finite-dimensional function space $\hat{\mathcal{B}} \coloneqq \operatorname{span} \mathcal{B}$ and

$$\hat{\mathcal{B}}_0 \coloneqq \left\{ w \in \hat{\mathcal{B}} \mid w|_{\Gamma_\mathrm{D}} = 0 \text{ a.e. in } \Gamma_\mathrm{D} \right\}, \tag{6.15}$$

we seek the Galerkin solution $\hat{u} \in \hat{\mathcal{B}}$ satisfying

$$\begin{aligned} \int_\Omega \langle \nabla \hat{u}, \nabla v \rangle \,\mathrm{d}x = \int_\Omega f v \,\mathrm{d}x + \int_{\Gamma_\mathrm{N}} g v \,\mathrm{d}s \quad \text{for all } v \in \hat{\mathcal{B}}_0, \\ \hat{u}|_{\Gamma_\mathrm{D}} = I_{\hat{\mathcal{B}}}(u_\mathrm{D}) \quad \text{on } \Gamma_\mathrm{D}, \end{aligned} \tag{6.16}$$

where $I_{\hat{\mathcal{B}}}(u_\mathrm{D}) \in \hat{\mathcal{B}}$ is an interpolation of u_D. We set $\hat{u}_0 \coloneqq \hat{u} - I_{\hat{\mathcal{B}}}(u_\mathrm{D}) \in \hat{\mathcal{B}}_0$ and reformulate the above problem to finding $\hat{u}_0 \in \hat{\mathcal{B}}_0$ such that

$$\int_\Omega \langle \nabla \hat{u}_0, \nabla v \rangle \,\mathrm{d}x = \int_\Omega f v \,\mathrm{d}x + \int_{\Gamma_\mathrm{N}} g v \,\mathrm{d}s - \int_\Omega \langle \nabla I_{\hat{\mathcal{B}}}(u_\mathrm{D}), \nabla v \rangle \,\mathrm{d}x \quad \text{for all } v \in \hat{\mathcal{B}}_0. \tag{6.17}$$

Since both left and right side of (6.16) are linear in v, it suffices to have the above equation fulfilled for all basis functions $v \in \mathcal{B}_0 = \{v_1, \dots, v_n\} = \mathcal{B} \cap \hat{\mathcal{B}}_0$ that are zero on the boundary. Since the right-hand side is also linear in $\hat{u}_0$, and $\hat{u}_0 \in \hat{\mathcal{B}}_0$ is a linear combination of these basis functions, (6.17) is equivalent to finding a vector $U = (u_1, \dots, u_n) \in \mathbb{R}^n$ such that

$$\underbrace{\left(\int_\Omega \langle \nabla v_i, \nabla v_j \rangle \,\mathrm{d}x\right)_{1 \le i,j \le n}}_{A \in \mathbb{R}^{n \times n}} \cdot U = \underbrace{\left(\int_\Omega f v_i \,\mathrm{d}x + \int_{\Gamma_\mathrm{N}} g v_i \,\mathrm{d}s - \int_\Omega \langle \nabla I_{\hat{\mathcal{B}}}(u_\mathrm{D}), \nabla v_i \rangle \,\mathrm{d}x\right)_{1 \le i \le n}}_{B \in \mathbb{R}^n}, \tag{6.18}$$

with $\hat{u} = \sum_{i=1}^n u_i v_i + I_{\hat{\mathcal{B}}}(u_\mathrm{D})$. We call A the *stiffness matrix* and B the *load vector*.

Discrete space and parametrization In all experiments shown below, the *physical domain* Ω (cf. Section 2.4) is the image of the *parametric domain* $\hat{\Omega} =]0, M] \times]0, N[$ under a *geometry map* $\mathrm{F} : \hat{\Omega} \to \mathbb{R}^2$ (cf. Section 2.2). Given a mesh $\mathcal{Q}$ and a spline basis $\mathcal{B}^\mathcal{Q} \in \{\mathcal{B}^\mathcal{Q}_\mathrm{THB}, \mathcal{B}^\mathcal{Q}_\mathrm{TS}\}$, the geometry map F uses NURBS (see Section 2.3) and is described through *control points* $C = \{c_b \mid b \in \mathcal{B}^\mathcal{Q}\} \subset \mathbb{R}^2$ and *weights* $W = \{w_b \mid b \in \mathcal{B}^\mathcal{Q}\} \subset [0, 1]$, namely

$$\mathrm{F}(x) \coloneqq \sum_{b \in \mathcal{B}^\mathcal{Q}} r_b(x) c_b \quad \text{and} \quad r_b(x) \coloneqq \frac{w_b b(x)}{\sum_{s \in \mathcal{B}^\mathcal{Q}} w_s s(x)}. \tag{6.19}$$

The control points $c_b \in C$ and weights $w_b \in W$ are given data and, since they define F, they fully describe the domain $\Omega = \mathrm{F}(\hat{\Omega})$. The basis $\mathcal{B}$ used for the discretization consists of so-called *pullback functions* (cf. Section 2.4) composed of the spline basis $\mathcal{B}^\mathcal{Q}$ and the inverse geometry map,

$$\mathcal{B} = \{b \circ \mathrm{F}^{-1} \mid b \in \mathcal{B}^\mathcal{Q}\}, \text{ and } \hat{\mathcal{B}} = \operatorname{span} \mathcal{B}. \tag{6.20}$$

Note as a side remark that F^{-1} does not exist for general data C and W, however it does exist in the experiments below.

Error estimator The Adaptive Algorithm (explained below in Section 2.5) is controlled by a standard residual local error estimator $\eta : \mathcal{Q} \to \mathbb{R}$ (see e.g. [53] for an application with THB-splines). Given the Galerkin solution $\hat{u} \in \hat{\mathcal{B}}$, it is defined by

$$\eta_\mathcal{Q}(\mathtt{Q}) \coloneqq \left(h_\mathtt{Q}^2 \left\|\Delta \hat{u} + f\right\|_\mathtt{Q}^2 + \sum_{E \in \mathcal{E}(\mathtt{Q})} h_E \left\|R_E(\hat{u})\right\|_E^2\right)^{1/2}, \tag{6.21}$$

where $\mathcal{E}(\mathtt{Q})$ is the set of edges of $\mathtt{Q}$, $h_\mathtt{Q}$ the diameter of $\mathtt{Q}$, and h_E the length (the 1D Lebesgue measure) of the edge E. The notation $\|\bullet\|_A$ abbreviates the L^2-norm

$\|\bullet\|_{L^2(A)}$. Given a normal vector ν_E for each edge E, the *edge residual* $R_E(\hat{u})$ is defined by

$$R_E(\hat{u}) \coloneqq \begin{cases} \frac{1}{2} \left[\!\left[\frac{\partial \hat{u}}{\partial \nu_E} \right]\!\right]_E & \text{if } E \text{ is an interior edge,} \\ g - \frac{\partial \hat{u}}{\partial \nu_E} & \text{if } E \text{ is a boundary edge in } \Gamma_{\mathrm{N}}, \\ 0 & \text{if } E \text{ is a boundary edge in } \Gamma_{\mathrm{D}}, \end{cases} \tag{6.22}$$

and we assume that any boundary edge is (up to its endpoints) either in Γ_{N} or in Γ_{D}. For any interior edge $E = \mathtt{Q} \cap \mathtt{Q}'$, the notation $[\![\bullet]\!]_E \coloneqq \bullet|_{\mathtt{Q}} - \bullet|_{\mathtt{Q}'}$ describes the jump along the edge E. Note that in all four methods that are compared in this chapter, none of the spline basis functions have jumps in their derivatives, and the same holds for the discrete solution $\hat{u}$. Provided that the Neumann boundary condition is met exactly (e.g. in the case $g = 0$), the above error estimator hence reduces to the volume contribution

$$\eta_{\mathcal{Q}}(\mathtt{Q}) \coloneqq h_{\mathtt{Q}} \left\| \Delta \hat{u} + f \right\|_{\mathtt{Q}}. \tag{6.23}$$

6.2.2 Linear elasticity

Data Let Ω, Γ_{D}, Γ_{N}, ν_{N}, u_{D} as above. For $u \in H^1(\Omega, \mathbb{R}^2)$, we define

$$\varepsilon(u) \coloneqq \left(\tfrac{1}{2}(\partial_i u_j + \partial_j u_i)\right)_{1 \le i,j \le 2} \quad \text{and} \quad \sigma(u)_{ij} \coloneqq \sum_{1 \le k,\ell \le 2} C_{ijk\ell}\, \varepsilon(u)_{k\ell} \text{ for } 1 \le i,j \le 2. \tag{6.24}$$

We call u the *displacement*, $\varepsilon(u)$ the *strain tensor* and $\sigma(u)$ the *stress tensor*, and C is some positive definite fourth order tensor that describes material properties.

Problem Find $u \in H^1(\Omega)$ such that

$$\begin{aligned} \int_\Omega \langle \sigma(u), \varepsilon(v) \rangle \,\mathrm{d}x = \int_\Omega f v \,\mathrm{d}x + \int_{\Gamma_{\mathrm{N}}} g v \,\mathrm{d}s \quad \text{for all } v \in H^1_0(\mathbb{R}^2), \\ u|_{\Gamma_{\mathrm{D}}} = u_{\mathrm{D}} \quad \text{a.e. on } \Gamma_{\mathrm{D}}. \end{aligned} \tag{6.25}$$

Discretization Given a basis $\mathcal{B}$ of a finite-dimensional function space $\hat{\mathcal{B}} \coloneqq \operatorname{span} \mathcal{B}$ and $\hat{\mathcal{B}}_0$ as above, we seek the Galerkin solution $\hat{u} \in \hat{\mathcal{B}}$ satisfying

$$\begin{aligned} \int_\Omega \langle \sigma(\hat{u}), \varepsilon(v) \rangle \,\mathrm{d}x = \int_\Omega f v \,\mathrm{d}x + \int_{\Gamma_{\mathrm{N}}} g v \,\mathrm{d}s \quad \text{for all } v \in \hat{\mathcal{B}}_0, \\ \hat{u}|_{\Gamma_{\mathrm{D}}} = I_{\hat{\mathcal{B}}}(u_{\mathrm{D}}) \quad \text{on } \Gamma_{\mathrm{D}}. \end{aligned} \tag{6.26}$$

Again, we set $\hat{u}_0 \coloneqq \hat{u} - I_{\hat{\mathcal{B}}}(u_{\mathrm{D}}) \in \hat{\mathcal{B}}_0$ and reformulate the above problem to finding $\hat{u}_0 \in \hat{\mathcal{B}}_0$ such that

$$\int_\Omega \langle \sigma(\hat{u}_0), \varepsilon(v) \rangle \,\mathrm{d}x = \int_\Omega f v \,\mathrm{d}x + \int_{\Gamma_{\mathrm{N}}} g v \,\mathrm{d}s - \int_\Omega \langle \sigma(I_{\hat{\mathcal{B}}}(u_{\mathrm{D}})), \varepsilon(v) \rangle \,\mathrm{d}x \quad \text{for all } v \in \hat{\mathcal{B}}_0. \tag{6.27}$$

Analogously to the derivation for the Poisson problem above, we compute the Galerkin solution by solving the equation

$$\underbrace{\left(\int_\Omega \langle \sigma(v_i), \varepsilon(v_j)\rangle \,\mathrm{d}x\right)_{1\le i,j\le n}}_{A\in\mathbb{R}^{n\times n}} \cdot U = \underbrace{\left(\int_\Omega f v_i \,\mathrm{d}x + \int_{\Gamma_\mathrm{N}} g v_i \,\mathrm{d}s - \int_\Omega \langle \sigma(I_{\hat{\mathcal{B}}}(u_\mathrm{D})), \varepsilon(v_i)\rangle \,\mathrm{d}x\right)_{1\le i\le n}}_{B\in\mathbb{R}^n}. \tag{6.28}$$

and setting $\hat{u} = \sum_{i=1}^n u_i v_i + I_{\hat{\mathcal{B}}}(u_\mathrm{D})$.

Error estimator Given the Galerkin solution $\hat{u} \in \hat{\mathcal{B}}$, we use the local error estimator described in [57], which is defined by

$$\eta_{\mathcal{Q}}(\mathtt{Q}) \coloneqq \left(h_{\mathtt{Q}}^2 \left\|\operatorname{div}\sigma(\hat{u}) + f\right\|_{\mathtt{Q}}^2 + \sum_{E\in\mathcal{E}(\mathtt{Q})} h_E \left\|R_E(\hat{u})\right\|_E^2\right)^{1/2}, \tag{6.29}$$

where the *edge residual* $R_E(\hat{u})$ is defined by

$$R_E(\hat{u}) \coloneqq \begin{cases} \frac{1}{2}\left[\!\left[\langle \nu_E, \sigma(\hat{u})\rangle\right]\!\right]_E & \text{if } E \text{ is an interior edge,} \\ g - \langle \nu_E, \sigma(\hat{u})\rangle & \text{if } E \text{ is a boundary edge in } \Gamma_\mathrm{N}, \\ 0 & \text{if } E \text{ is a boundary edge in } \Gamma_\mathrm{D}. \end{cases} \tag{6.30}$$

6.3 Experiments

We present below the results of our experiments, which serve as a basic comparison between the refinement routines REFINE_THB, REFINE_TS$_{2D}$, REFINE_THB$_{NN}$ and REFINE_TS$_{[29]}$. We will refer to REFINE_THB$_{NN}$ and REFINE_TS$_{[29]}$ as *greedy refinements* and to REFINE_THB and REFINE_TS$_{2D}$ as *safe refinements*, since the latter result in more widespread refinement and a larger number of degrees of freedom, but also provide more theoretical background that has been addressed in the previous chapters.

6.3.1 Worst case scenario

In this example, an initial square mesh with 64 elements is locally refined in the lower left corner, where only one element is marked for refinement in each refinement. The resulting Bézier meshes are presented in Figure 6.4. It can be seen that the greedy THB-spline refinement does only refine the marked element whereas the safe refinement routines extend the refinement region. Also the greedy T-spline refinement inserts additional control points in order to ensure analysis-suitability (cf. Definition 5.1.8). The total number of degrees of freedom (DOF) is plotted against the refinement steps in Figure 6.5 (a) to illustrate this behaviour.

The locality of the refinement comes at the cost of an increased interaction between differently-scaled basis functions in the case of greedy THB-spline refinement. In

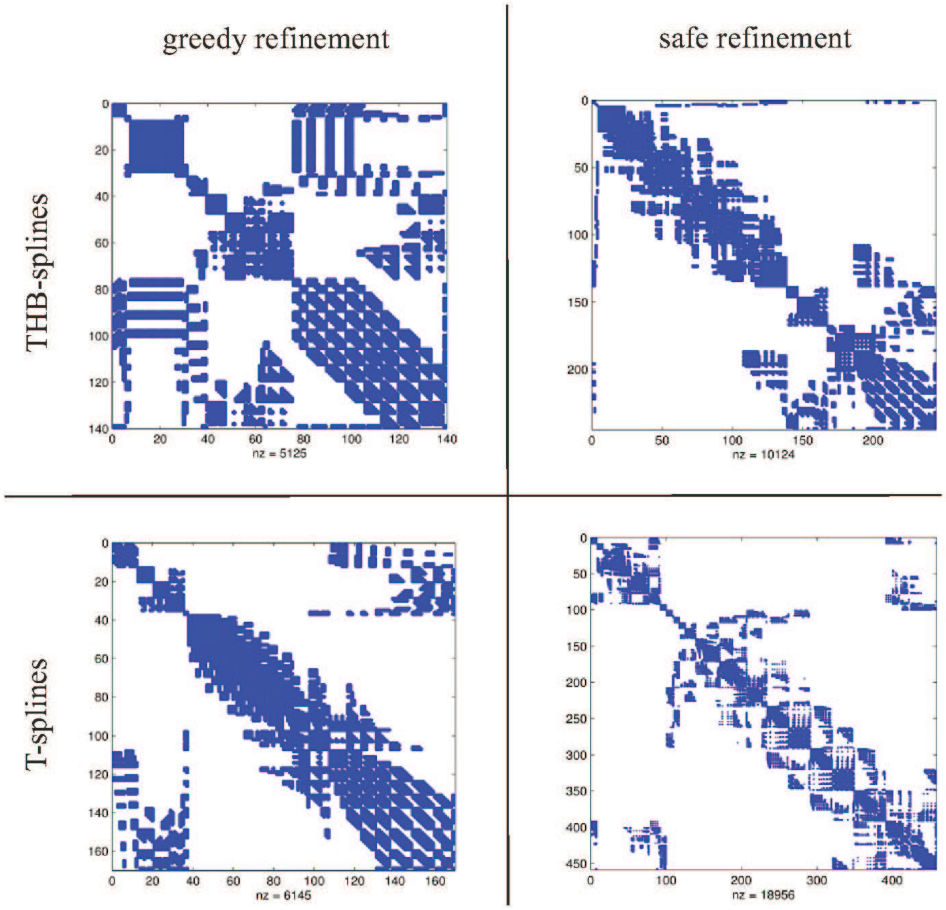

Figure 6.3 [41]: Worst case scenario: The sparsity patterns of the stiffness matrices after six refinement steps are illustrated. In particular the greedy THB-spline refinement results in a dense stiffness matrix.

this example, basis functions from the coarsest level interact with basis functions of the finest level. This leads to the occurrence of quasi-dense rows and columns and the loss of any band structure in the stiffness matrix, as it can be seen in Figure 6.3. The other refinement routines do not cause a degeneration of the stiffness matrix' structure.

The local mesh refinement also influences the behaviour of the condition number of the stiffness matrix. Gahalaut et al. [58] analyzed these condition numbers for NURBS-based isogeometric discretizations and uniform refinement, showing that the condition number increases linearly with respect to degrees of freedom. This is also reflected in our experiments. As expected, we observe for all kinds of local refinement that the condition numbers grow at higher rates, see Figure 6.5 (b). The rate is apparently independent of the type (T- or THB-splines) but does depend on the locality of refinement (greedy or safe), and thus on the grading of the mesh. However, if the condition numbers are compared with respect to the refinement step (cf. Figure 6.5 (c)), the safe THB-spline refinement produces higher condition numbers than the greedy one, and the T-splines higher condition numbers than the THB-splines. This shows that the number of additional degrees of freedom per refinement step may have a dominant influence on the condition number. Hence, for a clear comparison, the condition number has to be compared with respect to a

Figure 6.4 [41]: Refinement strategies: An initial square mesh with 64 elements is locally refined in the lower left corner using THB- and T-splines. The illustrated meshes are the Bézier meshes (see Definition 6.1.4).

quantity of main interest. For this reason the numerical error of the solution will be plotted over the condition number in the following examples. We emphasize that this discussion disregards appropriate preconditioning, which is beyond the scope of this thesis.

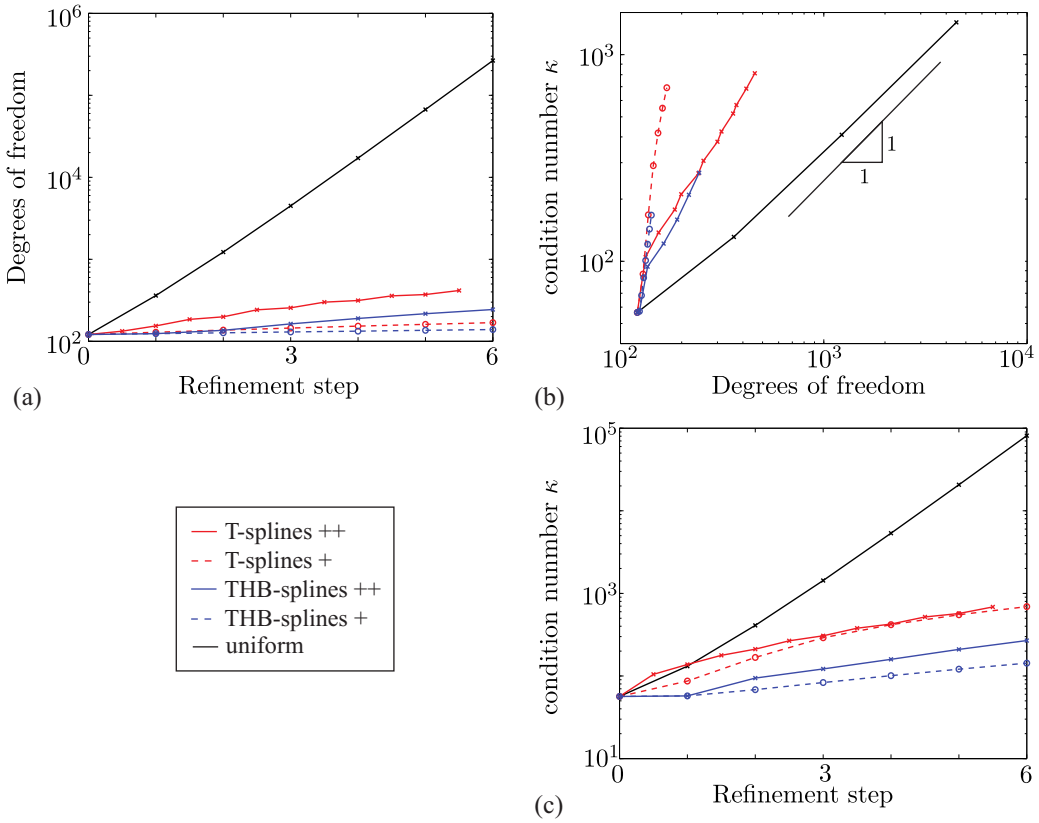

Figure 6.5 [41]: Worst case scenario: The relations between the total number of degrees of freedom, the condition number of the stiffness matrix and the refinement steps are illustrated. In the legend, "++" refers to safe refinements, and "+" to greedy refinements.

6.3.2 Poisson problem

In this example, the Poisson problem (cf. Section 6.2.1) is solved for the temperature u on two different two-dimensional domains. The first domain $\Omega_{\mathrm{L}} = \{(-1,1) \times (-1,1)\} \setminus \{(0,1) \times (0,1)\}$, referred to as the L-Shape, is characterized by a re-entrant corner with an opening angle of $\beta = 90°$ and a given exact solution

$$\bar{u} = r^{\frac{2}{3}} \sin \tfrac{2\phi - \pi}{3} \tag{6.31}$$

in polar coordinates (r, ϕ). The second domain $\Omega_{\mathrm{S}} = \{(-1,1) \times (-1,1)\}$, referred to as the slit domain, is characterized by a re-entrant corner with an opening angle of $\beta = 0°$ and a given exact solution

$$\bar{u} = r^{\frac{1}{2}} \sin \tfrac{\phi}{2} \ . \tag{6.32}$$

Both boundary value problems are illustrated in Figure 6.6. The boundary conditions are applied by setting $u = 0$ at the Dirichlet boundary Γ_{D} and the exact heat flux $g = \partial \bar{u} / \partial \nu_{\mathrm{N}}$ at the Neumann boundary Γ_{N}. The L-Shape is modelled by a single C^1-continuous B-spline patch, while the slit domain is modelled by a single B-spline patch with C^0-continuous lines at the axis of symmetry of the domain as indicated by the dashed lines in Figure 6.6.

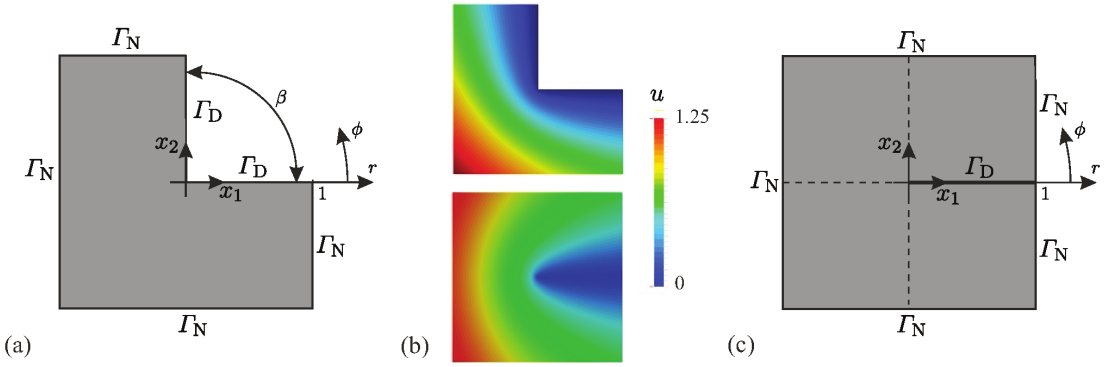

Figure 6.6 [41]: Poission problem: Domain and boundary conditions for **(a)** the L-shape and **(c)** the slit domain as well as **(b)** the corresponding analytical solutions.

In both problems, the geometry leads to a singularity of the solution at the re-entrant corner. In this case classical convergence theory does not hold, and the order of convergence with respect to the total number of degrees of freedom

$$k = -\tfrac{1}{2} \min\left(p, \tfrac{\pi}{2\pi - \beta}\right) \tag{6.33}$$

is governed by the angle β of the re-entrant corner [59]. For uniform h-refinement this leads to a convergence rate of $k = -1/3$ for all p for the L-shape and $k = -1/4$ for all p for the slit domain.

The optimal order of convergence $k = -p/2$ can be recovered by local mesh refinement in the vicinity of the singularity. The adaptive finite element method (cf. Section 2.5) will be applied below to solve the above problem with different refinement strategies. To select elements for refinement, the quantile marking is used. The associated parameter α has been adjusted manually for each refinement strategy, in order to achieve best possible convergence rates.

L-Shape

The initial mesh of the L-shape problem consists of 16 elements. Figure 6.7 shows the Bézier meshes after L refinement steps, as well as the marking parameters α. For the adaptive local refinement, the error in the H^1 norm is plotted over the total number of degrees of freedom (DOF) in Figure 6.8 (a). All refinement strategies recover the optimal order of convergence in the asymptotic range. Due to the coarse initial mesh, the safe refinements produce a greater amount of DOF in the pre-asymptotic range, which is in particular observed for the safe T-spline refinement. As a result, the safe refinements behave not as local as the greedy refinements but create more smoothly-graded meshes. To counteract the non-local refinements, the marking parameter for safe refinements is chosen higher such that a smaller number of elements is marked.

Particularly for the greedy THB-spline refinement, the computed stiffness matrix has a higher density. For all other refinement strategies no clear tendency is visible in the sparsity patterns in Figure 6.7.

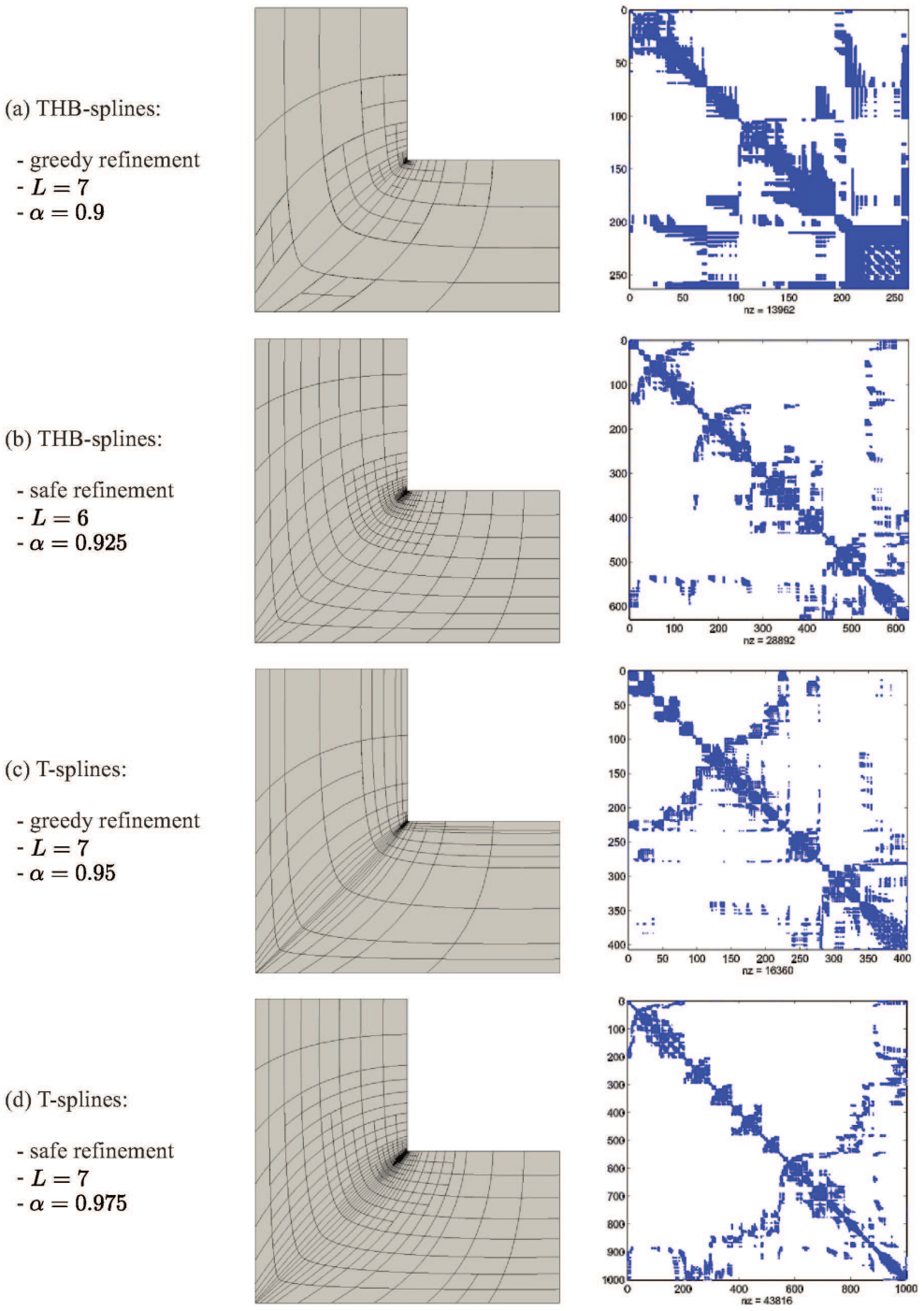

Figure 6.7 [41]: L-shape: The marking parameters α, the Bézier meshes and the sparsity patterns of the stiffness matrices after L refinement steps for all **(a)-(d)** refinement strategies. The safe refinement strategies result in widespread refinement, the greedy refinement strategies in more localized refinement. Again, the greedy THB-spline refinement creates the stiffness matrix with the highest density.

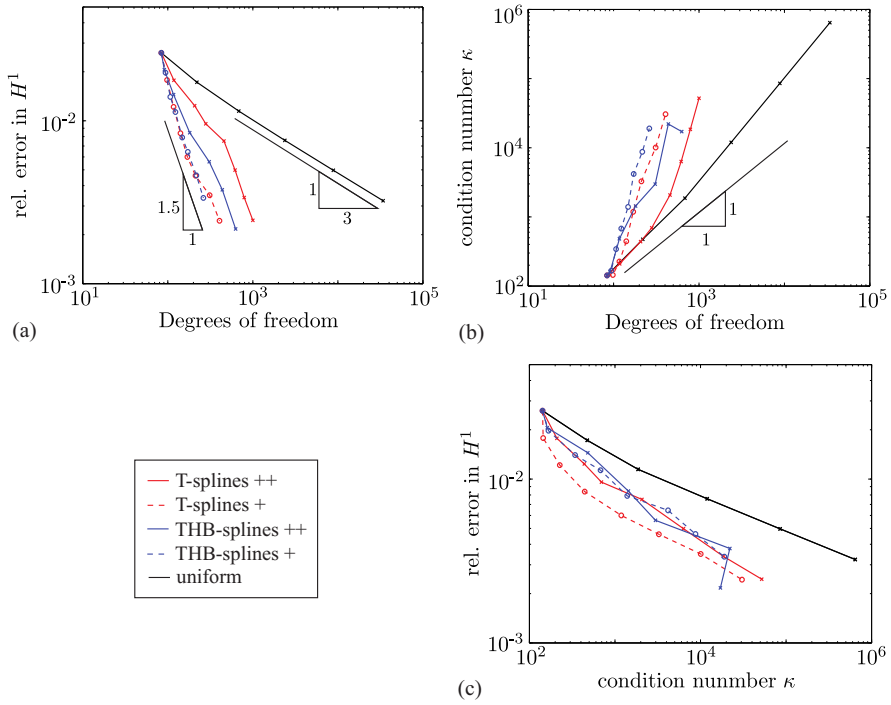

Figure 6.8: L-shape: The convergence rates as well as the relations between the condition number of the stiffness matrix, the numerical error of the solution and the total number of degrees of freedom are illustrated. **(a)** - All refinement strategies converge with the expected convergence rate $k = 1.5$ in the asymptotic range. As in Figure 6.5, "++" refers to safe refinements, and "+" to greedy refinements.

The condition number is plotted over the DOF in Figure 6.8 (b). Due to the geometric map of the L-shape, a rate higher than one is reached for uniform refinement. Regarding the local refinement, results similar to the previous example are obtained. However, the differences between the greedy and safe refinements are not as large as in the first experiment.

As mentioned above, also the error of the numerical solution with respect to the condition number (cf. Figure 6.8 (c)) is of interest. It can be seen that for the same order of accuracy, all local refinement techniques produce smaller condition numbers compared to the uniform case. This means, that for local refinement, the error of the solution decreases faster per DOF than the condition number increases per DOF. This is an important result, because it illustrates that the negative influence of a locally refined mesh on the condition number does not predominate the benefits of local refinement regarding the error level. The refinement strategies compared among themselves show similar results.

Slit domain

The initial mesh of the slit domain consists of 64 elements. The Bézier meshes after L refinement steps, as well as the marking parameters α are illustrated in Figure 6.10. As expected, the meshes of the safe refinement routines propagate the refinement area but produce smoothly-graded meshes. On the other hand, the greedy T-spline refinement leads to a mesh with very localized refinement and badly-shaped elements with aspect ratios up to 64. Concerning the sparsity patterns of the stiffness matrix, only the greedy THB-spline refinement creates matrices with a higher density, due to the increased interaction between the basis functions.

For the adaptive local refinement, the error in the H^1 norm is plotted over the total number of degrees of freedom (DOF) in Figure 6.9 (a). It can be seen that the error of the greedy refinement routines appear to converge with a higher rate in the pre-asymptotic range and later approach the theoretically predicted rate of $k = 1.5$. The safe refinement routines have a minor convergence rate in the pre-asymptotic range, but then also converge with the theoretical rate of $k = 1.5$. A reason for this behaviour can be found again in the relatively coarse initial mesh, which forces the safe T-spline refinement to refine almost the whole domain in the first refinement steps. As a result, the safe T-spline refinement requires six times more degrees of freedom than the greedy T-spline refinement for the same error level.

The condition number is plotted over the DOF in Figure 6.9 (b). Due to the badly shaped elements, the condition number for the greedy T-spline refinement increases fastest. The THB-spline refinements instead seem to benefit from their hierarchical structure together with the absence of a deforming geometry mapping. At a certain stage of refinement, the condition number does not increase further. This behaviour has been also found in [60] where HB-splines are compared against THB- and L-RB-splines. In the context of hierarchical Finite Elements [61], it is known and even proven that the condition number of the stiffness matrix scales with $O(\log(\texttt{DOF}))$ instead of $O(\texttt{DOF})$, due to orthogonalities with respect to the energy product between basis functions of different levels. In 1D, this leads to block-diagonal stiffness matrices; in higher dimensions, this effect is milder (see e.g. Figure 6.10 (a)), but still yields good conditioning. It seems that (Truncated) Hierarchical B-splines

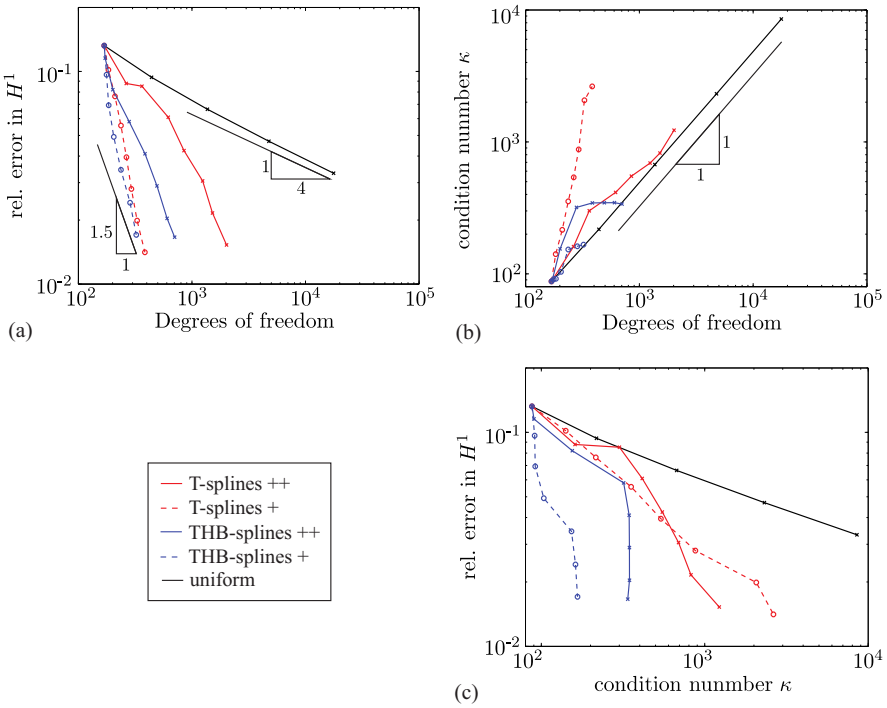

Figure 6.9 [41]: Slit domain: The convergence rates as well as the relations between the condition number of the stiffness matrix, the numerical error of the solution and the total number of degrees of freedom are illustrated. **(a)** - All refinement strategies converge with the expected convergence rate $k = 1.5$ in the asymptotic range.

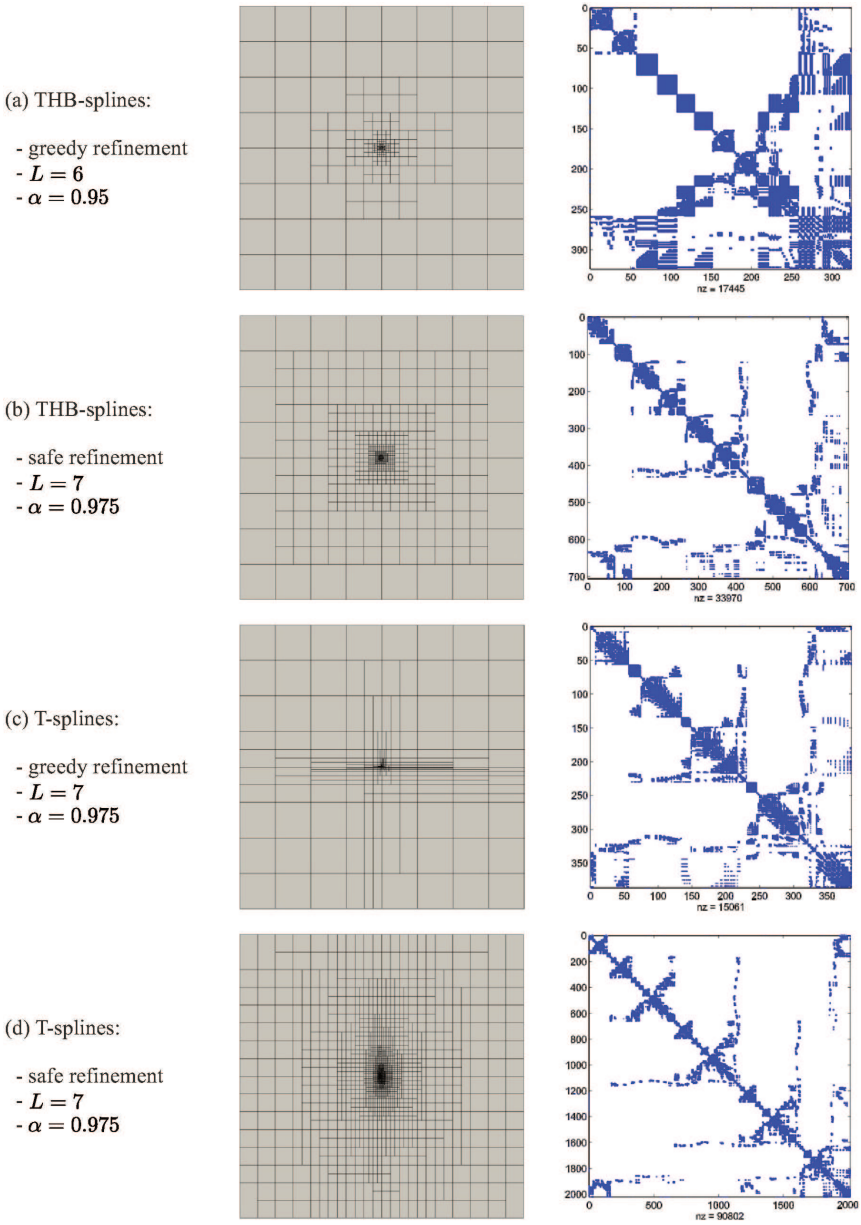

Figure 6.10 [41]: Slit domain: The marking parameters α, the Bézier meshes and the sparsity patterns of the stiffness matrices after L refinement steps for all **(a)**-**(d)** refinement strategies. Again, the safe refinement strategies result in widespread refinement. The greedy T-spline refinement yields very localized refinements with badly-shaped elements, and the greedy THB-spline refinement creates the stiffness matrix with the highest density and interaction.

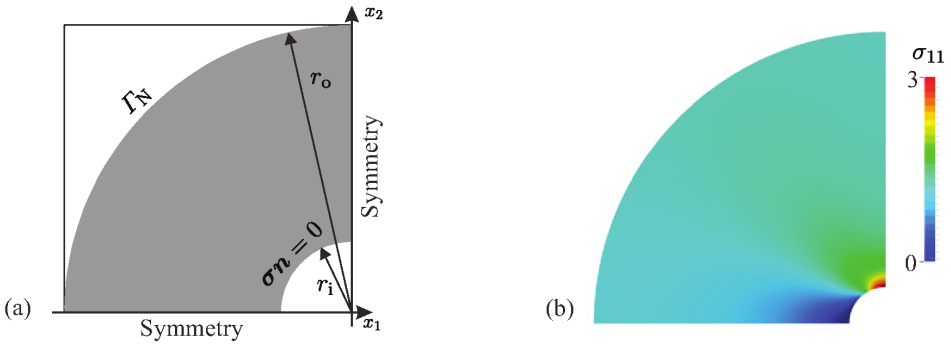

Figure 6.11 [41]: Infinite plate with a circular hole: **(a)** numerical analysis domain and boundary conditions, and **(b)** solution for σ_{11}.

share these benefits, however further investigation is needed in future.

Due to this effect, the greedy THB-spline refinement performs best if the numerical error is plotted over the condition number (cf. Figure 6.9 (c)). Since only a small amount of DOF is added during the refinement and due to the fact that the condition number grows slowly per DOF, an increased level of accuracy can be reached without increasing the condition number. But compared to the uniform refinement, also the T-spline refinements produce smaller condition numbers.

6.3.3 Linear elasticity

As a third example, an infinite plate with a circular hole under uniaxial in-plane tension σ_0 according to Figure 6.11 (a) is considered. The analytical solution is given by Timoshenko [62] in polar coordinates (r, ϕ),

$$\begin{aligned}
\bar{\sigma}_r &= \frac{\sigma_0}{2}\left[1 - \frac{r_\mathrm{i}^2}{r^2} + \left(1 - 4\frac{r_\mathrm{i}^2}{r^2} + 3\frac{r_\mathrm{i}^4}{r^4}\right)\cos(2\varphi)\right], \\
\bar{\sigma}_\varphi &= \frac{\sigma_0}{2}\left[1 + \frac{r_\mathrm{i}^2}{r^2} - \left(1 + 3\frac{r_\mathrm{i}^4}{r^4}\right)\cos(2\varphi)\right], \\
\bar{\sigma}_{r\varphi} &= \frac{\sigma_0}{2}\left(-1 - 2\frac{r_\mathrm{i}^2}{r^2} + 3\frac{r_\mathrm{i}^4}{r^4}\right)\sin(2\varphi),
\end{aligned} \tag{6.34}$$

where $r_\mathrm{i} = 1\mathrm{mm}$ is the radius of the hole. A numerical solution is conveniently obtained on the quarter of an annulus with Dirichlet boundaries to enforce the symmetry conditions, and a Neumann boundary Γ_N at the outer radius to enforce the exact normal stress. The uniaxial tensile stress $\sigma_0 = 1\mathrm{MPa}$ is applied in the x_1-direction and material parameters $E = 10^5\mathrm{Pa}$ and $\nu = 0.3$ are used. The computational domain is modelled by a single C^1-continous NURBS patch with an outer radius $r_\mathrm{o} = 8$.

The exact solution features a stress concentration at $(x, y) = (0, r_i)$ of $\sigma_{11} = 3\sigma_0$ as illustrated in Figure 6.11 (b). Due to the lack of a singularity, optimal convergence rates $k = -p/2$ can be obtained by uniform h-refinement. Local refinement does not improve this rate in the asymptotic limit [25, 56]. There is however a benefit of the adaptive refinement which increases with the locality of the stress concentration.

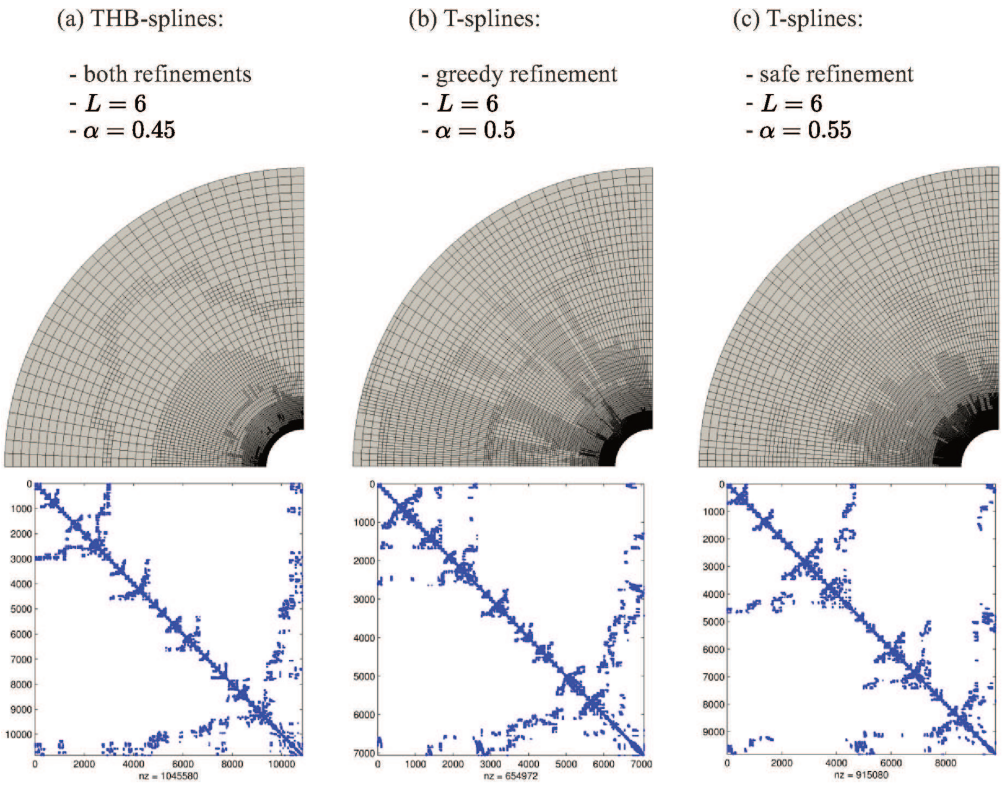

Figure 6.12 [41]: Infinite plate with a circular hole: The marking parameters α, the Bézier meshes and the sparsity patterns of the stiffness matrices after L refinement steps for all **(a)-(d)** refinement strategies. The greedy and safe THB-spline refinement show an identical refinement behaviour. Neither in the Bézier meshes, nor in the sparsity patterns, clear differences between the refinement strategies are visible.

That is, if the outer radius r_o is larger, the stress concentration is more localized in the computational domain, cf. Figure 6.12 (a), and an improved convergence can be achieved in the pre-asymptotic region.

This improvement can be obtained for all refinement techniques by setting the marking parameter around $\alpha = 0.5$ to generate a more extensive refinement. For this example the greedy and safe THB-spline refinement produce same results. The meshes after L refinement steps and the marking parameters α are illustrated in Figure 6.12. All refinement techniques lead to similar meshes. As a result, also the sparsity patterns are very similar and do not show any tendency. If the condition number is plotted over DOF (cf. Figure 6.13 (b)), no differences in the rate are visible between local and uniform refinement.

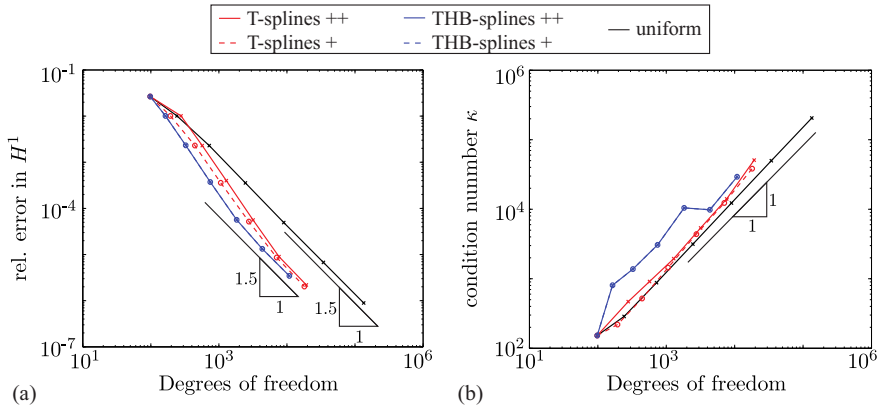

Figure 6.13 [41]: Infinite plate with a circular hole: The convergence rates as well as the condition number over the total number of degrees of freedom is plotted. **(a)** - The local refinement stategies improve the convergence rate in the pre-asymptotic regime, but reduce to $k = 1.5$ in the asymptotic region.

7 Outlook

The local mesh refinement for T-splines is a key aspect of this thesis. As mentioned in the introduction (cf. Chapter 1), T-splines have been introduced for purposes of Computer-Aided Design (CAD), and their main field of application involves locally reduced continuity in the sense of zero knot intervals and resulting multiple lines, as well as meshes that are not refinements of tensor-product meshes as assumed throughout all previous chapters, but refer to more complex topologies.

7.1 Zero Knot Intervals

We outline below an approach for the handling of zero knot intervals and multiple lines in the interior of the domain. The Definitions below are meant as a modification to Section 5.4 on the local refinement for multivariate T-splines.

Definition 7.1.1 (Initial mesh, elements)**.** We consider an arbitrary choice of *knot intervall sequences* $X_1, \dots, X_d$, with

$$X_j = \{[x_{j,0}, x_{j,1}], [x_{j,1}, x_{j,2}], \dots, [x_{j,n_j-1}, x_{j,n_j}]\}, \\ n_j \in \mathbb{N},\ x_{j,i} \in \mathbb{R} \text{ for all } i \in \{0, \dots, n_j\},\ x_{j,0} \leq \dots \leq x_{j,n_j} \quad (7.1)$$

for all $j \in \{1, \dots, d\}$. The initial mesh $\mathcal{Q}_0$ is defined as the tensor product of these intervall sequences

$$\mathcal{Q}_0 \coloneqq X_1 \times \dots \times X_d, \quad (7.2)$$

which is a set of axis-aligned boxes which we call *elements*.

Definition 7.1.2 (Embedded knot vectors)**.** Given $v = (v_1, \dots, v_d) \in \mathbb{R}^d$ and $j \in \{1, \dots, d\}$, we denote the *embedded global knot vector* by

$$\underline{\mathsf{K}}_j(v) \coloneqq \big\{(v_1, \dots, v_{j-1})\big\} \times \mathsf{K}_j(v) \times \big\{(v_{j+1}, \dots, v_d)\big\} \quad (7.3)$$

and, for $v \in \mathsf{N}$, the *embedded local knot vector* by

$$\underline{\mathsf{k}}_j(v) \coloneqq \big\{(v_1, \dots, v_{j-1})\big\} \times \mathsf{k}_j(v) \times \big\{(v_{j+1}, \dots, v_d)\big\}. \quad (7.4)$$

Embedded knot vectors contain points in $\mathbb{R}^d$ and are, similarly to $\mathsf{K}_j(v)$ and $\mathsf{k}_j(v)$, treated as ordered sets, and we assume that the elements of $\underline{\mathsf{K}}_j(v)$ and $\underline{\mathsf{k}}_j(v)$ are sorted in ascending order with respect to their j-th component.

Definition 7.1.3. Given a mesh $\mathcal{Q}$, an element $\mathtt{Q}$, and the above-defined embedded local knot vectors, we define *patch* of $\mathtt{Q}$ as

$$\operatorname{patch}(\mathcal{Q}, \mathtt{Q}) \coloneqq \{\mathtt{Q}' \in \mathcal{Q} \mid \exists\ v \in \mathsf{N},\ i, j \in \{1, \dots, d\}, i \neq j : \\ \#(\underline{\mathsf{k}}_j(v) \cap \mathtt{Q}) \geq 2 \leq \#(\underline{\mathsf{k}}_i(v) \cap \mathtt{Q}')\}. \quad (7.5)$$

The criterion $\#(\underline{\mathsf{k}}_j(v) \cap \mathtt{Q}) \geq 2$ means that the size of $\mathtt{Q}$ influences the distance between entries of $\mathsf{k}_j(v)$. Hence the patch of $\mathtt{Q}$ is the set of all elements $\mathtt{Q}' \in \mathcal{Q}$ that influence knot vectors of nodes of which a knot vector in an other dimension is influenced by $\mathtt{Q}$.

Corollary 7.1.4. *For $\mathtt{Q}, \mathtt{Q}' \in \mathcal{Q}$, the above definition implies the symmetry*

$$\mathtt{Q}' \in \operatorname{patch}(\mathcal{Q}, \mathtt{Q}) \;\Leftrightarrow\; \mathtt{Q} \in \operatorname{patch}(\mathcal{Q}, \mathtt{Q}'). \tag{7.6}$$

Definition 7.1.5 (Zero-volume elements)**.** We denote by $\mathcal{Z}(\mathcal{Q})$ all elements of $\mathcal{Q}$ that are degenerate in the sense of a vanishing volume due to a zero knot interval.

Algorithm 7.1.6 (Closure)**.** Given a mesh $\mathcal{Q}$ and a set of marked elements $\mathcal{M} \subseteq \mathcal{Q}$ to be refined, the *closure* $\textsc{closure\_ts}(\mathcal{Q}, \mathcal{M})$ of $\mathcal{M}$ is computed as follows.

$\widetilde{\mathcal{M}} \coloneqq \mathcal{M}$
repeat
  for all $\mathtt{Q} \in \widetilde{\mathcal{M}}$ **do**
    $\widetilde{\mathcal{M}} \coloneqq \widetilde{\mathcal{M}} \cup \left\{ \mathtt{Q}' \in \operatorname{patch}(\mathcal{Q}, \mathtt{Q}) \mid \ell(\mathtt{Q}') < \ell(\mathtt{Q}) \right\} \setminus \mathcal{Z}(\mathcal{Q})$
  end for
until $\widetilde{\mathcal{M}}$ stops growing
return $\textsc{closure\_ts}(\mathcal{Q}, \mathcal{M}) = \widetilde{\mathcal{M}}$

Algorithm 7.1.7 (Refinement)**.** Given a mesh $\mathcal{Q}$ and a set of marked elements $\mathcal{M} \subseteq \mathcal{Q}$ to be refined, $\textsc{refine\_ts}_{\mathrm{nD}}(\mathcal{Q}, \mathcal{M}, q)$ is defined by

$$\textsc{refine\_ts}_{\mathrm{nD}}(\mathcal{Q}, \mathcal{M}, q) \coloneqq \textsc{subdivide}(\mathcal{Q}, \textsc{closure\_ts}(\mathcal{Q}, \mathcal{M}), q). \tag{7.7}$$

Due to the design of Algorithm 7.1.6, the elements of $\mathcal{Z}(\mathcal{Q})$ are not refined, in order to not increase the multiplicity of lines. A key difficulty concerning this approach is the nesting of the patches (cf. Lemma 5.4.9). Given an admissible mesh $\mathcal{Q}$ and two nested elements $\mathtt{Q} \subseteq \hat{\mathtt{Q}}$, it is not yet proven if the corresponding patches are nested in the sense $\operatorname{patch}(\mathcal{Q}, \mathtt{Q}) \subseteq \operatorname{patch}(\mathcal{Q}, \hat{\mathtt{Q}})$. If it is the case, then we expect this modified refinement routine to fulfill all presented results in Section 5.4, plus the ability to refine meshes with multiple lines.

7.2 Local Refinement of Unstructured 2D meshes

In this chapter, we sketch an idea for the local refinement of two-dimensional meshes that do not have tensor-product structure, but do have an associated T-spline basis. In this context, we consider regular quadrilateral meshes as defined below.

Definition 7.2.1 (Unstructured mesh)**.** We call a finite set of convex and closed quadrilaterals $\mathcal{Q} \subset \mathcal{P}(\mathbb{R}^2)$ an *unstructured mesh* if it is regular, i.e., if any two distinct elements of $\mathcal{Q}$ have disjoint interior, and their intersection is either empty or exactly one common edge or one common vertex.

These unstructured meshes allow for the construction of a T-spline basis [63], involving so-called unstructured T-splines in the neighbourhood of extraordinary nodes (interior nodes that neighbour exactly 3 or more than 4 edges and boundary

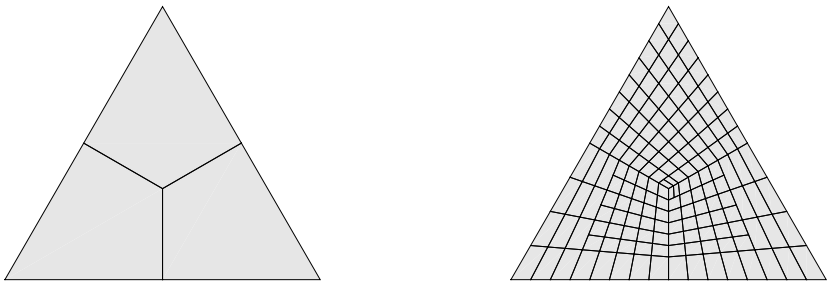

Figure 7.1: An unstructured mesh for a triangular domain (prototypical example): the initial mesh (left) and a refinement using REFINE_TS$_{\text{nD}}$ (right).

nodes that neighbour more than 4 edges). The refinement procedure REFINE_TS$_{\text{2D}}$ introduced in Chapter 5 is not appropriate for this case, because the absence of globally fixed parametric directions (i.e., the loss of a global notion of horizontal and vertical edges and T-junctions) yields that the subdivision of equally-leveled elements may produce crossing T-junction extensions. This means that REFINE_TS$_{\text{2D}}$ does not preserve analysis-suitability when applied to an unstructured mesh.

We classify below unstructured quadrilateral meshes by the minimal d that allows mapping the geometry into a d-dimensional structured mesh. We explain an adaptive refinement routine for a certain class of unstructured meshes, based on REFINE_TS$_{\text{nD}}$ applied in the multidimensional structured mesh.

7.2.1 Classification of unstructured meshes

In this section, we define k-unstructured meshes implicitely by the minimal space dimension k that allows for mapping the given geometry into a k-dimensional structured mesh. In order to come up with a more practical characterization of those meshes, we show a necessary criterion of k-unstructuredness, using constrained edge-coloring.

Definition 7.2.2 (k-unstructured mesh)**.** We call an unstructured mesh $\mathcal{Q}$ *k-unstructured* if there exists a globally continuous and invertible map $F : \mathbb{R}^2 \to \mathbb{R}^{k+2}$ that maps each element of $\mathcal{Q}$ to a square with vertices in $\mathbb{N}_0^{k+2}$ and side length 1.

0-unstructured meshes are called *structured*, and unstructured meshes that are not k-unstructured for any $k \in \mathbb{N}_0$ are called *totally unstructured*. If k is minimal such that $\mathcal{Q}$ is k-unstructured, we call $\mathcal{Q}$ *strictly k-unstructured*.

Remark. The constraint on the image squares to have integer coordinates implies that these squares have to be axis-parallel in $\mathbb{R}^{k+2}$. If $\mathcal{Q}$ is structured, then the image $F(\mathcal{Q}) \subset \mathcal{P}(\mathbb{R}^2)$ is a (possibly non-connected) subset of a uniform 2D mesh.

Definition 7.2.3 (Bipartite)**.** We call a mesh $\mathcal{Q}$ with vertices $\mathcal{V}$ and edges $\mathcal{E}$ *bipartite* if there is a map $\xi : \mathcal{V} \to \{0, 1\}$ with $v_1 \neq v_2$ for any $[v_1, v_2] \in \mathcal{E}$. If $\mathcal{Q}$ consists of quadrilaterals only, then this is equivalent to the absence of odd holes.

Definition 7.2.4 (Piecewise symmetric n-edge-coloring)**.** An *n-edge-coloring* of a mesh $\mathcal{Q}$ with edges $\mathcal{E}$ is a function $\chi : \mathcal{E} \to \{1, \dots, n\}$ such that any two adjacent edges have distinct values, i.e., $E_1 \cap E_2 \neq \emptyset \Rightarrow \chi(E_1) \neq \chi(E_2)$. We call an n-edge-coloring *piecewise symmetric (pws)* if it is a 2-edge-coloring on each quadrilateral.

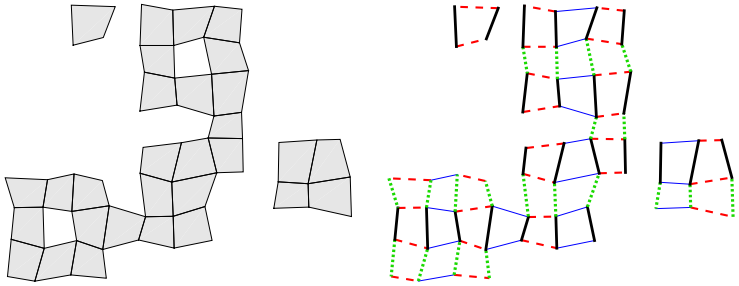

(a) structured mesh (b) pws. 4-edge-coloring

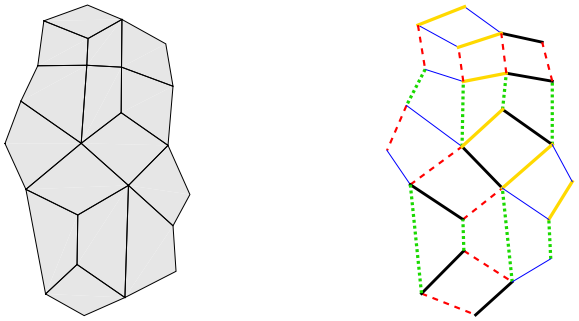

(c) 1-unstructured mesh (d) pws. 5-edge-coloring

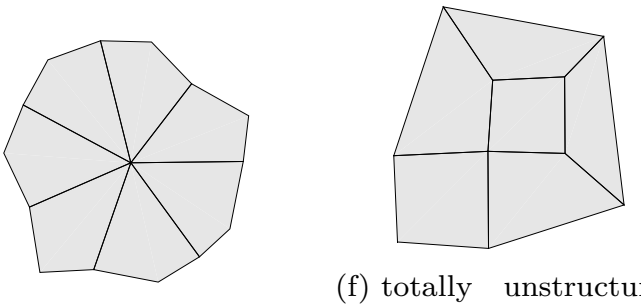

(e) 2-unstructured mesh (f) totally unstructured mesh

Figure 7.2: Examples of a structured, a 1-unstructured, a 2-unstructured, and a totally unstructured mesh.

Theorem 7.2.5. *If $\mathcal{Q}$ is k-unstructured, then it is bipartite and has a piecewise symmetric $(2k+4)$-edge-coloring.*

Proof. Consider a k-unstructured mesh $\mathcal{Q}$ with $k \in \mathbb{N}_0$ with vertices $\mathcal{V}$.

$\mathcal{Q}$ is bipartite: Define for any $v \in \mathcal{V}$ with $F(v) = (z_1, \dots, z_{k+2}) \in \mathbb{N}_0^{k+2}$

$$\xi(v) \coloneqq \left(\sum_{j=1}^{k+2} z_j \right) \bmod 2. \tag{7.8}$$

Since the image $F(E)$ of any edge $E = [v_1, v_2] \in \mathcal{E}$ is axis-parallel in $\mathbb{R}^{k+2}$ and has the length 1, the image vertices $F(v_1)$ and $F(v_2)$ differ in exactly one component, and the difference in that component is 1. Hence $\xi(v_1) \neq \xi(v_2)$.

$\mathcal{Q}$ has a piecewise symmetric $(2k+4)$-edge-coloring: We have to show that there is a labeling $\chi : \mathcal{E} \to \{1, \dots, 2k+4\}$ that returns an index $\chi(E)$ for any edge $E \in \mathcal{E}$, such that any two edges with a common vertex have distinct indices. At the same time, the four sides of any quadriliteral $Q \in \mathcal{Q}$ shall be labeled with two

indices, which means that any two opposing sides have the same index. For each edge $E \in \mathcal{E}(\mathcal{Q})$ with $F(E) = \{x_1\} \times \cdots \times \{x_{j-1}\} \times [x_j, x_j + 1] \times \{x_{j+1}\} \times \cdots \times \{x_{k+2}\}$, define

$$\chi(E) \coloneqq 2j - 1 + (x_j \bmod 2). \tag{7.9}$$

χ is an edge-coloring: Consider two distinct edges $E_1, E_2 \in \mathcal{Q}$ that share a vertex v. The images $F(E_1), F(E_2)$ are distinct (because F is invertible) and axis-parallel in $\mathbb{R}^{k+2}$, having the directions $1 \leq j_1, j_2 \leq k + 2$. If $F(E_1)$ and $F(E_2)$ are aligned, hence $j_1 = j_2$, then v is the startpoint of one and the endpoint of the other edge, which implies that $\chi(E_1)$ and $\chi(E_2)$ differ by one and hence cannot be equal. If $j_1 \neq j_2$, then (7.9) yields that $\chi(E_1)$ and $\chi(E_2)$ differ by more than 1 and cannot be equal.

χ is a 2-coloring on each quadrilateral: It suffices to show for an arbitrary edge E that the opposing edge E' in a quadrilateral $Q \supset E \cup E'$ satisfies $\chi(E') = \chi(E)$. W.l.o.g. let

$$\begin{aligned} F(Q) = \{x_1\} \times \cdots \times \{x_{i-1}\} \times [x_i, x_i + 1] \times \{x_{i+1}\} \times \ldots \\ \cdots \times \{x_{j-1}\} \times [x_j, x_j + 1] \times \{x_{j+1}\} \times \cdots \times \{x_{k+2}\} \end{aligned}$$

and

$$\begin{aligned} F(E) &= \{x_1\} \times \cdots \times \{x_i\} \times \cdots \times \{x_{j-1}\} \times [x_j, x_j + 1] \times \{x_{j+1}\} \times \cdots \times \{x_{k+2}\}, \\ F(E') &= \{x_1\} \times \cdots \times \{x_i + 1\} \times \cdots \times \{x_{j-1}\} \times [x_j, x_j + 1] \times \{x_{j+1}\} \times \cdots \times \{x_{k+2}\}. \end{aligned} \tag{7.10}$$

Then the definition of χ concludes the proof. □

Remark. Bipartiteness and the existence of a pws. $(2k + 4)$-edge-coloring is necessary, but not sufficient for k-unstructuredness. Two counterexamples are given in Figure 7.3. However, we conjecture that it is sufficient for n-unstructuredness for *some* $n \geq k$.

7.2.2 Refinement algorithm

We propose below a refinement strategy for k-unstructured meshes and their refinements (which may not be unstructured in the sense of Definition 7.2.1 because this definition excludes meshes with T-junctions). In essence, the algorithm consists of a refinement of the induced $(k + 2)$-dimensional mesh and the subsequent extraction of the interfaces of interest.

Definition 7.2.6 (Suitable meta-mesh, 2D extraction)**.** Let $\mathcal{Q}_0$ be a k-unstructured mesh in the sense of Definition 7.2.1, $k \in \mathbb{N}_0$, let F be the associated map from Definition 7.2.2, and $\hat{\mathcal{Q}}_0$ a set of $(k + 2)$-dimensional unit hypercubes. Denote by $\mathcal{F}_{2\mathrm{D}}(\hat{\mathtt{Q}})$ for any $(k+2)$-dimensional hypercuboid $\hat{\mathtt{Q}} \subset \mathbb{R}^{k+2}$ the set of two-dimensional faces on the boundary of $\hat{\mathtt{Q}}$. We call $\hat{\mathcal{Q}}_0$ a *suitable meta-mesh* of $\mathcal{Q}_0$ if

- each hypercube $\hat{\mathtt{Q}} \in \hat{\mathcal{Q}}_0$ has at least one 2D face in $F(\mathcal{Q}_0) \coloneqq \{F(\mathtt{Q}) \mid \mathtt{Q} \in \mathcal{Q}_0\}$, this is, $\mathcal{F}_{2\mathrm{D}}(\hat{\mathtt{Q}}) \cap F(\mathcal{Q}_0) \neq \emptyset$, and
- for each $\mathtt{Q} \in \mathcal{Q}_0$ there is exactly one hypercube $\hat{\mathtt{Q}}$ such that $F(\mathtt{Q}) \in \mathcal{F}_{2\mathrm{D}}(\hat{\mathtt{Q}})$.

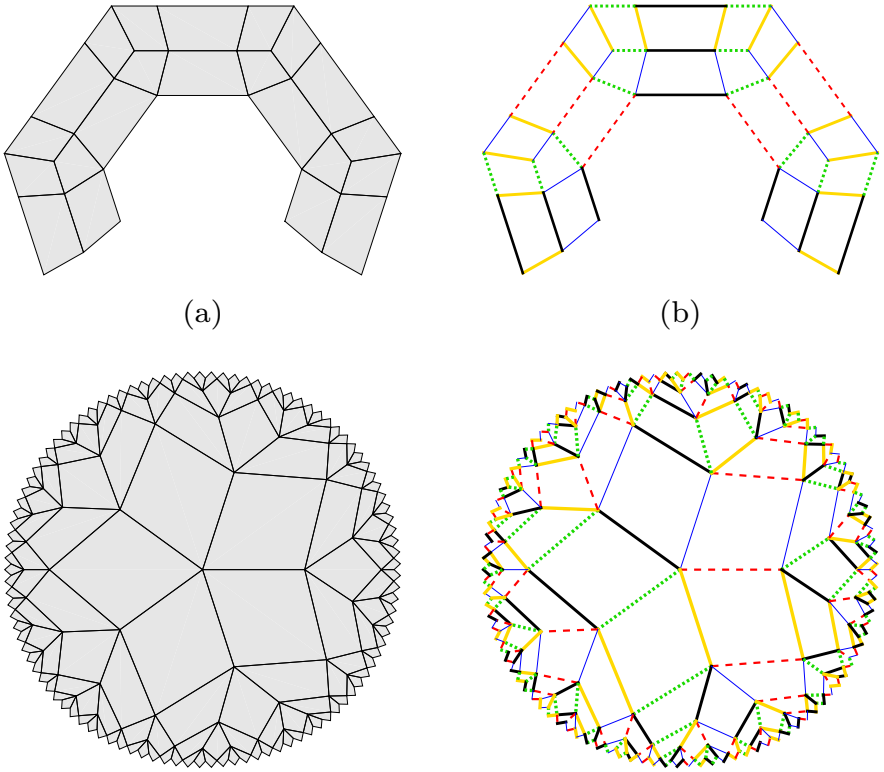

Figure 7.3: The two meshes in Figure 7.3a and 7.3c are bipartite and allow for a pws. 5-edge-coloring (7.3b and 7.3d, resp.), but they are *not* 1-unstructured. Both meshes allow for a continuous map to unit squares in $\mathbb{R}^3$, but the resulting mesh is self-overlapping in both cases, and hence the map is not invertible as required in Definition 7.2.2.

A suitable meta-mesh can be constructed by taking the set of *all* $(k+2)$-dimensional unit cubes $\hat{Q}$ satisfying $\mathcal{F}_{2D}(\hat{Q}) \cap F(\mathcal{Q}_0) \neq \emptyset$ and then, for each $Q \in \mathcal{Q}_0$ such that there are two hypercubes $\hat{Q}_1 \neq \hat{Q}_2$ with $F(Q) \in \mathcal{F}_{2D}(\hat{Q}_1) \cap \mathcal{F}_{2D}(\hat{Q}_2)$, omitting $\hat{Q}_1$ or $\hat{Q}_2$. We denote the suitable meta-mesh obtained by this construction by $\mathcal{Q}_0^{[k+2]}$.

For any refinement $\mathcal{Q}_j^{[k+2]}$ of $\mathcal{Q}_0^{[k+2]}$, we call

$$\mathcal{Q}_j := \text{extract}(\mathcal{Q}_j^{[k+2]}, \mathcal{Q}_0) := \{F^{-1}(S) \mid \exists\, \hat{Q} \in \mathcal{Q}_j^{[k+2]}, Q \in \mathcal{Q}_0 : \quad S \in \mathcal{F}_{2D}(\hat{Q}) \wedge S \subseteq F(Q)\} \tag{7.11}$$

the *2D extraction* of $\mathcal{Q}_j^{[k+2]}$, and $\mathcal{Q}_j^{[k+2]}$ the *meta-mesh* of $\mathcal{Q}_j$.

Algorithm 7.2.7 (Refinement for k-unstructured meshes)**.** The refinement for unstructured meshes is in essence REFINE_TS$_{nD}$ with an additional extraction step.

Input: k-unstructured initial mesh $\mathcal{Q}_0$,
meta-mesh $\mathcal{Q}^{[k+2]}$ of the refined mesh $\mathcal{Q}$,
marked elements $\mathcal{M} \subseteq \mathcal{Q}$ in the refined mesh.

Find the meta-mesh representation $\mathcal{M}^{[k+2]} \subseteq \mathcal{Q}^{[k+2]}$ of $\mathcal{M}$.

Set $\tilde{\mathcal{Q}}^{[k+2]} := \text{REFINE\_TS}_{nD}(\mathcal{Q}^{[k+2]}, \mathcal{M}^{[k+2]})$.

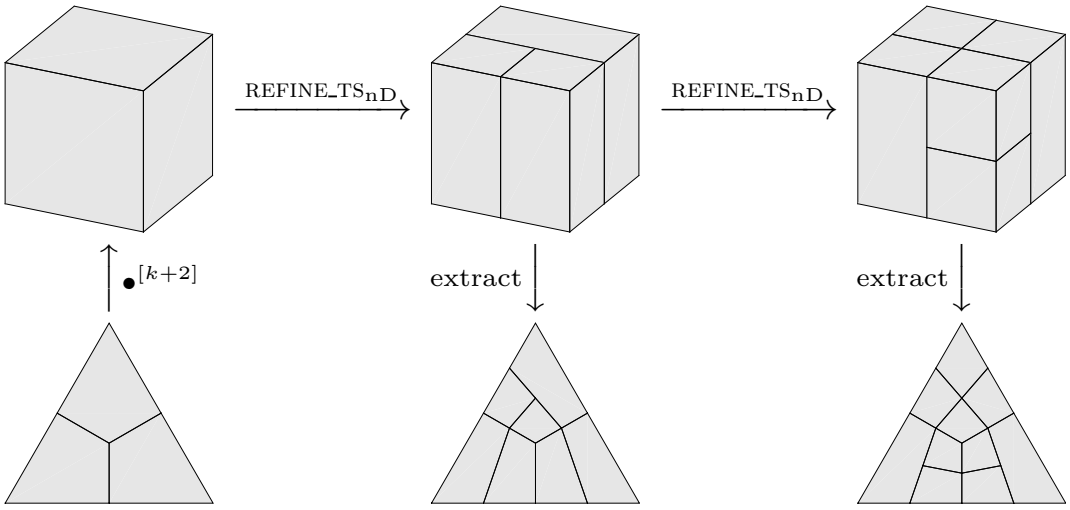

Figure 7.4: Example for the refinement of the 1-unstructured mesh from Figure 7.1. In the first refinement, the lower left element is marked, and in the second refinement step, its right-hand child element.

Set $\tilde{\mathcal{Q}} \coloneqq \mathrm{extract}(\tilde{\mathcal{Q}}^{[k+2]}, \mathcal{Q}_0)$.

Set $\mathcal{M} \coloneqq \mathcal{M} \cap \tilde{\mathcal{Q}}$.

while $\mathcal{M} \neq \emptyset$ **do**

Update the meta-mesh representation $\mathcal{M}^{[k+2]} \subseteq \mathcal{Q}^{[k+2]}$ of $\mathcal{M}$.

Set $\tilde{\mathcal{Q}}^{[k+2]} \coloneqq \mathrm{REFINE\_TS_{nD}}(\tilde{\mathcal{Q}}^{[k+2]}, \mathcal{M}^{[k+2]})$.

Set $\tilde{\mathcal{Q}} \coloneqq \mathrm{extract}(\tilde{\mathcal{Q}}^{[k+2]}, \mathcal{Q}_0)$.

Set $\mathcal{M} \coloneqq \mathcal{M} \cap \tilde{\mathcal{Q}}$.

end while

return $\tilde{\mathcal{Q}}, \tilde{\mathcal{Q}}^{[k+2]}$

An example of this algorithm is illustrated in Figure 7.4.

Linear independence

In order to argue on refinement and linear independence, we consider unstructured meshes and the associated spline spaces in a manifold setting, which is explained in [64]. The T-splines are constructed on a family (*proto-atlas*) of rectangular domains (*proto-charts*) and associated tensor-product meshes. Each proto-chart has associated a geometry map from the proto-chart to a part (*chart*) of the physical domain. The set of charts is called *atlas*, and their union is the physical domain. See Figure 7.5 for an example considering the triangle from Figures 7.1 and 7.4. The charts are supposed to overlap, and similarly, the proto-charts overlap in an abstract sense which is realized by so-called transition functions, see [64, Definition 1]. The T-splines that correspond to the unstructured mesh (constructed as in [63]) are linearly independent if on each proto-chart, the corresponding T-splines (including the T-splines from other overlapping proto-charts) are linearly independent. This is combined with a dual-compatibility criterion in [64, Theorem 1]. We conjecture that

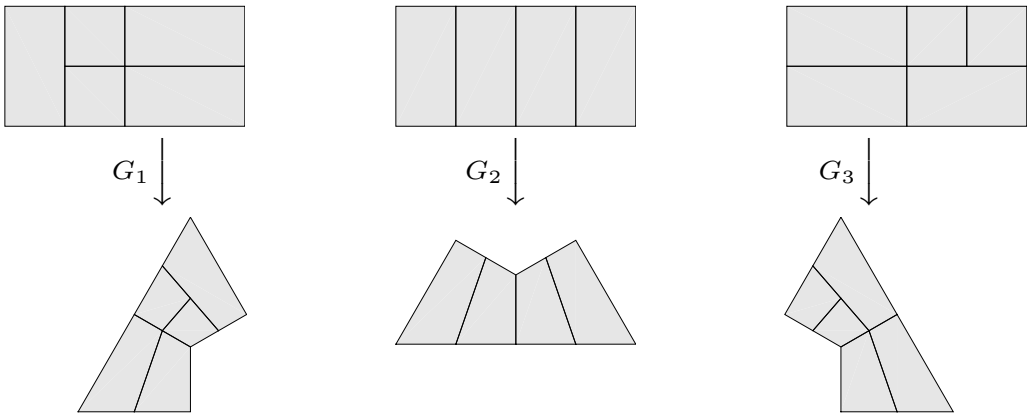

Figure 7.5: Proto-atlas (upper row) and atlas (lower row) of the triangle from Figure 7.4 after the first refinement.

Algorithm 7.2.7 preserves the linear independence of the T-splines, however this is not proven yet. Further properties of Algorithm 7.2.7 are the preservation of shape regularity (i.e., the mesh elements do not degenerate under refinement) and linear complexity, both inherited from REFINE_TS$_{\text{nD}}$.

8 Conclusions and Further Outlook

This thesis has presented and theoretically investigated local mesh refinement routines for the Adaptive Isogeometric Method with Hierarchical B-splines, Truncated Hierarchical B-splines, and T-splines in the two-dimensional and in the higher-dimensional setting. We addressed, for REFINE_HB and REFINE_THB, boundedness of the overlap of basis functions, boundedness of mesh overlays and linear complexity in the sense of a uniform upper bound on the ratio of generated and marked elements. The existence of an upper bound on the overlap of basis functions implies that the stiffness matrix of the linear system to solve is sparse, i.e., it has a bounded number of nonzero entries in each row and column. The upper bound on the number of elements in the coarsest common refinement (the overlay) of two meshes, as well as linear complexity from Theorems 3.1.12, 3.2.5 and 4.2.6 are crucial ingredients for a later proof of rate-optimality of the method, see [10, Equations (2.9) and (2.10)]. For REFINE_TS$_{2D}$ and REFINE_TS$_{nD}$, the overlap of basis functions is bounded a priori and did not need further investigation. We investigated the boundedness of mesh overlays, linear independence of the T-splines, nestedness of the T-spline spaces, and linear complexity as above. Altogether, we provided all properties for the REFINE step of the Adaptive Isogeometric Method that are needed for a proof of optimal convergence rates. In a selection of numerical experiments, the refinement routines REFINE_THB and REFINE_TS$_{2D}$ were applied in an adaptive method and have proven the performance predicted by the theory.

We outlined an approach for the handling of zero knot intervals and multiple lines in the interior of the domain, which are used in CAD applications for controlling the continuity of the spline functions, and we also sketched basic ideas for the local refinement of two-dimensional meshes that do not have tensor-product structure. We did not address the handling of even polynomial degrees for T-splines, which requires a generalization of anchor elements to the multidimensional setting, based on the techniques from [31]. We leave these three subjects as the major aspects of the ongoing and future work.

Bibliography

[1] M. Turner, R. Clough, H. Martin, and L. Topp, *Stiffness and deflection analysis of complex structures*, Journal of the Aeronautical Sciences **23** (1956), no. 9, 805–823.

[2] B. Galerkin, *Vestnik inzhenerov i tekhnikovi*, Tech **19** (1915), 897–908.

[3] I. Babuška and W. Rheinboldt, *A-posteriori error estimates for the finite element method*, International Journal for Numerical Methods in Engineering **12** (1978), no. 10, 1597–1615.

[4] I. Babuška and M. Vogelius, *Feedback and adaptive finite element solution of one-dimensional boundary value problems*, Numerische Mathematik **44** (1984), no. 1, 75–102.

[5] W. Dörfler, *A convergent adaptive algorithm for Poisson's equation*, SIAM Journal on Numerical Analysis **33** (1996), no. 3, 1106–1124.

[6] P. Morin, R. Nochetto, and K. Siebert, *Convergence of Adaptive Finite Element Methods*, SIAM Review **44** (2002), no. 4, 631–658.

[7] P. Binev, W. Dahmen, and R. DeVore, *Adaptive Finite Element Methods with convergence rates*, Numerische Mathematik **97** (2004), no. 2, 219–268.

[8] R. Stevenson, *Optimality of a standard Adaptive Finite Element Method*, Foundations of Computational Mathematics **7** (2007), no. 2, 245–269.

[9] J. Cascon, C. Kreuzer, R. Nochetto, and K. Siebert, *Quasi-Optimal Convergence Rate for an Adaptive Finite Element Method*, SIAM Journal on Numerical Analysis **46** (2008), no. 5, 2524–2550.

[10] C. Carstensen, M. Feischl, M. Page, and D. Praetorius, *Axioms of adaptivity*, Computers & Mathematics with Applications **67** (2014), no. 6, 1195–1253.

[11] T. Hughes, J. Cottrell, and Y. Bazilevs, *Isogeometric Analysis: CAD, Finite Elements, NURBS, exact geometry and mesh refinement*, Computer Methods in Applied Mechanics and Engineering **194** (2005), no. 39–41, 4135–4195.

[12] J. Cottrell, T. Hughes, and Y. Bazilevs, *Isogeometric Analysis: Toward integration of CAD and FEA*, John Wiley & Sons, Ltd, 2009.

[13] L. Beirão da Veiga, A. Buffa, G. Sangalli, and R. Vàzquez, *Mathematical analysis of variational isogeometric methods*, Acta Numerica **23** (2014), 157–287.

[14] D. Forsey and R. Bartels, *Hierarchical B-spline refinement*, Computers & Graphics **22** (1988), 205–212.

[15] R. Kraft, *Adaptive and linearly independent multilevel B–splines*, Surface Fitting and Multiresolution Methods (A. Le Méhauté, C. Rabut, and L. Schumaker, eds.), Vanderbilt University Press, Nashville, 1997, pp. 209–218.

[16] ———, *Adaptive und linear unabhängige Multilevel B–Splines und ihre Anwendungen*, Ph.D. thesis, Universität Stuttgart, 1998.

[17] A.-V. Vuong, C. Giannelli, B. Jüttler, and B. Simeon, *A hierarchical approach to adaptive local refinement in Isogeometric Analysis*, Computer Methods in Applied Mechanics and Engineering **200** (2011), no. 49-52, 3554–3567.

[18] D. Schillinger, L. Dede, M. Scott, J. Evans, M. Borden, E. Rank, and T. Hughes, *An isogeometric design-through-analysis methodology based on adaptive hierarchical refinement of NURBS, immersed boundary methods, and T-spline CAD surfaces*, Computer Methods in Applied Mechanics and Engineering **249** (2012), 116–150.

[19] C. Giannelli, B. Jüttler, and H. Speleers, *THB–splines: the truncated basis for hierarchical splines*, Computer Aided Geometric Design **29** (2012), 485–498.

[20] G. Kiss, C. Giannelli, U. Zore, B. Jüttler, D. Großmann, and J. Barner, *Adaptive CAD model (re-)construction with THB-splines*, Graphical models **76** (2014), no. 5, 273–288.

[21] C. Giannelli, B. Jüttler, S. Kleiss, A. Mantzaflaris, B. Simeon, and J. Špeh, *THB-splines: An effective mathematical technology for adaptive refinement in geometric design and Isogeometric Analysis*, Computer Methods in Applied Mechanics and Engineering **299** (2016), 337–365.

[22] T. Sederberg, J. Zheng, A. Bakenov, and A. Nasri, *T-Splines and T-NURCCs*, ACM Transactions on Graphics **22** (2003), no. 3, 477–484.

[23] T. Sederberg, D. Cardon, G. Finnigan, N. North, J. Zheng, and T. Lyche, *T-spline Simplification and Local Refinement*, ACM Transactions on Graphics **23** (2004), no. 3, 276–283.

[24] Y. Bazilevs, V. Calo, J. Cottrell, J. Evans, T. Hughes, S. Lipton, M. Scott, and T. Sederberg, *Isogeometric Analysis using T-splines*, Computer Methods in Applied Mechanics and Engineering **199** (2010), no. 5–8, 229–263, Computational Geometry and Analysis.

[25] M. Dörfel, B. Jüttler, and B. Simeon, *Adaptive Isogeometric Analysis by local h-refinement with T-splines*, Computer Methods in Applied Mechanics and Engineering **199** (2010), no. 5–8, 264–275, Computational Geometry and Analysis.

[26] A. Buffa, D. Cho, and G. Sangalli, *Linear independence of the T-spline blending functions associated with some particular T-meshes*, Computer Methods in Applied Mechanics and Engineering **199** (2010), no. 23–24, 1437–1445.

[27] X. Li and M. Scott, *On the nesting behavior of T-splines*, ICES Report 11-13, University of Texas at Austin (2011).

[28] X. Li, J. Zheng, T. Sederberg, T. Hughes, and M. Scott, *On linear independence of T-spline blending functions*, Computer Aided Geometric Design **29** (2012), no. 1, 63–76.

[29] M. Scott, X. Li, T. Sederberg, and T. Hughes, *Local refinement of analysis-suitable T-splines*, Computer Methods in Applied Mechanics and Engineering **213–216** (2012), 206–222.

[30] L. Beirão da Veiga, A. Buffa, D. Cho, and G. Sangalli, *Analysis-suitable T-splines are dual-compatible*, Computer Methods in Applied Mechanics and Engineering **249—252** (2012), 42–51, Higher Order Finite Element and Isogeometric Methods.

[31] L. Beirão da Veiga, A. Buffa, G. Sangalli, and R. Vàzquez, *Analysis-suitable T-splines of arbitrary degree: definition, linear independence and approximation properties*, Mathematical Models and Methods in Applied Sciences **23** (2013), no. 11, 1979–2003.

[32] Y. Zhang, W. Wang, and T. J. Hughes, *Solid T-spline construction from boundary representations for genus-zero geometry*, Computer Methods in Applied Mechanics and Engineering **249–252** (2012), 185–197, Higher Order Finite Element and Isogeometric Methods.

[33] W. Wang, Y. Zhang, L. Liu, and T. Hughes, *Trivariate solid T-spline construction from boundary triangulations with arbitrary genus topology*, Computer-Aided Design **45** (2013), no. 2, 351–360, Solid and Physical Modeling 2012.

[34] P. Morgenstern, *Globally structured three-dimensional analysis-suitable T-splines: Definition, linear independence and m-graded local refinement*, SIAM Journal on Numerical Analysis **54** (2016), no. 4, 2163–2186.

[35] X. Li and M. Scott, *Analysis-suitable T-splines: Characterization, refineability, and approximation*, Mathematical Models and Methods in Applied Sciences **24** (2014), no. 06, 1141–1164.

[36] A. Bressan, A. Buffa, and G. Sangalli, *Characterization of analysis-suitable T-splines*, Computer Aided Geometric Design **39** (2015), 17–49.

[37] A. Buffa, C. Giannelli, P. Morgenstern, and D. Peterseim, *Complexity of hierarchical refinement for a class of admissible mesh configurations*, Computer Aided Geometric Design **47** (2016), 83–92.

[38] P. Morgenstern and D. Peterseim, *Analysis-suitable adaptive T-mesh refinement with linear complexity*, Computer Aided Geometric Design **34** (2015), 50–66.

[39] G. Gantner, D. Haberlik, and D. Praetorius, *Adaptive IGAFEM with optimal convergence rates: Hierarchical B-splines*, arXiv:1701.07764 (2017).

[40] M. Feischl, G. Gantner, A. Haberl, and D. Praetorius, *Optimal convergence for adaptive IGA boundary element methods for weakly-singular integral equations*, Numerische Mathematik (2016), 1–36.

[41] P. Hennig, M. Kästner, P. Morgenstern, and D. Peterseim, *Adaptive mesh refinement strategies in Isogeometric Analysis – a computational comparison*, Computer Methods in Applied Mechanics and Engineering **316** (2017), 424 – 448, Special Issue on Isogeometric Analysis: Progress and Challenges.

[42] C. De Boor, *A practical guide to splines*, vol. 27, Springer-Verlag New York, 1978.

[43] R. Verfürth, *A posteriori error estimation techniques for finite element methods*, Oxford University Press, 2013.

[44] S. Kleiss, B. Jüttler, and W. Zulehner, *Enhancing Isogeometric Analysis by a Finite Element-based local refinement strategy*, Computer Methods in Applied Mechanics and Engineering **213–216** (2012), 168–182.

[45] L. Diening, C. Kreuzer, and R. Stevenson, *Instance optimality of the adaptive maximum strategy*, Foundations of Computational Mathematics **16** (2016), no. 1, 33–68.

[46] C. Kreuzer and M. Schedensack, *Instance optimal Crouzeix-Raviart Adaptive Finite Element Methods for the Poisson and Stokes problems*, IMA Journal of Numerical Analysis (2015).

[47] C. Carstensen and H. Rabus, *Axioms of adaptivity for separate marking*, arXiv:1606.02165 (2016).

[48] H. Rabus, *Quasi-optimal convergence of AFEM based on separate marking, Part I*, Journal of Numerical Mathematics **23** (2015), no. 2, 137–156.

[49] _____, *Quasi-optimal convergence of AFEM based on separate marking, Part II*, Journal of Numerical Mathematics **23** (2015), no. 2, 157–174.

[50] A. Målqvist and D. Peterseim, *Localization of elliptic multiscale problems*, Mathematics of Computation **83** (2014), no. 290, 2583–2603. MR 3246801

[51] P. Henning, P. Morgenstern, and D. Peterseim, *Multiscale partition of unity*, Meshfree Methods for Partial Differential Equations VII (M. Griebel and M. A. Schweitzer, eds.), Lecture Notes in Computational Science and Engineering, vol. 100, Springer International Publishing, 2015, Also available as INS Preprint No. 1315, pp. 185–204 (English).

[52] P. Hennig, *Adaptive isogeometric modelling using T-splines and hierarchical NURBS*, Master's thesis, TU Dresden, 2014.

[53] A. Buffa and C. Giannelli, *Adaptive isogeometric methods with hierarchical splines: Error estimator and convergence*, Mathematical Models and Methods in Applied Sciences **26** (2016), no. 01, 1–25.

[54] C. Giannelli, B. Jüttler, and H. Speleers, *Strongly stable bases for adaptively refined multilevel spline spaces*, Advances in Computational Mathematics **40** (2014), no. 2, 459–490.

[55] L. Schumaker, *Spline functions: Basic theory*, 3 ed., Cambridge Mathematical Library, Cambridge University Press, Cambridge, 2007.

[56] P. Hennig, S. Müller, and M. Kästner, *Bézier extraction and adaptive refinement of truncated hierarchical NURBS*, Computer Methods in Applied Mechanics and Engineering **305** (2016), 316–339.

[57] R. Verfürth, *A review of a posteriori error estimation techniques for elasticity problems*, Computer Methods in Applied Mechanics and Engineering **176** (1999), 419–440.

[58] K. Gahalaut, S. Tomar, and C. Douglas, *Condition number estimates for matrices arising in NURBS based isogeometric discretizations of elliptic partial differential equations*, arXiv:1406.6808 (2014).

[59] Z. Yosibash, *Singularities in elliptic boundary value problems and elasticity and their connection with failure initiation*, Springer New York, 2011.

[60] K. A. Johannessen, F. Remonato, and T. Kvamsdal, *On the similarities and differences between Classical Hierarchical, Truncated Hierarchical and LR B-splines*, Computer Methods in Applied Mechanics and Engineering **291** (2015), 64–101.

[61] H. Yserentant, *On the multi-level splitting of finite element spaces*, Numerische Mathematik **49** (1986), no. 4, 379–412.

[62] S. Timoshenko, *Theory of elasticity*, 3rd ed., McGraw-Hill Publishing Company, 10 1970.

[63] W. Wang, Y. Zhang, M. Scott, and T. Hughes, *Converting an unstructured quadrilateral mesh to a standard T-spline surface*, Computational Mechanics **48** (2011), no. 4, 477–498.

[64] G. Sangalli, T. Takacs, and R. Vázquez, *Unstructured spline spaces for isogeometric analysis based on spline manifolds*, Computer Aided Geometric Design **47** (2016), 61–82.

Index